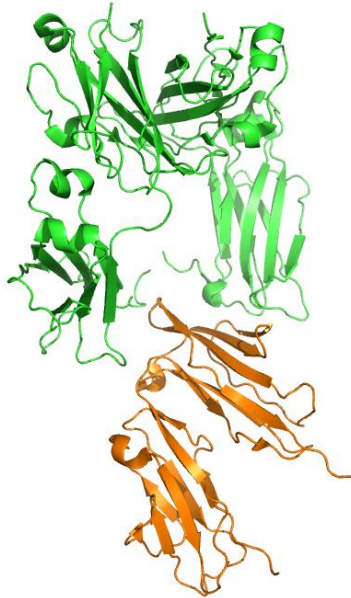


Investigating inhibitors of the IgE:high affinity receptor protein-protein interaction



Lucy Smith

A thesis submitted to Imperial College London in partial fulfilment
of the requirements for the degree of Doctor of Philosophy

Institute of Chemical Biology
Department of Chemistry
Imperial College London

December 2014

Declaration of originality

I declare that I have personally prepared this thesis and that the work described here is my own, carried out personally unless explicitly stated otherwise. All sources of information are acknowledged in the text and references.

Lucy Smith, December 2014

Copyright declaration

The copyright of this thesis rests with the author and is made available under a Creative Commons Attribution Non-Commercial No Derivatives licence. Researchers are free to copy, distribute or transmit the thesis on the condition that they attribute it, that they do not use it for commercial purposes and that they do not alter, transform or build upon it. For any reuse or redistribution, researchers must make clear to others the licence terms of this work.

Acknowledgements

Firstly I would like to thank my supervisors Professor Alan Spivey and Professor Robin Leatherbarrow in the Chemistry Department at Imperial College London for providing continued guidance and support throughout my PhD. I would also like to thank members of the Spivey, Leatherbarrow and Tate research groups for being lovely people to work with. Particular thanks to Dr Bingli Mo (for advice about peptide synthesis and ELISAs), Dr Maija Maskuniitty, Dr Neki Patel, Dr Manue Thinon, Jenny Ward and Rhiannon Beard (for general advice about peptide synthesis and LC-MS), Dr Will Heal, Dr Jennie Hutton and Dr Mark Rackham (for general chemistry and research advice) and finally to Dr Jimmy Sejberg and Dr Helena Dennison (for synthesising some of the compounds I used in my experiments).

I would like to thank my supervisor Dr Andrew Beavil at the Randall Division of Cell and Molecular Biophysics at King's College London for his support during my PhD and everyone at the Randall Division for making me welcome. Thanks to the MRC/Asthma UK Centre in Allergic Mechanisms of Asthma - Protein Production Facility for providing the proteins I used in my assays. Particular thanks to Dr Marie Pang (for guidance with protein labelling and the TR-FRET assay), Dr Nyssa Drinkwater (for guidance with protein crystallography and for taking me to Diamond), Professor Jim McDonnell (for help with SPR experiments), Dr Anthony Keeble, Dr Michael Kao, Dr Seema Agrawal and Dr Norhakim Yahya (for teaching me about protein expression and purification), Dr Anna Davies (for providing a protein I used in my SPR experiments) and Dr Rebecca Beavil (for general lab advice).

A big thank you goes to the Institute of Chemical Biology (ICB) Centre for Doctoral Training for being a friendly and supportive centre in which to work and for organising all the transferable skills courses, events and conferences throughout my PhD which have been thoroughly enjoyable and really enriched the PhD experience. Thank you also to the ICB and the EPSRC for funding my work.

Finally, and most importantly, I would like to give the biggest thank you to my family, boyfriend and close friends for their constant support in everything that I do.

Abstract

The protein-protein interaction (PPI) between immunoglobulin E (IgE) and its high affinity receptor (FcεRI) is an important part of the allergic response. Inhibition of the IgE:FcεRI interaction is a key strategy for the development of allergy treatments. This PPI has been validated as a therapeutic target by the humanised monoclonal antibody omalizumab, which binds to IgE and prevents the formation of the IgE:FcεRI complex and has proved successful at treating allergic asthma. However, small molecule inhibitors of the IgE:FcεRI PPI that are orally available would be a more desirable form of treatment.

This thesis describes the design, synthesis and testing of two series of inhibitors of the IgE:FcεRI interaction; small molecules based on the natural product aspercyclide A and short, linear peptides based on a key binding epitope of FcεRI. It also describes the development of a high-throughput time resolved fluorescence resonance energy transfer (TR-FRET) assay to test inhibitors and subsequent x-ray crystallography and SPR experiments to further investigate the mode of action of the inhibitors.

An analogue of aspercyclide A has shown inhibition of the IgE:FcεRI interaction in the micromolar range and an improved potency compared to the natural product itself. A number of 8-residue, linear peptides have been found to inhibit the IgE:FcεRI PPI in the micromolar range when tested in the TR-FRET assay. The most potent peptide has been biotinylated and immobilised for SPR experiments with IgE and FcεRI. These SPR experiments suggest that the peptide inhibits the IgE:FcεRI interaction by binding to the high affinity receptor rather than to IgE.

Publications and presentations arising from this research

Publications

- Smith, L. D.; Leatherbarrow, R. J.; Spivey, A. C. *Future Med. Chem.*, **2013**, *5*, 1423 – 1435.
- Sejberg, J. J. P.; Smith, L. D.; Leatherbarrow, R. J.; Beavil, A. J.; Spivey, A. C. *Tet. Lett.*, **2013**, *54*, 4970 – 4972.

Oral presentations

- Imperial College London Department of Chemistry Postgraduate Symposium
Imperial College London, 1st July 2014
- Protein-Protein Interactions Network Young Researchers Symposium
Imperial College London, 7th April 2014
- RSC Chemical Biology and Bio-Organic Chemistry Postgraduate Symposium
University of Warwick, 1st April 2014
- RSC Protein and Peptide Science Group Early Stage Researcher Meeting
Durham University, 11th November 2013
- Joint Centre for Doctoral Training Multidisciplinary Conference
Prince Philip House London, 13th – 14th June 2013
- Institute of Chemical Biology MRes Conference
Imperial College London, 7th September 2011
(first prize awarded)

Poster presentations

- Institute of Chemical Biology Advisory Board Meeting
Imperial College London, 15th January 2014
- RSC Biological and Medicinal Chemistry Sector Postgraduate Symposium
University of Cambridge, 13th December 2013
- London Universities Joint Chemical Biology Colloquium
Imperial College London, 28th November 2013
- Protein-Protein Interactions Network Young Researchers Symposium
University of Leeds, 10th September 2013
- Chemistry and Biology of Peptides Meeting
University of Nottingham, 18th July 2013
- Imperial College London Graduate School Summer Research Symposium
Imperial College London, 12th July 2013
- Imperial College London Department of Chemistry Postgraduate Symposium
Imperial College London, 2nd July 2013
- RSC Protein and Peptide Science Group Early Stage Researcher Meeting
Burlington House London, 30th November 2012
- Protein-Protein Interactions Network Young Researchers Symposium
University of Leeds, 13th September 2012
- Joint Centre for Doctoral Training Life Sciences Conference
University of Warwick, 17th – 18th May 2012

Contents

Acknowledgements.....	3
Abstract.....	4
Publications and presentations arising from this research	5
List of abbreviations.....	13
List of figures.....	17
List of tables.....	19
List of schemes.....	20
Chapter 1: Introduction	21
1.1 Allergies.....	21
1.2 Treatments for allergies	22
1.2.1 Anti-histamines, bronchodilators and corticosteroids	22
1.2.2 Omalizumab	23
1.3 The IgE:FcεRI PPI.....	24
1.4 Targeting PPIs with peptides and small molecules	30
1.5 Peptide inhibitors of the IgE:FcεRI PPI	31
1.5.1 Peptides based on IgE	32
1.5.2 Peptides based on FcεRI	33
1.5.3 Peptides unrelated to IgE or FcεRI.....	36
1.5.4 Overview of peptide inhibitors of the IgE:FcεRI PPI	39
1.6 Natural product inhibitors of the IgE:FcεRI PPI.....	40
1.6.1 Aspercyclide A and analogues.....	40
1.7 Other inhibitors of the IgE:FcεRI PPI	42
1.7.1 Synthetic fluorescein dyes	42
1.7.2 Oligonucleotides	42
1.7.3 Designed ankyrin repeat proteins.....	43
1.8 Testing inhibitors of the IgE:FcεRI PPI.....	44

1.8.1	<i>In vitro</i> binding assays	45
1.8.2	Cell-based activity assays	51
1.8.3	Biophysical assays and structural techniques.....	52
1.9	Aims and objectives of PhD	55
Chapter 2: Assay development and biophysical/structural techniques.....		56
2.1	ELISA	56
2.2	Development of the TR-FRET assay.....	58
2.2.1	Choice of fluorophores	58
2.2.2	Format of the TR-FRET assay	60
2.2.3	Fluorescent labelling of proteins	61
2.2.4	Purification of IgE-Fc-A647.....	64
2.2.5	Optimisation of the assay conditions	66
2.2.6	Comparison of ELISA vs TR-FRET assay	69
2.3	Expression and purification of IgE C ϵ 2 and C ϵ 3 domains	70
2.3.1	Expression and purification of IgE C ϵ 3 domain	70
2.3.2	Expression of IgE C ϵ 2 domain	73
2.4	Development of SPR experiments with immobilised IgE-Fc and $\alpha\gamma$	73
2.4.1	Immobilisation of $\alpha\gamma$	74
2.4.2	Binding of IgE-Fc to immobilised $\alpha\gamma$	75
2.4.3	Immobilisation of biotin-IgE-Fc.....	76
2.4.4	Binding of $\alpha\gamma$ to immobilised biotin-IgE-Fc.....	76
2.4.5	Inhibition of IgE-Fc binding to immobilised $\alpha\gamma$ by free $\alpha\gamma$	76
Chapter 3: Small molecule inhibitors of the IgE:Fc ϵ RI PPI.....		77
3.1	Aspercyclide A and analogues.....	77
3.1.1	Design and synthesis of aspercyclide A and analogues.....	77
3.1.2	Testing aspercyclide A and analogues with the TR-FRET assay	78
3.1.3	Testing aspercyclide A and analogues with the ELISA	79

3.1.4	Soak crystallisation of (+)-aspercyclide A C19 methyl ether (+)-1 with IgE-Fc	82
3.1.5	Novartis data for aspercyclide A and analogues.....	84
3.2	Dibenzofurans	85
3.2.1	Design and synthesis of dibenzofurans	85
3.2.2	Testing dibenzofurans with the TR-FRET assay.....	85
3.2.3	Testing dibenzofurans with the ELISA.....	86
3.2.4	Soak crystallisation of dibenzofuran (\pm)-11 with IgE-Fc.....	90
3.2.5	SPR experiments with dibenzofuran (\pm)-11	91
3.2.6	Novartis data for dibenzofurans	92
Chapter 4: Peptide inhibitors of the IgE:Fc ϵ RI PPI		93
4.1	Design and synthesis of peptide inhibitors	93
4.1.1	Peptide design.....	93
4.1.2	Solid phase peptide synthesis	96
4.1.3	Biotin-labelled peptides	101
4.2	Testing peptide inhibitors with the ELISA	106
4.3	Testing peptide inhibitors with the TR-FRET assay	106
4.4	Testing biotin-peptide inhibitors with the TR-FRET assay	108
4.5	Testing biotin-peptide inhibitors with streptavidin in the TR-FRET assay	109
4.6	X-ray crystallography experiments.....	110
4.6.1	Co-crystallisations of peptides with IgE-Fc	110
4.6.2	Soak crystallisations of peptides with IgE-Fc	114
4.7	SPR experiments.....	115
4.7.1	SPR with immobilised proteins	115
4.7.2	SPR with immobilised biotin-peptide	115
Chapter 5: Summary and future work		121
5.1	Summary.....	121
5.1.1	Small molecules	121

5.1.2	Peptides.....	122
5.2	Future work.....	124
5.2.1	Small molecules.....	124
5.2.2	Peptides.....	124
5.2.3	Other future directions for investigating inhibitors of the IgE:FcεRI interaction.....	125
Chapter 6: Experimental.....		127
6.1	Expression and purification of IgE-Fc and αγ	127
6.2	TR-FRET assay.....	127
6.2.1	TR-FRET assay general directions.....	127
6.2.2	TR-FRET assay buffers	128
6.2.3	Labelling of IgE-Fc with Alexa Fluor 647 NHS ester	128
6.2.4	Labelling of αγ with Tb chelate isothiocyanate	128
6.2.5	Optimisation of TR-FRET assay.....	129
6.2.6	TR-FRET inhibition assay format	129
6.2.7	TR-FRET inhibition assay data analysis.....	130
6.3	ELISA	130
6.3.1	ELISA general directions.....	130
6.3.2	ELISA buffers.....	131
6.3.3	ELISA inhibition assay format.....	131
6.3.4	ELISA inhibition assay data analysis.....	132
6.4	Expression and purification of Cε2 and Cε3	132
6.4.1	Expression and purification of Cε2 and Cε3 general directions.....	132
6.4.2	Buffers and solutions for expression of Cε2 and Cε3.....	133
6.4.3	Buffers for purification of Cε2 and Cε3.....	133
6.4.4	Buffers and solutions for SDS-PAGE.....	133
6.4.5	Expression of Cε2 and Cε3	134
6.4.6	Purification of Cε3.....	135

6.5	SPR experiments.....	136
6.5.1	SPR general directions	136
6.5.2	SPR buffers	136
6.5.3	Immobilisation of $\alpha\gamma$ onto CM5 sensor chip.....	136
6.5.4	Initial binding of IgE-Fc to immobilised $\alpha\gamma$	136
6.5.5	Immobilisation of IgE-Fc onto CM5 sensor chip	137
6.5.6	Initial binding of $\alpha\gamma$ to immobilised IgE-Fc.....	137
6.5.7	Inhibition assay with dibenzofuran (\pm)-11, IgE-Fc and immobilised $\alpha\gamma$	137
6.5.8	Immobilisation of b-Phe(3)-peptide onto SA sensor chip	137
6.5.9	Initial binding of IgE-Fc to immobilised b-Phe(3)-peptide	138
6.5.10	Initial binding of $\alpha\gamma$ to immobilised b-Phe(3)-peptide.....	138
6.5.11	Binding assays of IgE-Fc, $\alpha\gamma$ and IgG ₄ to immobilised b-Phe(3)-peptide	138
6.6	Protein crystallography	139
6.6.1	Protein crystallography general directions.....	139
6.6.2	Protein crystallography buffers and solutions.....	139
6.6.3	Co-crystallisations	139
6.6.4	Soak crystallisations	140
6.7	Synthesis of aspercyclide A and analogues.....	141
6.8	Synthesis of dibenzofuran and analogues.....	142
6.9	Peptide synthesis.....	142
6.9.1	Peptide synthesis general directions	143
6.9.2	Automated SPPS.....	143
6.9.3	Cleavage from resin and side-chain deprotection of peptides.....	144
6.9.4	On-resin biotin labelling of peptides	144
6.9.5	LC-MS analysis and purification of peptides.....	145
6.9.6	LC-MS characterisation data for all pure peptides	146
6.9.7	Other peptides used in experiments	147

6.10	Novartis testing of small molecules and peptides.....	147
7	References.....	148
8	Appendices	155
8.1	Aspercyclide A and analogues – ELISA inhibition assay IC ₅₀ curves.....	155
8.2	Aspercyclide A and analogues – TR-FRET inhibition assay IC ₅₀ curves	159
8.3	Dibenzofurans – ELISA inhibition assay IC ₅₀ curves	162
8.4	Dibenzofurans – TR-FRET inhibition assay IC ₅₀ curves.....	169
8.5	LC-MS chromatograms and mass spectra of pure peptides	171
8.6	Peptides - ELISA inhibition assay IC ₅₀ curves.....	181
8.7	Peptides - TR-FRET inhibition assay IC ₅₀ curves	182
8.8	Biotin-peptides – TR-FRET inhibition assay IC ₅₀ curves.....	191
8.9	Biotin-peptides and streptavidin – TR-FRET inhibition assay IC ₅₀ curves	195

List of abbreviations

$\alpha\gamma$ – Fc ϵ R1 α -IgG₄-Fc (Fc ϵ R1 α fused to C γ 2 – C γ 3 domains of IgG₄)

$\alpha\gamma$ -Tb – $\alpha\gamma$ conjugated to Tb chelate donor fluorophore

Ala – alanine

APS – ammonium persulfate

Arg – arginine

Asn – asparagine

Asp – aspartic acid

Bip – biphenylalanine

Boc – *tert*-butyloxycarbonyl

BSA – bovine serum albumin

CD – circular dichroism

CM – carboxymethylated dextran matrix

COSY – correlation spectroscopy

Cs124 – carbostyryl 124 (7-amino-4-methyl-2(1*H*)-quinoline)

CSP-HPLC – chiral stationary phase high performance liquid chromatography

Cys – cysteine

DARPin – designed ankyrin repeat protein

DIPEA – *N,N*-diisopropylethylamine

DMF – *N,N*-dimethylformamide

DMSO – dimethylsulfoxide

DNA – deoxyribose nucleic acid

DSC/F – differential scanning calorimetry/fluorimetry

DTPA – diethylenetriaminepentaacetic acid

DTT – dithiothreitol

E. coli - *Escherichia coli*

ED₅₀ – effective dose required to produce therapeutic response in 50% of cases

EDC – 1-ethyl-3-(3-dimethylaminopropyl)carbodiimide

EDTA – ethylenediaminetetraacetic acid

ee – enantiomeric excess

ELISA – enzyme-linked immunosorbent assay

Eq – equation

eq – equivalents

ESI – electrospray ionisation

Fab – antigen binding fragment of antibody

Fc – constant fragment of antibody

FcεRI – high affinity receptor of IgE

FcεRII / CD23 – low affinity receptor of IgE
(**derCD23** – soluble monomeric lectin head domain of CD23)

sFcεRIα – soluble fragment of the extracellular domains of the α-chain of FcεRI

Fmoc – fluorenylmethoxycarbonyl

FPLC – fast protein liquid chromatography

FRET – Förster/fluorescence resonance energy transfer

Gln – glutamine

Glu – glutamic acid

Gly – glycine

h – hour

HATU – 1-[bis(dimethylamino)methylene]-1*H*-1,2,3-triazolo[4,5-*b*]pyridinium 3-oxide hexafluorophosphate

HBS – HEPES buffered saline

HBTU – 2-(1*H*-benzotriazol-1-yl)-1,1,3,3-tetramethyluronium hexafluorophosphate

HCTU – 1-[bis(dimethylamino)methylene]-5-chlorobenzotriazolium 3-oxide hexafluorophosphate

HEPES – 4-(2-hydroxyethyl)-1-piperazineethanesulfonic acid

His – histidine

HPLC – high performance liquid chromatography

HRP – horseradish peroxidase

HSQC – heteronuclear single quantum correlation (spectroscopy)

HTRF – homogenous time-resolved FRET

HTS – high throughput screening

IC – Imperial College London

IC₅₀ – inhibitor concentration required to inhibit activity by 50%

IgE – immunoglobulin E

IgE-Fc – constant fragment of IgE consisting of Cε2 – Cε4 domain pairs

IgE-Fc₃₋₄ – subfragment of IgE-Fc consisting of Cε3 – Cε4 domain pairs

IgE-Fc-A647 – IgE-Fc conjugated to Alexa Fluor 647 acceptor fluorophore

Ile – isoleucine

IPTG – isopropyl β -D-1-thiogalactopyranoside
ITC – isothermal titration calorimetry
K_a – association constant
KCL – King’s College London
K_d – dissociation constant
k_{off} – dissociation rate (off-rate)
LC-MS – liquid chromatography mass spectrometry
Leu – leucine
LRET – lanthanide resonance energy transfer
Lys – lysine
MCD – mast cell degranulating (peptide)
Met – methionine
min – minute
MS – mass spectrometry
MW – molecular weight
NHS – *N*-hydroxysuccinimide
NMM – 4-methylmorpholine
NMP – 1-methyl-2-pyrrolidinone
NMR – nuclear magnetic resonance
NOESY – nuclear Overhauser effect spectroscopy
OD – optical density
OPD – *ortho*-phenylenediamine
PBS – phosphate buffered saline
PBS-T – phosphate buffered saline with 0.1% v/v Tween[®] 20
PDB – Protein Data Bank
PEG – polyethylene glycol
Phe – phenylalanine
PMSF – phenylmethylsulfonyl fluoride
PPI – protein-protein interaction
ppm – parts per million
Pro – proline
PyBOP – (benzotriazol-1-yloxy)tripyrrolidinophosphonium hexafluorophosphate
RBL – rat basophilic leukaemia (cell line)

ROESY – rotating frame nuclear Overhauser effect spectroscopy
rpm – revolutions per minute
Rt – retention time
rt – room temperature
s - second
SAR – structure activity relationship
S/B – signal to background ratio
SDS-PAGE – sodium dodecyl sulfate polyacrylamide gel electrophoresis
SEC – size exclusion chromatography
Ser – serine
SMILES – simplified molecular-input line-entry system
S/N – signal to noise ratio
SOC medium – super optimal broth with catabolite repression medium
SPPS – solid phase peptide synthesis
SPR – surface plasmon resonance
STD – saturation transfer difference (NMR)
TBE – tris/boric acid/EDTA
TBME – *tert*-butylmethylether
TBTU – *N,N,N',N'*-tetramethyl-*O*-(benzotriazol-1-yl)uronium tetrafluoroborate
TFA – trifluoroacetic acid
Thr – threonine
TIS – triisopropylsilane
T_m – melting temperature
TMEDA – tetramethylethylenediamine
TOCSY – total correlation spectroscopy
TOF – time of flight
TR-FRET – time resolved fluorescence resonance energy transfer
Tris – tris(hydroxymethyl)aminomethane
Trp – tryptophan
TTHA - triethylenetetraamine-*N,N,N',N'',N''',N''''*-hexaacetic acid
Tyr – tyrosine
UV – ultraviolet
Val – valine

List of figures

Figure 1: Structures of antihistamines diphenhydramine (Benadryl) and loratadine (Claritin)	23
Figure 2: Schematic representation of the structures of antibodies IgE and IgG	24
Figure 3: Crystal structure of IgE-Fc showing the asymmetric conformation	25
Figure 4: Crystal structure of interaction between IgE-Fc ₃₋₄ and sFcεRIα showing key binding sites	26
Figure 5: Crystal structure of interaction between IgE-Fc ₃₋₄ and derCD23.....	28
Figure 6: Crystal structure of IgE-Fc bound to αεFab and trapped in extended conformation.....	29
Figure 7: AB loop peptide and 2,2'-tolan peptide inhibitors based on IgE Cε3 domain.....	32
Figure 8: Cyclo(L-262) peptide and cyclo(rD-262) peptide inhibitors based on C-C' loop of FcεRI...	33
Figure 9: Ro25-7162 peptide and Ro25-9960 peptide inhibitors based on C-strand of FcεRI	34
Figure 10: IgE-Trap peptide and PepE peptide inhibitors based on C'-E loop and B-C loop of FcεRI	35
Figure 11: β-hairpin peptide and ζ-peptide inhibitors identified using phage display.....	36
Figure 12: Co-crystal structure of ζ-peptide bound to binding site 2 of FcεRI	37
Figure 13: D-PAM peptide inhibitor developed from affinity purification of antibodies.....	38
Figure 14: Val(6)Ala(12)MCD peptide inhibitor optimised from bee venom peptide.....	39
Figure 15: Structures of Aspercyclides A, B and C	40
Figure 16: Structures of synthetic fluorescein dyes Rose Bengal and Ethyl Eosin	42
Figure 17: Schematic of data variability bands and separation band for a HTS assay	44
Figure 18: Overlap of the emission and excitation spectra of a donor and acceptor fluorophore...	47
Figure 19: Improvement in FRET signal due to time delay	50
Figure 20: Structures of Tb chelate donor fluorophore and Alexa Fluor 647 acceptor fluorophore	58
Figure 21: Emission spectrum for Tb chelate donor fluorophore	59
Figure 22: Excitation and emission spectra for Alexa Fluor 647 acceptor fluorophore	60
Figure 23: Size exclusion chromatogram of αγ-Tb.....	63
Figure 24: Size exclusion chromatogram of IgE-Fc-A647	65
Figure 25: Preparative size exclusion chromatogram of IgE-Fc-A647 and IgE-Fc.....	66
Figure 26: TR-FRET binding curves for IgE-Fc-A647 and αγ-Tb.....	67
Figure 27: TR-FRET inhibition curves for unlabelled IgE-Fc	68
Figure 28: TR-FRET inhibition curves for unlabelled αγ	68
Figure 29: Elution trace from Ni ²⁺ affinity column for first purification of IgE-Fc Cε3 domain	71
Figure 30: Elution trace from gel filtration column for second purification of IgE-Fc Cε3 domain...	71
Figure 31: SDS-PAGE gel showing IgE-Fc Cε3 domain.....	72
Figure 32: ¹ H NMR spectrum of IgE Cε3 domain	72

Figure 33: Crystal photo and x-ray diffraction - soak crystallisation of (+)-1 with IgE-Fc.....	82
Figure 34: Crystal photo and x-ray diffraction for soak crystallisation of (±)-11 with IgE-Fc	90
Figure 35: SPR sensorgrams for inhibition assay of IgE-Fc and immobilised $\alpha\gamma$ with (±)-11	92
Figure 36: Structure of linear, 8-mer peptide based on C-strand of C-C' loop of Fc ϵ RI	93
Figure 37: Structures of peptides.....	95
Figure 38: LC-MS UV trace (A) and ES- mass spectrum (B) for pure Bip(3)-peptide	100
Figure 39: Structures of biotin-labelled peptides and linker-peptide	102
Figure 40: Analytical LC-MS UV traces for crude and pure b-Phe(3)-peptide	104
Figure 41: Analytical LC-MS UV traces for crude and pure b-link-Phe(3)-peptide	105
Figure 42: TR-FRET inhibition assay curves for Bip(3)-peptide.....	107
Figure 43: Crystal photos and x-ray diffractions - first co-crystallisations of peptides and IgE-Fc..	111
Figure 44: Crystal photos - second co-crystallisations of peptides and IgE-Fc.....	113
Figure 45: SPR sensorgrams and Langmuir isotherm - IgE-Fc binding to immobilised b-Phe(3)-peptide	118
Figure 46: SPR sensorgrams and Langmuir isotherm - IgG ₄ binding to immobilised b-Phe(3)-peptide	119
Figure 47: SPR sensorgrams and Langmuir isotherm - $\alpha\gamma$ binding to immobilised b-Phe(3)-peptide	120
Figure 48: Structures of (+)aspercyclyde A and its benzoxathiazine-2,2-dioxide derivative	122
Figure 49: Structures of the most active peptides Phe(3)-peptide and Bip(3)-peptide.....	123

List of tables

Table 1: Peptide inhibitors of the IgE:FcεRI PPI in order of potency	40
Table 2: Categorisation of assay quality by Z-factor	45
Table 3: Comparison of advantages and disadvantages of ELISA vs TR-FRET assay.....	69
Table 4: TR-FRET inhibition assay IC ₅₀ values for aspercyclide A and analogues	78
Table 5: ELISA inhibition assay IC ₅₀ values for aspercyclide A and analogues.....	80
Table 6: Data collection statistics for soak crystallisation of (+)-1 with IgE-Fc.....	83
Table 7: TR-FRET inhibition assay IC ₅₀ values for dibenzofurans (±)-11 and (±)-12.....	86
Table 8: ELISA inhibition assay IC ₅₀ values for dibenzofurans (±)-11 and (±)-12	87
Table 9: ELISA inhibition assay IC ₅₀ values for dibenzofuran analogues of (±)-11.....	88
Table 10: ELISA inhibition assay IC ₅₀ values for dibenzofuran (±)-23 and ligand 8.....	89
Table 11: Data collection for soak crystallisation of (±)-11 with IgE-Fc.....	91
Table 12: Peptides investigated	94
Table 13: Biotin-labelled peptides and linker-peptide synthesised	101
Table 14: ELISA inhibition assay IC ₅₀ values for peptides	106
Table 15: TR-FRET inhibition assay IC ₅₀ values for peptides	107
Table 16: TR-FRET inhibition assay IC ₅₀ values for biotin-peptides	109
Table 17: TR-FRET inhibition assay IC ₅₀ values for biotin-peptides at lower concentrations.....	109
Table 18: TR-FRET inhibition assay IC ₅₀ values for biotin-peptides with streptavidin.....	110
Table 19: Data collection statistics - first co-crystallisations of peptides and IgE-Fc	112
Table 20: Data collection statistics - second co-crystallisations of peptides and IgE-Fc	113
Table 21: Data collection statistics - soak crystallisation of IgE-Fc and Trp(3)-peptide	114
Table 22: Aspercyclide A and analogues used in experiments	141
Table 23: Dibenzofurans and analogues used in experiments	142
Table 24: LC-MS characterisation data for all pure peptides synthesised during PhD	146
Table 25: Other peptides used in experiments.....	147

List of schemes

Scheme 1: Overview of the allergic response.....	22
Scheme 2: Overview of a general ELISA for measuring a PPI	46
Scheme 3: Overview of a general FRET assay for measuring a PPI	48
Scheme 4: Overview of ELISA inhibition assay	57
Scheme 5: Oxidation of OPD by the enzyme HRP	57
Scheme 6: Overview of TR-FRET inhibition assay	61
Scheme 7: Mechanism for labelling of a lysine residue of $\alpha\gamma$ with Tb chelate isothiocyanate.....	62
Scheme 8: Mechanism for labelling of a lysine residue of IgE-Fc with Alexa Fluor 647 NHS ester...	64
Scheme 9: Overview of SPR experiments with immobilised proteins.....	74
Scheme 10: Activation of carboxyl groups of SPR sensor chip surface with EDC and NHS.....	75
Scheme 11: Dennison's Heck-Mizoroki reaction of bromide intermediates.....	85
Scheme 12: Overview of Fmoc SPPS of Phe(3)-peptide using TentaGel S rink amide resin	97
Scheme 13: Mechanism for deprotection of an Fmoc group from the N-terminus of a peptide	98
Scheme 14: Mechanism for coupling of an Fmoc-amino acid to the N-terminus of a peptide	99
Scheme 15: Overview of biotinylation of the N-terminus of a resin-bound peptide.....	103
Scheme 16: Overview of SPR experiments with immobilised b-Phe(3)-peptide.....	116

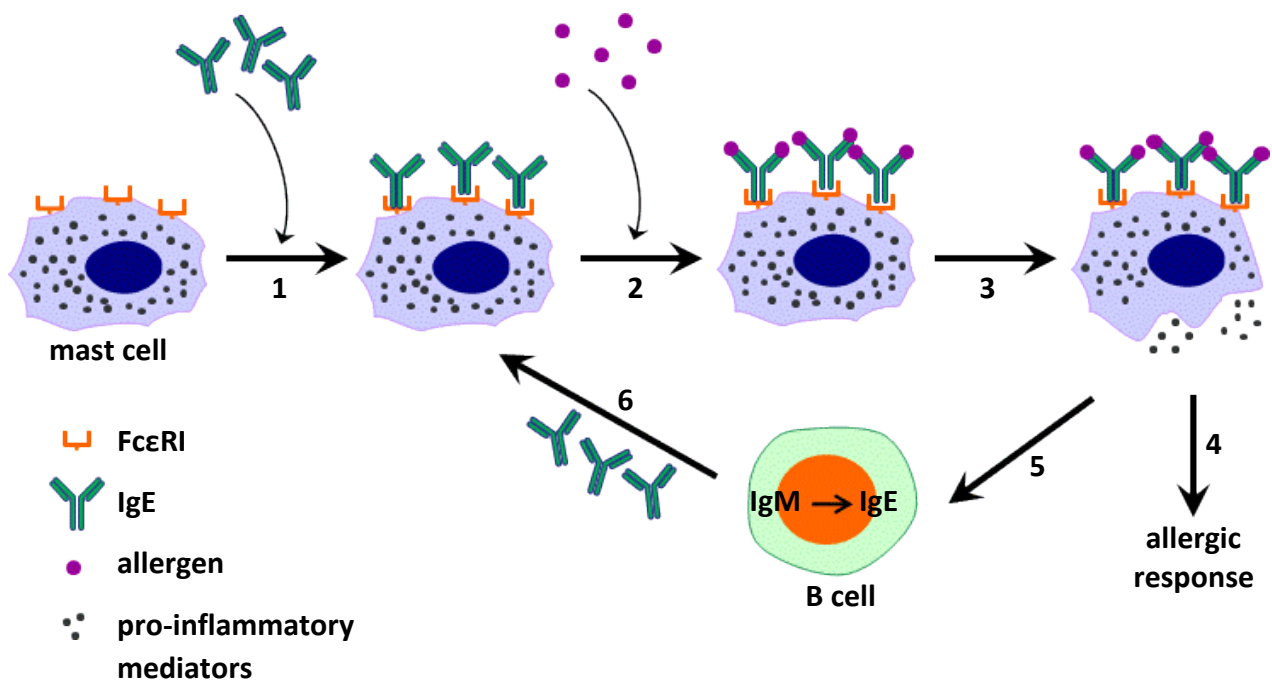
Chapter 1: Introduction

1.1 Allergies

Allergies are becoming increasingly prevalent in developed countries with 39% of children and 30% of adults in the UK suffering from the most common allergies including asthma, allergic rhinitis (hay fever) and eczema.^{1,2} Allergic reactions produce unpleasant symptoms such as running nose and eyes, itchiness and sneezing which reduce quality of life for sufferers. Severe allergies can result in serious acute conditions or potentially fatal anaphylaxis.³ Allergies also make up 6% of general practice consultations and 0.8% of hospital admissions in the UK, placing a financial burden on the NHS.¹

Allergies are mainly caused by the antibody immunoglobulin E (IgE) causing immediate or type I hypersensitivity reactions in the body. A key component of the allergic response is the protein-protein interaction (PPI) between IgE and its high affinity receptor (FcεRI).^{4,5} FcεRI is found on the surfaces of mast cells in the mucosal linings of the nose, mouth, lungs, skin and digestive tract and on the surfaces of basophils, a granulocyte white blood cell.^{4,5} In an allergy patient, increased amounts of IgE are produced which have binding specificity for a particular allergen to which the patient is sensitive. This IgE circulates within the bloodstream and then binds to FcεRI. If that particular allergen is then inhaled, ingested or contacts the skin, the allergen can bind to receptor-bound IgE, cross-linking the IgE molecules and causing the receptors to aggregate.³ This activates the mast cell and, after a series of intracellular PPIs, degranulation of the mast cell occurs where various proinflammatory mediators such as histamines and cytokines are released.⁴

These mediators then interact with their receptors in the local tissue which causes inflammation and vasodilation, resulting in symptoms characteristic of the organ affected.⁴ For instance, activation of mast cells in the mucosal lining of the respiratory tract causes asthma and results in symptoms including inflamed, swollen airways, shortness of breath and wheezing.^{5,6} This initial reaction can happen within minutes and constitutes the acute or early phase of the allergic response.⁴ The late phase of the allergic response, which occurs a few hours later, involves CD40-ligand and interleukins which are expressed by mast cells during degranulation. These mediators interact with B-cells in the local tissue and cause the B-cells to switch from producing the IgM antibody isotype to producing IgE, which maintains mast cell sensitisation and allergic symptoms via what is known as a 'positive feedback loop' (Scheme 1).^{4,5}



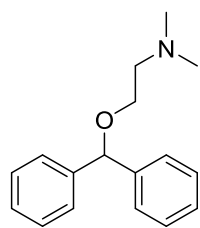
Scheme 1: Overview of the allergic response

1 = IgE binds to FcεRI on mast cell surface, 2 = allergen binds to FcεRI-bound IgE, 3 = mast cell activation and degranulation, 4 = mediators interact with local tissue causing allergic response, 5 = mediators interact with local B cells causing class-switching to IgE isotype, 6 = increased IgE synthesis causing persistent mast cell sensitisation via a positive feedback loop.

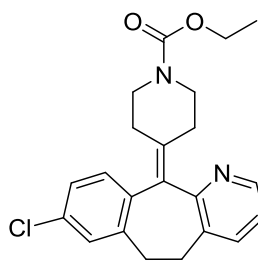
1.2 Treatments for allergies

1.2.1 Anti-histamines, bronchodilators and corticosteroids

The most common treatments for allergies are antihistamines, which benefit from being inexpensive, widely available over the counter and moderately effective at relieving symptoms of various common allergies particularly hay fever, as well as dust, pet and skin allergies.⁷ Antihistamines are small molecule antagonists of the H₁ histamine receptor, which block the effect of histamine and therefore prevent cells in the local tissue from causing inflammation and vasodilation. Examples include the first generation antihistamine diphenhydramine (trade name Benadryl)⁸ and the second generation antihistamine loratadine (trade name Claritin)⁹, the structures of which are shown in Figure 1.



Diphenhydramine



Loratadine

Figure 1: Structures of antihistamines diphenhydramine (Benadryl) and loratadine (Claritin)

The main disadvantage of antihistamines is that their lack of selectivity for the H₁ histamine receptor means they cause unpleasant side-effects, mainly drowsiness but also dizziness and nausea. Second generation antihistamines are more selective for the H₁ histamine receptor than first generation antihistamines therefore side-effects are reduced to some extent, but they can still occur in some patients.

Inhaled bronchodilators¹⁰ and corticosteroids¹¹ are also used to treat the symptoms of asthma. Bronchodilators are small molecule β 2-adrenergic receptor agonists which relax airway smooth muscle, dilate the airways and increase airflow to the lungs, making it easier to breathe. An example of a short-acting bronchodilator is salbutamol (trade name Ventolin), which provides fast, temporary relief from asthma symptoms. Corticosteroids work by reducing inflammation of the airways and lungs and can be used as a long-term treatment for asthma. However, not all asthma patients have a positive response to these types of treatments.

1.2.2 Omalizumab

The humanised monoclonal antibody omalizumab (trade name Xolair), manufactured by Novartis/Genentech, has been used effectively to treat moderate to severe allergic asthma and works by targeting the PPI between IgE and Fc ϵ RI.¹²⁻¹⁴ Omalizumab binds to free IgE, reducing levels of free IgE in the bloodstream and preventing the formation of the IgE:Fc ϵ RI PPI and subsequent mast cell degranulation. A benefit of omalizumab binding to free IgE, rather than receptor-bound IgE, is that this avoids a potential agonist effect of omalizumab where cross-linking of IgE and aggregation of receptors could occur which could lead to possible anaphylaxis.¹³

Despite clinical success, the use of omalizumab has some downsides. Due to its high molecular weight, administration is via a subcutaneous injection required every 2 – 4 weeks, which is not

suitable for patients with a high body mass index, and it is also an expensive form of treatment.¹² However, omalizumab demonstrates that the IgE:FcεRI PPI is a viable therapeutic target and that inhibiting the formation of this PPI can prevent the allergic response from occurring. All of the allergy treatments mentioned in this section have various drawbacks and there is an unmet need for improvements in allergy treatments. A selective, small molecule inhibitor of the IgE:FcεRI PPI that would be inexpensive to produce and would be orally available without causing side-effects would be a huge advance and would meet this need for improved treatments.

1.3 The IgE:FcεRI PPI

IgE is a large, globular protein and one of the five immunoglobulin isotypes found in the human body (the others are IgA, IgD, IgG and IgM).⁴ IgE is the least abundant of the immunoglobulins, with a concentration of ~ 150 ng/mL in serum, compared to ~ 10 mg/mL for IgG.⁴ IgE is a monomer consisting of two heavy chains and two light chains. The variable regions of the heavy and light chains constitute the two identical antigen binding sites and these, along with the adjacent light chain constant regions and the Cε1 domain pair, form the antigen binding fragment (Fab).⁴ The Cε2, Cε3 and Cε4 domain pairs form the constant fragment (Fc) which contains receptor binding sites. The structure of IgE is similar to that of IgG, which is the most abundant immunoglobulin and provides the majority of immunity against invading pathogens, however IgE has an extra disulfide-linked Cε2 domain pair which makes IgE less flexible than IgG (Figure 2).^{15,16}

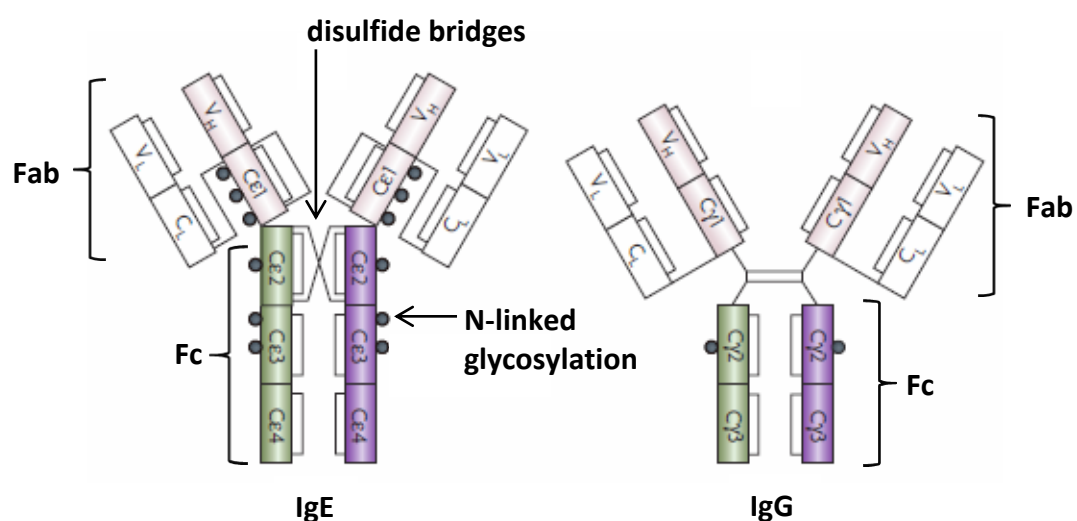


Figure 2: Schematic representation of the structures of antibodies IgE and IgG
 Image taken from reference⁵. Antigen binding fragment (Fab) and constant fragment (Fc) are labelled, along with disulfide bridges (solid lines) and sites of N-linked glycosylation (grey circles). IgE has an extra disulfide-linked domain pair and is therefore less flexible than IgG.

The two C ϵ 2 domains of IgE are linked by two crossed disulfide bridges which form between Cys(241) on the first domain and Cys(328) on the second domain and vice versa.¹⁶ The interaction between the two C ϵ 2 domains is unusual for immunoglobulin domain pairs, in that the domains associate due to polar buried surface areas, rather than the usual non-polar. The crystal structure of the Fc region of IgE (known as IgE-Fc) showed that this C ϵ 2 domain pair folds back onto the IgE-Fc region in such a way that one C ϵ 2 domain makes extensive contact with the C ϵ 3 and C ϵ 4 domain pairs but the other C ϵ 2 domain does not, meaning IgE has an overall asymmetric or bent conformation (Figure 3).¹⁶

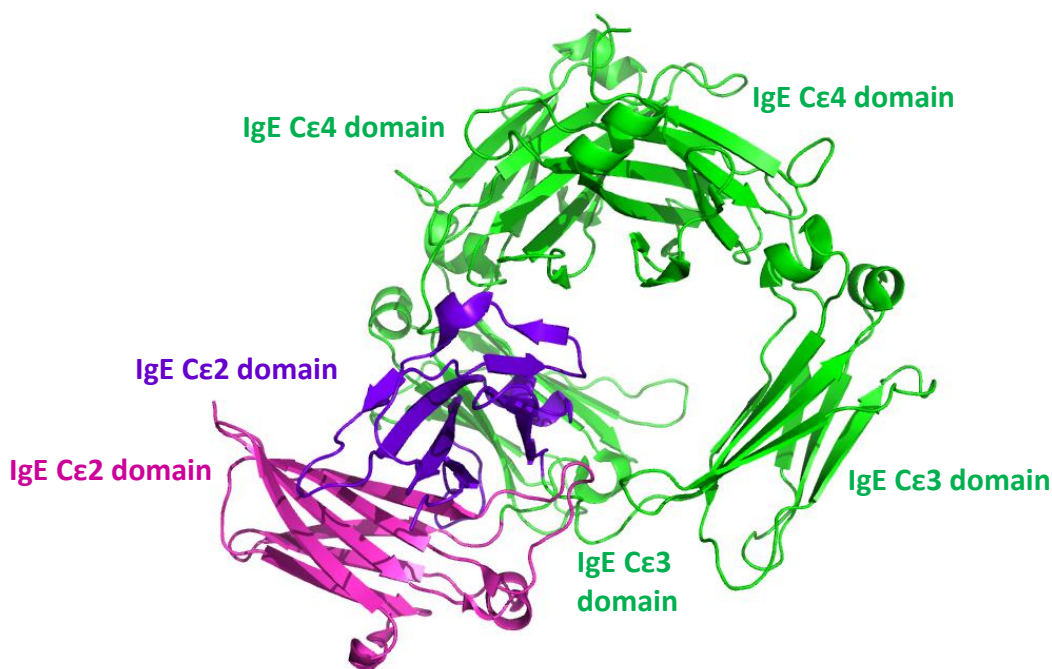


Figure 3: Crystal structure of IgE-Fc showing the asymmetric conformation

IgE-Fc C ϵ 3 and C ϵ 4 domain pairs are shown in green, one of the IgE-Fc C ϵ 2 domains is shown in pink and the other is shown in purple. IgE-Fc has an overall asymmetric conformation where the C ϵ 2 domain pair folds back onto the IgE-Fc region. Protein data bank (PDB) code 1LS0¹⁶, figure constructed using PyMOL.

IgE binds to two receptors; the high affinity receptor Fc ϵ RI, which is involved in the allergic response as discussed above, and the low affinity receptor Fc ϵ RII (also known as CD23), which is important in regulating IgE levels.⁴ The high affinity receptor Fc ϵ RI is expressed in large quantities on the surfaces of mast cells and basophils and is a heterotetramer, consisting of an α -chain, a β -chain and two γ -chains.⁴ The α -chain is a type I integral membrane protein and its extracellular domains contain binding sites for IgE. The β -chain and γ -chains are involved in cell signalling and cytoplasmic functions. In 2000, the crystal structure of a subfragment of IgE-Fc consisting of the C ϵ 3-C ϵ 4 domain pairs (known as IgE-Fc₃₋₄) bound to a soluble fragment of the extracellular domains of the α -chain of Fc ϵ RI (known as sFc ϵ RI α) was first solved.¹⁵

This crystal structure revealed that one receptor molecule binds to one dimeric IgE-Fc molecule in an asymmetric fashion through two key binding epitopes or ‘hotspots’ on FcεR1α that each interact with one of the Cε3 domains of IgE-Fc.¹⁵ Binding site 1 comprises the C-C’ loop of the D2 domain, where Tyr(131) of the C’-strand of the loop projects into a hydrophobic pocket made of the Cε3 domain and the Cε2-Cε3 linker region of IgE-Fc.^{15,17} Binding site 2 comprises four solvent-exposed tryptophan residues at the D1-D2 interface region, where Trp(87) and Trp(110) sandwich around Pro(426) of the IgE-Fc Cε3 domain (Figure 4).^{15,17}

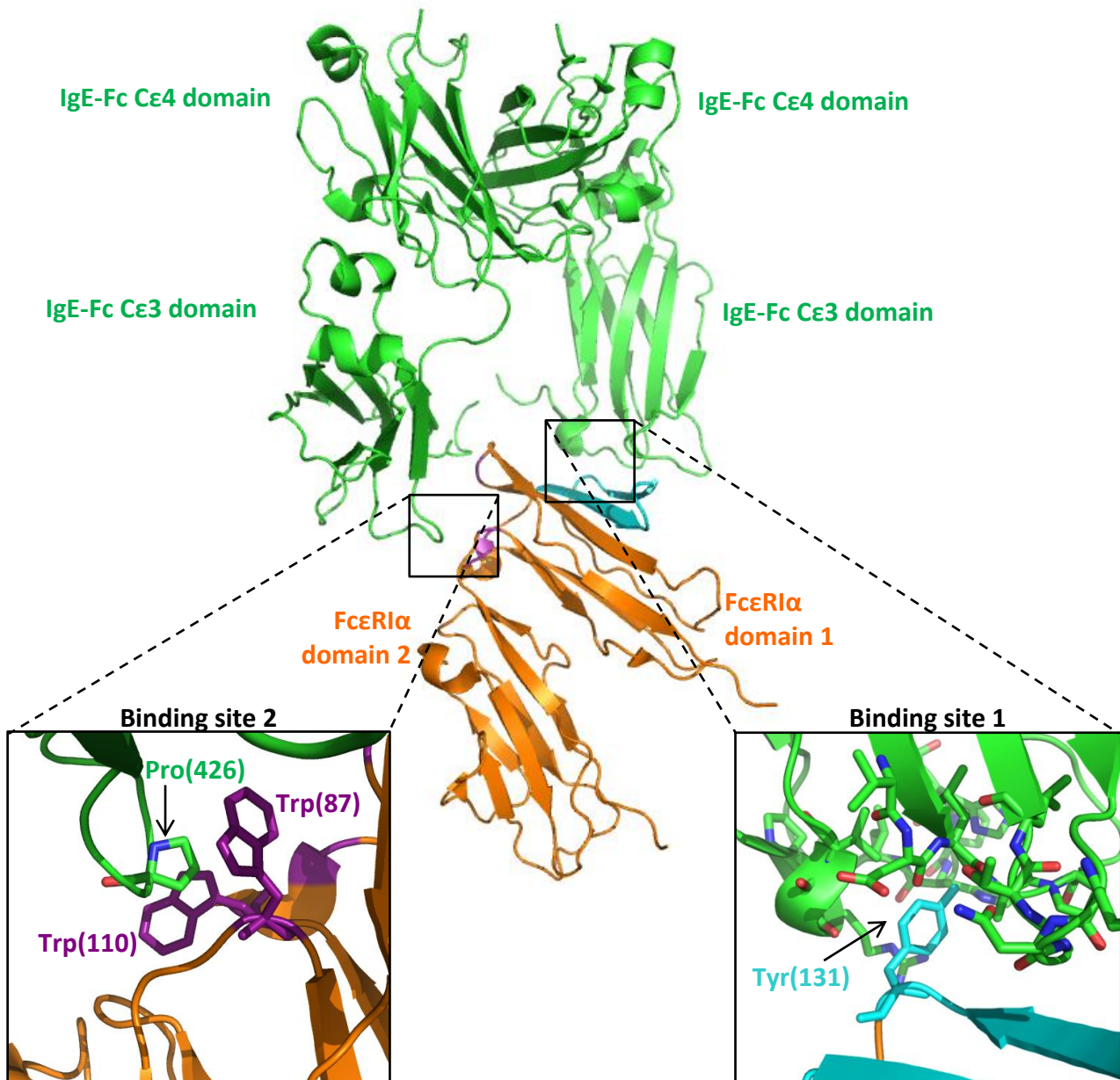


Figure 4: Crystal structure of interaction between IgE-Fc₃₋₄ and sFcεR1α showing key binding sites
 IgE-Fc₃₋₄ (a subfragment of IgE-Fc consisting of the Cε3 and Cε4 domain pairs) is shown in green and sFcεR1α (a soluble fragment of the extracellular domains of the α-chain of the high affinity receptor FcεRI) is shown in orange. Binding site 1 (the C-C’ loop of sFcεR1α) is shown in pale blue. At binding site 1, the receptor Tyr(131) projects into a hydrophobic pocket of IgE-Fc. Binding site 2 (the D1-D2 linker region of sFcεR1α) is shown in purple. At binding site 2, receptor Trp(87) and Trp(110) sandwich around Pro(426) of IgE-Fc. PDB code 1F6A¹⁵, figure constructed using PyMOL.

The binding affinity of IgE and FcεRI is very high ($K_d \sim 0.1$ nM) which is up to five times higher than the affinity of IgG binding to its receptors FcγRI, FcγRII and FcγRIII.^{4,15,16} This is mainly attributed to a low dissociation rate of the IgE:FcεRI interaction ($k_{off} = 2 \times 10^{-4} \text{ s}^{-1}$) and also due to the large number of aromatic residues of FcεRI that are occluded within the extensive buried interface of $\sim 1850 \text{ \AA}^2$.^{15,16} As revealed by surface plasmon resonance (SPR) studies on the binding kinetics of the IgE:FcεRI interaction, there are two binding phases observed.^{18,19} The interaction comprises a lower affinity phase ($K_a \sim 2.9 \times 10^7 \text{ M}^{-1}$) and a higher affinity phase ($K_a \sim 2.7 \times 10^9 \text{ M}^{-1}$) with the dissociation dominated by the higher affinity phase.¹⁹ This biphasic interaction is due to a conformational change occurring between two states of the IgE:FcεRI complex, where IgE rearranges after first engaging with FcεRI.^{20,21}

More recently, x-ray crystallography²² and fluorescence resonance energy transfer (FRET) experiments²³ have been used to show that these conformational transformations occur in both FcεRI and the IgE Cε2 and Cε3 domains for the maximum affinity interaction. After the initial formation of the IgE:FcεRI complex, the two IgE Cε3 domains move apart making IgE-Fc more bent, which allows FcεRI to interact with subsites on both of the two Cε3 domains.^{22,23} In free IgE-Fc only one of these Cε3 domain subsites is accessible to FcεRI. It has been shown that both Cε3 domains need to engage with FcεRI for maximum affinity²⁴ and that a reduction in affinity of the IgE:FcεRI interaction causes a reduction in the allergic response²⁵ both *in vitro* and *in vivo*. Whilst this conformational change is occurring in IgE, a cavity between one Cε2 domain and one Cε3 domain becomes closed. This may present an opportunity for allosteric inhibition of the IgE:FcεRI interaction; if a small molecule could fit into the cavity and prevent it from closing, the conformational changes could not occur and FcεRI would only be able to access one of the Cε3 subsites and not both.

The binding between IgE and its low affinity receptor CD23 also gives further insights into allosteric inhibition of the IgE:FcεRI interaction. CD23 is expressed on the membranes of B-cells and is structurally distinct from most other immunoglobulin receptors as it belongs to the C-type lectin superfamily.⁵ The membrane-bound form of CD23 consists of three lectin domain 'heads' projecting from the membrane on a triple α-helical coiled-coil stalk. IgE binds to CD23 with a lower affinity than it binds to FcεRI ($K_d \sim 0.1 - 1 \text{ μM}$ for binding of IgE to a single CD23 domain head and $K_d \sim 1 - 10 \text{ nM}$ for binding of IgE to the CD23 trimer due to avidity effects).⁵

It has recently been found, using x-ray crystallography and nuclear magnetic resonance (NMR) experiments that the CD23 binding sites and the FcεRI binding sites are at opposite ends of the IgE Cε3 domain, but that IgE cannot bind both receptors at once.^{26,27} The crystal structure of the IgE:CD23 interaction showed that IgE-Fc₃₋₄ binds to two molecules of the soluble monomeric lectin head domain of CD23 (known as derCD23), with each derCD23 binding at the IgE Cε3-Cε4 interface (Figure 5).²⁶

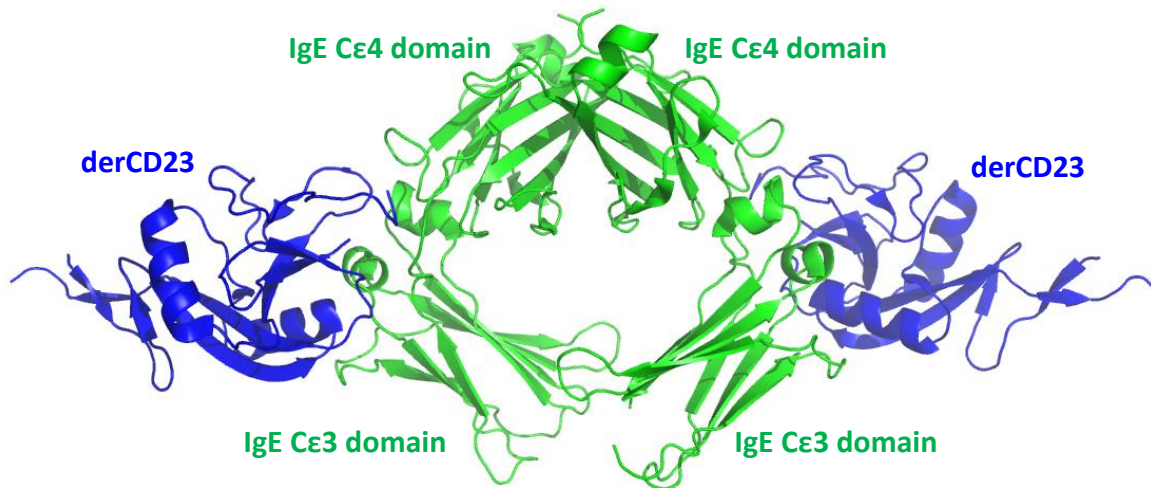


Figure 5: Crystal structure of interaction between IgE-Fc₃₋₄ and derCD23

IgE-Fc₃₋₄ is shown in green and two derCD23 fragments (a soluble fragment of the low affinity receptor CD23) are shown in dark blue. PDB code 4EZM²⁶, figure constructed using PyMOL.

The conformation changes required to bind one receptor have been proposed not to be compatible with binding the other receptor and vice versa, reflecting an allosteric mechanism. IgE Cε3 domains bind only FcεRI when they are in the 'open' conformation and bind only CD23 when they are in the 'closed' conformation. As CD23 binds to the IgE Cε3-Cε4 interface, an inhibitor that binds to IgE at this site could keep IgE in the 'closed' conformation and prevent the conformational changes required for it to move to the 'open' conformation and bind to FcεRI, suggesting that allosteric inhibition of the IgE:FcεRI interaction would be possible.^{28,29} Further x-ray crystallography studies on the interaction between IgE-Fc₃₋₄ and CD23 by Dhaliwal *et al.* revealed that calcium-dependent structural changes in CD23 increase its affinity for IgE³⁰ and found that conformational flexibility occurs in two key IgE-binding loops of CD23³¹ and in IgE-Fc₃₋₄³² to accommodate the formation of the IgE:CD23 complex. An understanding of these conformational changes may prove to be important for allosteric inhibition of the IgE:FcεRI interaction, or for targeting the IgE:CD23 interaction itself with the aim of modulating the production of IgE.

Very recent x-ray crystallography and other experiments by Drinkwater *et al.* revealed that IgE-Fc can actually adopt a fully extended, symmetrical conformation in solution.³³ This was achieved by ‘trapping’ IgE-Fc in the extended conformation, by complexing it to two IgG Fab fragments (known as aεFabs) that bound to IgE-Fc, one on each side. In this complex, the IgE Cε2 domains show the greatest structural change, ‘unbending’ so that they no longer have an extensive intramolecular interface with the Cε3-Cε4 domains (Figure 6).³³ It was found that aεFab allosterically inhibited IgE from binding to FcεRI; IgE was trapped in an extended conformation when complexed with aεFab and so binding sites 1 and 2 were both disrupted and it could not engage with FcεRI. aεFab also sterically inhibited IgE from binding to FcεRI; aεFab could compete with FcεRI for binding to free, bent IgE-Fc, since modelling of a single aεFab onto the IgE:FcεRI complex shows a clash between the aεFab and FcεRI.³³ This work gives a more complete overview of the structure and conformational changes of IgE and may provide a further avenue for inhibition of the IgE:FcεRI complex; if FcεRI-bound IgE could be encouraged to ‘unbend’ it may be able to dissociate from the receptor.

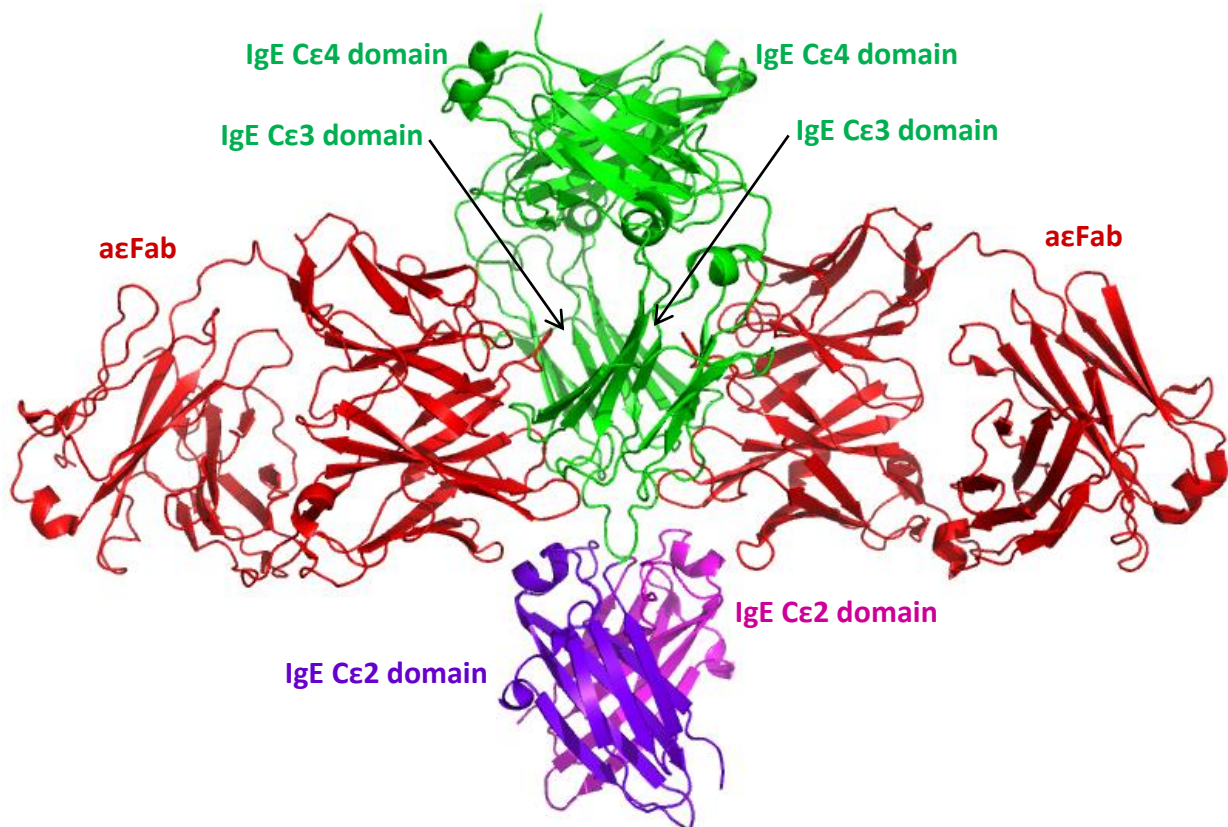


Figure 6: Crystal structure of IgE-Fc bound to aεFab and trapped in extended conformation
IgE-Fc (the Cε2 – Cε4 domains) is shown in green and the two aεFabs (IgE-binding IgG Fab fragments) are shown in red. PDB code 4J4P³³, figure constructed using PyMOL.

1.4 Targeting PPIs with peptides and small molecules

The number of PPIs is vast and they play a crucial role in almost all biological processes and are implicated in a variety of diseases. PPIs are therefore an increasingly important focus for therapeutic intervention and there have been a number of comprehensive reviews published on inhibiting PPIs.³⁴⁻³⁹ It would be attractive for a PPI to be targeted by a small, orally available 'drug-like' molecule, however due to the complex nature of interacting protein surfaces, the development of such small molecule inhibitors is very challenging.³⁶ Firstly, protein surfaces that come into contact during a PPI are usually large ($\sim 1500 - 3000 \text{ \AA}^2$) and flat, without the grooves and pockets found on protein surfaces that interact with small molecules such as enzymes and G protein-coupled receptors.³⁶ Furthermore, the key binding regions on interacting proteins are often non-contiguous which means they can be difficult to mimic with small molecules or with peptides derived from contiguous sequences.³⁶ Finally, ligands that bind to proteins do not translate well to the design of PPI inhibitors, therefore high throughput screening (HTS) of compound libraries does not always find effective small molecule 'drug-like' inhibitors of PPIs.³⁵

However, several strategies for targeting PPIs have been employed to develop effective PPI inhibitors regardless of these challenges. Systematic mutation of individual contact residues of a PPI to alanine, a technique known as alanine scanning, can identify relative contributions of individual residues to the overall binding affinity. These key epitopes or 'hotspots' usually consist of aromatic residues tryptophan and tyrosine⁴⁰, due to their hydrophobic nature and lack of rotatable bonds meaning there is only a small entropic penalty on binding, and mimicking these hotspots with synthetic molecules can modulate a PPI.³⁵ Information about key features of protein interfaces has also led to the discovery of various biological molecules that can recognise these features and modulate a PPI, including artificial antibodies, small proteins, functional oligonucleotides and unnatural biopolymers.³⁵ Small molecules have also been found to modulate PPIs, including Cu(II) complexes and tetraphenylporphyrin derivatives³⁵ and certain molecular structures such as the biphenyl moiety⁴¹ have been found to bind to a range of proteins and could be used as a 'scaffold' for drug design.

Peptides have also had widespread use for studying and inhibiting PPI binding interfaces and can be particularly effective at mimicking protein hotspots. Traditionally, peptides have not been considered desirable as drugs or drug leads due to them not conforming to the criteria of Lipinski's rule of five (MW < 500, hydrogen bond donors < 5, hydrogen bond acceptors < 10, CLogP < 5)⁴²

and therefore displaying poor oral availability and also as they are typically hydrolysed by protease enzymes. However, there are many modifications to peptides that can improve their pharmacokinetics, for instance structurally constrained, cyclic peptides may adopt particular conformations that make them less susceptible to proteolytic degradation than linear peptides.⁴³⁻⁴⁵ Furthermore, inhibitors of PPIs tend to have a higher MW (up to 800 – 900) than inhibitors of a typical enzyme-substrate interaction and many PPI inhibitors do not conform to Lipinski's rule of five.^{36,37} Unnatural amino acids can be included in a peptide to potentially improve its affinity, selectivity and metabolic stability.^{46,47} Other modified peptides, such as 'retro-inverso' peptides and β -peptides could also give improved activity and stability.³⁷ Finally, molecules that mimic a peptide's secondary structure, such as α -helix, β -sheet or β -turn peptidomimetics can be a method of developing more 'drug-like' molecules from existing peptide inhibitors.³⁷

Natural products provide a range of molecular scaffolds and are good starting points from which to prepare extensive compound libraries for high throughput screening against a PPI.³⁷ New chemical methods can also allow substituents on the core scaffold to be modified to give compounds with high molecular diversity.³⁷ In addition, the chemical structure of a natural product is usually predisposed to bind with a high affinity and specificity to a biological target. As such, natural products have been the starting point for the majority of approved therapeutics and are the main source of compounds that target PPIs.³⁷

1.5 Peptide inhibitors of the IgE:Fc ϵ RI PPI

Despite the IgE:Fc ϵ RI PPI being a challenging target for inhibition, there have been a number of inhibitors developed, including small molecules, peptides and small proteins, and these have been recently reviewed by Smith *et al.*⁴⁸ Peptides are the most widely studied type of inhibitors of the IgE:Fc ϵ RI interaction. Very early work in this area, carried out by Hamburger, used short, linear peptides to study the binding interface between IgE and Fc ϵ RI and discovered a pentapeptide based on IgE that competed with IgE for binding to mast cells in human skin.^{49,50} Other early work, by Stanworth *et al.*, also discovered linear peptides 12 – 15 residues long that could compete with IgE for binding to mast cells and studied peptides as synthetic vaccines for the treatment of allergies.⁵¹⁻⁵³ Since this work, peptides have continued to be studied and most of the inhibitors of the IgE:Fc ϵ RI interaction reported in the literature are disulfide-constrained, cyclic peptides. These peptides mimic key binding epitopes of either IgE or Fc ϵ RI or have been identified by other means such as phage display.

1.5.1 Peptides based on IgE

AB loop peptide and 2,2'-tolan peptide

Helm *et al.* studied peptides derived from IgE and found that the exposed Ω -loop and the AB β -strand of the IgE C ϵ 3 domain was a key binding hotspot for the interaction of IgE with Fc ϵ RI.⁵⁴ A disulfide-constrained, cyclic peptide mimicking this region known as the 'AB-loop peptide', containing loop residues Leu(340) – Cys(358), inhibited IgE-triggered 5-hydroxytryptamine release from a rat basophilic leukemia (RBL) cell line transfected with Fc ϵ RI ($IC_{50} \sim 12 \mu M$).⁵⁴ The aforementioned crystal structure of the IgE:Fc ϵ RI complex was then solved, which showed that these regions of the IgE C ϵ 3 domain do not make direct contact with Fc ϵ RI during the IgE:Fc ϵ RI interaction^{15,17}, which could suggest a potential allosteric mechanism of inhibition for the AB-loop peptide.

Spivey, Helm *et al.* later replaced the disulfide bridge with the more rigid 2,2'-diphenylacetylene (2,2'-tolan) bridge in an attempt to improve affinity, however this peptide had a similar activity to the original peptide.⁵⁵ Spivey *et al.* then synthesised a 9-residue, tolan-bridged peptide comprising only loop residues Pro(345) – Ser(353) known as the '2,2'-tolan peptide'.⁵⁶ However, when tested with an enzyme-linked immunosorbent assay (ELISA), this peptide was less active than the original peptide ($IC_{50} \sim 660 \mu M$).⁵⁶ Despite this loss of activity, the reduction in flexibility of the 2,2'-tolan peptide, compared to the AB loop peptide, may increase the chances of obtaining a co-crystal structure of this peptide bound to Fc ϵ RI which might allow its mode of action to be determined. The structures of the AB loop peptide and the 2,2'-tolan peptide can be seen in Figure 7.

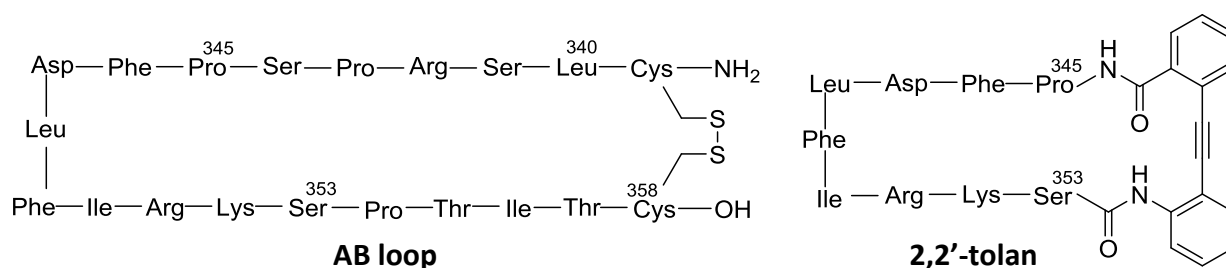


Figure 7: AB loop peptide and 2,2'-tolan peptide inhibitors based on IgE C ϵ 3 domain

Peptides were synthesised by Spivey *et al.* The AB loop peptide contains residues Leu(340) – Cys(538) of the IgE C ϵ 3 domain and inhibits the IgE:Fc ϵ RI interaction ($IC_{50} \sim 12 \mu M$).⁵⁴ The 2,2'-tolan peptide contains residues Pro(345) – Ser(353) of the IgE C ϵ 3 domain and inhibits the IgE:Fc ϵ RI interaction ($IC_{50} \sim 660 \mu M$).⁵⁶ (NB: -NH₂ denotes free N-terminus, -OH denotes free C-terminus).

1.5.2 Peptides based on FcεRI

As discussed previously, binding site 1 of FcεRI, comprising the C-C'-loop, is a key region for interaction with IgE and as such a number of peptides mimicking this region have been developed with the aim that they bind to IgE and inhibit the IgE:FcεRI interaction. It is advantageous for an inhibitor to bind to IgE, rather than to FcεRI, as binding to FcεRI could cause a possible agonist effect and mast cell degranulation.

Cyclo(L-262) peptide and cyclo(rD-262) peptide

McDonnell *et al.* designed a disulfide-constrained cyclic peptide mimicking the C-C'-loop of FcεRI known as the 'cyclo(L-262) peptide', which contained residues Ile(119) – Tyr(129) of FcεRI and was found by 2D NMR to adopt a stable β-hairpin structure in solution.^{44,57,58} This peptide was found to bind to IgE ($K_d = 2.6 \mu\text{M}$) when tested with an SPR assay and was also found to inhibit sensitisation of RBL cells with IgE when tested with a β-hexosaminidase release assay ($IC_{50} = 30 \mu\text{M}$).^{44,57} A peptide with a reversed sequence and inverted chirality known as the 'cyclo(rD-262) peptide' was also synthesised in an attempt to obtain enhanced proteolytic stability whilst keeping the 3D structure the same.^{44,57} It was found by circular dichroism (CD) spectroscopy that the cyclo(rD-262) peptide did indeed adopt a mirror image structure in solution, however the activity was slightly reduced when tested with the β-hexosaminidase release assay ($IC_{50} = 100 \mu\text{M}$).^{44,57} The structures of both peptides can be seen in Figure 8.

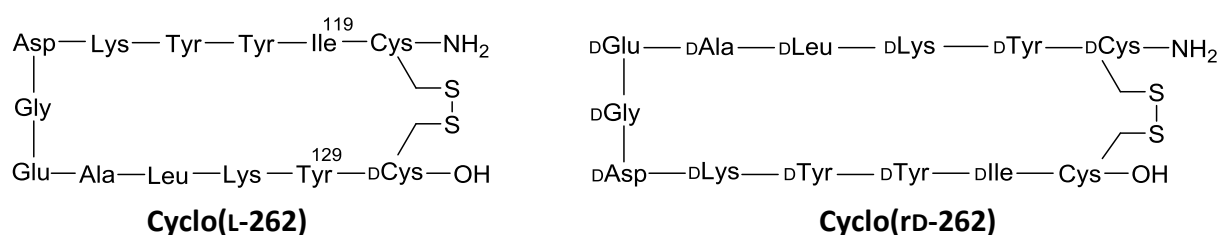


Figure 8: Cyclo(L-262) peptide and cyclo(rD-262) peptide inhibitors based on C-C' loop of FcεRI

Peptides were synthesised by McDonnell *et al.* Cyclo(L-262) peptide contains residues Ile(119) – Tyr(129) of FcεRI and inhibits the IgE:FcεRI ($IC_{50} = 30 \mu\text{M}$) and cyclo(rD-262) peptide has a reverse sequence and inverted chirality to cyclo(L-262) peptide and inhibits the IgE:FcεRI ($IC_{50} = 100 \mu\text{M}$).^{44,57} (NB: -NH₂ denotes free N-terminus, -OH denotes free C-terminus).

Ro25-7162 peptide and Ro25-9960 peptide

Danho *et al.* carried out similar work and synthesised a variety of linear and disulfide-constrained cyclic peptides mimicking the C-C' loop C-strand and the adjacent F-strand of FcεRI.⁵⁹ The most potent of these was a 21-residue, disulfide-constrained, cyclic peptide known as 'Ro25-7162 peptide' which inhibited IgE binding ($IC_{50} = 40 \mu M$) using an undisclosed binding assay, however molecular dynamics and NMR studies showed that this peptide had a flexible conformation in solution.⁵⁹ To try to stabilise the β -strand conformation, a series of dimeric peptides were then synthesised with the disulfide bridge between the middle of the two strands. The most potent of these was an 8-residue, disulfide-constrained homodimer based on the C-strand of FcεRI known as 'Ro25-9960 peptide' which inhibited IgE binding more strongly than the original cyclic peptide ($IC_{50} = 2 \mu M$).⁵⁹ The structures of both peptides can be seen in Figure 9.

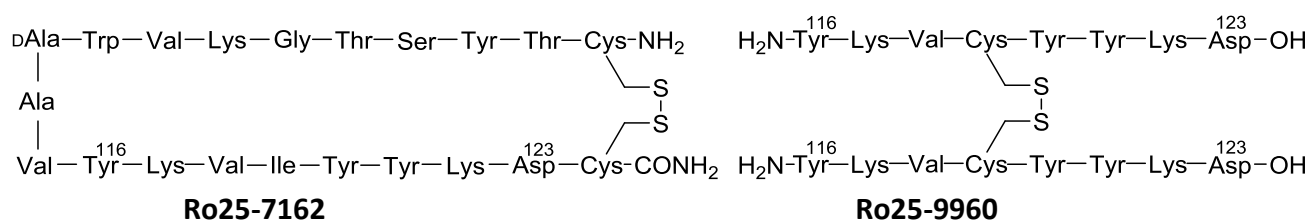


Figure 9: Ro25-7162 peptide and Ro25-9960 peptide inhibitors based on C-strand of FcεRI

Peptides were synthesised by Danho *et al.* and inhibit the IgE:FcεRI interaction (Ro25-7162 $IC_{50} = 40 \mu M$ and Ro25-9960 $IC_{50} = 2 \mu M$).⁵⁹ (NB: -NH₂ denotes free N-terminus, -CONH₂ denotes amidated C-terminus).

IgE-Trap peptide and PepE peptide

More recently, Sandomenico *et al.* used a comparable approach and synthesised a polypeptide that comprised the C'-E loop (residues 129 – 134), the B-C loop (residues 110 – 113) and the F-G loop (residues 151 – 162) of FcεRI, to reproduce both binding site 1 and binding site 2.⁶⁰ Asn(133) was mutated to Lys(133) to allow attachment between the peptide sequences and Ser(162) was mutated to Cys(162) to allow a disulfide bridge to form between it and Cys(151). This peptide, known as 'IgE-Trap peptide', inhibited the IgE:FcεRI interaction when tested with an ELISA ($IC_{50} = 70 \mu M$) and flow cytometry using RBL cells.⁶⁰

Subsequent SPR studies found that the C'-E loop and the B-C loop displayed cooperativity for binding to IgE and that the F-G loop had little contribution for binding to IgE. A further peptide was therefore synthesised consisting of only the C'-E loop and the B-C loop, known as 'PepE peptide'.⁶¹ In PepE peptide, the C'-E loop and the B-C loop were attached via an additional β -Ala residue, rather than directly attached as in the 'IgE Trap peptide', to better reflect the actual distance

between these loops in the protein. PepE peptide bound strongly to IgE when tested with an SPR binding assay ($K_d = 500 \text{ nM}$) which was approximately a 30-fold increase in affinity compared to IgE Trap peptide.⁶¹ PepE peptide was also found to inhibit the IgE:FcεRI interaction when tested with an SPR competition assay ($IC_{50} = 32 \text{ } \mu\text{M}$) which was approximately four times lower than for IgE Trap peptide, and PepE peptide was also found to inhibit the release of β -hexosaminidase from RBL cells.⁶¹ It is noteworthy that PepE peptide has a lower molecular weight than the original IgE Trap peptide, yet binding affinity has improved. The structures of both peptides can be seen in Figure 10.

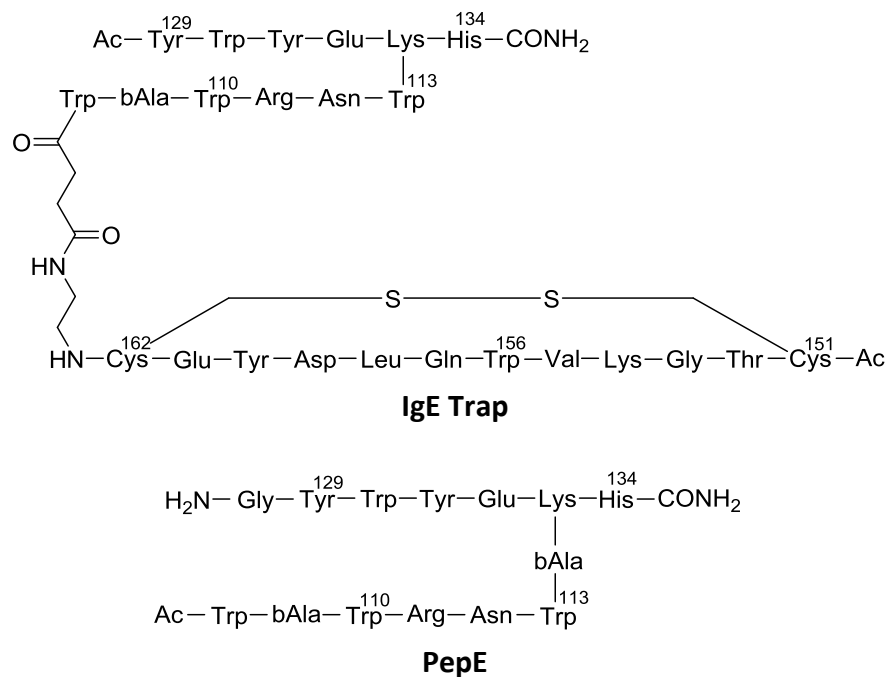


Figure 10: IgE-Trap peptide and PepE peptide inhibitors based on C'-E loop and B-C loop of FcεRI

Peptides were synthesised by Sandomenico *et al.* and inhibit the IgE:FcεRI interaction (IgE Trap $IC_{50} = 70 \text{ } \mu\text{M}$ ⁶⁰, PepE peptide $IC_{50} = 32 \text{ } \mu\text{M}$ ⁶¹). (NB: Ac denotes acetylated N-terminus, $-\text{NH}_2$ denotes free N-terminus, $-\text{CONH}_2$ denotes amidated C-terminus, bAla denotes a β -alanine residue).

PepE peptide was recently tested *in vivo* using a line of mice sensitive to IgE-mediated systemic anaphylaxis.⁶² Mice that received a single dose of PepE before sensitisation were fully protected from anaphylaxis, whereas control mice reacted strongly with core body temperature drops and increased levels of mouse mast cell protease in the serum.⁶² However, PepE that was administered after sensitisation had no effect on IgE-mediated anaphylaxis. This suggests that PepE is able to bind to IgE and prevent the formation of the IgE:FcεRI complex, but it cannot disrupt the IgE:FcεRI complex once it has formed.

1.5.3 Peptides unrelated to IgE or FcεRI

***β*-hairpin peptide and *ζ*-peptide**

There are a number of alternative methods to using protein hotspots that have been used to develop peptide inhibitors of the IgE:FcεRI interaction, such as phage display. Nakamura *et al.* at Genentech carried out binding selections using FcεRI and polyvalent peptide-phage libraries to identify novel peptides that bound to FcεRI and inhibited IgE binding.⁶³ Optimisation with monovalent phage display yielded peptides with micromolar binding affinity for FcεRI that were also able to inhibit histamine release. Analogous peptides containing a disulfide bond were then synthesised and the most potent was a 15-residue, disulfide-constrained, cyclic peptide known as 'β-hairpin peptide' due to its 3D structure in solution, as determined by 2D NMR spectroscopy.⁶³ The β-hairpin peptide was found to inhibit allergen-induced activation of RBL cells when tested with a cell-based potency assay (IC₅₀ = 1 μM).⁶³

Further optimisation using an expanded series of peptide-phage libraries gave a series of disulfide-constrained, bicyclic peptides that had a zeta 3D structure in solution and the most potent was a 21-residue peptide known as 'ζ-peptide'.⁶⁴ The ζ-peptide had an improved activity (IC₅₀ = 32 nM) and is the most potent peptide inhibitor of the IgE:FcεRI reported to date.⁶⁴ The structures of both peptides can be seen in Figure 11.

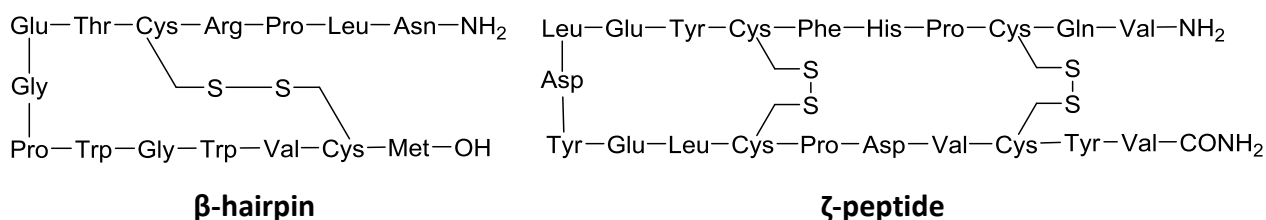


Figure 11: β-hairpin peptide and ζ-peptide inhibitors identified using phage display

Peptides were developed by Nakamura *et al.* and inhibit the IgE:FcεRI interaction (β-hairpin peptide IC₅₀ = 1 μM⁶³, ζ-peptide IC₅₀ = 32 nM⁶⁴). (NB: -NH₂ denotes free N-terminus, -OH denotes free C-terminus, -CONH₂ denotes amidated C-terminus).

Receptor mutagenesis experiments and 2D NMR spectroscopy revealed that both the β-hairpin peptide and the ζ-peptide bound competitively to binding site 2 of FcεRI, despite their different sequences, and that the key residue on both peptides was a proline.⁶⁵ Binding site 2 of FcεRI (see Figure 4) comprises residues Trp(87) and Trp(110) of FcεRI which sandwich around Pro(426) of IgE, so it would seem likely that these peptides mimic the Pro(426) of IgE and therefore compete with IgE for binding to FcεRI. X-ray crystallography experiments confirmed this and the co-crystal

structure of ζ -peptide bound to Fc ϵ RI shows that a proline residue does sit in between the tryptophans of Fc ϵ RI (Figure 12).⁶⁵ These peptides undoubtedly show high activity against the IgE:Fc ϵ RI interaction and this appears to be the only example of a co-crystal structure of a peptide inhibitor bound to either of the proteins which is significant. The only downside could be if the proline-tryptophan interaction was found at other PPI interfaces then these peptides may suffer from a lack of selectivity for the IgE:Fc ϵ RI interaction.

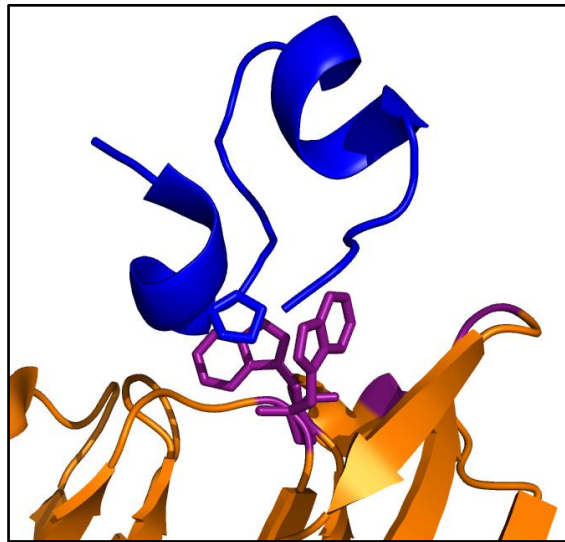


Figure 12: Co-crystal structure of ζ -peptide bound to binding site 2 of Fc ϵ RI

ζ -peptide (dark blue) synthesised by Nakamura and co-workers. Pro(16) of ζ -peptide is sandwiched between Trp(87) and Trp(110) (both purple) of Fc ϵ RI (orange). PDB code 1RPQ⁶⁵, figure constructed using PyMOL.

D-PAM peptide

The development of peptides for the purification of antibodies using affinity chromatography has also enabled researchers to discover peptides that bind to IgE. Fassina *et al.* screened synthetic, tetrameric, tripeptides for inhibition of the interaction between various immunoglobulins and protein A using an ELISA.⁶⁶⁻⁶⁸ A peptide known as protein A mimetic (PAM) peptide was selected from this screen, immobilised onto a solid support and used in affinity columns for purifying IgA, IgE, IgG, IgM and IgY.⁶⁹⁻⁷²

Verdoliva *et al.* then synthesised the inverse form of this peptide known as 'D-PAM peptide' for a more effective purification of IgG.⁷³ D-PAM peptide comprises four subunits of the tripeptide (R)Tyr-(R)(S)Thr-(R)Arg on a scaffold of a Gly and three (S)Lys residues.⁷⁴ D-PAM peptide was also studied for the treatment of the inflammatory disease systemic lupus erythematosus.^{74,75} Rossi *et al.* more recently studied D-PAM peptide as a potential allergy treatment and it was found to bind

selectively to IgE when tested using ELISA and SPR experiments, inhibit β -hexosaminidase release from RBL cells ($IC_{50} = 5 \mu M$) and suppress rat passive cutaneous anaphylaxis.⁷⁶ However, D-PAM was not found to disrupt the interaction between IgE and Fc ϵ RI which suggests it may only bind to IgE that is already bound to Fc ϵ RI. It could work by adding a broad positive charge to the Fc ϵ RI-bound IgE, causing repulsion between IgE molecules and preventing them from cross-linking and activating the cell. The structure of D-PAM peptide can be seen in Figure 13.

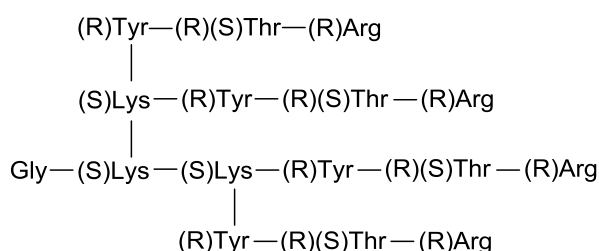


Figure 13: D-PAM peptide inhibitor developed from affinity purification of antibodies
 D-PAM peptide was synthesised by Verdoliva *et al.* and inhibits the IgE:Fc ϵ RI interaction ($IC_{50} = 5 \mu M$)⁷⁶.

Val(6)Ala(12) MCD peptide

Natural products extracted from the venom of bees, wasps and ants have the potential to be used as pharmaceuticals.⁷⁷ Buku *et al.* studied a series of biologically active peptides extracted from the venom of the European honey bee and found a disulfide-constrained, bicyclic peptide, known as mast cell degranulating (MCD) peptide.⁷⁸⁻⁸⁵ At low concentrations MCD peptide was found to have histamine-releasing activity and at high concentrations it was found to have anti-inflammatory activity and was therefore interesting for its application to inflammation and allergies.⁷⁸⁻⁸¹ Further investigation found that MCD peptide was able to bind to RBL mast cell surfaces by receptor-mediated endocytosis and prevent the binding of IgE.⁸²

MCD peptide was then prepared synthetically and this peptide also competed with IgE for binding Fc ϵ RI when tested with a fluorescence polarisation assay ($IC_{50} = 114 \mu M$).⁸² Alanine scanning on MCD peptide found that substituting Pro(12) for Ala(12) gave a more potent peptide, known as Ala(12)MCD peptide⁸²⁻⁸⁴, which bound strongly to Fc ϵ RI when tested using RBL cells transfected with fluorescent IgE ($IC_{50} = 40 nM$).⁸⁵ Ala(12)MCD peptide also displayed low histamine-releasing activity when tested using peritoneal mast cells ($ED_{50} = 212 \mu M$).⁸⁵ Further analogous peptides were synthesised and substituting Lys(6) for Val(6) gave a peptide, known as Val(6)Ala(12)MCD peptide, that still bound strongly to Fc ϵ RI ($IC_{50} = 600 nM$) and almost completely inhibited mast

cell secretion when tested using a β -hexosaminidase release assay ($ED_{50} = 6.6 \mu\text{M}$).⁸⁵ Binding affinity in the nanomolar range is noteworthy and a positive feature of this peptide inhibitor, however at 22 residues long this peptide has quite a high molecular weight therefore may have limited therapeutic potential without the use of a delivery vehicle. In addition, the fact that Val(6)Ala(12)MCD peptide binds to Fc ϵ RI, rather than IgE, could be undesirable for the reasons mentioned previously. The structure of this peptide can be seen in Figure 14.

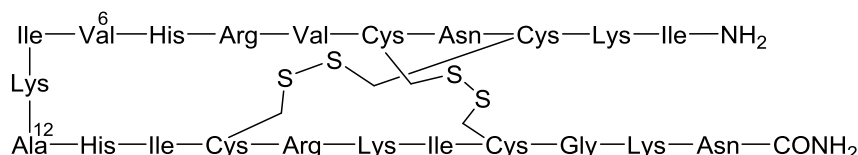


Figure 14: Val(6)Ala(12)MCD peptide inhibitor optimised from bee venom peptide

Val(6)Ala(12)MCD peptide was synthesised by Buku *et al.* and inhibits the IgE:Fc ϵ RI interaction ($IC_{50} = 600 \text{ nM}$).⁸⁵ (NB: $-\text{NH}_2$ denotes free N-terminus, $-\text{CONH}_2$ denotes amidated C-terminus).

1.5.4 Overview of peptide inhibitors of the IgE:Fc ϵ RI PPI

As described in this section, there are a variety of disulfide-constrained, cyclic peptide inhibitors of the IgE:Fc ϵ RI interaction that have been reported in the literature. These peptides are either based on functional epitopes of IgE or Fc ϵ RI or have been identified by other means such as phage display and show inhibition in the micromolar to nanomolar range. A summary of these peptide inhibitors can be seen in Table 1 and they are listed in order of potency. The peptides have molecular weights in the range of $\sim 1300 - 2500$ and Table 1 shows that in general the larger peptides are better able to inhibit the IgE:Fc ϵ RI interaction than the smaller peptides. For example, the most active peptide inhibitor, ζ -peptide, has MW 2534 and $IC_{50} = 32 \text{ nM}$ whereas the least active peptide inhibitor, 2,2'-tolan peptide, has MW 1324 and $IC_{50} = 660 \mu\text{M}$.

Name/ Synthesised by	MW	Method of development	Binding partner	IC ₅₀ / assay type
ζ-peptide Nakamura <i>et al.</i> ⁶⁴	2534	Phage display	FcεRI	32 nM activation of RBL cells
[Val6,Ala12] MCD peptide Buku <i>et al.</i> ⁸⁵	2532	Isolated from been venom	FcεRI	600 nM β-hexosaminidase release
Ro 25-9660 peptide Danho <i>et al.</i> ⁵⁹	2161	Mimics FcεRI	Unknown	2 μM undisclosed binding assay
D-PAM peptide Rossi <i>et al.</i> ⁷⁶	2141	Affinity purification	IgE	5 μM β-hexosaminidase release
Cyclo(L-262) peptide McDonnell <i>et al.</i> ⁵⁷	1567	Mimics FcεRI	IgE	30 μM β-hexosaminidase release
PepE peptide Sandomenico <i>et al.</i> ⁶¹	1994	Mimics FcεRI	IgE	32 μM SPR
2,2'-tolan peptide Spivey <i>et al.</i> ⁵⁶	1324	Mimics IgE	Unknown	660 μM ELISA

Table 1: Peptide inhibitors of the IgE:FcεRI PPI in order of potency

1.6 Natural product inhibitors of the IgE:FcεRI PPI

1.6.1 Aspercyclide A and analogues

Singh *et al.* used an IgE:FcεRI binding ELISA to screen natural product extracts of microbial origin and identified a fungal extract that displayed activity.⁸⁶ Following fractionation of the extract using a bioassay, three novel compounds were isolated; aspercyclides A, B and C and the only active compound of these was aspercyclide A which inhibited IgE binding (IC₅₀ = 200 μM) (Figure 15).⁸⁶ Despite the only moderate affinity of aspercyclide A, it has a low molecular weight of 410 so its ability to inhibit a high affinity PPI is significant and it is an interesting starting point for the design and synthesis of analogues.

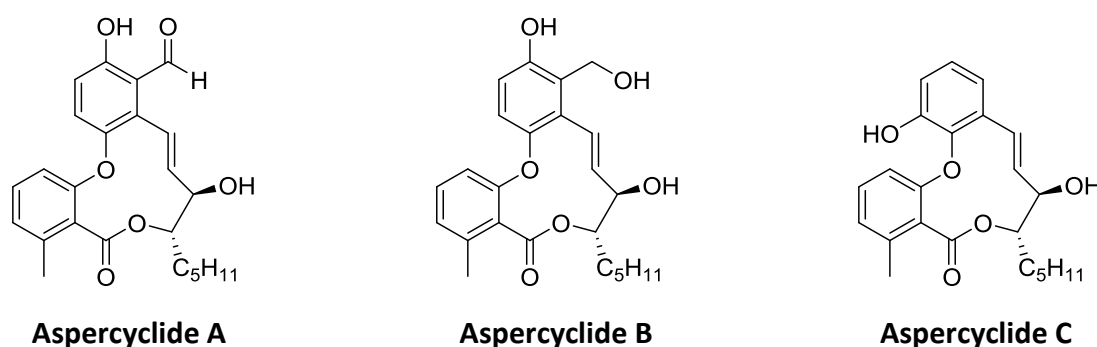


Figure 15: Structures of Aspercyclides A, B and C

Furstner *et al.* then reported the total synthesis of (+)-aspercyclide A, which employed a diastereoselective Nozaki-Hiyama-Kishi reaction as the key cyclisation step to form the core of the molecule.⁸⁷ This synthesis was completed in 14 steps, however (+)-aspercyclide A was unstable and purification resulted in decomposition, therefore this synthetic route may be of limited use for analogue synthesis. Also, since the NHK reaction installs both stereocentres at the same time, it is likely that the diastereomeric ratio would vary between analogues. Yoshino *et al.* later reported another total synthesis of (+)-aspercyclide A, which employed an intramolecular oxidative diaryl ether formation of a diphenol and phenolic oxidation to give the aryl C-O bond.⁸⁸ This synthesis was also completed in 14 steps with control of chemo-, stereo- and region-selectivity, however no biological data was reported for (+)-aspercyclide A. They also later reported a similar synthesis of the related but inactive compound (+)-aspercyclide C.⁸⁹

Spivey *et al.* reported the total synthesis of (±)-aspercyclide A and its C19 methyl ether, employing a Heck-Mizoroki reaction as they key macrocyclisation step.⁹⁰ The synthesis of (±)-aspercyclide A was completed in 8 steps and its C19 methyl ether completed in 7 steps, with one less step needed for this compound as it used a commercially available acetal as the starting material. Both compounds were tested with an ELISA and displayed similar activities to those first reported by Singh; (±)-aspercyclide A (IC₅₀ = 95 μM) and (±)-aspercyclide A C19 methyl ether (IC₅₀ = 110 μM).⁹⁰ Spivey *et al.* then reported a new synthesis of (±)-aspercyclide A C19 methyl ether, which used a Pd(0)-catalysed, fluororous-tagged, germyl-Stille reaction as they key macrocyclisation step.⁹¹ The enantiomers were separated by chiral stationary phase high-performance liquid chromatography (CSP-HPLC) and the (+)-enantiomer was 10 times more active than the (-)-enantiomer when tested using an ELISA (IC₅₀ = 40 μM for (+)-enantiomer and IC₅₀ = 483 μM for the (-)-enantiomer).⁹¹

Spivey *et al.* went on to develop the enantioselective synthesis of (+)-aspercyclide A using Krische iridium-catalysed diastereo- and enantioselective alkoxyallylation to form the key *anti*-diol intermediate, and this (+)-aspercyclide A inhibited the IgE:FcεRI interaction as before when tested with an ELISA (IC₅₀ = 5 - 200 μM).⁹² It was considered, however, that the benzaldehyde of aspercyclide A could potentially react irreversibly with amines of protein lysine residues to form Schiff bases and lead to toxicity.⁹³ In order to check that the activity of (+)-aspercyclide A was not due to such non-specific binding, an analogue containing a benzoxathiazine moiety in place of the aldehyde was synthesised and this compound also inhibited the IgE:FcεRI interaction with a similar

potency ($IC_{50} = 160 - 460 \mu M$).⁹² This work forms part of this PhD thesis and so will be discussed further in Chapter 3.

Aspercyclide A is a good starting point for the synthesis of further analogues with the aim of improving affinity, but it would be important to determine the mode of action of these compounds to facilitate the development of more potent analogues, as it is not currently known whether they bind to IgE or FcεRI.

1.7 Other inhibitors of the IgE:FcεRI PPI

1.7.1 Synthetic fluorescein dyes

The Heska Corporation reported another class of small molecule inhibitors of the IgE:FcεRI interaction, the synthetic fluorescein dyes K₂-rose bengal, Na₂-rose bengal and ethyl eosin (Figure 16).^{94,95} These dyes exhibited a range of activities when tested using functional whole-cell assays and rat passive cutaneous anaphylaxis models ($IC_{50} = 0.48 - 5.0 \text{ mM}$).^{94,95} The binding mode of these compounds is not reported, but it is thought to be non-specific binding therefore the compounds are likely to have limited potential for development for therapeutic use.

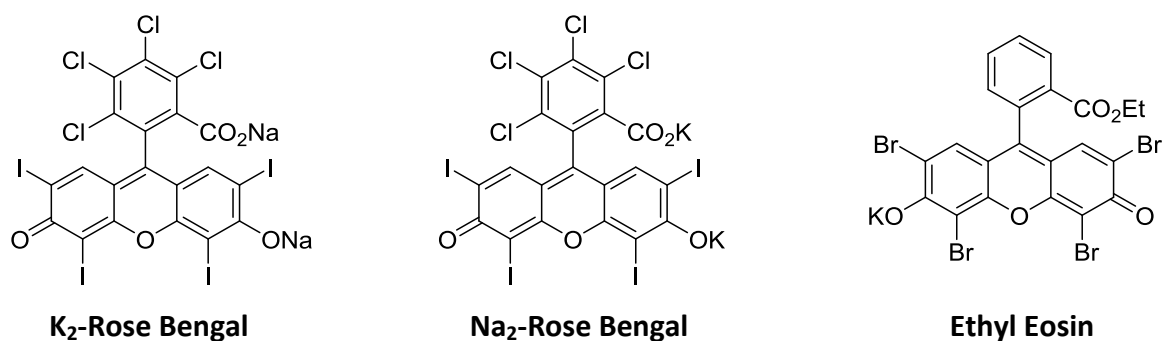


Figure 16: Structures of synthetic fluorescein dyes Rose Bengal and Ethyl Eosin

1.7.2 Oligonucleotides

Wiegand *et al.* reported various oligonucleotide inhibitors of the IgE:FcεRI interaction, discovered using a systematic enrichment of ligands by exponential enrichment method (SELEX).⁹⁶ Three libraries of oligonucleotides were found to bound to IgE with high affinity; 25-nucleotide RNA ligands ($K_d \sim 35 \text{ nM}$), 35-nucleotide RNA ligands ($K_d \sim 30 \text{ nM}$) and 37-nucleotide single-stranded DNA ligands ($K_d \sim 10 \text{ nM}$).⁹⁶ An RBL cell-based ELISA was used to test the ability of the oligonucleotides to inhibit the IgE:FcεRI interaction and it was found they bound to two distinct but overlapping sites on the IgE Cε3 domain. Oligonucleotides are reasonably large molecules (MW $\sim 7 - 20 \text{ kDa}$) so may have limited therapeutic use by oral administration.

1.7.3 Designed ankyrin repeat proteins

Eggel *et al.* reported the use of ribosome display and ELISA screening to identify a series of designed ankyrin repeat proteins (DARPin) that inhibited the IgE:FcεRI interaction.⁹⁷ Two monovalent DARPins that recognised different epitopes of FcεRI were identified from SPR experiments and these were fused together to create the bispecific DARPin known as C-A3-30/B-A4-85. This DARPin bound to FcεRI with very high affinity ($K_d = 0.067$ nM), inhibited the IgE:FcεRI interaction and prevented IgE-mediated degranulation from RBL cells transfected with FcεRI.⁹⁷ A similar method was used to identify the bivalent DARPin known as E2_79/E2_79 which bound with a high affinity to the IgE Cε3 domain ($K_d = 0.88$ nM) and inhibited the release of proinflammatory mediators from RBL cells expressing FcεRI ($IC_{50} = 0.54$ nM).⁹⁸ DARPins that bind to IgE may be a possible alternative allergy treatment to omalizumab after extensive *in vivo* studies. Eggel *et al.* then went on to describe a fusion protein known as DE53-Fc, which consisted of IgE-Fc fused to a DARPin that specifically bound to IgE, which could attach FcεRI-bound IgE to the low-affinity IgG receptor FcγRII and inhibit allergen-induced activation of basophils.⁹⁹

Kim *et al.* later reported the co-crystal structure of DARPin E2_79 bound to IgE-Fc₃₋₄, where residue 335 of IgE was mutated to Cys(335) to keep IgE-Fc₃₋₄ in the closed conformation where it cannot bind to FcεRI.¹⁰⁰ This co-crystal structure showed that DARPin E2_79 bound to the IgE Cε3 domain but did not interact with those residues involved in binding to FcεRI, which led to the suggestion that DARPin E2_79 bound to the IgE:FcεRI complex and partially overlapped with IgE residues binding to FcεRI at binding site 2. Kinetic modelling and SPR studies indicated that E2_79 bound to FcεRI-bound IgE with a 2:1 stoichiometry and was thought to cause dissociation of the IgE:FcεRI complex by competing for binding to FcεRI at site 2, partially exposing these interfaces and causing full dissociation in what was referred to as a 'facilitated dissociation' mechanism.¹⁰⁰

Eggel *et al.* then assessed the therapeutic potential of the DARPin E2_79 in comparison to omalizumab.¹⁰¹ They showed that DARPin E2_79 could remove IgE from FcεRI in a dose-dependent manner, when tested with competitive ELISA and SPR experiments. Omalizumab was also found to act in the same way as DARPin E2_79 but to a lesser extent. It was also found that DARPin E2_79 could remove IgE from primary human basophils expressing FcεRI which prevented IgE-dependent cell activation and subsequent release of proinflammatory mediators. Further studies on the pharmacokinetics of DARPins would be required, but they seem promising to be studied as a potential alternative to omalizumab for allergy treatment.

1.8 Testing inhibitors of the IgE:FcεRI PPI

To effectively test inhibitors of the IgE:FcεRI PPI, or indeed any PPI, a sensitive, reproducible and robust assay is required in order to distinguish between compounds that display a range of activities.¹⁰² In addition, if an assay is also simple, automatable, high-throughput and cost-effective it can be amenable to HTS, whereby large numbers of compounds in a library are quickly tested against a target in order to identify active compounds or 'hits' for further studies.¹⁰³ Some useful parameters for measuring the suitability or quality of an assay are signal to background ratio (S/B) and signal to noise ratio (S/N):¹⁰²

$$S/B = \frac{\text{mean signal}}{\text{mean background}} \quad (\text{Eq. 1}) \quad S/N = \frac{\text{mean signal} - \text{mean background}}{\text{standard deviation of background}} \quad (\text{Eq. 2})$$

However, the S/B and S/N are not always reliable parameters for assay quality as they do not fully take into account signal and background variability and the dynamic range of the signal. The data variability band for a given signal is defined by the mean of the signal ± 3 standard deviations, which gives a 99.73% confidence limit.¹⁰² A 'hit' would be a signal that was significantly shifted away from the mean of the general sample population. The difference between the data variability band for the sample and for the control, known as the separation band, is a useful 'window' for defining hit compounds and is also referred to as the usable dynamic range of an assay (Figure 17).

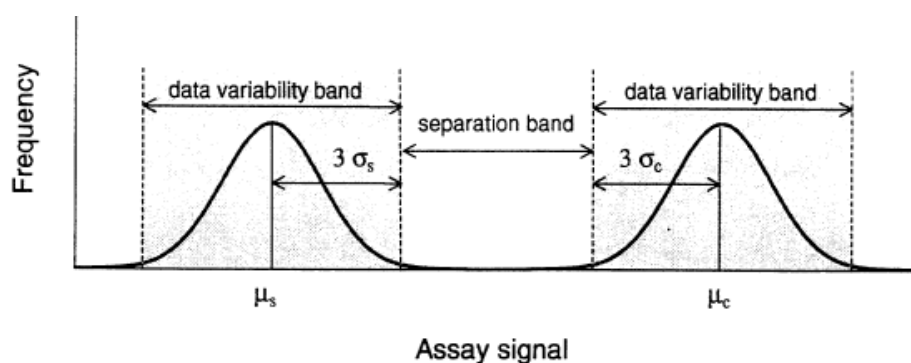


Figure 17: Schematic of data variability bands and separation band for a HTS assay

The data variability band for a signal is the mean (μ) ± 3 standard deviations (σ). The difference between the data variability band for the sample (s) and for the control (c) is known as the separation band and is a useful 'window' for defining hit compounds.

As there are various units in which this separation band can be expressed, it is useful to have a simple, dimensionless parameter to describe it and this is known as the Z-factor. The Z-factor is defined as the ratio of the separation band to the assay signal dynamic range and is preferable to S/B and S/N as it takes into account data variability and the dynamic range and it can be used to compare assays of different format since it has no dimensions:¹⁰²

$$\text{Z-factor} = 1 - \frac{(3 \times \text{standard deviation of sample}) + (3 \times \text{standard deviation of control})}{|\text{mean of sample} - \text{mean of control}|} \quad (\text{Eq. 3})$$

The Z-factor is always less than or equal to 1 and the higher the Z-factor the better the assay, since a good assay has a large signal dynamic range and a low data variability. An assay can be categorised according to its Z-factor (Table 2).

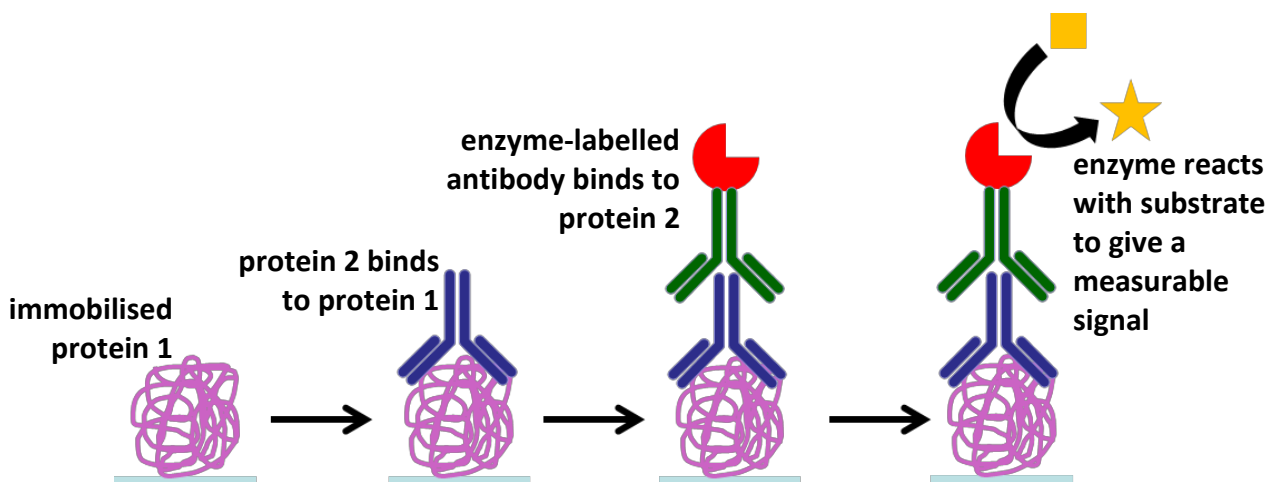
Z-factor	Assay Quality
1	Ideal
0.5 – 1	Excellent
0 – 0.5	Good
0	Poor
< 0	Screening impossible

Table 2: Categorisation of assay quality by Z-factor

1.8.1 *In vitro* binding assays

Enzyme-linked immunosorbent assay (ELISA)

Since being first described in 1971 by Engvall and Perlmann¹⁰⁴ and also by Van Weemen and Schuurs¹⁰⁵, ELISAs have had widespread use as a biochemical assay, as a diagnostic tool in medicine, in toxicology and even in the food industry.¹⁰⁶ ELISAs can be used to measure PPI binding and therefore the competition between a PPI and a small molecule inhibitor.¹⁰⁷ This is achieved by immobilising the first protein to a multi-well plate surface, blocking any unbound sites on the plate surface, then allowing the second protein to bind to the first protein. After washing off any unbound protein, the second protein is then detected by adding an enzyme-labelled antibody which binds to the second protein. The enzyme substrate is then added, which reacts with the enzyme to produce a measurable readout which is proportional to the amount of second protein bound (Scheme 2). Washing between each of these steps removes any substance not specifically bound.



Scheme 2: Overview of a general ELISA for measuring a PPI

ELISAs have the benefit of being highly adaptable. The first protein can be immobilised by passive adsorption to the plate (as in Scheme 2), by antibody capture or by using a biotinylated protein and streptavidin capture.¹⁰⁷ The second protein can be detected by directly labelling the second protein with an enzyme, by adding an enzyme-labelled antibody that binds to the second protein (as in Scheme 2) or by using a biotinylated second protein and using enzyme-labelled streptavidin. Finally, the enzyme can react with its substrate to give absorbance, fluorescence or luminescence readouts. Another benefit is that ELISAs are usually very sensitive assays as the signal is amplified as a result of using an enzyme. However, the drawbacks of ELISAs are that they require multiple steps, which can reduce throughput and can also result in false positive results due to the number of secondary reagents used.

Despite these drawbacks, ELISAs are widely used and they have been applied to test the inhibition of the 2,2'-tolan peptide⁵⁶, the IgE Trap peptide^{60,61}, the DPAM peptide⁷⁶, aspericyclide A compounds^{86,90,91}, oligonucleotides⁹⁶ and DARPins⁹⁷ against the IgE:FcεRI interaction.

Förster/Fluorescence resonance energy transfer (FRET) assay

An alternative assay to the ELISA for measuring the competition between a PPI and a small molecule inhibitor, that is potentially higher throughput, is the FRET assay.^{108,109} FRET was originally described by Förster¹¹⁰ in 1948 and has since found numerous applications in biological sciences. FRET is the process of non-radiative energy transfer between a donor fluorophore and an acceptor fluorophore, which both have specific spectral properties. This energy transfer occurs

when the emission spectrum of the donor fluorophore overlaps with the excitation spectrum of the acceptor fluorophore (Figure 18).

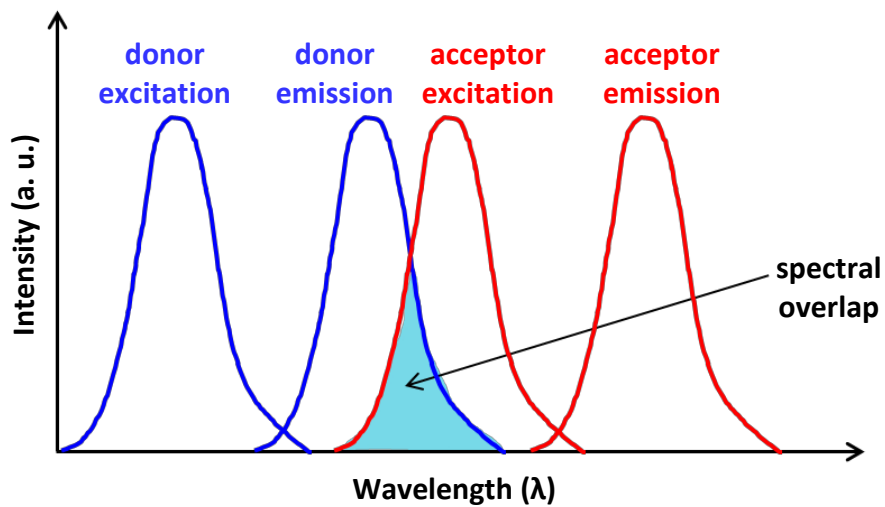
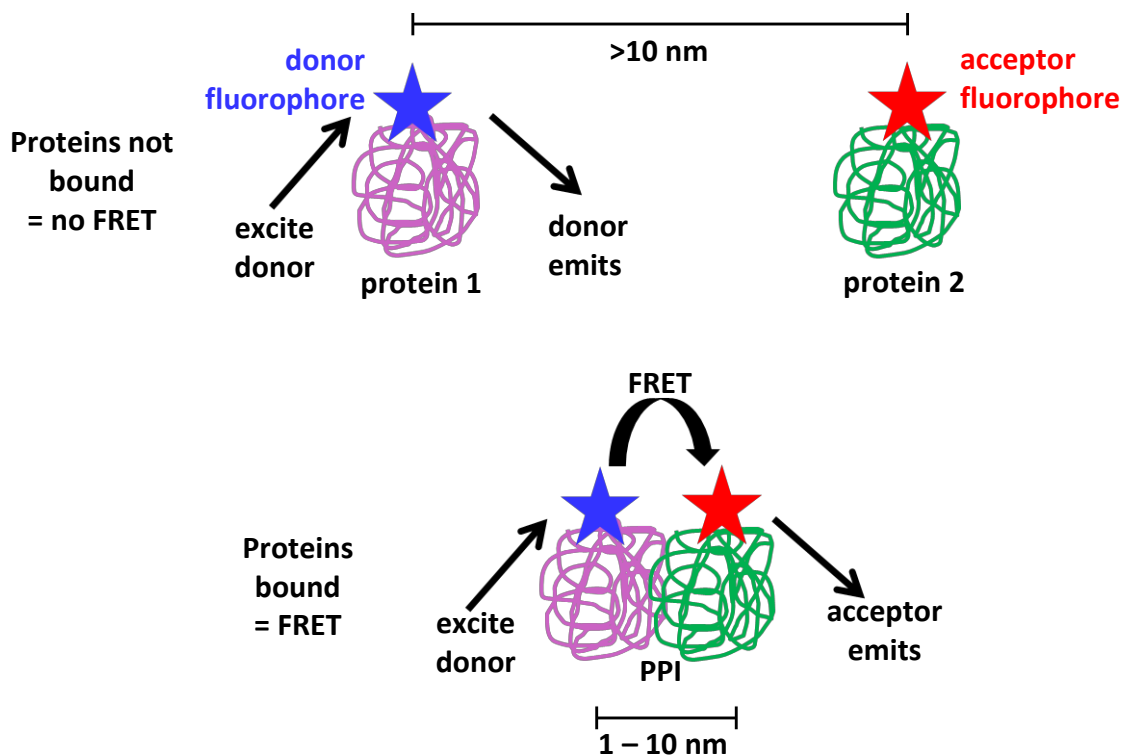


Figure 18: Overlap of the emission and excitation spectra of a donor and acceptor fluorophore

The emission spectrum of the donor fluorophore and the excitation spectrum of the acceptor fluorophore overlap, meaning FRET can occur between the two fluorophores.

When the donor fluorophore is excited, energy is transferred to the acceptor fluorophore via long-range dipole-dipole interactions, and emission from the acceptor is observed (Scheme 3). The ratio of the acceptor emission to the donor emission, following excitation, comprises the assay readout and is proportional to the amount of protein complex formed. This energy transfer only occurs when the two fluorophores are in close proximity to each other, usually within 10 nm or less, which makes it a very useful technique for measuring the interaction of two proteins as this is the distance over which many proteins interact.



Scheme 3: Overview of a general FRET assay for measuring a PPI

FRET efficiency (E_{FRET}) is measured by the following equation¹⁰⁷:

$$E_{\text{FRET}} = \frac{1}{1 + (r/R_0)^6} \quad (\text{Eq. 4})$$

where r is the distance between the fluorophores and R_0 is the Förster distance at which FRET efficiency is 50% for the specific donor/acceptor fluorophore pair. The energy transfer is inversely proportional to the sixth power of distance between the fluorophores, meaning FRET is extremely sensitive to even small changes in distance. R_0 depends on the spectral overlap of the donor emission spectrum and the acceptor excitation spectrum. A large spectral overlap means FRET can be observed over longer distances, however 10 nm is the limit for most donor/acceptor pairs.

A variety of fluorophores can be used for a FRET assay, from small molecules¹⁰⁷ such as fluorescein, tetramethylrhodamine, 5-((2-aminoethyl)amino)naphthalene-1-sulfonic acid (EDANS), 4-([4-(dimethylamino)phenyl]azo)benzoic acid (DABCYL), cyanines and Alexa Fluor compounds to biologically encoded proteins such as green fluorescent protein (GFP)¹¹¹. The main benefit to the FRET assay is that it is carried out in solution, so no immobilisation or washing steps are needed

and no secondary reagents are required to detect the amount of proteins bound. This makes the FRET assay faster and more amenable to HTS than the ELISA.

An intramolecular FRET assay has been applied to study the IgE:FcεRI interaction by Hunt *et al.*, who labelled IgE-Fc with biologically encoded proteins to measure the conformational changes on binding to FcεRI.²³ Monomeric red fluorescent protein (mRFP) was fused to the IgE-Fc Cε2 domain and enhanced green fluorescent protein (eGFP) was fused to the IgE-Fc Cε4 domain, positioning the fluorophores ~ 9 nm apart so FRET could occur. On binding of this labelled IgE to FcεRI, IgE became more bent, so the fluorophores moved closer together and the FRET signal increased.

Despite the benefits and widespread use of FRET assays, there are some drawbacks. Autofluorescence from the buffer and from the compounds being tested may affect the signal and light scattering from precipitated compounds and coloured compounds can absorb excitation and emission radiation. Another problem is that a wide acceptor excitation spectrum may cause the acceptor to be excited directly by incident light. Finally, FRET assays do require the proteins to be labelled with fluorophores, which may affect the protein function. A variation of the FRET assay known as a time-resolved FRET (TR-FRET) or a homogeneous time-resolved FRET (HTRF) has been developed which overcomes some of these challenges.

Time resolved – fluorescent resonance energy transfer (TR-FRET) assay

TR-FRET uses donor fluorophores with long emission half-lives of up to 1500 μs, most notably chelates of the lanthanides terbium³⁺ (Tb³⁺) and europium³⁺ (Eu³⁺).¹¹²⁻¹²⁰ The long lifetimes of these lanthanides means that a time delay of 50 – 150 μs can be introduced between excitation of the donor and measurement of the acceptor emission.¹¹⁴ This time delay means that any autofluorescence from the buffer or inhibitors being tested and any acceptor excitation from incident light will have decayed (these occur on the ns timescale) before the measurement of the acceptor emission (Figure 19). Another benefit of the TR-FRET assay is that the lanthanides have a slightly larger proximity limit for FRET to occur, of up to 20 nm, which means that larger biomolecular complexes could be measured.¹¹⁴ The use of these lanthanides means this technique can also be referred to as lanthanide resonance energy transfer (LRET).

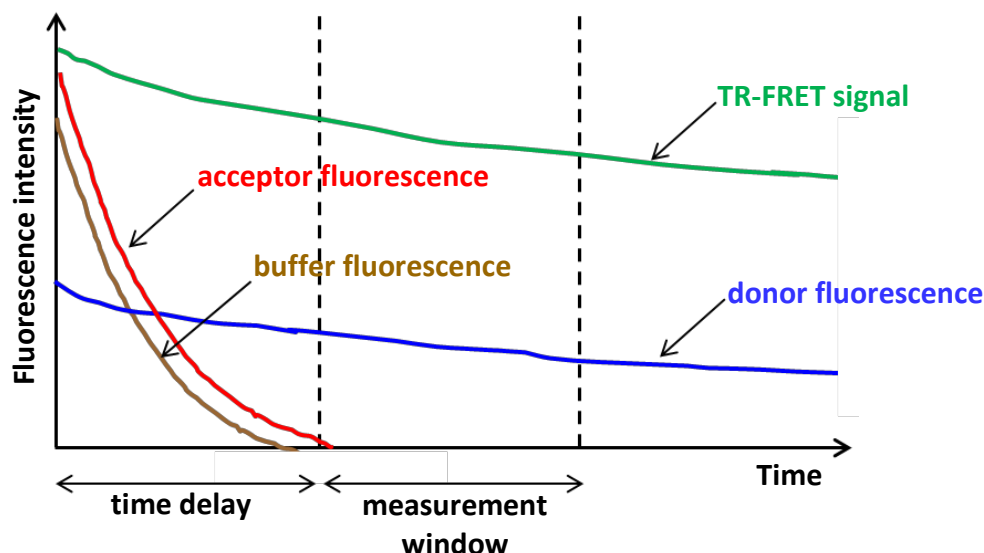


Figure 19: Improvement in FRET signal due to time delay

A time delay of 50 – 150 μs after donor excitation and before measurement means that autofluorescence from buffer or inhibitors has decayed.

Polyaminocarboxylates¹¹³ are commonly used as chelates for Tb^{3+} and Eu^{3+} , with the 8-dentate diethylenetriaminepentaacetic acid (DTPA) chelate^{115,116,119} being the most popular, but other chelates such as triethylenetetraaminehexanoic acid (TTHA)¹²¹ are also used as well. The chelate is covalently linked to a chromophore such as 7-amino-4-methyl-2(1H)-quinoline (carbostyryl 124 or cs124)^{113,115,116,119}, or a derivative of this¹²², which acts as an ‘antenna’ or sensitiser to absorb the excitation light. The chelate is also linked to an amine-reactive functional group¹¹⁵ (eg. an isothiocyanate) or a thiol-reactive functional group^{116,119} (eg. a maleimide) for attachment to a protein.

TR-FRET assays have been used to study the interactions between IgE and its receptors $\text{Fc}\epsilon\text{RI}$ and CD23. Kim *et al.* applied the technique of TR-FRET for monitoring and finding inhibitors of the IgE: $\text{Fc}\epsilon\text{RI}$ interaction, using a Tb donor fluorophore attached to an anti-His-tag antibody (known as Tb-Ab), an Alexa Fluor 488 acceptor fluorophore attached to IgE-Fc (known as A488-IgE-Fc) and His-tagged $\text{Fc}\epsilon\text{RI}\alpha$ (known as His- $\text{Fc}\epsilon\text{RI}\alpha$).¹²³ In the assay Tb-Ab bound to His- $\text{Fc}\epsilon\text{RI}\alpha$, then A488-IgE-Fc bound to His- $\text{Fc}\epsilon\text{RI}\alpha$ to form a complex and FRET occurred between Tb-Ab and A488-IgE-Fc. They tested the DARPin E2_79¹⁰⁰ as an inhibitor of the IgE: $\text{Fc}\epsilon\text{RI}$ interaction, as described in section 1.7.3, and found that it caused a concentration-dependent reduction in the FRET signal, demonstrating this TR-FRET assay was a robust method for testing inhibitors of the IgE: $\text{Fc}\epsilon\text{RI}$ interaction.

Dhaliwal *et al.*²⁶ and Borthakur *et al.*²⁷ used TR-FRET for monitoring the binding of IgE to its receptors FcεRI and CD23. IgE-Fc was labelled with the acceptor fluorophore Alexa Fluor 647 (known as A647-IgE-Fc) and each receptor was labelled with a Tb chelate donor fluorophore (known as Tb-derCD23 and Tb-sFcεRIα). TR-FRET experiments showed that unlabelled sFcεRIα could displace Tb-derCD23 from IgE and that unlabelled derCD23 could displace Tb-sFcεRIα from IgE, which confirmed that IgE cannot bind both receptors at once.²⁶

Drinkwater *et al.* recently used intramolecular TR-FRET to study the conformations of IgE-Fc and how it flexes between acutely bent and extended conformations.³³ The IgE-Fc Cε2 domain was labelled with a Tb chelate donor fluorophore and the IgE-Fc Cε4 domain was labelled with biotin and then conjugated to streptavidin labelled with the acceptor fluorophore Alexa Fluor 488. FRET occurred between the donor and acceptor fluorophores due to the acutely bent conformation of IgE which brought them into close proximity. As IgE became extended, on trapping in the extended conformation by αεFab as described in section 1.3, there was a decrease in FRET due to the fluorophores moving apart.

Fluorescence anisotropy/polarisation assay

Fluorescence anisotropy or polarisation is another fluorescence technique that is used to study the binding of proteins and a small molecule inhibitor or ligand.^{107,124,125} If a small molecule inhibitor labelled with a fluorophore is excited with polarised light, it emits light that has a degree of polarisation inversely proportional to the rate that the molecule is rotating. Since small molecules tend to rotate faster than large molecules, they will emit depolarised light. If the fluorescently-labelled small molecule then binds to a protein, it rotates much more slowly and therefore if it is excited with polarised light, it will emit light that remains polarised. The change in polarisation of emitted light can therefore be used to measure the extent of the binding of the small molecule to the protein.

1.8.2 Cell-based activity assays

Whilst the ELISA, TR-FRET and other binding assays described in section 1.8.1 can determine the ability of a compound to bind to one of the proteins and inhibit the PPI between IgE and FcεRI, it is important to also test if an inhibitor can actually prevent the subsequent downstream cellular activity as a result of the IgE:FcεRI PPI. Various cell-based assays have been used to test if inhibitors can prevent mast cell degranulation (the release of proinflammatory mediators from a

mast cell). RBL cells are most commonly used for studying allergies, as they are physiologically similar to mast cells but are a more stable cell line in tissue culture.¹²⁶ The ability of an inhibitor to inhibit passive sensitisation of RBL cells with IgE and prevent the release of the mast cell enzyme β -hexosaminidase is a technique that has been used with the cyclo(L-262) peptide^{44,57}, the PepE peptide⁶¹, the D-PAM peptide⁷⁶ and the Val(6)Ala(12)MCD peptide⁸⁵. Another mediator of mast cell degranulation is 5-hydroxytryptamine (serotonin) and the AB loop peptide was tested for its ability to inhibit IgE-triggered 5-hydroxytryptamine secretion from RBL cells transfected with Fc ϵ RI.⁵⁴ RBL cell based assays have also been used to test the β -hairpin peptide⁶³ and the DARPin C-A3-30/B-A4-85⁹⁷ inhibitors of the IgE:Fc ϵ RI interaction.

1.8.3 Biophysical assays and structural techniques

Surface Plasmon Resonance (SPR)

SPR is a useful biophysical technique that can be used to study PPIs.¹⁰⁷ SPR is a phenomenon that occurs when light is reflected off a conducting film positioned between two substances with a different refractive index. In a typical SPR experiment, the conducting film is a thin gold layer onto which the first protein is immobilised. Microfluidics are then used to inject a solution containing the second protein over the immobilised protein. Formation of the protein-protein complex causes a change in refractive index of the sample, which changes the angle/intensity of the reflected light and is a measurable signal. The first SPR instrument was developed by Biacore (now part of GE Healthcare) and so sometimes this technique can be referred to as 'Biacore', however SPR is now widely used and many other companies also market SPR instruments.

As well as measuring PPIs, SPR can also be used to measure the competitive inhibition of a PPI by an inhibitor and also the binding of an inhibitor directly to an immobilised protein. The change in signal is proportional to the change in mass on the conducting film (since proteins have near identical refractive index values). It is therefore usually easier to measure binding of a second protein to an immobilised protein (which would give a large increase in mass on the surface), rather than to measure binding of a small molecule to an immobilised protein (which would give a small increase in mass on the surface). However, many instruments are now sensitive enough to detect even these small changes in mass. SPR is a very versatile technique and can measure binding stoichiometry, reversibility and affinity through kinetic or steady-state experiments and binding can be monitored in real time.^{127,128}

SPR has been widely used to study the interactions of inhibitors of the IgE:FcεRI PPI. The binding affinity of cyclo(L-262) peptide to IgE was measured with SPR^{44,57}, IgE-Trap peptide was found to bind selectively to IgE over other immunoglobulins when tested with SPR⁶⁰, the binding affinity of PepE peptide to IgE was measured with SPR, competition experiments were also carried out to measure the inhibition of the IgE:FcεRI interaction with PepE peptide⁶¹ and D-PAM peptide was found to bind specifically and selectively to IgE using SPR experiments⁷⁶. SPR has also been used to measure how DARPins can modulate the IgE:FcεRI interaction and it was found by SPR that DARPin E2_79 bound with a 2:1 stoichiometry to IgE that was already bound to FcεRI and caused the dissociation of the IgE:FcεRI complex.¹⁰⁰

X-ray crystallography

X-ray crystallography is sometimes referred to as the 'gold standard' technique for determining how a small molecule interacts with its protein target. Obtaining a high resolution x-ray co-crystal structure of a protein with a small molecule bound, can give valuable information on exactly what contacts are made between the small molecule and the protein at the binding site and can facilitate the development of molecules that bind with a higher affinity. A co-crystal structure can be obtained either by soak crystallisation (soaking the compound into crystals of the protein) or by co-crystallisation (growing protein crystals in the presence of the compound). However, it can sometimes be challenging to obtain a co-crystal structure; if the protein does not crystallise well, if the compound binding to the protein causes changes in the protein structure that prevent crystallisation, or if the compound has poor affinity or solubility.

X-ray crystallography has been widely used to study the interaction between IgE and FcεRI (as described in section 1.3). It has also been used to obtain a co-crystal structure of the ζ-peptide bound to FcεRI⁶⁵ (Figure 12), which appears to be the only published co-crystal structure of an inhibitor of the IgE:FcεRI interaction bound to one of the proteins.

Nuclear magnetic resonance (NMR) spectroscopy

NMR spectroscopy is an alternative technique to x-ray crystallography for determining a protein structure and for carrying out experiments with proteins and small molecules.¹²⁹ Firstly, NMR experiments can measure the signal changes for a small molecule as it binds to a protein. An example of this type of experiment is saturation transfer difference (STD) NMR, where energy is transferred from the solvent or protein to the small molecule.¹³⁰ The signal changes for the small

molecule indicate which parts of the molecule are involved in binding to the protein. STD NMR is a particularly useful technique as it can be used to measure transient and weak binding inhibitors.

Alternatively, NMR experiments can measure the signal changes for a protein as it interacts with a small molecule. 2D NMR experiments with isotopically-labelled proteins are commonly used, and one example is ^{15}N - ^1H heteronuclear single-quantum correlation (HSQC) spectroscopy.^{34,107} ^{15}N - ^1H HSQC gives a signal for every hydrogen bound to a ^{15}N atom, therefore each residue in a protein will give one signal and any residues with nitrogen-containing side chains will give additional signals. If a small molecule is bound to the protein, any conformational changes in the protein can be identified due to changes in signals, which would suggest the part of the protein involved in binding. There is a vast array of other 2D NMR techniques that can also be used to study proteins. These techniques include homonuclear through-bond correlation methods such as correlation spectroscopy (COSY) and total correlation spectroscopy (TOCSY) and through-space correlation methods such as nuclear Overhauser effect spectroscopy (NOESY) and rotating frame nuclear Overhauser effect spectroscopy (ROESY).^{34,107,129}

Various 2D NMR techniques have been used to study peptide inhibitors of the IgE:Fc ϵ RI interaction. TOCSY and NOESY were used to show that cyclo(L-262) and cyclo(rD-262) peptide inhibitors adopted a stable β -hairpin structure in solution.⁵⁸ TOCSY, NOESY, COSY and ROESY were used to determine that the β -hairpin peptide and the ζ -peptide inhibitors adopted stable β -hairpin structures in solution.^{63,64}

Isothermal titration calorimetry (ITC)

ITC is a useful technique for measuring the thermodynamics of binding of a small molecule to a protein, by measuring the heat absorbed or generated by the interaction.¹⁰⁷ This allows the binding affinity, enthalpy, entropy and stoichiometry to be determined. ITC is useful as it directly measures the energy of binding meaning no labels are required and it is carried out in solution. However, for weak inhibitors the heat of binding can only be small and in general relatively large quantities of the protein partners are required to obtain useful results.

Differential scanning calorimetry (DSC) and differential scanning fluorimetry (DSF/thermal shift assay)

These techniques are based on the fact that when a small molecule binds to a protein, the resulting complex is more stable than the protein by itself, therefore the melting temperature (T_m) of the protein increases.¹⁰⁷ By measuring the increase in T_m as a compound binds to a protein, the binding affinity can be determined. DSC measures the heat absorbed by the protein as the temperature is increased. DSF measures the binding of a hydrophobic fluorophore to the protein as the temperature is increased. The fluorophore binds non-specifically to the hydrophobic parts of the protein that get exposed as the protein melts, and this binding causes an increase in fluorescence.

1.9 Aims and objectives of PhD

The long-term goal of this area of research is to identify a potent and selective small molecule inhibitor of the PPI between IgE and FcεRI which has good oral bioavailability, favourable pharmacological properties and could potentially be developed to have therapeutic use in the treatment of allergies. With this in mind, the overall aim of the PhD was to investigate inhibitors of the IgE:FcεRI interaction by designing and synthesising small molecule and peptide inhibitors and developing and using binding assays, biophysical experiments and structural techniques to test these inhibitors. The study of peptide inhibitors of the IgE:FcεRI interaction builds upon work carried out in the MRes research project and this will be discussed in Chapter 4. Specific objectives for the PhD were to:

- 1) Develop and optimise a TR-FRET assay to test inhibitors of the IgE:FcεRI interaction
- 2) Develop SPR experiments with immobilised IgE and FcεRI
- 3) Express and purify individual domains of IgE for further experiments
- 4) Test aspericyclide A and analogues as inhibitors of the IgE:FcεRI PPI in the previously developed ELISA and the new TR-FRET assay
- 5) Test dibenzofurans as inhibitors of the IgE:FcεRI PPI in the ELISA and TR-FRET assays
- 6) Synthesise additional peptide inhibitors to add to peptide library developed during MRes research project
- 7) Test all peptides in the TR-FRET assay
- 8) Carry out x-ray crystallography experiments with IgE-Fc and the most potent peptides and small molecules

Chapter 2: Assay development and biophysical/structural techniques

2.1 ELISA

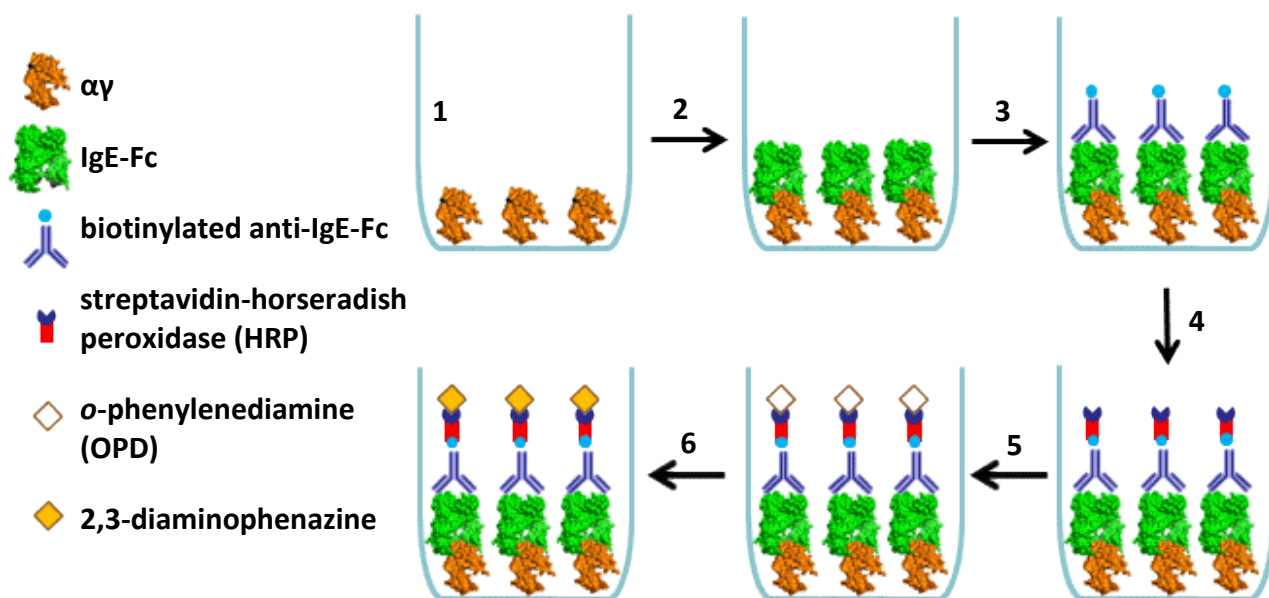
An ELISA was used to test inhibitors of the IgE:FcεRI interaction, employing the methodology developed previously as part of the MRes research project¹³¹. This ELISA methodology is described in this section and more details can be found in section 6.3.

The two proteins used for the ELISA were IgE-Fc and FcεRIα-IgG₄-Fc (the extracellular domains of the α-chain of FcεRI fused to the C_γ2 – C_γ3 domains of IgG₄), which is referred to as α_γ. These proteins were kindly provided by the MRC/Asthma UK Centre in Allergic Mechanisms of Asthma, Protein Production Facility at the Randall Division of Cell and Molecular Biophysics, King's College London (KCL). As discussed in section 1.3, IgE-Fc consists of the Cε2, Cε3 and Cε4 domain pairs which contain key sites for binding of IgE-Fc to the high affinity receptor FcεRI. The α_γ fusion protein is a substitute for sFcεRIα as it is easier to express in large quantities and considerably cheaper than sFcεRIα.

The first step of the ELISA was immobilisation of α_γ to a flat-bottom F96 MaxiSorp 96-well plate by passive adsorption of a solution of α_γ (0.02 μM) for 16 hours at 4 °C. This was followed by washing with phosphate buffered saline (PBS) with 0.1% Tween 20 surfactant (PBS-T), the Tween 20 acts as a detergent to prevent non-specific protein binding, to remove any α_γ that was not adsorbed to the plate. Bovine serum albumin (BSA) was then added to the plate for 1 hour at 37 °C to block any exposed plate surface and prevent any other substances binding non-specifically to the plate, followed by washing with PBS-T. A solution of IgE-Fc (0.033 nM), that had been pre-incubated for 1 hour at room temperature (rt) with the inhibitor, was then added to the plate and incubated at 37 °C for 1 hour, followed by washing with PBS-T. Inhibitors were prepared in 12 different concentrations, with a maximum concentration of 1 mM and 2-fold dilutions to obtain each new concentration, and a minimum concentration of 0.5 μM. A potent inhibitor should be able to prevent the IgE-Fc from binding to the immobilised α_γ on the plate and the next stage of the assay involves the detection of the amount of IgE-Fc:α_γ complex formed.

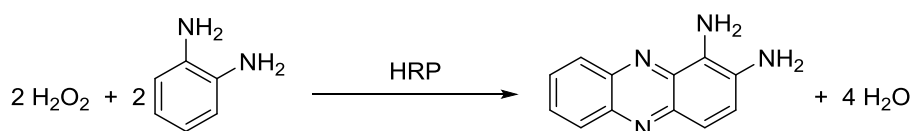
Biotinylated anti-IgE-Fc was then added for 1 hour at 37 °C, which would bind to any IgE-Fc that was bound to the immobilised α_γ, followed by washing with PBS-T. Streptavidin conjugated to the enzyme horseradish peroxidase (HRP) was then added for 1 hour at 37 °C, which would bind to

any biotinylated anti-IgE-Fc, followed by washing with PBS only. Finally, a solution of the chromogenic enzyme substrate *ortho*-phenylenediamine (OPD) was added for 4 minutes at rt in the dark, following which the enzymatic reaction was quenched with 3 M HCl. The colourless OPD was oxidised by HRP to give the orange/brown product 2,3-diaminophenazine and the absorbance at 492 nm was then measured using a Multiskan EX Microplate Photometer. The amount of absorbance was proportional to the amount of IgE-Fc bound to $\alpha\gamma$; the lower the absorbance, the less IgE-Fc: $\alpha\gamma$ complex formed and therefore the more potent the inhibitor. An overview of the ELISA can be seen in Scheme 4 and the enzymatic reaction can be seen in Scheme 5.



Scheme 4: Overview of ELISA inhibition assay

1 = immobilisation of $\alpha\gamma$ onto the 96-well plate, 2 = addition of IgE-Fc which bound to immobilised $\alpha\gamma$, 3 = addition of biotinylated anti-IgE-Fc antibody which bound to IgE-Fc, 4 = addition of streptavidin conjugated to the enzyme HRP which bound to biotinylated anti-IgE-Fc, 5 = addition of the enzyme substrate OPD, 6 = oxidation of OPD by the enzyme HRP to generate the coloured product 2,3-diaminophenazine. Between each addition step extensive washing was carried out to remove any substance not specifically bound.



Scheme 5: Oxidation of OPD by the enzyme HRP

Oxidation of the chromogenic substance OPD by HRP with H_2O_2 formed the soluble, orange-brown product 2,3-diaminophenazine in the final stage of the ELISA inhibition assay. The oxidation reaction was quenched with 3M HCl after 4 min then the plate was read spectrophotometrically at 492 nm. The amount of signal was proportional to the amount of IgE-Fc bound to immobilised $\alpha\gamma$.

2.2 Development of the TR-FRET assay

Even though the ELISA described in section 2.1 has been used for testing inhibitors of the IgE:FcεRI, it does have some drawbacks, mainly that the multiple processing steps and extensive washing required between each step can reduce assay throughput. One main aim of this PhD was therefore to develop and optimise a simple and robust TR-FRET assay for testing inhibitors of the IgE:FcεRI, which would potentially be higher throughput than the ELISA.

The two proteins used for the TR-FRET assay were IgE-Fc and $\alpha\gamma$ as described in section 2.1. It was planned to label one protein with a long lifetime donor fluorophore and one protein with an acceptor fluorophore. On binding of IgE-Fc to $\alpha\gamma$, the fluorophores would be in close enough proximity that FRET would occur between them. If a compound that inhibited the formation of the IgE-Fc: $\alpha\gamma$ complex was also present, then the amount of FRET would decrease. The inhibitor would be added in increasing concentrations, allowing a dose-response curve to be plotted and therefore IC_{50} values be calculated to allow a comparison between the inhibitors. The IC_{50} value is defined as the concentration of inhibitor required to reduce the response by 50%.

2.2.1 Choice of fluorophores

As discussed in section 1.8.1, TR-FRET requires a long lifetime donor fluorophore (usually a lanthanide chelate) and an acceptor fluorophore, where the donor emission spectrum overlaps with the acceptor excitation spectrum. A Tb chelate was chosen as the donor fluorophore and Alexa Fluor 647 was chosen as the acceptor fluorophore (Figure 20).

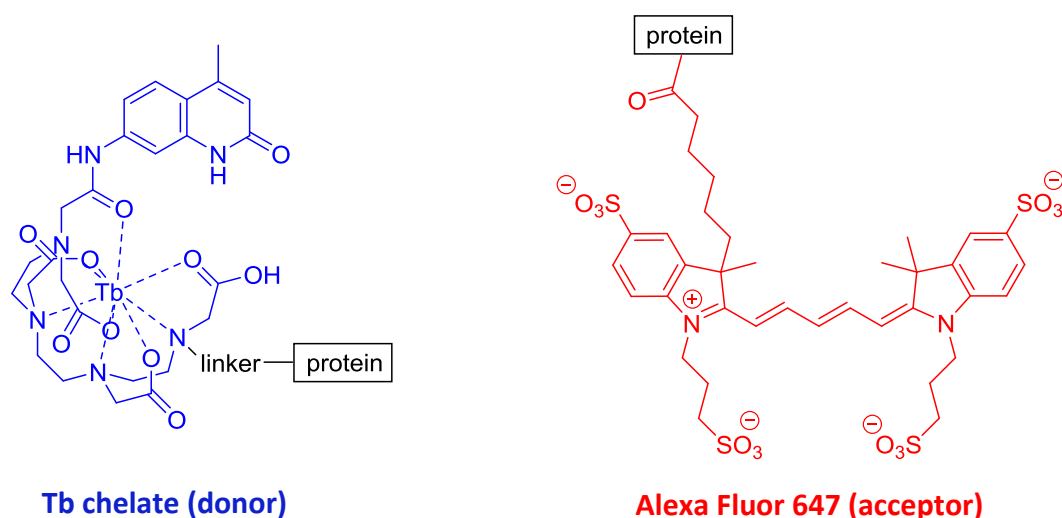


Figure 20: Structures of Tb chelate donor fluorophore and Alexa Fluor 647 acceptor fluorophore

Tb chelate donor fluorophore

A Tb chelate fluorophore, with an isothiocyanate reactive group for attachment to the protein, was purchased from Invitrogen/Life Technologies. Although the exact structure of the chelate is not disclosed by the manufacturers, it was thought to be a DTPA chelate with a cs124 antenna attached and a linker such as ethylenediamine between the chelate and the isothiocyanate group, as in the papers by Selvin *et al.*^{112,115,116,118} Terbium chelates are excited at a wavelength of 340 nm and their emission spectrum displays four sharp, distinct peaks at 490 nm, 546 nm, 585 nm and 620 nm (Figure 21).^{112,116,118}

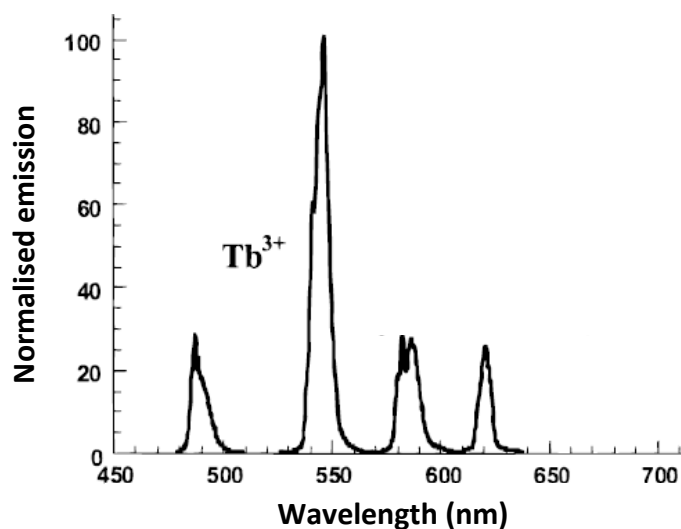


Figure 21: Emission spectrum for Tb chelate donor fluorophore

The chelate consists of DTPA with a cs124 antenna. Figure adapted from reference.¹¹⁶

Alexa Fluor 647 acceptor fluorophore

An Alexa Fluor 647 fluorophore with an *N*-hydroxysuccinimide (NHS) ester reactive group comes from an extensive library of Alexa Fluor fluorophores originally produced by Molecular Probes (now Invitrogen/Life Technologies) whose excitation and emission spectra cover the visible and the near infrared spectrum.¹³² The number refers approximately to the maximum excitation wavelength of the dye in nm. Alexa Fluor fluorophores are synthesised by sulfonation of existing fluorophores including rhodamine, fluorescein and cyanine dyes, which makes them negatively charged and hydrophilic.¹³² They generally tend to be brighter, more photostable and less sensitive to pH than the original dyes.¹³³ Alexa Fluor 647 has a maximum excitation wavelength of 650 nm and a maximum emission wavelength of 668 nm (Figure 22).¹³⁴ This particular fluorophore was chosen as an acceptor as the Tb chelate emission peak at 620 nm overlaps with the excitation peak at 650 nm for Alexa Fluor 647.

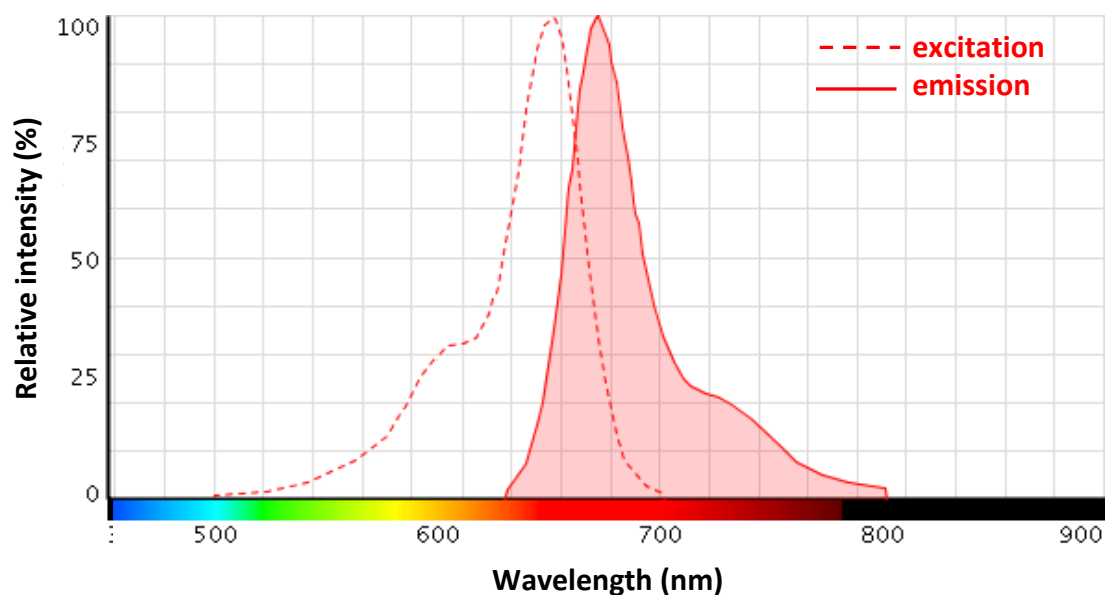


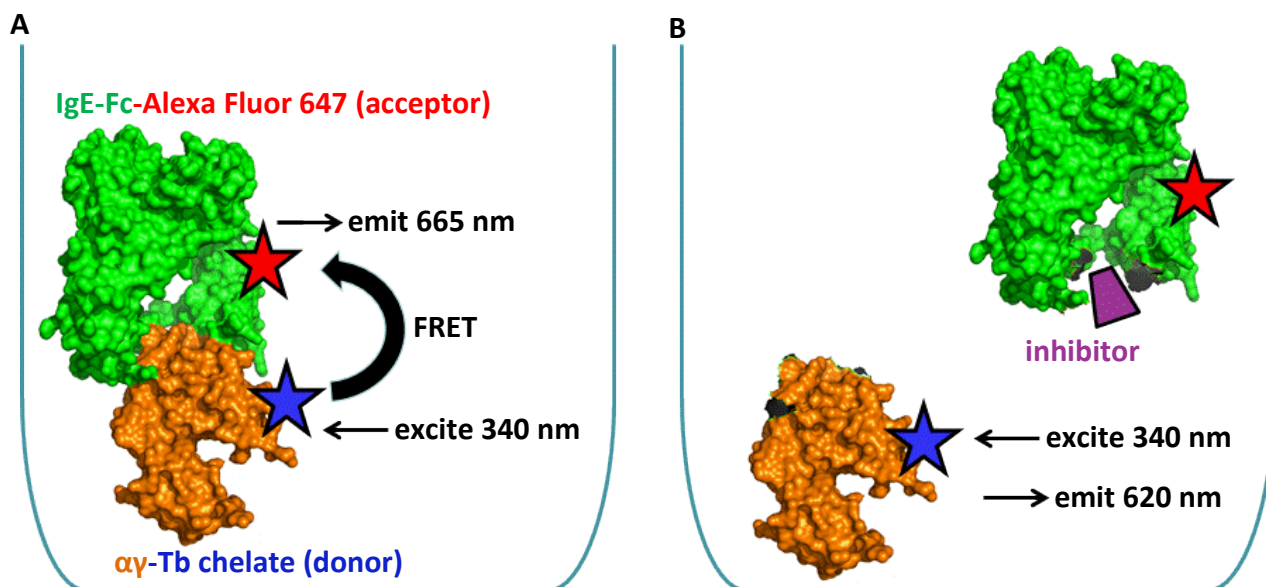
Figure 22: Excitation and emission spectra for Alexa Fluor 647 acceptor fluorophore
 Maximum excitation wavelength is 650 nm (dashed line) and maximum emission wavelength is 688 nm (solid line). Image adapted from www.lifetechnologies.com Fluorescence SpectraViewer (accessed Nov 2014).

2.2.2 Format of the TR-FRET assay

It was decided to label IgE-Fc with Alexa Fluor 647 and to label $\alpha\gamma$ with Tb chelate. If no inhibitors were present (Scheme 4 A), the labelled IgE-Fc and $\alpha\gamma$ would bind to each other and this would bring the fluorophores into close proximity. If the Tb chelate donor fluorophore was excited using a wavelength of 340 nm, then the energy it emits at 620 nm would non-radiatively transfer to and excite the Alexa Fluor 647 acceptor fluorophore, due to the Tb chelate emission peak at 620 nm overlapping with the Alexa Fluor 647 broad excitation peak centred at 650 nm. The Alexa Fluor 647 would then emit at 665 nm. The Tb chelate donor emission would be measured at 620nm and the Alexa Fluor 647 acceptor emission would be measured at 665nm. The ratio between these values, known as the TR-FRET ratio, would give the signal for this assay.

If an inhibitor was added (Scheme 4 B), the extent to which it inhibited the interaction between labelled IgE-Fc and $\alpha\gamma$ would be reflected in the reduction in the TR-FRET ratio; the more potent the inhibitor the more the TR-FRET ratio would be reduced. A time delay of 100 μ s would be allowed, before taking the emission measurements, so that any autofluorescence from the buffer or inhibitors or any acceptor excitation from incident light would have decayed, giving a more accurate measurement. This assay has the benefit of being homogenous (i.e. all components are in

solution) with no washing steps required or secondary reagents needed, therefore it should be relatively simple to carry out and higher throughput than the ELISA.



Scheme 6: Overview of TR-FRET inhibition assay

A = inhibitor not present therefore IgE-Fc and α are bound and FRET occurs. Excitation at 340 nm of Tb chelate donor fluorophore on α causes non-radiative transfer of energy to Alexa Fluor 647 acceptor fluorophore on IgE-Fc due to its close proximity, this causes excitation of the Alexa Fluor 647, which then emits at 665 nm. B = inhibitor present therefore inhibition of the IgE-Fc: α interaction occurs causing loss of FRET. Excitation of Tb chelate donor fluorophore on α occurs, but energy transfer to Alexa Fluor 647 cannot take place as it is too far away, therefore only emission at 620 nm from the Tb chelate is observed.

2.2.3 Fluorescent labelling of proteins

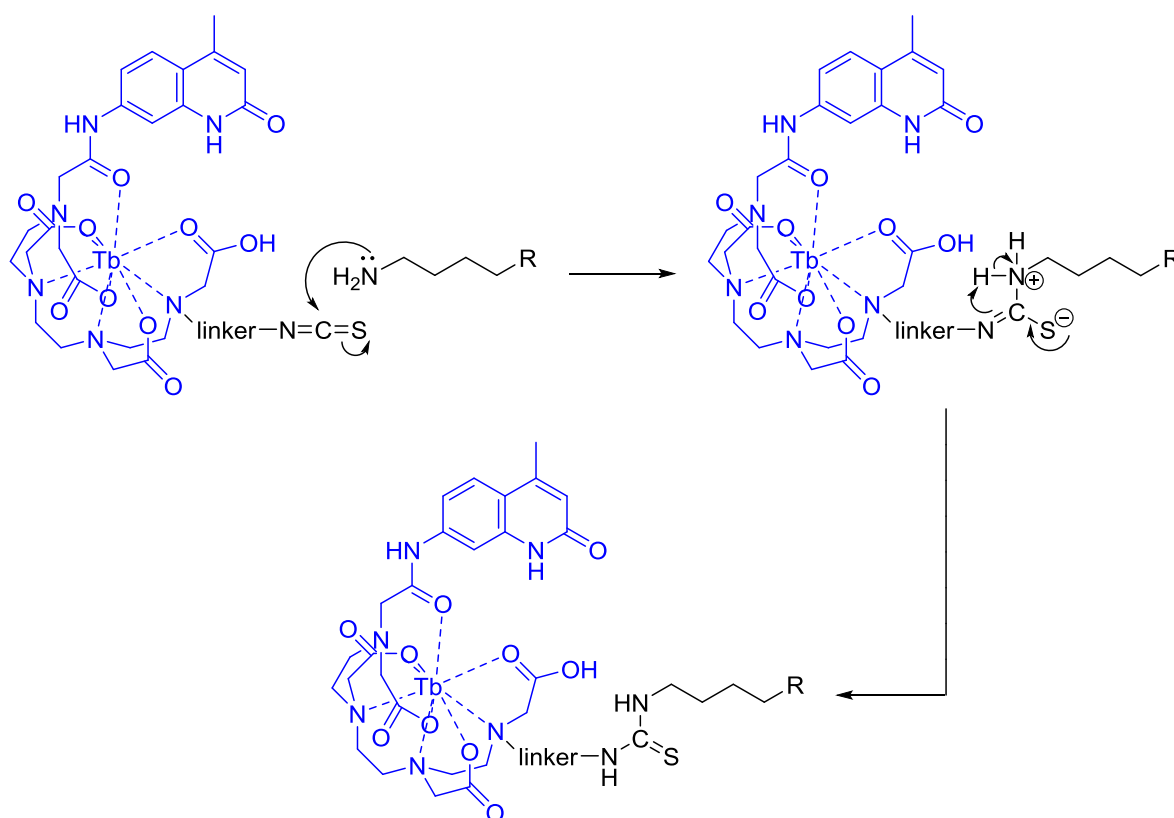
With the design of the TR-FRET assay decided, the first stage was to label the IgE-Fc and α proteins with the fluorophores. In both cases, labelling was achieved via the covalent reaction of the amine groups of the protein lysine residues with the amine-reactive group on the fluorophore, which meant that labelling was non-specific. The advantage of this method, over a site-specific reaction on the protein, is that there is no need for protein modification and it is a relatively simple reaction to carry out.

The disadvantage could be that multiple labelling reactions may each give a slightly different dye:protein ratio, depending on the extent of the lysine labelling, and it may be difficult to control this. It may be that one particular dye:protein ratio would give the highest TR-FRET signal. Another potential issue could be if key binding regions of the proteins were labelled by a fluorophore, this may affect the ability of the two proteins to interact with each other as they would do without the label present. However, the fluorophores are much smaller molecules than the proteins, so this

was not envisaged to be a problem, and the lysine labelling was carried out in the first instance as it was the simplest technique.

Labelling of $\alpha\gamma$ with Tb chelate isothiocyanate

For the labelling of $\alpha\gamma$ with Tb chelate isothiocyanate, a solution of Tb chelate isothiocyanate (final concentration 378 μM) in dimethylsulfoxide (DMSO) was added to a solution of $\alpha\gamma$ (final concentration 37.8 μM) in carbonate buffer and allowed to react in the dark for 3 hours with vigorous shaking, according to the manufacturer's instructions (Scheme 7). The resulting fluorescently-labelled protein (known as $\alpha\gamma\text{-Tb}$) was then dialysed into PBS at 4 $^{\circ}\text{C}$ for 48 hours in the dark to remove any unreacted fluorophore. Further experimental details can be found in section 6.2.4.



Scheme 7: Mechanism for labelling of a lysine residue of $\alpha\gamma$ with Tb chelate isothiocyanate

To determine the degree of labelling and to check that the dialysis had removed all the unreacted dye, $\alpha\gamma\text{-Tb}$ was subjected to size exclusion chromatography (SEC). This technique uses a porous solid phase to separate molecules according to their size. A solution is passed through a column which contains porous beads; smaller molecules travel through the pores in the beads and elute

more slowly, whereas larger molecules cannot fit through the pores and so elute more quickly. Absorbance, measured at a particular wavelength, detects when a substance elutes.

A solution of $\alpha\gamma$ -Tb in PBS was subjected to analytical SEC using a Superdex 200 5 x 150 mm gel filtration column and a dual wavelength of 280 nm (protein absorption) and 343 nm (Tb chelate absorption). Absorbance at 280 nm and at 343 nm both peaked at approximately 3 minutes, which indicated that the $\alpha\gamma$ was successfully labelled with Tb chelate (Figure 23). Free Tb chelate isothiocyante is a much smaller molecule than $\alpha\gamma$ -Tb so would elute later at approximately 10 minutes. The absence of a 343 nm absorbance peak at 10 minutes indicated that any unreacted Tb chelate isothiocyante was successfully removed during the dialysis. The final concentration of $\alpha\gamma$ -Tb was determined using a spectrophotometer and found to be 5.1 μ M and a dye:protein ratio of 6.3:1 was achieved (see section 6.2.4 for the calculation used to determine this ratio).

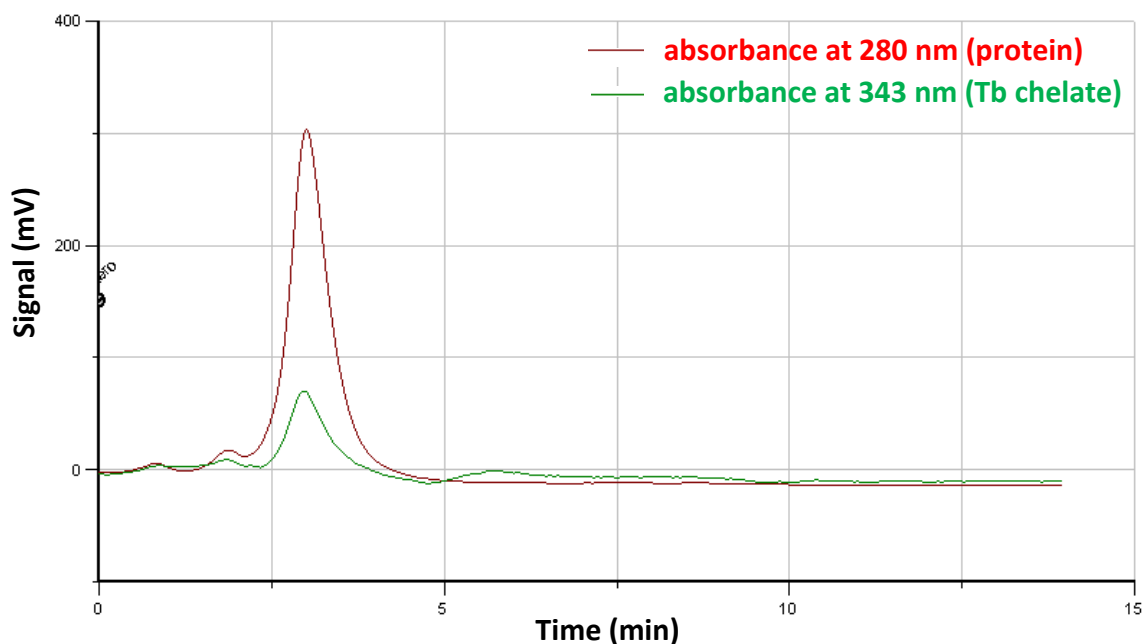
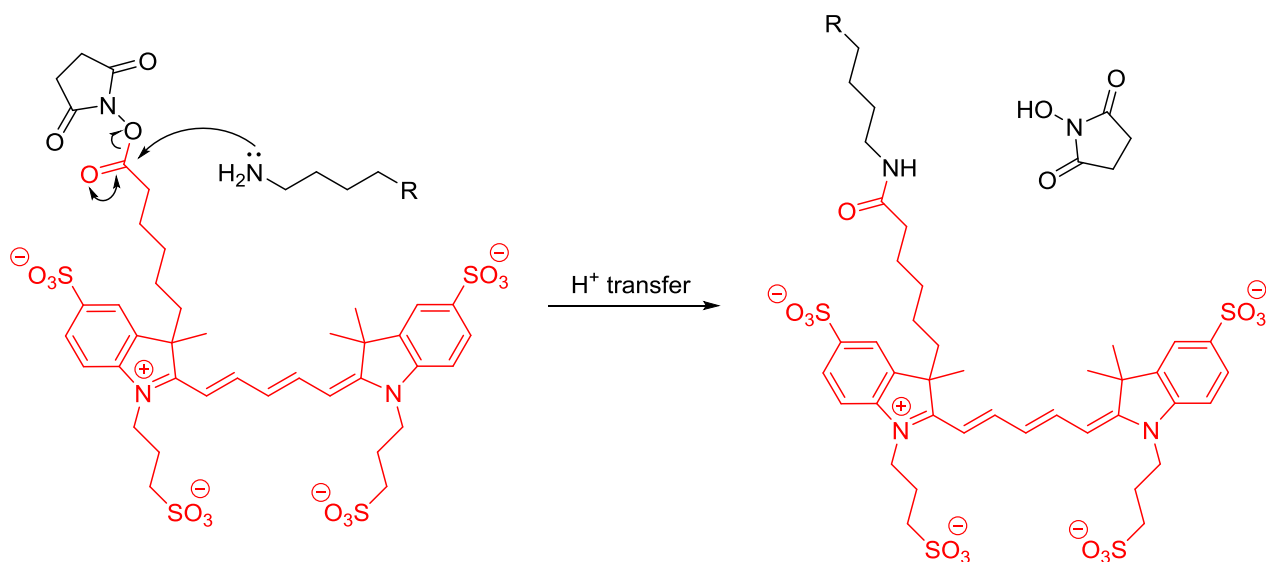


Figure 23: Size exclusion chromatogram of $\alpha\gamma$ -Tb

Red trace = absorbance at 280 nm (for $\alpha\gamma$), green trace = absorbance at 343 nm (for Tb chelate). Peaks for 280 nm and 343 nm at approximately 3 min were concurrent which indicated the successful labelling of $\alpha\gamma$ with Tb chelate. No peak between 10 and 15 minutes for 343 nm indicated that any unreacted Tb chelate isothiocyante had been removed from the labelled protein during dialysis.

Labelling of IgE-Fc with Alexa Fluor 647 NHS ester

The IgE-Fc was labelled with Alexa Fluor 647 NHS ester (carried out by Dr Marie Pang, KCL). A 2.5-fold molar excess of fluorophore was used and the resultant fluorescently-labelled protein (known as IgE-Fc-A647) had a dye:protein ratio of 1.9:1 (Scheme 8).



Scheme 8: Mechanism for labelling of a lysine residue of IgE-Fc with Alexa Fluor 647 NHS ester

2.2.4 Purification of IgE-Fc-A647

At a later time during the course of the research described in this thesis, it was thought that IgE-Fc-A647 had decomposed, therefore IgE-Fc-A647 was subjected to analytical SEC using a Superdex 200 10 x 300 mm gel filtration column and measuring protein absorbance at 280 nm. The chromatogram showed the presence of a main peak at 17 minutes (for IgE-Fc-A647) and a less intense peak at 20 minutes which was assumed to be for a smaller, degraded fragment of IgE-Fc-A647 (Figure 24). Another small peak at 32 minutes was likely to be for unreacted Alexa Fluor 647 isothiocyanate.

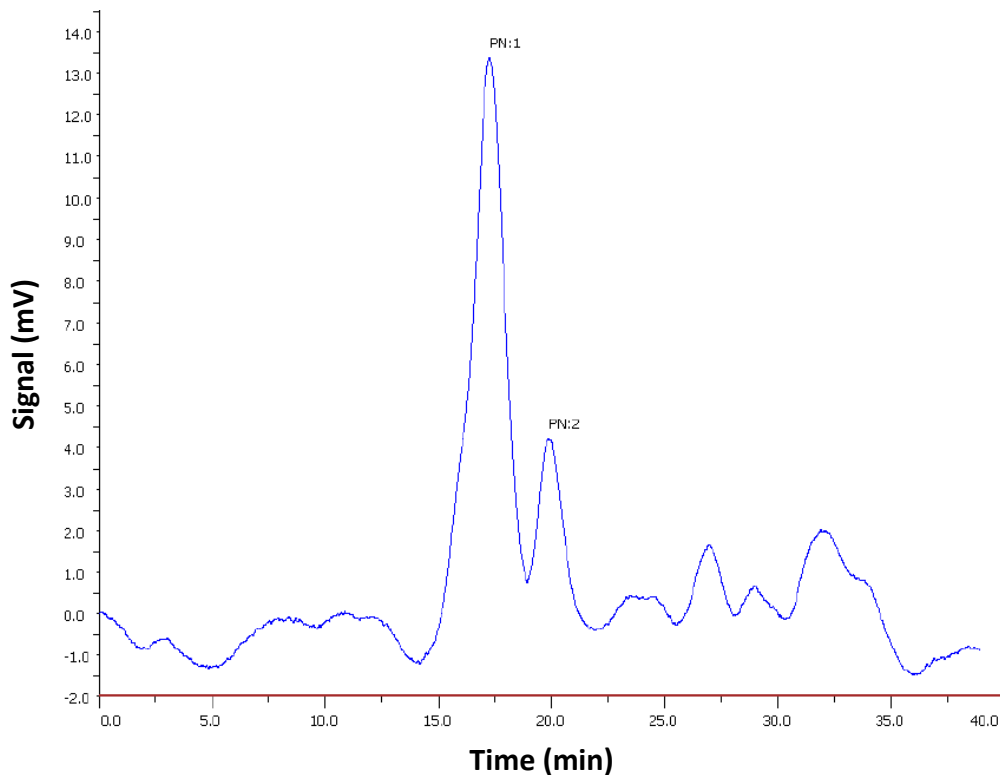


Figure 24: Size exclusion chromatogram of IgE-Fc-A647

Absorbance was measured at 280 nm. Peak at 17 min indicated IgE-Fc-A647, peak at 20 min indicated degraded IgE-Fc-A647 and peak at 32 min indicated unreacted Alexa Fluor 647.

IgE-Fc-A647 was therefore purified using preparative SEC to remove any degraded protein and unreacted dye using a Superdex 75 10 x 300 mm gel filtration column and measuring protein absorbance at 280 nm. The chromatogram showed the peak at 12 minutes was for the pure IgE-Fc-A647 and that degraded protein and unreacted dye were successfully removed (Figure 25). A sample of unlabelled IgE-Fc was also subjected to preparative SEC to check that the fractions containing pure IgE-Fc-A647 were correct and both chromatograms are overlaid in Figure 25. This showed that the peak at 12 minutes was for the pure IgE-Fc-A647 and that fractions 3 and 4 were pure.

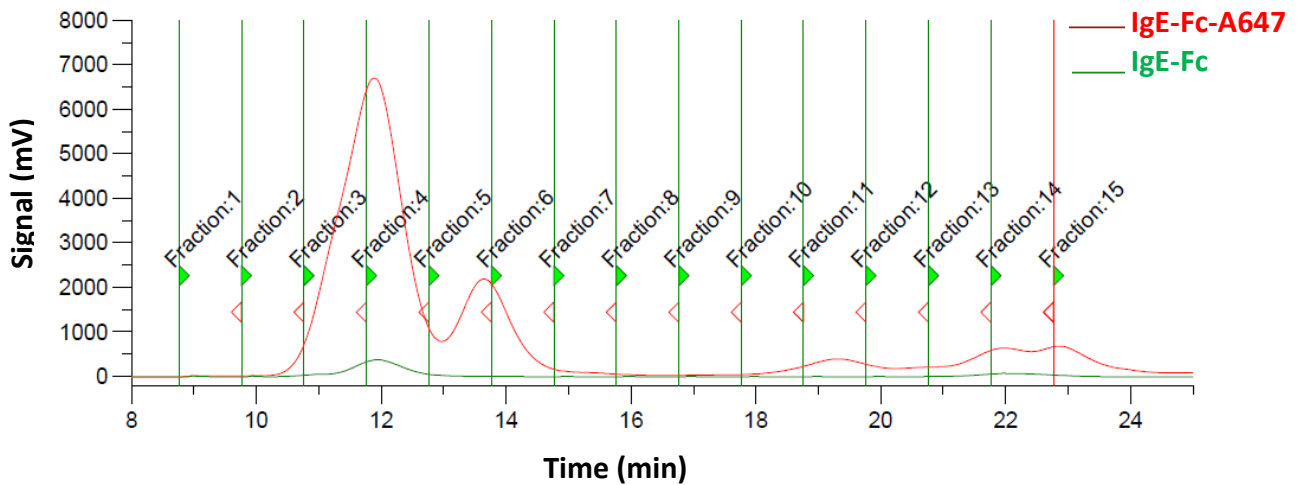


Figure 25: Preparative size exclusion chromatogram of IgE-Fc-A647 and IgE-Fc

Red trace = absorbance at 280 nm for IgE-Fc-A647. Peak at 12 min was for IgE-Fc-A647, peak at 13.5 min was for degraded IgE-Fc-A647 and peaks at 19.2 min, 22 min and 23 min were for free Alexa Fluor 647. Green trace = absorbance at 343 nm for unlabelled IgE-Fc. Peak at 12 min was concurrent with the peak for IgE-Fc-A647. Fractions 3 and 4 contained pure IgE-Fc-A647.

2.2.5 Optimisation of the assay conditions

Initial binding assays

To determine if the binding of IgE-Fc and $\alpha\gamma$ could be measured using TR-FRET, initial binding assays were first carried out between IgE-Fc-A647 and $\alpha\gamma$ -Tb. Assays were carried out in opaque, flat bottom 384-well plates at room temperature. TR-FRET dilution buffer was used for all assays, however the exact buffer composition was undisclosed by the manufacturers (Invitrogen). Various other buffers, including PBS, tris(hydroxymethyl)aminomethane (tris) and 4-(2-hydroxyethyl)-1-piperazineethanesulfonic acid (HEPES), were tested by co-workers at KCL, however the TR-FRET buffer was found to give by far the highest TR-FRET signal (unpublished results, Dr Marie Pang, KCL), which is why it was used for the assays.

As the K_d of the IgE:Fc ϵ RI interaction is $\sim 0.1 \text{ nM}^{4,15,16}$ it was anticipated that IgE-Fc-A647 and $\alpha\gamma$ -Tb concentrations in the low nanomolar range would be suitable. The concentration of $\alpha\gamma$ -Tb was initially fixed at 0.5 nM, 1 nM, 2 nM and 5 nM and in each case IgE-FcA647 was added in increasing amounts until a 10-fold molar excess was achieved. The plate was then read using an Artemis HTRF-compatible microplate reader. The plate was excited at 340 nm and, following a time delay of 100 μs , absorbance was measured at 620 nm and 665 nm. The TR-FRET ratio was calculated by the following equation:

$$\text{TR-FRET ratio} = \frac{\text{emission at 665 nm}}{\text{emission at 620 nm}} \times 10,000 \quad (\text{Eq. 5})$$

For each assay the TR-FRET ratio was plotted against the concentration of IgE-Fc-A647 using a 4-parameter logistic to give dose-response or binding curves (Figure 26).

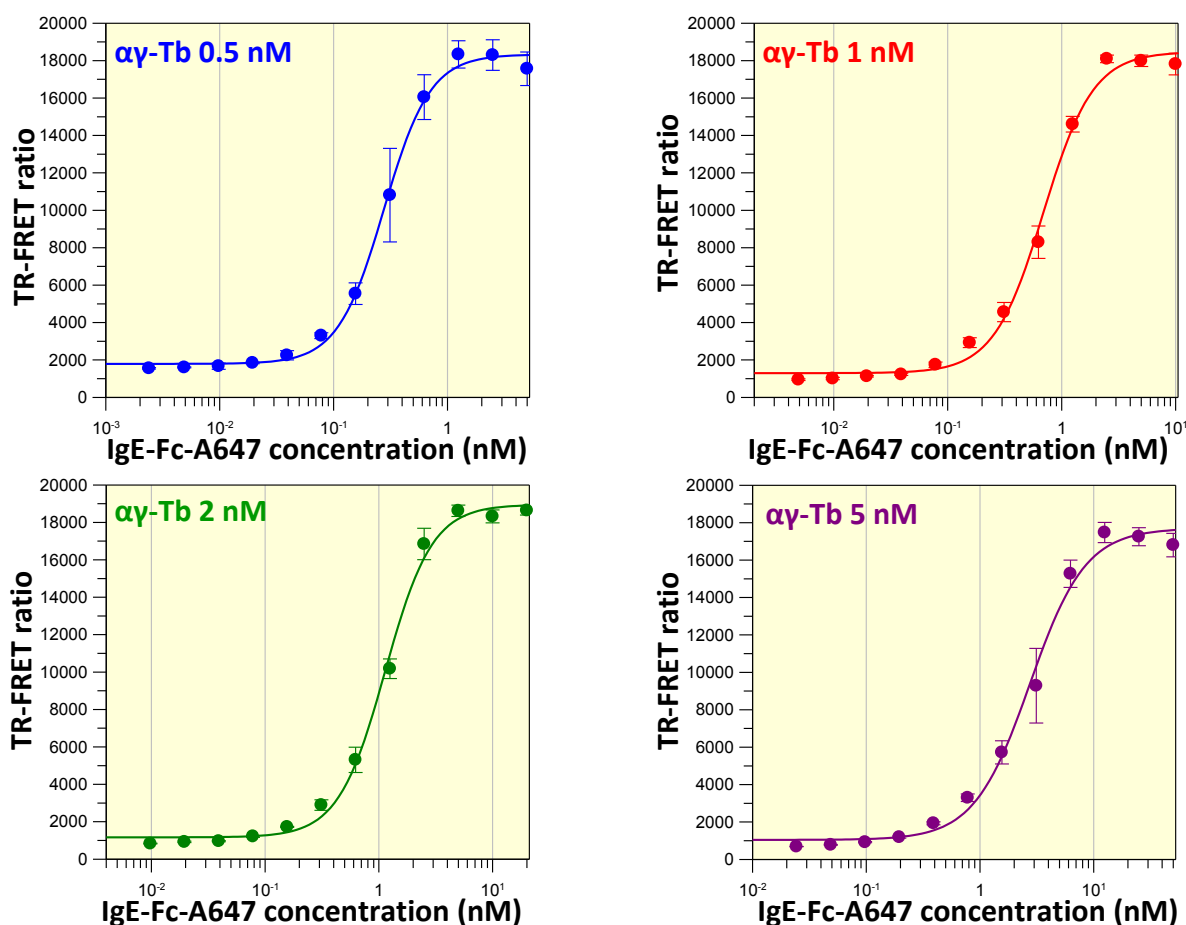


Figure 26: TR-FRET binding curves for IgE-Fc-A647 and α -Tb

The concentration of α -Tb was fixed at 0.5 nM, 1 nM, 2 nM and 5 nM and in each case IgE-Fc-A647 was added in increasing concentrations up to a 10-fold molar excess.

It can be seen that for each binding assay, a high TR-FRET signal of $\sim 19,000$ was achieved. It was therefore decided to use α -Tb at the lowest concentration of 0.5 nM, as this would use the least material whilst still giving a high signal. A concentration of 1.25 nM was chosen for IgE-Fc-A647 as this is at the highest point of the binding curve for α -Tb at 0.5 nM.

Initial inhibition assays

It was then investigated if these concentrations of IgE-Fc-A647 and α -Tb were suitable for an inhibition assay, using unlabelled proteins as inhibitors. The concentration of α -Tb was fixed at 0.5 nM, the concentration of IgE-Fc-A647 was fixed at 1.25 nM and unlabelled IgE-Fc was added in increasing amounts until a 10-fold molar excess was achieved. This assay was also repeated with unlabelled α as an inhibitor. The order of addition was investigated in each case; the unlabelled protein inhibitor was incubated for 1 hour either with IgE-Fc-A647 or with α -Tb, before the other

labelled protein was added. The plate was then read straightaway after the addition of the final protein. The inhibition curves for unlabelled IgE-Fc as an inhibitor can be seen in Figure 27 and the inhibition curves for unlabelled $\alpha\gamma$ as an inhibitor can be seen in Figure 28.

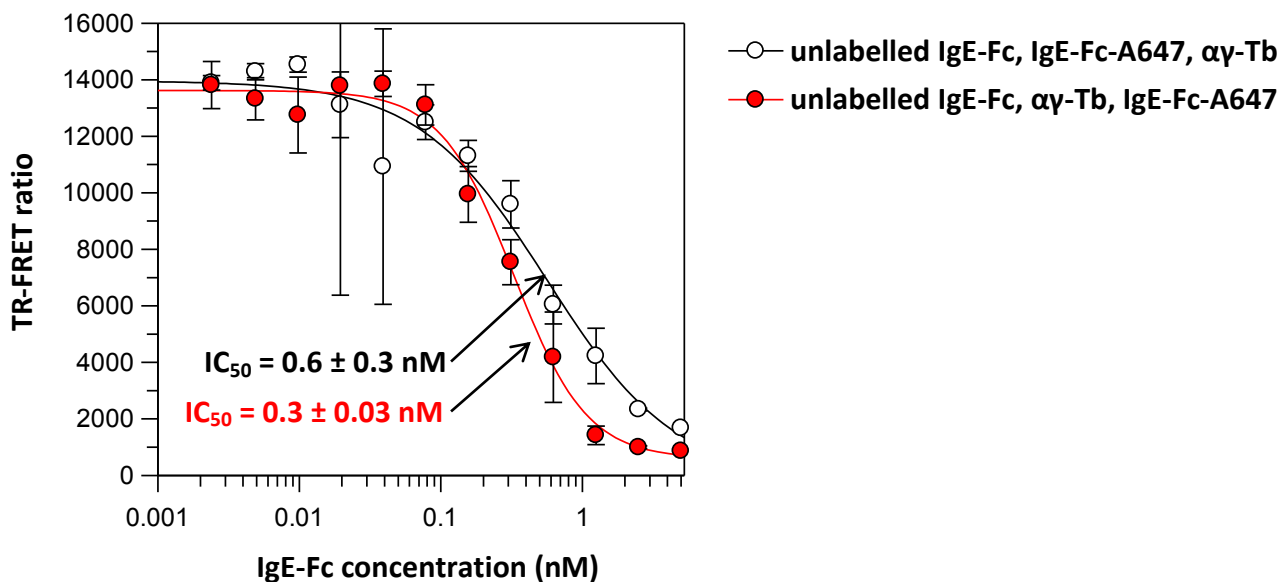


Figure 27: TR-FRET inhibition curves for unlabelled IgE-Fc

The concentration of $\alpha\gamma$ -Tb was fixed at 0.5 nM, the concentration of IgE-Fc-A647 was fixed at 1.25 nM and increasing concentrations of unlabelled IgE-Fc were used up to a 10-fold molar excess. The key denotes the order in which the proteins were added. Unlabelled IgE-Fc was incubated with the first labelled protein for 1 hour, before addition of the second labelled protein.

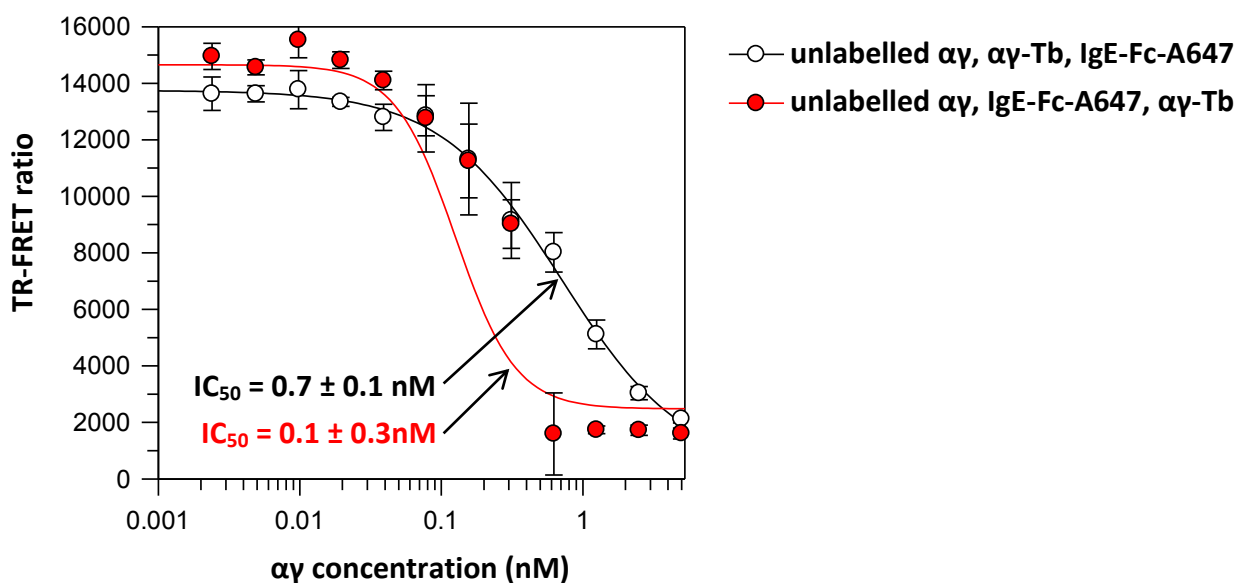


Figure 28: TR-FRET inhibition curves for unlabelled $\alpha\gamma$

The concentration of $\alpha\gamma$ -Tb was fixed at 0.5 nM, the concentration of IgE-Fc-A647 was fixed at 1.25 nM and increasing concentrations of unlabelled $\alpha\gamma$ were used up to a 10-fold molar excess. The key denotes the order in which the proteins were added. Unlabelled $\alpha\gamma$ was incubated with the first labelled protein for 1 hour, before addition of the second labelled protein.

Figures 27 and 28 show that good inhibition curves are obtained when using unlabelled proteins as inhibitors of the interaction between IgE-Fc-A647 and $\alpha\gamma$ -Tb. In all cases, when the unlabelled protein inhibitor concentration reached a 10-fold molar excess, the TR-FRET signal was reduced to a background level. This indicated that the concentrations of labelled proteins were suitable to use in subsequent inhibition assays with small molecules or peptides. It can also be seen that the IC₅₀ values are similar, within error, regardless of the order of addition of the proteins suggesting that the proteins are in equilibrium.

The incubation time once all proteins had been added was also investigated. After initial reading of the plate, all proteins were incubated for a further hour then the plate was read again. However, this gave an almost identical result, likely due to the high affinity of the IgE:Fc ϵ RI interaction, therefore it was not deemed necessary for any incubation after all proteins were added in subsequent inhibition assays.

2.2.6 Comparison of ELISA vs TR-FRET assay

The main advantages and disadvantages of the ELISA and the TR-FRET inhibition assays are summarised in Table 3. The S/B and the Z-factor were calculated with equations 1 and 3 respectively and using the data from the inhibition assay of **Bip(3)-peptide** (this peptide will be discussed in more detail in Chapter 4).

ELISA S/B: 14.7 , Z-factor: 0.97		TR-FRET S/B: 12.6 , Z-factor: 0.79	
Advantages	Disadvantages	Advantages	Disadvantages
No need to label proteins	Multiple processing steps, takes ~ 1 day per assay	Few processing steps, takes ~ 0.5 day per assay	Labelling of proteins required
Larger volumes in 96-well plate - easier handling	Extensive washing required	Homogenous, no washing required	Smaller volumes in 384-well plate - more difficult handling
	Larger volumes - uses more material	Smaller volumes - uses less material	
	Higher protein concentration - uses more material	Lower protein concentration - uses little material	

Table 3: Comparison of advantages and disadvantages of ELISA vs TR-FRET assay

It can be seen from Table 3 that the main advantages of the TR-FRET assay over the ELISA are that this assay is carried out in solution, with no need to add secondary reagents or carry out extensive washing steps and the assay uses lower volumes and concentrations therefore conserving material. These factors make the TR-FRET assay more attractive for testing libraries of inhibitors. The Z-factors in both cases are high (0.97 for the ELISA and 0.70 for the TR-FRET assay) and a good S/B is achieved (14.7 for the ELISA and 12.6 for the TR-FRET assay). Whilst these parameters are slightly higher for the ELISA, they are still very good for the TR-FRET assay and the advantages of the TR-FRET assay are such that this was chosen as the assay of choice for future inhibitor testing.

2.3 Expression and purification of IgE Cε2 and Cε3 domains

In addition to IgE-Fc, it would be useful to have individual domains of IgE to use in experiments and investigate their interaction with inhibitors, therefore it was decided to express the Cε2 and Cε3 domains of IgE. The Cε3 domains constitute the key region of IgE that interacts with FcεRI (see section 1.3) and it was therefore thought that if a compound inhibited the interaction between IgE and FcεRI by binding to IgE, it would likely bind to the Cε3 domain. The Cε2 domain of IgE does not interact with FcεRI, therefore it would be unlikely that a compound would inhibit the IgE:FcεRI interaction by binding to Cε2, although this could be possible if an allosteric mechanism of inhibition was adopted. It was thought that the Cε2 and Cε3 proteins could be used in subsequent SPR experiments, for compounds that had exhibited inhibition in the ELISA or TR-FRET assays. These proteins could also be used for STD NMR experiments and, if they were ¹⁵N-labelled, used for ¹⁵N-HSQC NMR experiments.

2.3.1 Expression and purification of IgE Cε3 domain

Cε3 was expressed in BL21 *Escherichia coli* (*E. coli*) cells grown in minimal media and induced with isopropyl β-D-1-thiogalactopyranoside (IPTG) when optical density (OD) had reached at least 0.6, according to the procedures of McDonnell *et al.*¹³⁵⁻¹³⁷ Sodium dodecyl sulfate polyacrylamide gel electrophoresis (SDS-PAGE) analysis of induced and uninduced cells was used to confirm that expression had taken place. Cε3 formed inclusion bodies which were solubilised in a buffer containing 6 M guanidinium chloride denaturant to ensure the protein was unfolded. To ensure the intradomain disulfide bond form correctly between Cys(358) and Cys(418), refolding was carried out using a Ni²⁺ affinity column. The amount of refolding buffer was gradually increased, which meant that the guanidinium-containing solubilisation buffer was gradually decreased, allowing the disulfide bond to form (Figure 29). After elution from the Ni²⁺ column, refolded Cε3

was then run through a gel filtration column to remove any unfolded protein. The elution trace (Figure 30) shows a single peak for Cε3 confirming that the refolding and purification steps were successful. Further details of the Cε3 expression and purification procedures can be found in section 6.4.

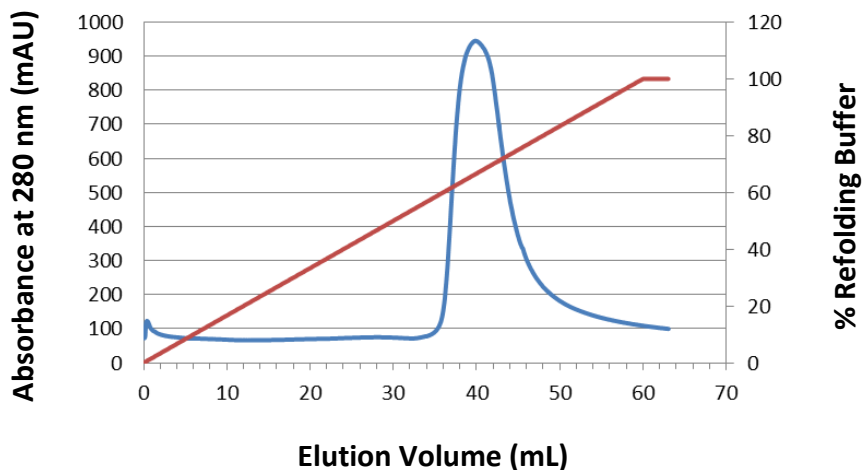


Figure 29: Elution trace from Ni²⁺ affinity column for first purification of IgE-Fc Cε3 domain
Blue line = absorbance at 280 nm, red line = % of refolding buffer (increased from 0 – 100% with simultaneous decrease of guanidinium chloride from 100 – 0%).

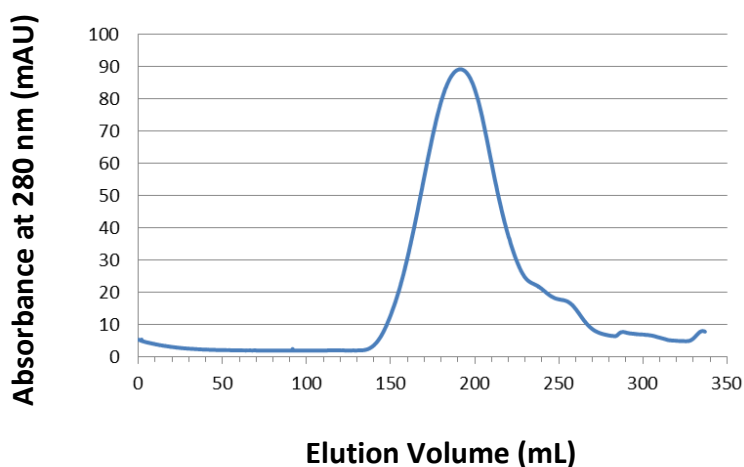


Figure 30: Elution trace from gel filtration column for second purification of IgE-Fc Cε3 domain
Blue line = absorbance at 280 nm. Single peak indicated successful purification of Cε3.

SDS-PAGE analysis was then used to determine the purity of Cε3 and this was carried out with 5 μg, 10 μg and 20 μg of Cε3. The SDS-PAGE gel (Figure 31) showed that refolded, pure Cε3 was mainly monomeric, with a MW of ~ 14.3 kDa, but that small amounts of dimeric and trimeric Cε3 were also present. This meant that Cε3 may need further purification before being used in any experiments with inhibitors. The gel also showed that 5 μg was a large enough amount of Cε3 for visualisation by SDS-PAGE.

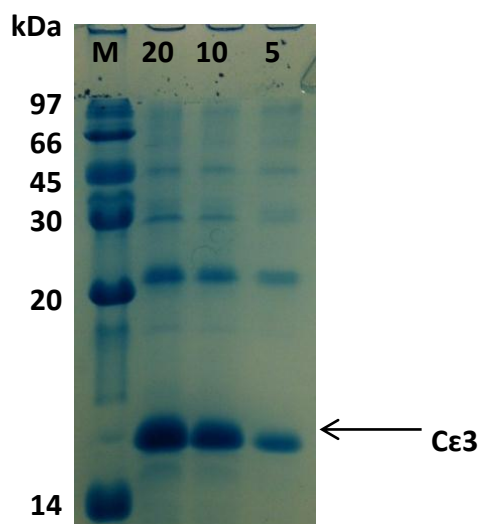


Figure 31: SDS-PAGE gel showing IgE-Fc Cε3 domain

M = molecular weight marker and 20, 10 and 5 refer to the amount in μg of Cε3.

^1H NMR spectroscopy was used to characterise Cε3 and the ^1H NMR spectrum (Figure 32) was typical of a molten globule such as Cε3, which typically lack rigid tertiary structure.^{136,137} The peak at $\delta \sim 1$ parts per million (ppm) is indicative of methyls in a molten globule, as for a well folded protein these would normally appear more upfield at around 0.5 ppm. The broad peak at $\delta \sim 8.3$ ppm indicates that there is little dispersion of the amide backbone chemical shifts. Finally, the weak but broad signal at $\delta \sim 10$ ppm is for the tryptophan residues of Cε3.

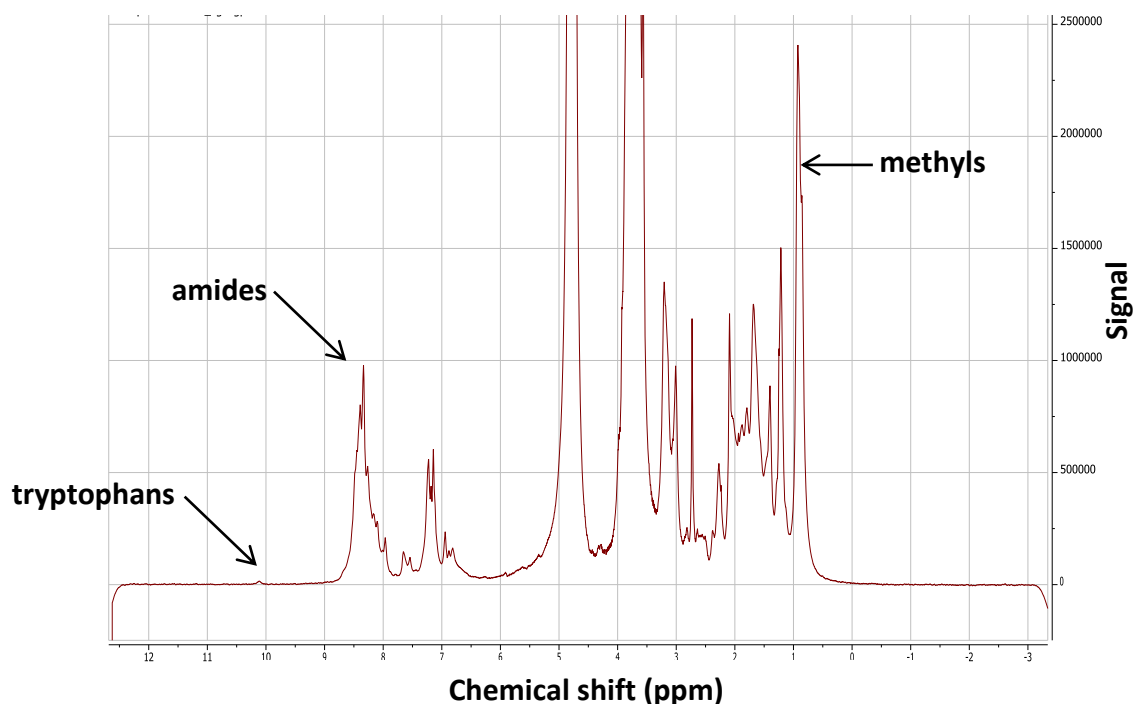


Figure 32: ^1H NMR spectrum of IgE Cε3 domain

Spectrum showed peaks for methyls ($\delta \sim 1$ ppm), amides ($\delta \sim 8.3$ ppm) and tryptophans ($\delta \sim 10$ ppm).^{136,137}

Mass spectrometry (MS) was also used to characterise pure Cε3, however the presence of strong polyethylene glycol (PEG) signals in the mass spectrum, with characteristic peaks 44 Da apart, obscured the mass spectrum of the protein. The Cε3 could have been contaminated with PEG from the dialysis tubing (when Cε3 was dialysed into H₂O for the MS experiments), although the tubing was thoroughly washed before dialysis. The dialysis was carried out again, with more extensive washing of the tubing and a longer dialysis time, then the MS was repeated. However, despite these precautions, the presence of PEG signals still swamped the spectrum. Further details of all analysis and characterisation procedures can be found in section 6.4.

2.3.2 Expression of IgE Cε2 domain

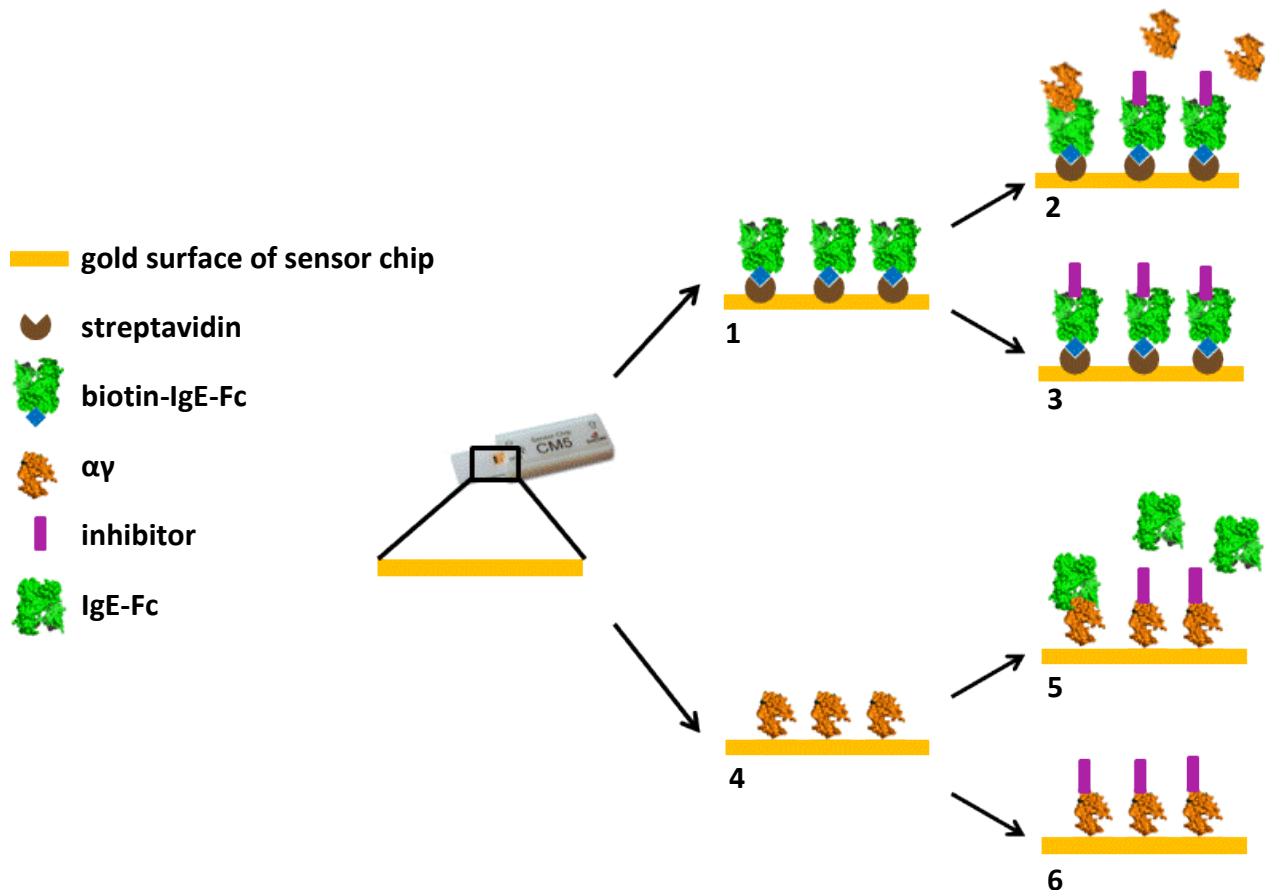
Cε2 was also successfully expressed using the same procedures as for Cε3 (see section 6.4 for full details) and Cε2 cell pellets are ready for purification.

2.4 Development of SPR experiments with immobilised IgE-Fc and αγ

As discussed in section 1.8.3, SPR is a very useful biophysical technique that has been widely used to study the interactions of inhibitors with IgE and FcεRI. It was decided to develop and use SPR experiments with immobilised IgE-Fc and immobilised αγ and carry out inhibition assays with any compounds that displayed inhibition in the ELISA or TR-FRET assays. If αγ was immobilised to the SPR sensor chip and a solution of IgE-Fc injected over the chip, the binding of IgE-Fc to αγ should be detected by an increase in signal. If a pre-incubated solution of IgE-Fc and an inhibitor was injected over the chip, the extent to which the inhibitor prevented binding of IgE-Fc to immobilised αγ would be shown by a smaller increase in signal (or no increase if none of the IgE-Fc bound to αγ). This inhibition assay could also be carried out the other way round, with IgE-Fc immobilised to the chip and a solution of αγ and an inhibitor injected over the chip. If any inhibition was seen in either of these experiments, it was planned to monitor the direct binding of the inhibitor to each of the immobilised proteins, which would hopefully shed some light on which protein the inhibitor was binding to.

A CM5 sensor chip was chosen for the SPR experiments as it comprises a carboxymethylated dextran matrix (CM) on top of the gold chip surface which allows a covalent attachment of the protein to the chip. The carboxyl groups of the dextran matrix are activated, then allowed to react with the primary amine of the lysine residues of the protein to form an amide bond. This method is suitable for immobilising αγ, however for IgE-Fc if the attachment to the chip was via the lysine

residues this would orientate the IgE-Fc into an inactive conformation due to the position of the lysines at the C ϵ 3 domain of IgE-Fc. It was therefore decided to immobilise streptavidin onto the chip (in the same way as the α immobilisation), then to inject biotinylated IgE-Fc over the chip (biotin-IgE-Fc provided by Dr Marie Pang, KCL). The biotin was positioned in a site-specific manner to the IgE-Fc to ensure an active conformation of the protein once immobilised. An overview of the inhibition assays and direct binding assays with both immobilised proteins can be seen in Scheme 9.



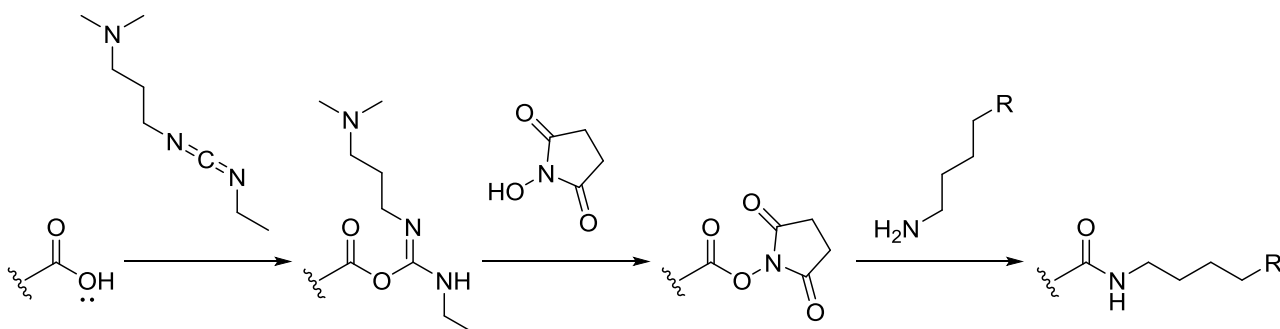
Scheme 9: Overview of SPR experiments with immobilised proteins

1 = immobilisation of biotin-IgE-Fc onto a streptavidin coated SPR chip, 2 = inhibition assay with injection of a mixture of α and inhibitor, 3 = direct binding assay with injection of inhibitor only, 4 = immobilisation of α onto SPR chip, 5 = inhibition assay with injection of a mixture of IgE-Fc and inhibitor, 6 = direct binding assay with injection of inhibitor only.

2.4.1 Immobilisation of α

All SPR experiments were carried out at room temperature using a Biacore T200 instrument. More details on the experimental procedures can be found in section 6.5. Prior to the α immobilisation, the carboxymethylated dextran matrix on the chip surface was first activated with 1-ethyl-3-(3-dimethylaminopropyl)carbodiimide (EDC) and NHS to form reactive esters. α (100 nM) was then added, the lysine residues of which reacted with the active esters on the chip surface to form a

stable amide linkage (Scheme 10). An increase of ~ 1000 resonance units was achieved, indicating the $\alpha\gamma$ was successfully immobilised. Ethanolamine was then added to cap any unreacted NHS esters on the chip surface to prevent further reaction and ensure that IgE-Fc or any inhibitors that were subsequently injected would only bind specifically to $\alpha\gamma$ and not react directly with the chip. All immobilisation steps were carried out in HEPES buffered saline (HBS).



Scheme 10: Activation of carboxyl groups of SPR sensor chip surface with EDC and NHS

EDC coupled to carboxyl group of carboxymethylated dextran matrix on surface of SPR sensor chip to form an unstable *o*-acylisourea intermediate. NHS then coupled to the carboxyl group forming the more stable NHS ester. The NHS-ester then reacted with the primary amine of the lysine residues of the protein to form an amide bond and a stable conjugate.

2.4.2 Binding of IgE-Fc to immobilised $\alpha\gamma$

IgE-Fc (10 nM) was injected over the chip containing immobilised $\alpha\gamma$, to check the $\alpha\gamma$ was active and able to bind IgE-Fc. An increase of ~ 300 resonance units was observed which indicated that the proteins were successfully bound. Due to the slow off-rate between IgE-Fc and $\alpha\gamma$ ^{15,16}, the dissociation of IgE-Fc and a corresponding return to baseline would take approximately 2 days, therefore the IgE-Fc was removed with an injection of glycine pH 2.5.

The SPR running buffer was then changed from HBS to PBS with 2% DMSO and 0.005% Tween 20. This was because PBS was used in the ELISA so it was more consistent and it was thought that when adding inhibitors there would need to be a small percentage of DMSO to aid compound solubility. The IgE-Fc binding to immobilised $\alpha\gamma$ was repeated in the new SPR running buffer and an increase of ~ 30 resonance units was observed, which was approximately 30 pg/mm². This was lower than the increase when HBS was used, which could have been due to the addition of DMSO in the buffer. However, the IgE-Fc binding and removal was reproducible when repeated twice more, with an increase of ~ 30 resonance units being observed each time, therefore this $\alpha\gamma$ -chip was deemed suitable for subsequent inhibition assays with IgE-Fc and inhibitors.

2.4.3 Immobilisation of biotin-IgE-Fc

Prior to the IgE-Fc immobilisation, the carboxymethylated dextran matrix on the chip surface was activated with EDC and NHS to form reactive esters. Streptavidin (160 nM) was then added, the lysine residues of which reacted with the active esters on the chip surface to form a stable amide linkage. An increase of ~ 1000 resonance units was achieved, indicating the streptavidin was successfully immobilised to the chip. Ethanolamine was then added to cap any unreacted NHS esters on the chip surface. Biotin-IgE-Fc (125 nM) was then added, which bound to the streptavidin coated chip and gave an increase of ~ 900 resonance units, indicating successful immobilisation. All immobilisation steps were carried out in HBS.

2.4.4 Binding of $\alpha\gamma$ to immobilised biotin-IgE-Fc

$\alpha\gamma$ (10 nM) was injected over the chip containing immobilised biotin-IgE-Fc, to check the IgE-Fc was active and able to bind $\alpha\gamma$, and this binding experiment was carried out in PBS with 2% DMSO. An increase of ~ 30 resonance units was observed, which was approximately 30 pg/mm^2 and indicated that the $\alpha\gamma$ was successfully bound to IgE-Fc. This was the same increase in resonance units as seen with IgE-Fc binding to immobilised $\alpha\gamma$ (section 2.4.2) which implied that the two proteins could bind equally well to each other, regardless of which one was immobilised to the chip. The $\alpha\gamma$ was then removed using glycine pH 2.5. This was repeated once more with the same result, which confirmed the reproducibility of the $\alpha\gamma$ binding and removal and indicated that the IgE-Fc-chip was ready to be used in subsequent inhibition assays.

2.4.5 Inhibition of IgE-Fc binding to immobilised $\alpha\gamma$ by free $\alpha\gamma$

To see if IgE-Fc could be prevented from binding to immobilised $\alpha\gamma$ by free $\alpha\gamma$, a solution of IgE-Fc (10 nM) and $\alpha\gamma$ (10 nM) was injected over the immobilised $\alpha\gamma$. No change in signal was observed, which indicated that the IgE-Fc was successfully inhibited by free $\alpha\gamma$, as would be expected.

Chapter 3: Small molecule inhibitors of the IgE:FcεRI PPI

3.1 Aspercyclide A and analogues

3.1.1 Design and synthesis of aspercyclide A and analogues

As discussed in section 1.6.1, the natural product aspercyclide A isolated by Singh *et al.* was reported to display inhibition of the IgE:FcεRI interaction when tested with an ELISA ($IC_{50} = 200 \mu\text{M}$).⁸⁶ This was an interesting starting point for the design of small molecule inhibitors of this PPI and there have since been a number of total syntheses of (+)-aspercyclide A reported.^{87,88,90,91} Most recently, the total synthesis of (+)-aspercyclide A and an analogue as well as their ELISA inhibition assay results was reported by Spivey *et al.*⁹² The ELISA testing of these compounds, and of other unpublished analogues, forms part of this PhD research and is described in this section.

Initial work in the Spivey group at Imperial College London (IC) on aspercyclide A was to synthesise the racemic (\pm)-aspercyclide A C19 methyl ether of the natural product. This compound had the advantage over the natural product that its synthesis started from a commercially available acetal so one less synthetic step was required and it displayed an improved activity when tested in an ELISA to that reported by Singh *et al.* for the natural product itself (IC_{50} for (\pm)-aspercyclide A C19 methyl ether = $110 \mu\text{M}$).⁹⁰ Racemic (\pm)-aspercyclide A C19 methyl ether (**\pm -1**) was synthesised by Dr Jimmy Sejberg, IC.⁹¹ This synthesis used a Pd(0)-catalysed germyl-Stille reaction as the key macrocyclisation step. Optical resolution of the racemic compound by CSP-HPLC was also used to separate the (+)-enantiomer (**+1**) in 98.4% enantiomeric excess (ee).⁹¹

The enantioselective synthesis of the natural product (+)-aspercyclide A was later carried out also by Dr Jimmy Sejberg, which employed a Krische iridium-catalysed, diastereo- and enantioselective alkoxyallylation to form the key *anti*-diol intermediate (two batches of this compound were synthesised: **+2a** and **+2b**).⁹² In order to check that the activity of aspercyclide A was not due to the benzaldehyde forming a Schiff base with the protein lysine residues, three analogues were also synthesised by Dr Jimmy Sejberg, where the benzaldehyde moiety was replaced with a different functional group. The first was an aldoxime **+3**, which was synthesised by the reaction of (+)-aspercyclide A with hydroxylammonium chloride. The second was a benzisoxazole **+4** which was synthesised by reacting the aldoxime **+3** with 2,3-dichloro-5,6-dicyano-1,4-benzoquinone (DDQ) and PPh_3 . The final analogue was a benzoxathiazine-2,2-dioxide **+5** which was made by reacting (+)-aspercyclide A with sulfamoyl chloride (see Table 4).

3.1.2 Testing aspercyclide A and analogues with the TR-FRET assay

(±)-Aspercyclide A C19 methyl ether (**(±)-1**), (+)-aspercyclide A C19 methyl ether (**(+)-1**) and (+)-aspercyclide A (**(+)-2a**) were tested with the TR-FRET assay. The concentration of IgE-Fc-A647 was fixed at 1.25 nM, the concentration of $\alpha\gamma$ -Tb was fixed at 0.5 nM and the inhibitor was prepared in 12 different concentrations, starting at 1 mM with 2-fold dilutions to a final concentration of 0.49 μ M. For each compound, two TR-FRET assays were carried out to investigate the order of addition of the proteins. Either the compound was pre-incubated with IgE-Fc-A647 for 1 hour, before adding $\alpha\gamma$ -Tb then reading the plate, or alternatively the compound was pre-incubated with $\alpha\gamma$ -Tb for 1 hour, before adding IgE-Fc-A647 and reading the plate. Further experimental details can be found in section 6.2.6 and the TR-FRET assay results are shown in Table 4.

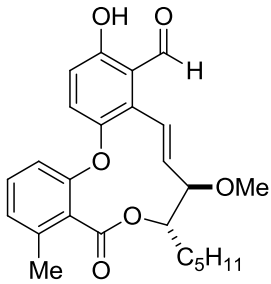
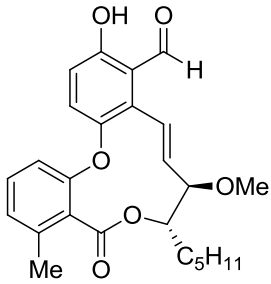
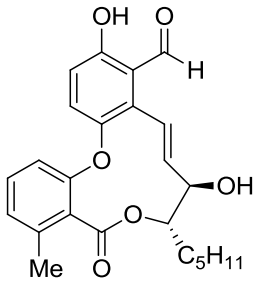
Compound reference	Structure	IC ₅₀ (μ M)	
		Pre-incubated with IgE-Fc-A647	Pre-incubated with $\alpha\gamma$ -Tb
((±)-1) (JS-039)		>1000	>1000
((+)-1) (JS-039-E1)		>1000	>1000
((+)-2a) (JS-291)		>1000	>1000

Table 4: TR-FRET inhibition assay IC₅₀ values for aspercyclide A and analogues

NB: The references in parenthesis indicate the Spivey research group compound reference number.

Unfortunately none of the compounds tested in the TR-FRET assays showed any inhibition of the interaction between IgE-Fc-A647 and $\alpha\gamma$ -Tb as they all had IC_{50} values of > 1 mM. This could have been because the fluorophores on the proteins were preventing the compounds from binding as they would do in the ELISA where unlabelled proteins are used. Or it could have been that the compounds were inhibiting the PPI, but they were also interfering with the TR-FRET assay in some way, for instance by autofluorescing, although this should have been accounted for with the 100 μ s time delay. Another possibility could be that their previous ELISA results were false positives, due to the number of processing steps and multiple reagents involved in the ELISA. It was therefore decided to test these aspercyclide A compounds with the ELISA described in section 2.1 to see if they displayed any activity.

3.1.3 Testing aspercyclide A and analogues with the ELISA

(\pm)-Aspercyclide A C19 methyl ether (\pm)-**1**, (+)-aspercyclide A (+)-**2a** and (+)-**2b** and the three analogues of (+)-aspercyclide with the benzaldehyde replaced with another functional group (+)-**3**, (+)-**4** and (+)-**5** were tested with the ELISA (see section 6.3.3 for the experimental details) and the results are shown in Table 5.

Compound reference	Structure	IC ₅₀ (μM)	Compound reference	Structure	IC ₅₀ (μM)
(±)-1 (JS-039)		>1000	(+)-3 (JS-287)		>1000
(+)-2a (JS-291)		424 ± 27 540 ± 220	(+)-4 (JS-289)		>1000
(+)-2b (JS-256-P)		>1000	(+)-5 (JS-312)		162 ± 5 463 ± 19

Table 5: ELISA inhibition assay IC₅₀ values for aspercyclide A and analogues

NB: The references in parenthesis indicate the Spivey research group compound reference number.

Multiple IC₅₀ values indicate the assay has been repeated on a different occasion.

It can be seen from Table 5 that (±)-aspercyclide A C19 methyl ether (**(±)-1**) did not show inhibition of the IgE:FcεRI interaction when tested in the ELISA. However, (+)-aspercyclide A (**(+)-2a**) did show moderate inhibition, for the two times this assay was carried out (IC₅₀ = 424 μM - 538 μM). This was likely to have been because it was enantiomerically pure (and it was found earlier that the (+)-enantiomer of the C19 methyl ether compound was 10-fold more active than the (-)-enantiomer).⁹¹ However, the other sample of the same compound (**(+)-2b**) did not display any activity, which could have been because it had a slightly different solubility or possibly because it contained residual contaminants from the synthesis. Neither the aldoxime analogue (**(+)-3**) nor the benzisoxazole analogue (**(+)-4**) of (+)-aspercyclide A displayed any activity. However, pleasingly, the benzoxathiazine-2,2-dioxide analogue of (+)-aspercyclide A (**(+)-5**) inhibited the IgE:FcεRI interaction with a slightly higher potency (IC₅₀ = 162 μM - 463 μM). These values are comparable to the ELISA IC₅₀ value of 200 μM first reported by Singh *et al.*⁸⁶ and to the ELISA IC₅₀ values reported by Spivey

et al.^{90,91} for (±)-aspercyclide A C19 methyl ether. These results also indicated that the activity of **(+)-5** was not attributed to the benzaldehyde moiety forming a Schiff base with protein lysine residues, which is consistent also with a specific binding mode and the difference in activity between the two enantiomers. These results for the (+)-aspercyclide A **(+)-2a** and its benzoxathiazine derivative **(+)-5** were published recently.⁹²

A challenging aspect of the ELISA testing of these compounds was that the compounds tended to display poor solubility when diluted from the 50 mM stock solution in DMSO to the 1 mM assay solution in PBS with 2% DMSO. This would mean that if not all the compound had gone into solution, the ELISA may not have given accurate results if the insoluble material was removed during the extensive washing steps and therefore the concentration of the compound in solution was not as high as it should have been. Alternatively, any insoluble compound could have bound non-specifically to the various components of the assay and the compound could have appeared to be more active than it actually was.

To overcome these solubility issues, the ELISA was repeated multiple times with variations in the assay conditions using compound **(±)-1**. The assay solution of **(±)-1** was made up in carbonate buffer pH 9.6, rather than PBS pH 7.3, in the hope that the more basic pH would deprotonate the compound and increase aqueous solubility. However, the ELISA did not work with the carbonate buffer, probably due to the sensitivity of the proteins to changes in pH. The original ELISA was then repeated using PBS 5% DMSO, rather than PBS 2% DMSO, in the hope the increased DMSO content would aid solubility, however this technique did not result in any improvement on the solubility of the compound. Finally, the original assay was carried out as normal, but the compound was first heated in a water bath up to ~ 50 °C, with intermittent vigorous shaking, which was successful in ensuring all of the compound was dissolved and it was also found that the high temperature did not cause any decomposition of the compound. This technique for dissolving was used to varying degrees for all compounds tested in the ELISA, to ensure complete dissolution into the aqueous buffer for use in the assay.

3.1.4 Soak crystallisation of (+)-aspercyclide A C19 methyl ether (+)-1 with IgE-Fc

Obtaining an x-ray co-crystal structure of aspercyclide A or an analogue bound to either IgE-Fc or FcεRI would give valuable information on what contacts are made between the inhibitor and the protein and would facilitate the development of molecules that bind with a higher affinity. As it is not known which protein of the IgE:FcεRI interaction is targeted by aspercyclide A, it was decided to first carry out crystallisation experiments with IgE-Fc and an aspercyclide A compound, as IgE-Fc was readily available and the crystallisation conditions had been previously established.^{16,22,33}

(±)-Aspercyclide A C19 methyl ether **(+)-1** was chosen, as this was previously found to inhibit the IgE:FcεRI interaction with ELISA ($IC_{50} = 40 \mu\text{M}$) reported by Spivey *et al.*⁹¹ and there was a large enough quantity of this compound available for the experiments (unfortunately there was not enough of the more active compound **(+)-5** available). Soak crystallisations were carried out, where the compound was added into crystals of IgE-Fc, as a compound of this size should fit through the protein crystal channels. Soak crystallisations were carried out using **(+)-1** (2.5 mM) and 4 – 6 apo crystals of IgE-Fc (crystals provided by Dr Nyssa Drinkwater, KCL). After incubation at 18 °C for 5 – 10 days, individual crystals were frozen in liquid nitrogen and x-ray diffraction data was collected at the Diamond Light Source synchrotron (data collection carried out by Dr Nyssa Drinkwater, KCL). Further experimental details can be found in section 6.6. Figure 33 shows a photo of the crystal used for the data collection and the x-ray diffraction pattern obtained and Table 6 shows the data collection statistics.

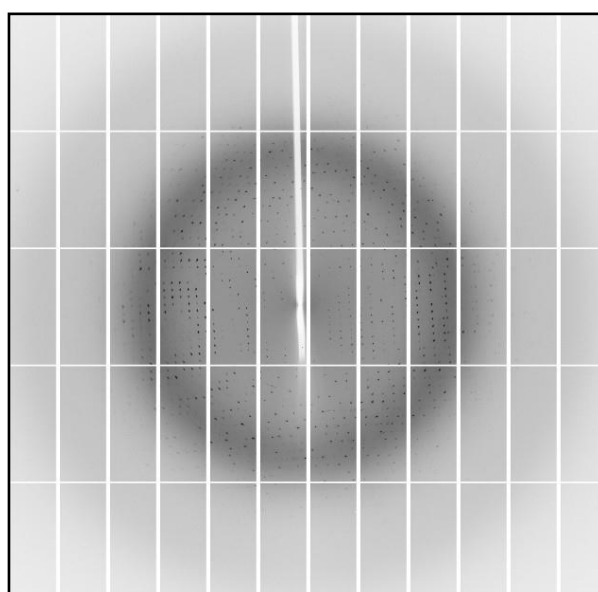
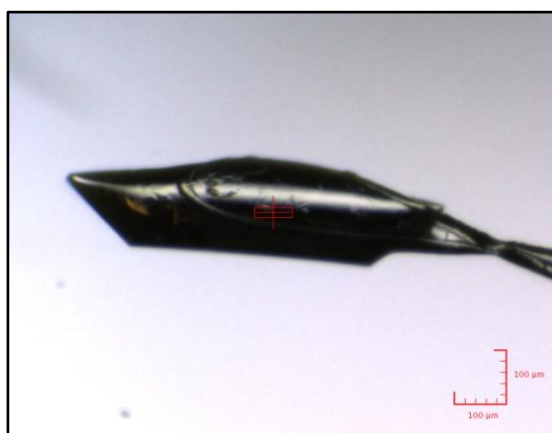


Figure 33: Crystal photo and x-ray diffraction - soak crystallisation of **(+)-1** with IgE-Fc

Resolution (Å)	2.29
R_{merge}	0.092
I/sigma	13.8
Completeness (%)	98.0
Multiplicity	3.9
Average unit cell	a = 129.31, b = 74.60, c = 79.78
Space group	P 2 ₁ 2 ₁ 2

Table 6: Data collection statistics for soak crystallisation of (+)-1 with IgE-Fc

It can be seen from Table 6 that the crystal diffracted to a high resolution of 2.29 Å with ideal data collection statistics for the subsequent solving of the crystal structure. The crystal structure was solved by molecular displacement using a high resolution structure of IgE:Fc (PDB code 2WQR²²) and the CCP4 software Phenix Refine and Coot. Weak electron density was found, that did not match to the IgE-Fc structure, therefore **(+)-1** was modelled into the structure using its simplified molecular-input line-entry system (SMILES) code. A second round of refinement was carried out, however unfortunately the electron density refinement did not improve enough to confirm if the compound was bound to IgE-Fc.

This result could indicate that **(+)-1** does not bind to IgE-Fc, but binds instead to FcεRI, which is why a co-crystal structure of **(+)-1** bound to IgE-Fc was not obtained. Alternatively, **(+)-1** could bind to IgE-Fc, but not with a high enough affinity for a co-crystal structure to be obtained. Further x-crystallography experiments could be carried out, for instance co-crystallisations with IgE-Fc instead of soak crystallisations, or using IgE-Fc₃₋₄ instead of IgE-Fc, as this protein is more flexible and may give different packing forms. The receptor protein sFcεRIα could be used instead for crystallisation experiments, as this may be the protein with which **(+)-1** interacts, although sFcεRIα is more expensive and less easily crystallised than IgE-Fc, so potency may need to be improved before it would be worth using this protein.

3.2.6 Novartis data for aspercyclide A and analogues

The (±)-aspercyclide A C19 methyl ether **(±)-1**, (+)-aspercyclide A **(+)-2b** and the benzothiazine analogue of (+)-aspercyclide A **(+)-5** were also tested in an ELISA by a collaborator at Novartis, Horsham (Dr Jeffrey Stonehouse) in order to confirm the earlier ELISA results. **(±)-1** showed no inhibition of the IgE:FcεRI interaction which confirmed the earlier result, **(+)-2b** displayed inhibition of the IgE:FcεRI interaction but an IC₅₀/EC₅₀ value could not be calculated from the data and **(+)-5** inhibited the interaction (EC₅₀ = 124 – 156 μM). These are pleasing results and confirm the ELISA activity reported earlier for these compounds (Table 4).

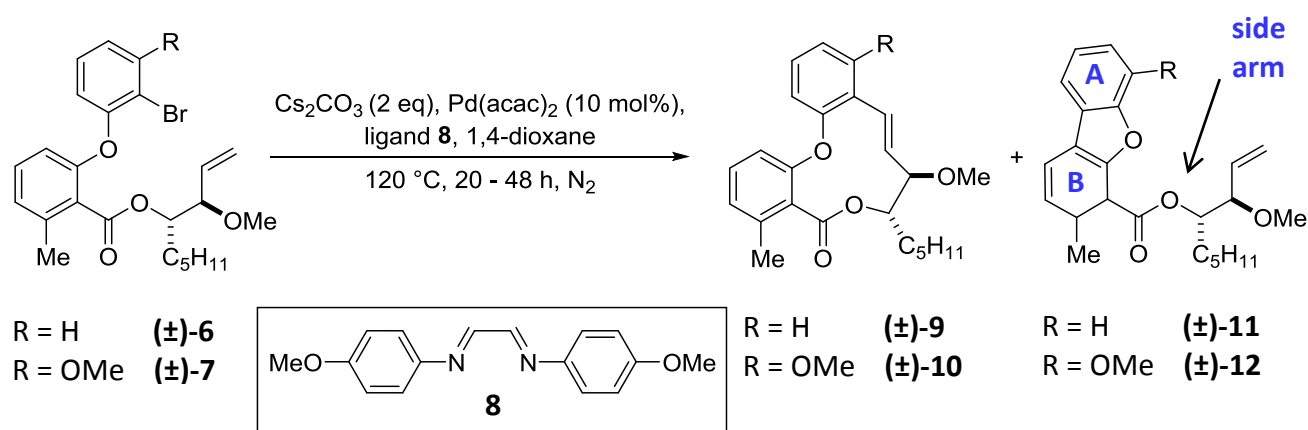
The same compounds were also tested by Novartis in a FRET assay, however none of the compounds displayed inhibition in this assay. This also confirms the earlier result where it was found that **(±)-1a** and **(+)-2a** did not display activity in the TR-FRET assay (Table 3).

(±)-1, **(+)-2b** and **(+)-5** were also tested for binding to immobilised IgE-Fc and full length IgE in SPR experiments carried out by Novartis. The benzothiazine derivative of (+)-aspercyclide A **(+)-5** was found to display weak binding to both IgE-Fc and full length IgE when tested at 200 μM, however this binding was not enough for the compound to be considered as a 'hit' by Novartis. Further details can be found in section 6.10.

3.2 Dibenzofurans

3.2.1 Design and synthesis of dibenzofurans

Further work in the Spivey group at IC was to synthesise more analogues of aspercyclide A to try to build up information about the structure activity relationship (SAR) of these compounds. Heck-Mizoroki reactions of bromide intermediates (**±**)-**6** and (**±**)-**7** were carried out (by Dr Helena Dennison, IC) which made use of ligand **8**. As well as forming the desired aspercyclide A C19 methyl ether analogues (**±**)-**9** and (**±**)-**10**, the dibenzofuran by-products (**±**)-**11** and (**±**)-**12** were also formed (Scheme 11).¹³⁸



Scheme 11: Dennison's Heck-Mizoroki reaction of bromide intermediates¹³⁸

A and B denote the two benzene rings of the dibenzofuran compounds and side-arm denotes the large substituent on ring B.

It was decided to isolate dibenzofurans (**±**)-**11** and (**±**)-**12** and test them as potential inhibitors of the IgE:FcεRI interaction, as it would be interesting to see if compounds containing this different scaffold could also inhibit the interaction.

3.2.2 Testing dibenzofurans with the TR-FRET assay

The dibenzofuran compounds (**±**)-**11** and (**±**)-**12** were tested in the TR-FRET assay using the same procedure as before and the results can be seen in Table 7.

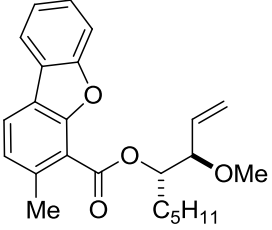
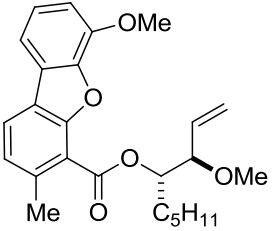
Compound reference	Structure	IC ₅₀ (μM)	
		Pre-incubated with IgE-Fc-A647	Pre-incubated with αγ-Tb
(±)-11 (HJD-107)		>1000	>1000
(±)-12 (HJD-115)		>1000	>1000

Table 7: TR-FRET inhibition assay IC₅₀ values for dibenzofurans (±)-11 and (±)-12

NB: The references in parenthesis indicate the Spivey research group compound reference number.

Unfortunately, neither of the dibenzofurans (±)-11 and (±)-12 inhibited the IgE:FcεRI interaction when tested with the TR-FRET assay. As mentioned in section 3.1.2, this lack of inhibition could have been because the fluorophores on the proteins were preventing the compounds from binding as they would do to the native protein. Or it could have been that the compounds were inhibiting the interaction between IgE and FcεRI, but were interfering with the TR-FRET assay by possibly autofluorescing. It was decided to test these dibenzofurans with the ELISA to confirm the results.

3.2.3 Testing dibenzofurans with the ELISA

The dibenzofuran (±)-11 had previously been tested in an ELISA by collaborators at KCL and it was found to show good activity against the IgE:FcεRI interaction (IC₅₀ = 2 μM, unpublished data, Dr Fabienne Saab and Dr Mary Holdom, KCL). Dibenzofurans (±)-11 and (±)-12 were tested with the ELISA described in section 2.1 and the results can be seen in Table 8.

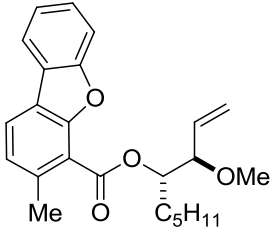
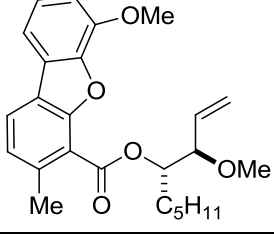
Compound reference	Structure	IC ₅₀ (μM)
(±)-11 (HJD-107)		3 ± 0.1 5 ± 0.3
(±)-12 (HJD-115)		205 ± 51

Table 8: ELISA inhibition assay IC₅₀ values for dibenzofurans (±)-11 and (±)-12

NB: The references in parenthesis indicate the Spivey research group compound reference number. Multiple IC₅₀ values indicate the assay has been repeated on a different occasion.

It can be seen that dibenzofuran **(±)-11** showed good inhibition of the IgE:FcεRI PPI (IC₅₀ = 3 μM - 5 μM). This is consistent with the ELISA IC₅₀ value reported by collaborators at KCL, however it is unusual that this compound exhibited no inhibition at all in the TR-FRET assay (Table 7) and this could indicate that both sets of ELISA results were false positives. As there are multiple processing steps involved in the ELISA, this may have resulted if **(±)-11** was inhibiting the binding of biotinylated anti-IgE-Fc to IgE-Fc for instance, or inhibiting the enzymatic reaction of OPD by the enzyme HRP. However, the thorough washing between each stage of the assay should have ensured that there was no inhibitor left when these secondary reagents were added. The false positive hypothesis could be investigated by carrying out a modified ELISA, with either IgE-Fc or αγ not present, to see if the ELISA signal was still inhibited by **(±)-11**. The other dibenzofuran **(±)-12** showed inhibition of the IgE:FcεRI interaction to a lesser extent (IC₅₀ = 205 μM), which indicated that the methoxy substituent is not tolerated in this position on ring A.

Since **(±)-11** displayed such promising activity against the IgE:FcεRI interaction, a series of analogues were synthesised by Dr Helena Dennison, IC¹³⁸ in order to build up SAR data for these compounds. In these dibenzofuran analogues, either the methoxy group, the pentyl group or both groups were not present on the side arm of ring B, and for each case, the methyl substituent on ring B was either present or not present (compounds **13**, **14**, **15**, **(±)-16**, **17**, **18** and **19**). It would be interesting to find out if the dibenzofuran scaffold was required for activity or not, so a bromide

analogue (**±**)-**20**, where only ring B was present, was synthesised (Dr Jimmy Sejberg, IC). Conversely, it would also be interesting to determine if the side arm of ring B was required for the activity or not, so analogue **21**, with a carboxylic acid group in place of the side arm on ring B, was also synthesised (Dr Jimmy Sejberg, IC). Finally, the commercially available compound dibenzofuran-4-carboxylic acid **22** was also obtained. All of these compounds were then tested with the ELISA and the compound structures and ELISA IC₅₀ results can be seen in Table 9.

Compound reference	Structure	IC ₅₀ (μM)	Compound reference	Structure	IC ₅₀ (μM)
13 (HJD-205)		576 ± 122	18 (HJD-214)		>1000
14 (HJD-210)		>1000	19 (HJD-212)		>1000
15 (HJD-211)		>1000	(±)-20 (JS-004/26)		>1000
(±)-16 (HJD-186)		>1000	21 (JS-322)		462 ± 89
17 (HJD-213)		>1000	22		>1000

Table 9: ELISA inhibition assay IC₅₀ values for dibenzofuran analogues of (±**)-11**

NB: The references in parenthesis indicate the Spivey research group compound reference number.

It can be seen that compounds **13** and **21** displayed a moderate inhibition of the IgE:FcεRI interaction ($IC_{50} = 576 \mu\text{M}$ and $462 \mu\text{M}$ respectively), but none of the other inhibitors showed any activity. This indicates that the methyl substituent is required on ring B and that the dibenzofuran core is also important, but that the exact nature of the side arm is less important. It was unexpected that of all these analogues, only two showed a moderate activity, which was 100-fold weaker than that of (\pm)-**11**. It therefore seemed likely that the (\pm)-**11** ELISA IC_{50} value was indeed a false positive and that this compound was inhibiting a different component of the ELISA and not actually the IgE:FcεRI interaction.

In order to confirm the activity, or lack thereof, of (\pm)-**11** this compound was re-synthesised (by Dr Jimmy Sejberg, IC) which is referred to as (\pm)-**23** and this was also tested in the ELISA. The ligand **8** from the Heck-Mizoroki reaction in Scheme 11 (synthesised by Dr Daniel Offerman, IC) was also tested in the ELISA, in case a very small amount of this ligand could have been contaminating the sample of (\pm)-**11** and causing the activity. These ELISA results can be seen in Table 10.

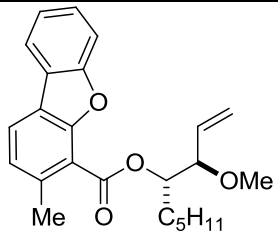
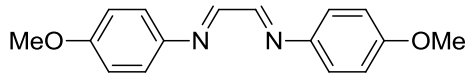
Compound reference	Structure	IC_{50} (μM)
(\pm)- 23 (JS-331)		>1000 >1000
8 (DAO-268)		>1000

Table 10: ELISA inhibition assay IC_{50} values for dibenzofuran (\pm)-23** and ligand **8****

NB: The references in parenthesis indicate the Spivey research group compound reference number. Multiple IC_{50} values indicate the assay has been repeated on a different occasion.

The re-synthesised dibenzofuran (\pm)-**23** was tested twice but did not show any inhibition of the IgE:FcεRI interaction. This seems to confirm that the original sample of this compound, (\pm)-**11**, was a false positive, or was possibly contaminated with a small amount of another much more active compound, however all compounds were analysed by liquid chromatography-mass spectrometry

(LC-MS) to confirm their purity before testing in all assays. Ligand **8** did not inhibit the IgE:FcεRI interaction, indicating that it was unlikely to be this ligand that was contaminating the sample and contributing to the activity. At the same time as the synthesis and testing of these new analogues of (**±**)-**11**, other biophysical and structural experiments were also being carried out on (**±**)-**11**, which are discussed below.

3.2.4 Soak crystallisation of dibenzofuran (**±**)-**11** with IgE-Fc

Soak crystallisation experiments were carried out using (**±**)-**11** (2.5 mM) and 4 – 6 apo crystals of IgE-Fc (crystals provided by Dr Nyssa Drinkwater, KCL). After incubation at 18 °C for 5 – 10 days, individual crystals were frozen in liquid nitrogen and x-ray diffraction data was collected at the Diamond Light Source synchrotron (data collection carried out by Dr Nyssa Drinkwater). Figure 34 shows a photo of the crystal used for the data collection as well as the x-ray diffraction pattern obtained and Table 11 shows the data collection statistics.

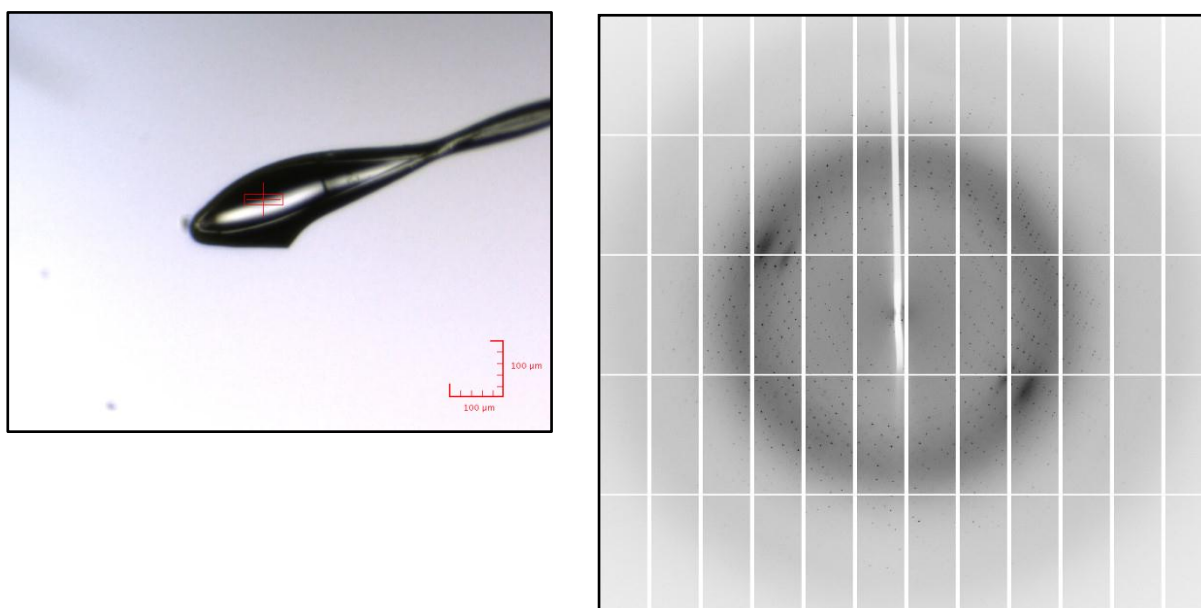


Figure 34: Crystal photo and x-ray diffraction for soak crystallisation of (±**)-**11** with IgE-Fc**

Resolution (Å)	2.15
R_{merge}	0.064
I/sigma	18.2
Completeness (%)	99.7
Multiplicity	3.9
Average unit cell	a = 129.08, b = 74.67, c = 79.29
Space Group	P 2 ₁ 2 ₁ 2

Table 11: Data collection for soak crystallisation of (±)-11 with IgE-Fc

It can be seen from Table 11 that the data collection statistics for this experiment are good and the crystal diffracted to a high resolution of 2.15 Å. Crystal structures were solved as described in section 3.1.4, by molecular displacement using a high resolution structure of IgE:Fc (PDB code 2WQR²²). As for the aspercyclide compound, weak electron density was found, that did not match to the IgE-Fc structure, therefore (±)-11 was modelled into the structure using its SMILES code. A second round of refinement was carried out, however the electron density refinement did not improve enough to confirm if the compound was bound to IgE-Fc. This result could indicate that (±)-11 does not bind to IgE-Fc, but binds instead to FcεRI, or that it does bind to IgE-Fc, but not with a high enough affinity for a co-crystal to be obtained. The additional crystallisation experiments described in section 3.1.4 could be carried out for (±)-11, but in light of the ELISA results of analogues of (±)-11 and the re-synthesised compound (±)-23, it seems likely that this compound does not actually inhibit the IgE:FcεRI interaction.

3.2.5 SPR experiments with dibenzofuran (±)-11

SPR experiments were carried out, using the SPR chip with immobilised αγ as described in section 2.4. An initial experiment was carried out, to see if (±)-11 could inhibit the binding of IgE-Fc to immobilised αγ. A solution of IgE-Fc (10 nM) with (±)-11 (10 μM), that had been pre-incubated for 1 hour, was injected over the αγ-chip. An increase of ~ 30 resonance units was observed, which was the same increase as when no inhibitor was present, which indicated that no inhibition was taking place. An inhibition assay was then set up to confirm this, where various different concentrations of (±)-11 were used. Solutions of (±)-11 at 10 different concentrations (160 μM to 0.3 μM) and IgE-Fc (10 nM in each solution) were pre-incubated for 1 hour, before being injected

over the α -chip. A glycine injection between each different solution was used to remove any IgE-Fc bound to the chip. The sensorgrams for this inhibition assay can be seen in Figure 35.

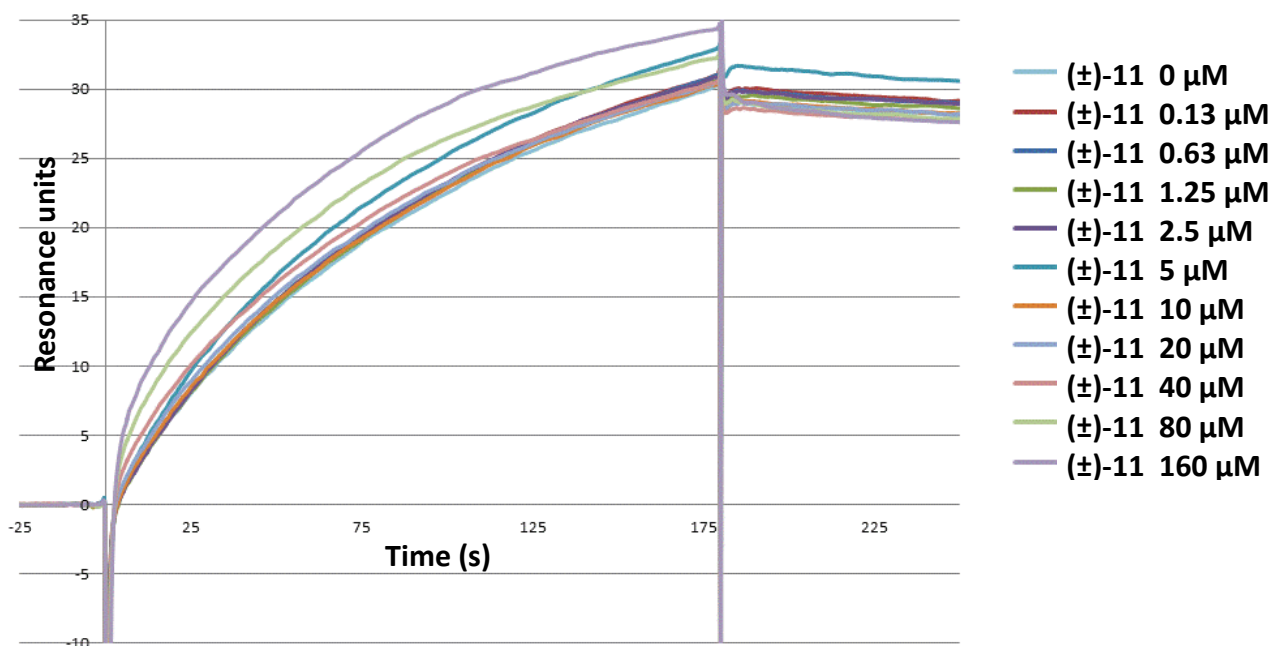


Figure 35: SPR sensorgrams for inhibition assay of IgE-Fc and immobilised α with (±)-11

These sensorgrams show that for the highest concentration of (±)-11 of 160 μ M, there is a higher signal. However, it would be expected that at the highest concentration of (±)-11, there would be less IgE-Fc binding to immobilised α which would result in a lower signal. This result could imply that the compound was binding non-specifically to the chip itself, however there was only a small difference of \sim 5 resonance units between no inhibitor present and 160 μ M inhibitor present, so it would seem that the compound was not inhibiting IgE-Fc binding to immobilised α . This is also consistent with the fact that (±)-11 did not show binding to IgE-Fc in the crystallography experiments.

3.2.6 Novartis data for dibenzofurans

The dibenzofurans **13**, (±)-**16**, **21** and (±)-**23** were tested for their ability to inhibit the IgE:Fc ϵ RI interaction in an ELISA and a FRET inhibition assay and for their ability to bind to immobilised IgE-Fc and full length IgE in SPR experiments by a collaborator at Novartis, Horsham (Dr Jeffrey Stonehouse). No inhibition or binding was observed for any of these compounds by Novartis. This mainly confirms the results found earlier. There was a moderate inhibition seen in my ELISA for **13** and **21** (Table 8) but it may have been because my ELISA is more sensitive than the Novartis ELISA.

Chapter 4: Peptide inhibitors of the IgE:FcεRI PPI

As discussed in section 1.5, peptides have been widely investigated as inhibitors of the interaction between IgE and FcεRI. A number of disulfide-constrained, cyclic peptides have been reported, that inhibit this interaction with IC₅₀ values in the micromolar to nanomolar range. The design, synthesis and testing of peptide inhibitors of the IgE:FcεRI interaction forms the main part of this PhD research and is discussed in this section.

4.1 Design and synthesis of peptide inhibitors

4.1.1 Peptide design

An 8-residue, linear peptide was synthesised which consisted of residues Tyr(116) to Asp(123) of the C-strand of the C-C' loop of FcεRI, a hotspot region of FcεRI which binds to the IgE Cε3 domain and the IgE Cε2-Cε3 linker region (Figure 36).

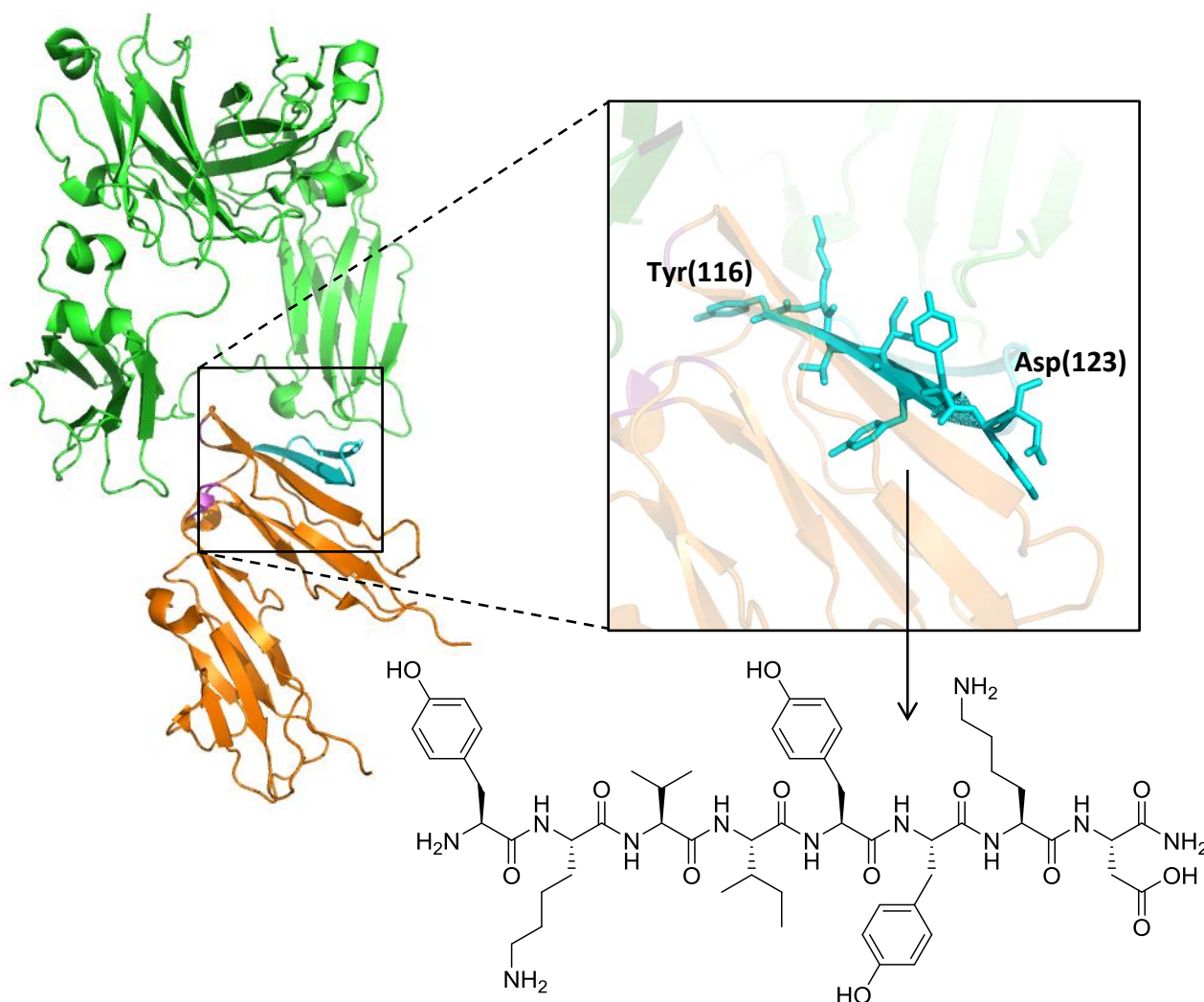


Figure 36: Structure of linear, 8-mer peptide based on C-strand of C-C' loop of FcεRI
IgE-Fc₃₋₄ is shown in green, sFcεRIα is shown in orange and binding site 1 is shown in pale blue.

It was originally envisaged that this peptide (based on the key binding epitope of FcεRI) may mimic this region and therefore compete with FcεRI for binding to IgE-Fc. However, it was found (by Dr Bingli Mo, IC) that the reverse sequence of this peptide (which was synthesised by Dr Bingli Mo in error) inhibited the IgE:FcεRI interaction when tested with an ELISA ($IC_{50} \sim 100 \mu M$) but that the actual C-strand peptide sequence from FcεRI (Figure 36) did not show any inhibition.¹³⁹ This could imply that the original C-strand peptide was not actually mimicking the FcεRI hotspot region and therefore its mode of action of inhibition could actually involve binding to either protein, or indeed binding to the complex. Subsequent alanine scanning of the reverse-sequence peptide found that Tyr(3) was a key residue for binding affinity (Dr Bingli Mo, IC).¹³⁹ During the MRes research project, the reverse-sequence peptide was synthesised, along with analogues where Tyr(3) was substituted for other aromatic residues Phe, Trp and His.¹³¹ These peptides were tested in an ELISA and it was found that the reverse-sequence peptide inhibited the IgE:FcεRI interaction ($IC_{50} = 219 \mu M$) and the peptide with Phe in position 3 had improved inhibition ($IC_{50} = 99 \mu M$).¹³¹

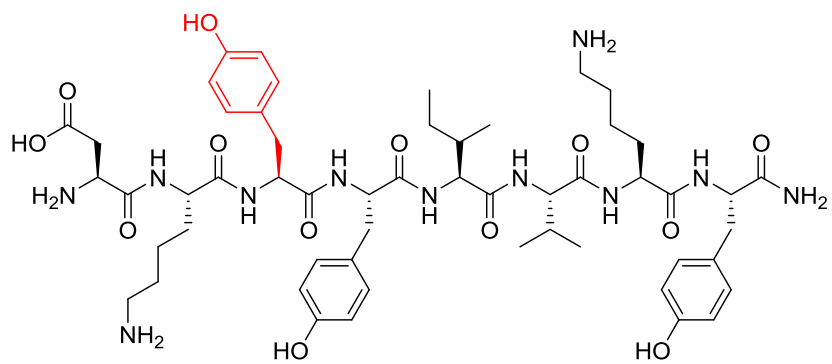
During this PhD research, these peptides were re-synthesised and another analogue with the unnatural amino acid biphenylalanine (Bip) substituted at position 3 was also synthesised to further investigate the SAR and to see if a larger group was tolerated at this position. It was planned to then use the TR-FRET assay to test the peptides, and compare the results to the ELISA results obtained previously. It was also planned to carry out structural and biophysical experiments, including x-ray crystallography and SPR assays, on the most active peptides, to ascertain their mode of action of inhibition. An overview of the peptides used during this PhD and any previous ELISA IC_{50} values can be seen in Table 12 and their structures can be seen in Figure 37.

Peptide name	Peptide sequence	Previous ELISA IC_{50} (μM)
C-strand-peptide	H ₂ N-Tyr-Lys-Val-Ile-Tyr-Tyr-Lys-Asp-CONH ₂	>1000 ^a
Parent-peptide (reverse sequence of C-strand)	H ₂ N-Asp-Lys- Tyr -Tyr-Ile-Val-Lys-Tyr-CONH ₂	219 ± 8 ^b
Phe(3)-peptide	H ₂ N-Asp-Lys- Phe -Tyr-Ile-Val-Lys-Tyr-CONH ₂	99 ± 17 ^b
Trp(3)-peptide	H ₂ N-Asp-Lys- Trp -Tyr-Ile-Val-Lys-Tyr-CONH ₂	204 ± 13 ^b
His(3)-peptide	H ₂ N-Asp-Lys- His -Tyr-Ile-Val-Lys-Tyr-CONH ₂	>1000 ^b
Bip(3)-peptide	H ₂ N-Asp-Lys- Bip -Tyr-Ile-Val-Lys-Tyr-CONH ₂	not yet tested

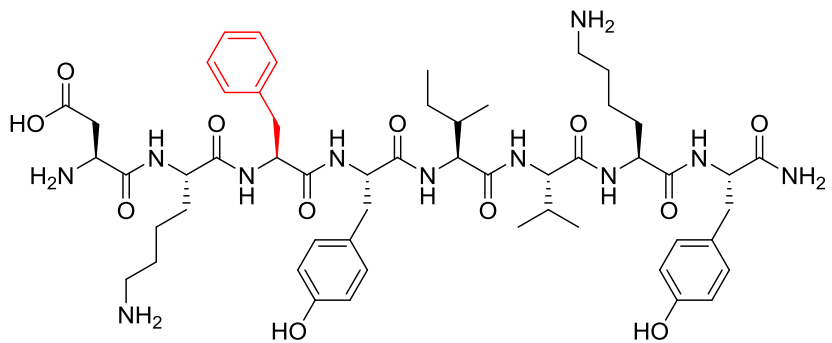
Table 12: Peptides investigated

^aELISA carried out by Dr Bingli Mo, IC.¹³⁹ ^bELISA carried out during MRes research project.¹³¹ Residues in position 3 are shown in bold. (NB: H₂N- denotes free N-terminus, -CONH₂ denotes amidated C-terminus).

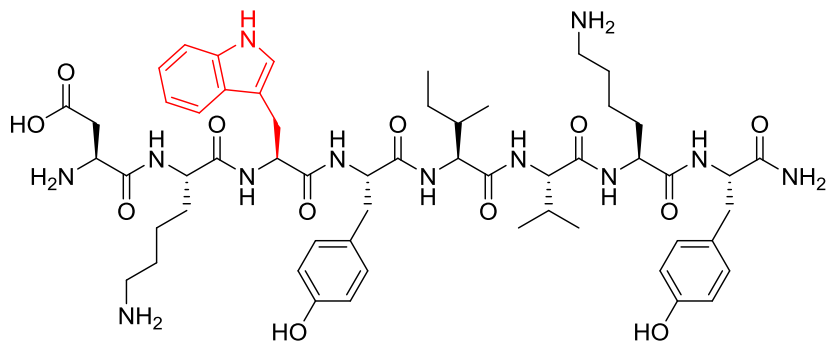
Parent-peptide



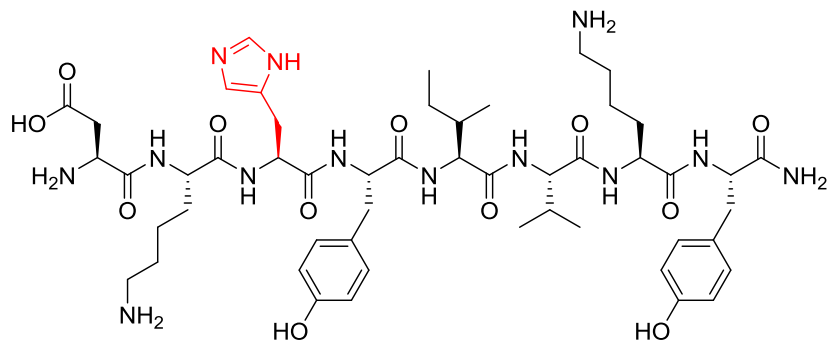
Phe(3)-peptide



Trp(3)-peptide



His(3)-peptide



Bip(3)-peptide

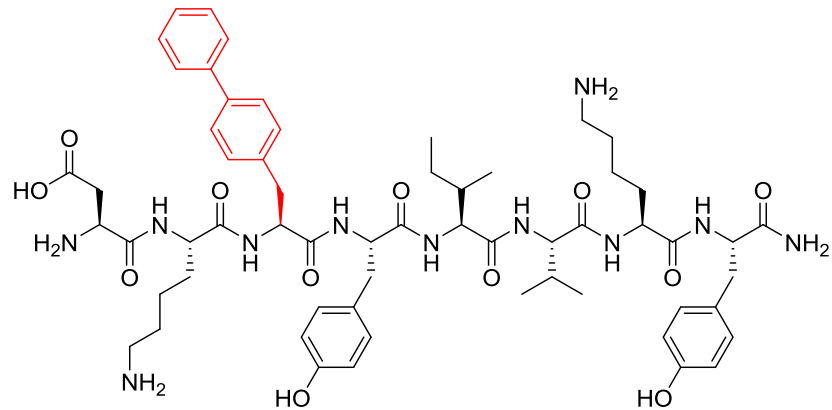


Figure 37: Structures of peptides

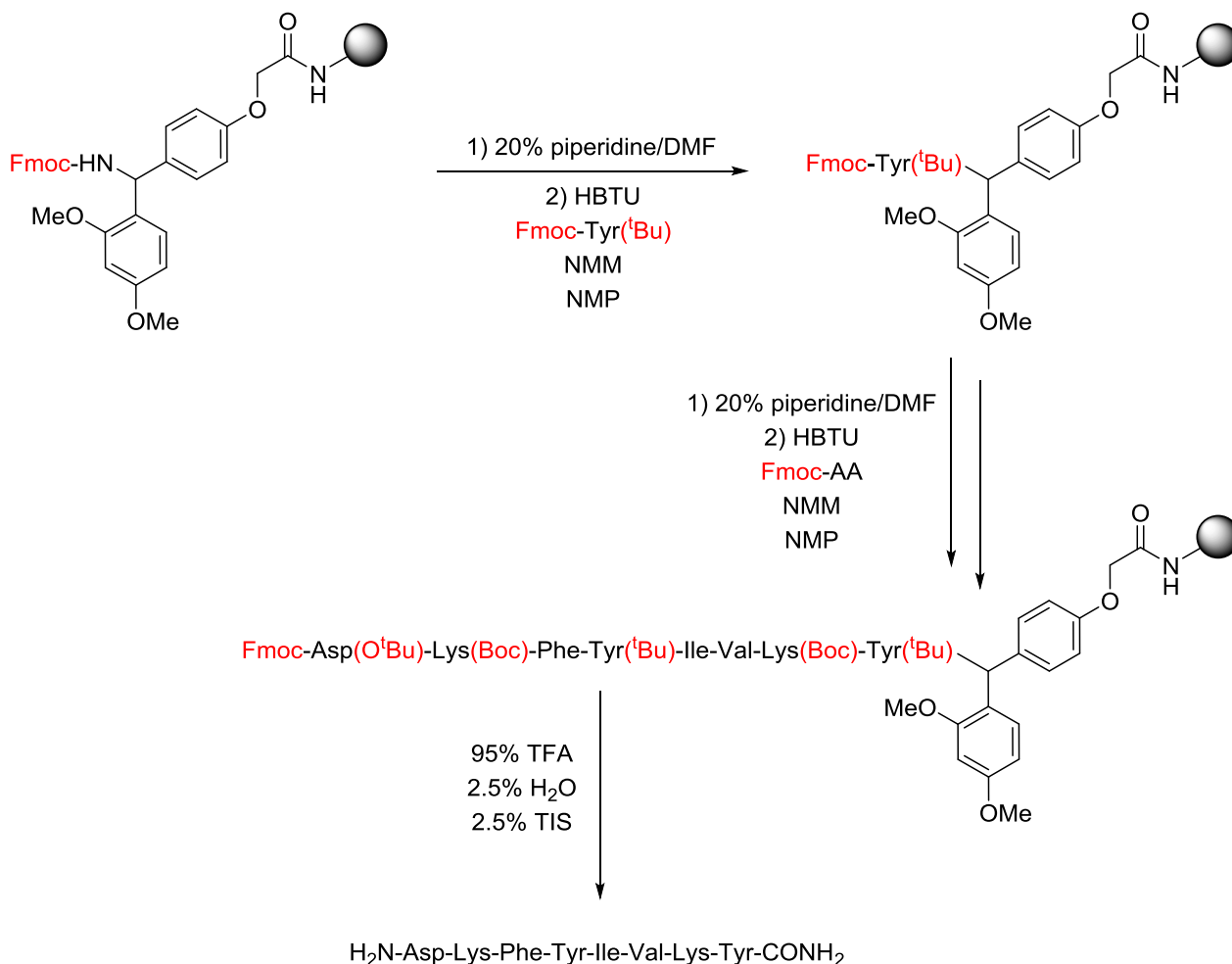
4.1.2 Solid phase peptide synthesis

Peptides were synthesised by automated solid phase peptide synthesis (SPPS), a method which has been widely used in peptide research for many years. SPPS, originally developed by Merrifield in the 1960s, uses a polystyrene resin, to which each amino acid is coupled in turn to build up the peptide from the C-terminus to the N-terminus.¹⁴⁰ The major benefit of this technique is that the insolubility of the resin allows reagents and by-products to be easily removed by simply washing the resin and a wide variety of resins are available for various peptide applications. The repetitive nature of SPPS lends itself to automation and instruments can simultaneously carry out the synthesis of a number of different peptide sequences of up to 30 residues in length. The most common method of SPPS makes use of fluorenylmethoxycarbonyl (Fmoc) as a temporary amine protecting group for each amino acid, which is removed before each coupling reaction with a mild base.^{141,142} The incoming amino acid is activated and then coupled to the deprotected amine of the previous residue.^{143,144}

Peptides were synthesised by automated Fmoc SPPS using an Intavis AG ResPep SL instrument. A TentaGel S Rink Amide Resin was used, which is a copolymer consisting of a low crosslinked polystyrene matrix onto which PEG is attached via an ethyl ether linker. The linker increases resin stability and the PEG group has hydrophilic and hydrophobic properties, therefore the TentaGel resins have been found to give good peptide yields. This Rink amide resin was chosen so that the C-terminus was left with an amide functionality following cleavage from the resin. Peptides were synthesised with a C-terminal amide, as this was previously found (by Dr Bingli Mo) to give peptides an improved potency over the C-terminal free carboxylic acid group.

The first step in the synthesis was removal of the Fmoc protecting group from the resin using 20% piperidine in dimethylformamide (DMF), then the C-terminal Fmoc-protected amino acid was activated and coupled to the resin using 2-(1*H*-benzotriazol-1-yl)-1,1,3,3-tetramethyluronium hexafluorophosphate (HBTU) and 4-methylmorpholine (NMM) in 1-methyl-2-pyrrolidinone (NMP). The resin was then washed with DMF to remove any side-products or unreacted material and a solution of 5% acetic anhydride in DMF was added to cap any unreacted N-terminal amine on the growing peptide, followed by another washing step. This process was repeated until the peptide was the desired length, then the resin-bound peptide was removed from the synthesiser, washed with DMF, dichloromethane, methanol and diethyl ether and dried under vacuum. The peptide was then cleaved from the resin, with simultaneous removal of the N-terminal Fmoc group and

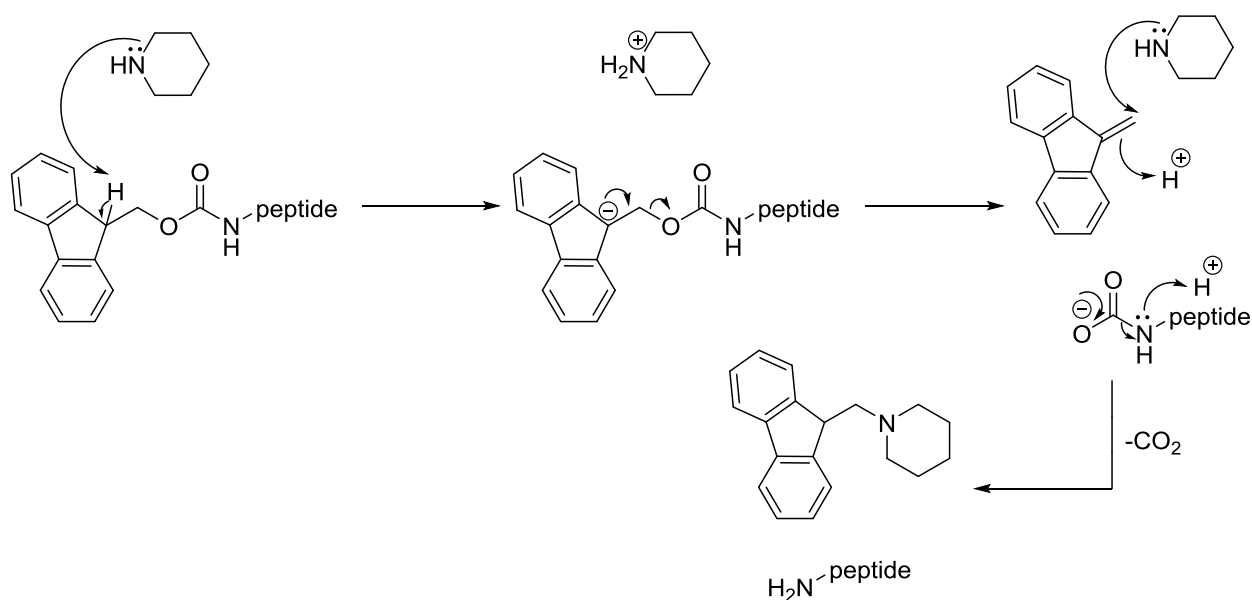
the side chain protecting groups, with 95% trifluoroacetic acid (TFA), 2.5% H₂O and 2.5% triisopropylsilane (TIS). The free peptide was then precipitated from the TFA solution with ice-cold *tert*-butylmethylether (TBME). Further details of the experimental procedure can be found in section 6.9 and an overview of the synthesis (for **Phe(3)-peptide**) is shown in Scheme 12.



Scheme 12: Overview of Fmoc SPPS of Phe(3)-peptide using TentaGel S Rink amide resin

The Fmoc protecting group was removed from the resin using 20% piperidine in DMF. The Fmoc-protected amino acid (with side-chain protecting group shown in parenthesis) was then coupled using HBTU and NMM. The Fmoc deprotection and amino acid coupling cycle was repeated until the peptide was the desired length. The peptide was then cleaved from the resin using 95% TFA, 2.5% TIS and 2.5% H₂O which also removed any side chain protecting groups to leave the free peptide with a C-terminal amide.

The mechanism for the Fmoc deprotection at the N-terminus of a peptide involves piperidine abstracting the dibenzylic proton from the Fmoc group, following which the resulting aromatic anion undergoes E1C_B elimination to generate dibenzofulvene and a carbamic acid terminated peptide. Piperidine then adds to the dibenzofulvene to form a side-product, which can be removed by washing, and loss of carbon dioxide from the carbamic acid terminated peptide leaves the free amine, ready for the subsequent coupling reaction (Scheme 13).

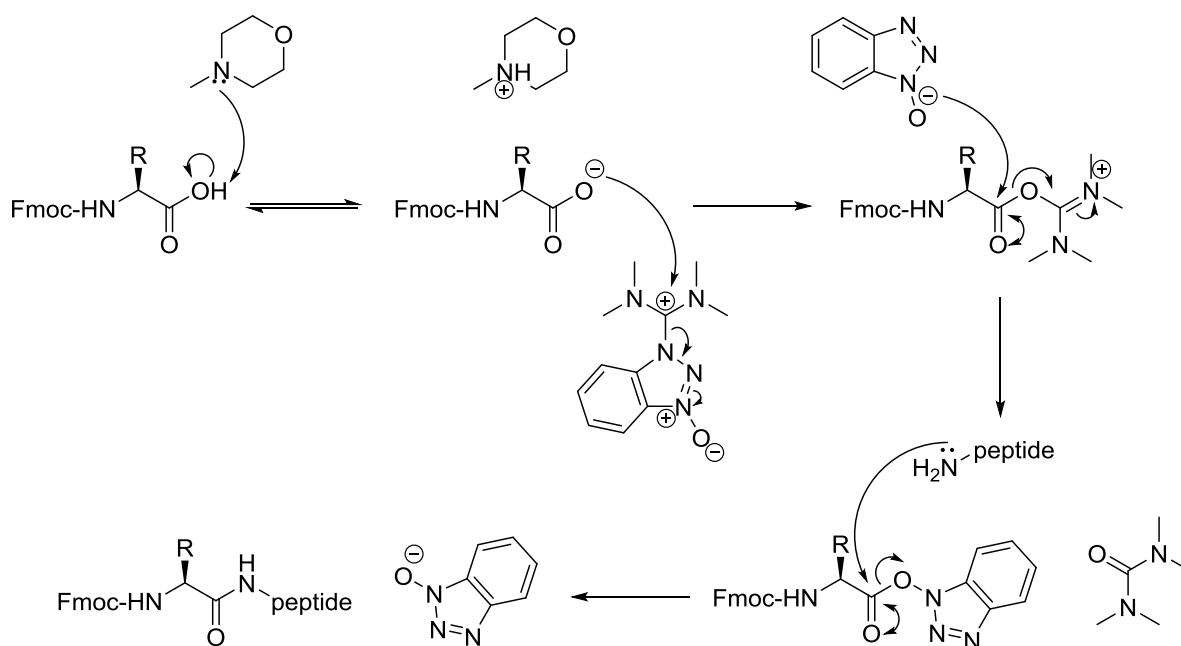


Scheme 13: Mechanism for deprotection of an Fmoc group from the N-terminus of a peptide

The dibenzyl proton of the Fmoc group is abstracted by piperidine to leave an aromatic anion, which eliminates dibenzofulvene to leave a carbamic acid terminated peptide. CO_2 is eliminated from the peptide to leave the free N-terminus and the excess piperidine adds to the dibenzofulvene to give a by-product.

Coupling of the subsequent amino acid requires activation of the amino acid carboxylate to generate an active ester which would be a better leaving group. Commonly used activating/coupling agents are uronium or phosphonium salts of non-nucleophilic anions, including HBTU, 1-[bis(dimethylamino)methylene]-1*H*-1,2,3-triazolo[4,5-*b*]pyridinium 3-oxide hexafluorophosphate (HATU), 1-[bis(dimethylamino)methylene]-5-chlorobenzotriazolium 3-oxide hexafluorophosphate (HCTU), *N,N,N',N'*-tetramethyl-*O*-(benzotriazol-1-yl)uronium tetrafluoroborate (TBTU) and (benzotriazol-1-yloxy)tripyrrolidinophosphonium hexafluorophosphate (PyBOP).

HBTU was used for this peptide synthesis, as it produces hydroxybenzotriazolyl esters that are highly reactive towards nucleophiles. The HBTU activation/coupling mechanism begins with deprotonation of the amino acid carboxyl group by the organic base NMM. The deprotonated carboxyl group then attacks HBTU to form an *O*-acyl isourea activated intermediate and the benzotriazolyl anion, this anion then attacks the intermediate to form a hydroxybenzotriazolyl active ester and tetramethyl urea as a by-product. The N-terminal amine group of the peptide then couples to this active ester to form the new amide bond and the benzotriazolyl anion is regenerated (Scheme 14).



Scheme 14: Mechanism for coupling of an Fmoc-amino acid to the N-terminus of a peptide

The carboxyl group of the amino acid is deprotonated by NMM and then attacks HBTU to form an O-acyl isourea intermediate and a benzotriazolyl anion. The anion attacks the intermediate to form a hydroxybenzotriazolyl active ester and leave tetramethyl urea as by-product. The free N-terminus of the peptide then couples to the ester to form an amide bond the regenerate the benzotriazolyl anion.

The success of the peptide synthesis was determined by analytical LC-MS and peptides were then purified by preparative LC-MS, both of which were carried out using mobile phases of methanol and H₂O, with 0.1% formic acid, and a linear gradient of 5 – 98% methanol. The syntheses of all peptides during the PhD were successful and characterisation data can be found in section 6.9.6. An example of an LC-MS ultraviolet (UV) trace and negative electrospray (ES-) mass spectrum for the pure **Bip(3)-peptide** can be seen in Figure 38. This presence of a single, sharp peak in both the UV trace and the mass spectrum indicates the high level of purity achieved for this peptide and is typical of all peptides synthesised during the PhD (other spectra can be seen in appendix section 8.5).

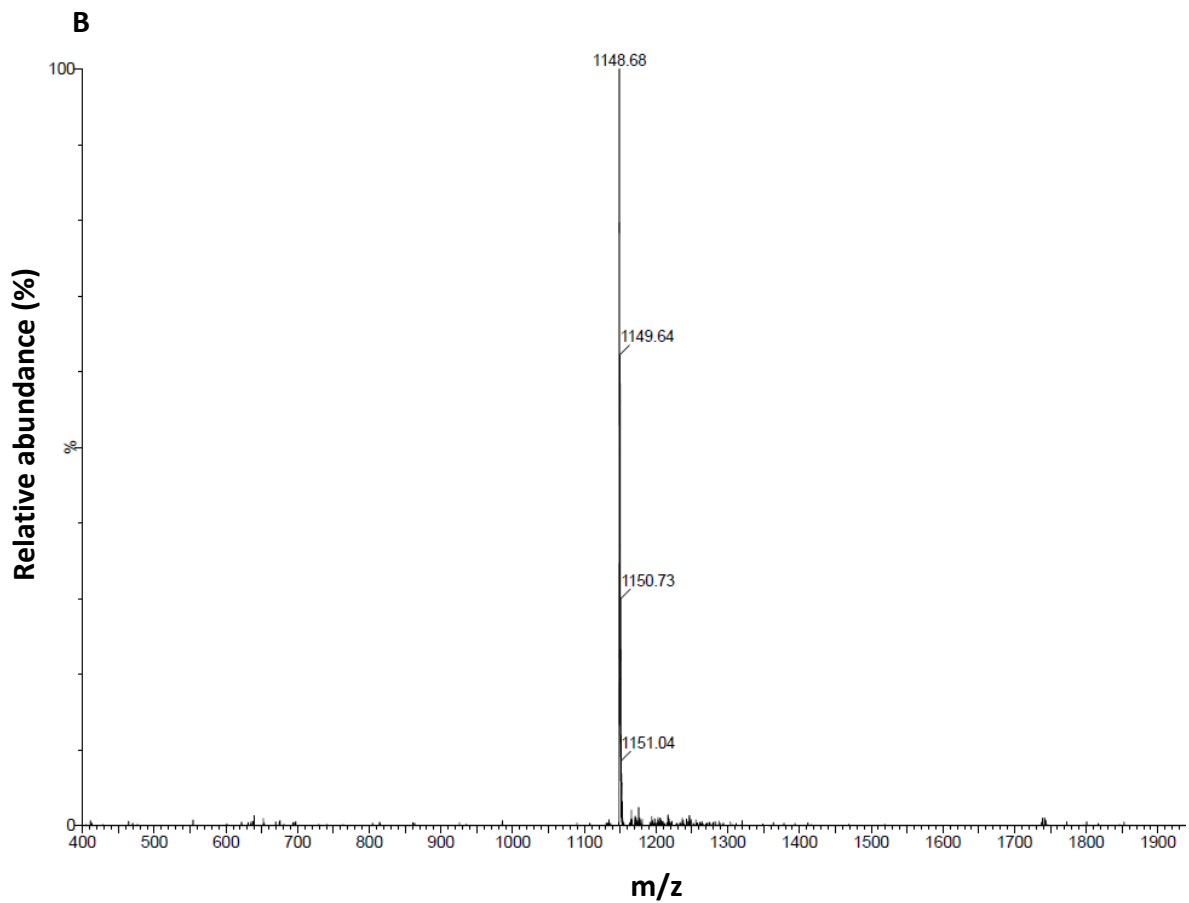
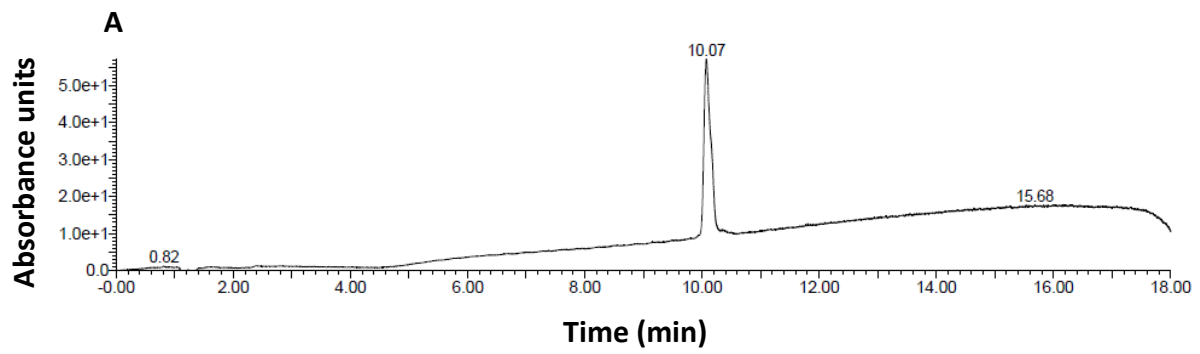


Figure 38: LC-MS UV trace (A) and ES- mass spectrum (B) for pure Bip(3)-peptide
Single, sharp peaks at $R_t = 10.07$ min in the UV trace and at $m/z = 1148.68$ in the mass spectrum indicate the purity of the peptide.

4.1.3 Biotin-labelled peptides

It was later decided to synthesise biotin-labelled peptides for use in SPR experiments. It was envisaged that a peptide could be labelled with biotin for immobilisation onto an SPR chip and either IgE-Fc or $\alpha\gamma$ could then be injected over the chip and might bind to the immobilised peptide (these experiments are discussed in section 4.7). **Phe(3)-peptide** was chosen to be labelled with biotin as it was the most active peptide in the library. It was decided to attach the biotin to the N-terminus of the peptide, both directly to the N-terminal residue and via a linker made of three glycine residues. The corresponding peptide with the N-terminal linker but without the biotin label was also synthesised to investigate the effect of the linker by itself. It was chosen to attach the biotin to the N-terminus as it meant the labelling reaction could be carried out whilst the peptide was still attached to the solid phase resin and the side chain groups were protected, which should ensure that no competing side-reactions occur and the labelling efficiency is high. It also allows for the simple removal of reagents after the reaction.

If having the biotin attached to the N-terminus rendered the peptide unsuitable for the SPR experiments, it was thought that the biotin could instead be attached to the C-terminus of the peptide (by using a resin which comprised a biotin that would be left attached to the C-terminus after cleavage) or that the biotin could be added to a residue side chain. However, this would involve a more complicated synthesis perhaps employing an orthogonal protecting group strategy. Therefore, the N-terminal biotin labelling was employed in the first instance. An overview of the biotin-labelled peptides and the corresponding unlabelled linker-peptide synthesised during this research can be seen in Table 13 and their structures can be seen in Figure 39.

Peptide name	Peptide sequence
b-Phe(3)-peptide	biotin -Asp-Lys-Phe-Tyr-Ile-Val-Lys-Tyr-CONH ₂
b-link-Phe(3)-peptide	biotin-Gly-Gly-Gly -Asp-Lys-Phe-Tyr-Ile-Val-Lys-Tyr-CONH ₂
link-Phe(3)-peptide	H ₂ N- Gly-Gly-Gly -Asp-Lys-Phe-Tyr-Ile-Val-Lys-Tyr-CONH ₂

Table 13: Biotin-labelled peptides and linker-peptide synthesised

Biotin-labelled peptides were synthesised to use for subsequent SPR experiments. Residues in bold show how the peptide sequence differs from that of the parent peptide. (NB: biotin- denotes biotinylated N-terminus, H₂N- denotes free N-terminus, -CONH₂ denotes amidated C-terminus).

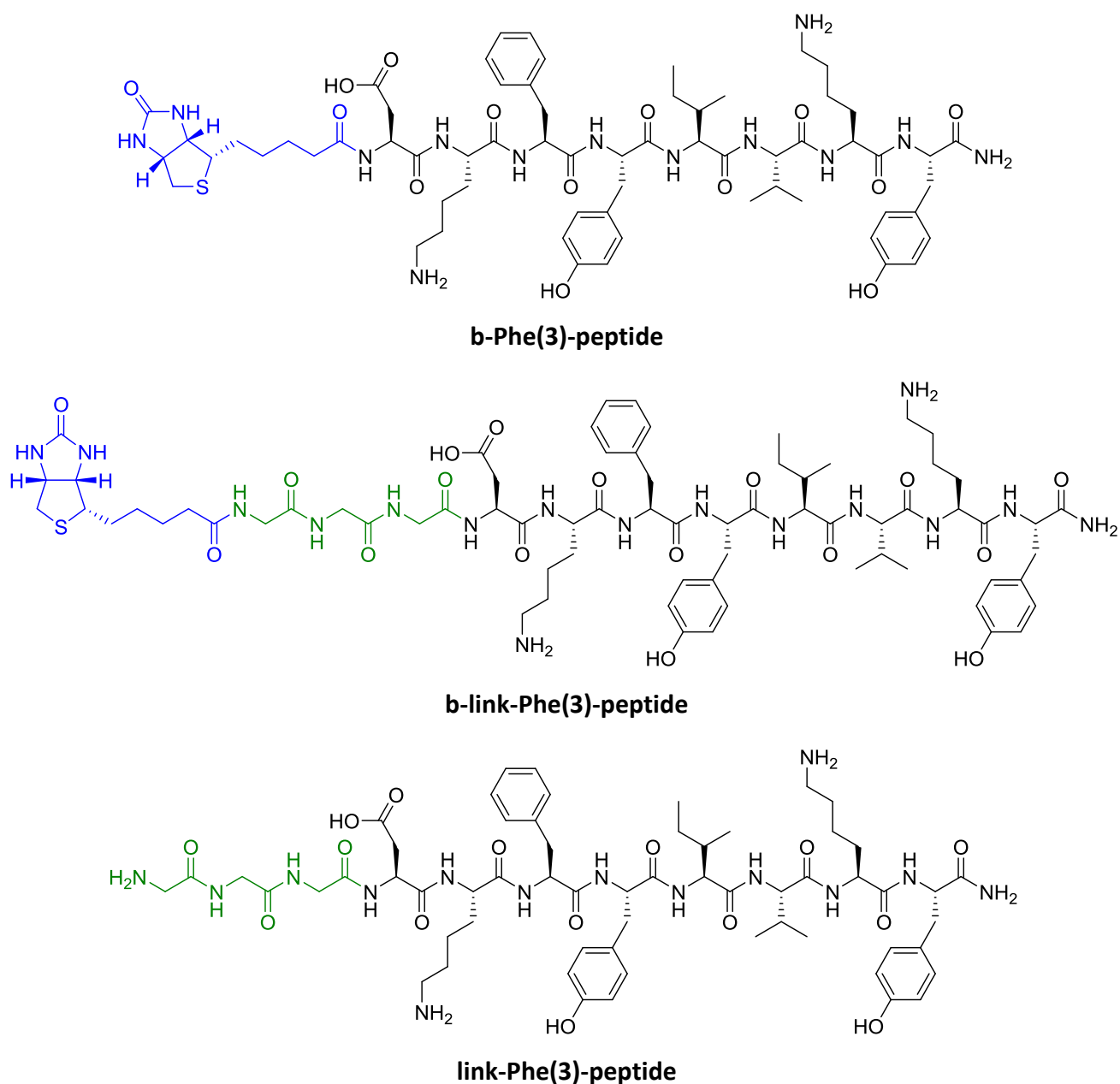
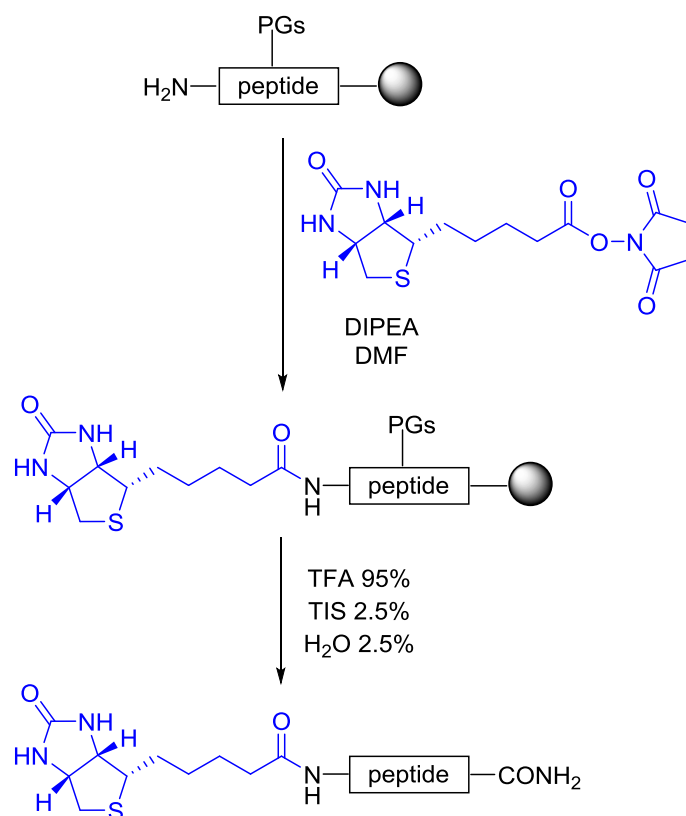


Figure 39: Structures of biotin-labelled peptides and linker-peptide

The biotin group is shown in blue and the linker made of 3 Gly residues is shown in green.

The biotin-labelling reaction was achieved by allowing a solution of biotin-NHS ester (5 equivalents (eq)) and *N,N*-diisopropylethylamine (DIPEA) (1 eq) to react with the resin-bound **Phe(3)-peptide**, following which the reagents were removed by filtration and the resin washed with DMF. Cleavage from the resin and side-chain deprotection was then carried out as before. More details of the experimental procedures can be found in section 6.9.4 and an overview of the synthesis is seen in Scheme 15.



Scheme 15: Overview of biotinylation of the N-terminus of a resin-bound peptide

The N-terminus of the resin-bound peptide was biotinylated using biotin-NHS ester and DIPEA. The biotinylated peptide was then cleaved from the resin using a mixture of 95% TFA, 2.5% TIS and 2.5% H₂O which also removed any side chain protecting groups to leave the free peptide with an N-terminal biotin group and a C-terminal amide.

The first biotin-labelling reaction was carried out, to synthesise **b-Phe(3)-peptide**, at rt for 1 hour, then the solution removed, the resin washed and the reaction repeated for a further 1 hour with fresh biotin-labelling solution. However, after cleavage from the resin and analysis by LC-MS, it was found that not all of the peptide had been biotinylated. The UV trace from the analytical LC-MS of crude **b-Phe(3)-peptide** (Figure 40, A) showed a peak at retention time (Rt) = 8.99 min for the unlabelled peptide and a peak at Rt = 10.07 min for the biotinylated peptide. The reaction could not have gone to completion for a number of reasons; for example if the biotin NHS ester reagent had decomposed, or if the resin was not 'swollen' enough in solvent before the reaction. However, it seemed most likely that the reaction time was too short. Even though not all the peptide **b-Phe(3)-peptide** was labelled, the peptides eluted one minute apart, so it was easy to separate and isolate the two peptides by preparative LC-MS and the UV trace for pure biotin-labelled peptide (Figure 40, B) shows that all unlabelled peptide was removed and a single sharp peak for only the biotin-labelled peptide was observed.

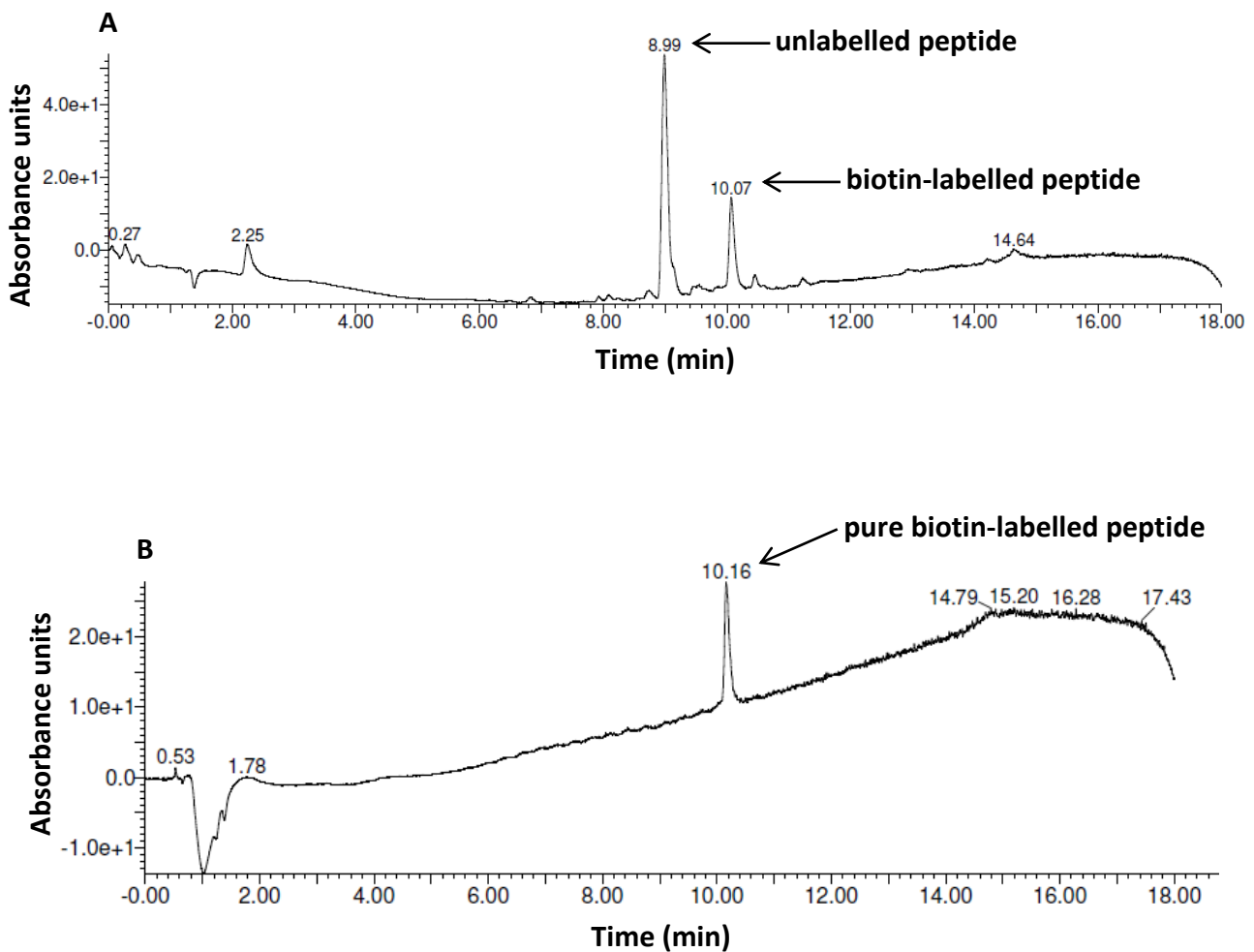


Figure 40: Analytical LC-MS UV traces for crude and pure b-Phe(3)-peptide

A = UV trace for crude biotinylated peptide showed that a mixture of unlabelled peptide (Rt = 8.99 min) and biotinylated peptide (Rt = 10.07 min) was obtained after cleavage from the resin and side-chain deprotection. B = UV trace for pure biotinylated peptide shows that the unlabelled peptide was successfully removed to leave only a peak for the pure biotinylated peptide (Rt = 10.16 min).

In order to improve the yield of the biotin-labelled peptide, the next time the labelling reaction was carried out, to synthesise **b-link-Phe(3)-peptide**, the reaction time was increased to 16 hours. This time only biotin-labelled peptide was seen in the UV trace from the analytical LC-MS of crude **b-link-Phe(3)-peptide** (Figure 41, A) indicating that the increased reaction time was key to improving the yield. However, this peptide did contain the glycine linker which could also have been a factor in making the synthesis more successful. Since there was an N-terminal glycine, rather than an aspartic acid, there could have been less steric hindrance during the reaction. The **b-link-Phe(3)-peptide** was then successfully purified using preparative LC-MS and the UV trace for the pure peptide can be seen in Figure 41, B.

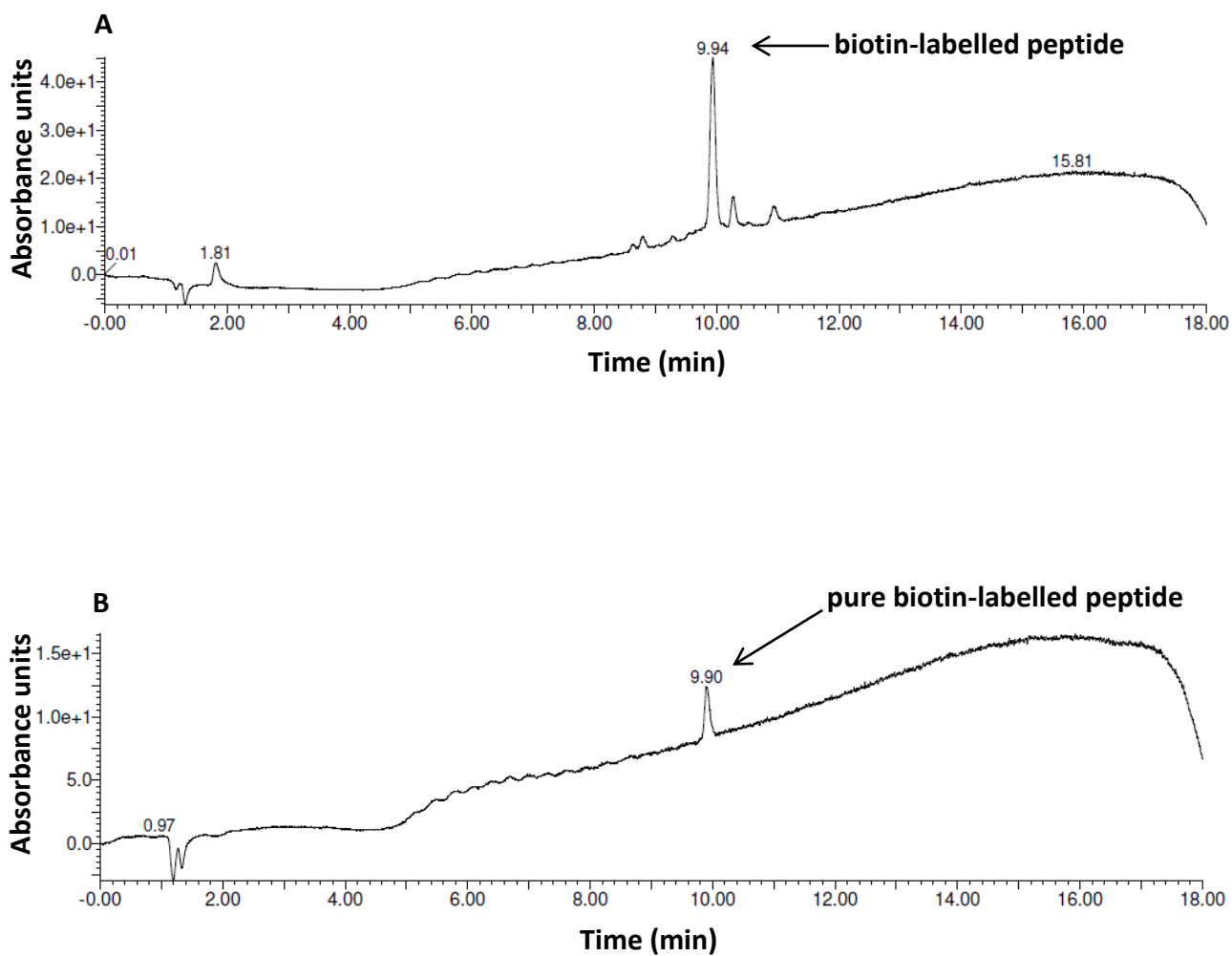


Figure 41: Analytical LC-MS UV traces for crude and pure b-link-Phe(3)-peptide

A = UV trace for crude biotinylated peptide showed that only biotinylated peptide (Rt = 9.94 min) was obtained after cleavage from the resin and side-chain deprotection, which indicated that all peptide was labelled during the biotinylation reaction. B = UV trace for pure biotinylated peptide (Rt = 9.90 min).

4.2 Testing peptide inhibitors with the ELISA

Two of the peptides synthesised during the PhD, the **C-strand peptide** and the **Bip(3)-peptide**, had not previously been tested with the ELISA. These peptides were therefore tested using the ELISA methodology described earlier and the IC_{50} values can be seen in Table 14.

Peptide name	Peptide sequence	IC_{50} (μ M)
C-strand peptide	H ₂ N-Tyr-Lys-Val-Ile-Tyr-Tyr-Lys-Asp-CONH ₂	>1000
Bip(3)-peptide	H ₂ N-Asp-Lys- Bip -Tyr-Ile-Val-Lys-Tyr-CONH ₂	173 ± 12

Table 14: ELISA inhibition assay IC_{50} values for peptides

It can be seen from Table 13, that the **C-strand peptide**, which consists of the sequence found in the C-strand hotspot region of FcεRI, did not inhibit the IgE:FcεRI interaction and this confirms the previous result (Dr Bingli Mo, IC).¹³⁹ The **Bip(3)-peptide** did inhibit the interaction ($IC_{50} = 173 \mu$ M) which is in the same range as the **parent peptide** and the **Phe(3)-peptide** tested previously.¹³¹ It is promising that this peptide shows inhibition of the PPI, as it indicates that the larger biaryl group is tolerated at this position, and it is advantageous as the biaryl group has been previously reported not only to confer increased activity and selectivity but also stability to proteolytic degradation.¹⁴⁵

4.3 Testing peptide inhibitors with the TR-FRET assay

All peptides were then tested in the TR-FRET assay, using the methodology described earlier, to compare IC_{50} values to those obtained in the ELISA and to see if the TR-FRET assay was higher throughput than the ELISA and would be a more efficient assay for testing further libraries of peptide inhibitors. Examples of the TR-FRET inhibition curves for **Phe(3)-peptide** can be seen in Figure 42 and the TR-FRET assay IC_{50} values for all peptides can be seen in Table 15.

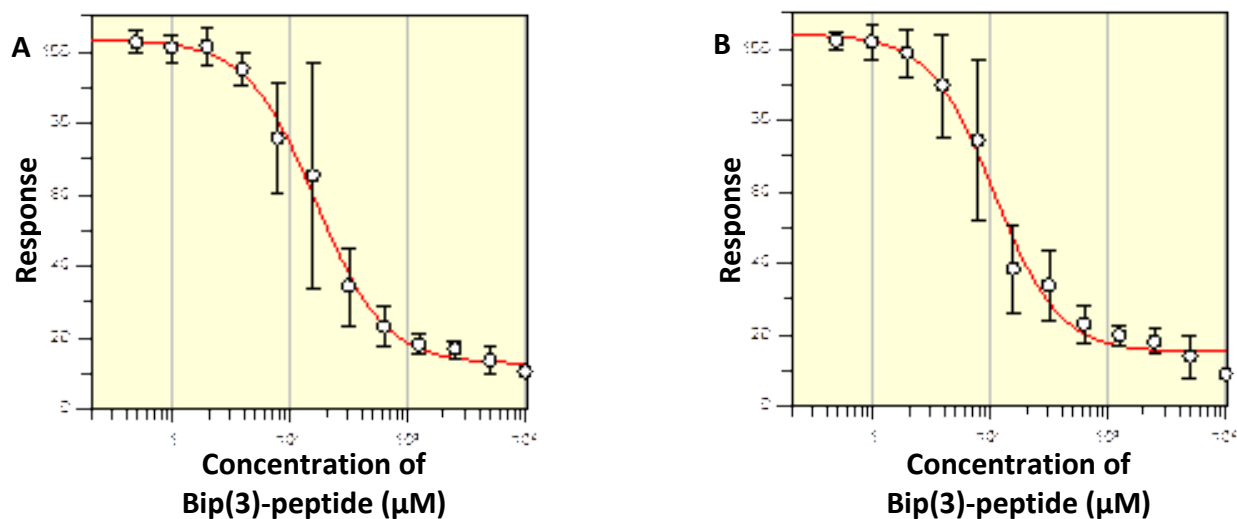


Figure 42: TR-FRET inhibition assay curves for Bip(3)-peptide

A = **Bip(3)-peptide** preincubated with IgE-Fc-A647 ($IC_{50} = 16 \pm 1 \mu M$). B = **Bip(3)-peptide** preincubated with $\alpha\gamma$ -Tb ($IC_{50} = 11 \pm 1 \mu M$).

Peptide name	Peptide sequence	IC_{50} (μM) Pre-inc. IgE-Fc	IC_{50} (μM) Pre-inc. $\alpha\gamma$
C-strand-peptide	H ₂ N-Tyr-Lys-Val-Ile-Tyr-Tyr-Lys-Asp-CONH ₂	>1000	>1000
parent- peptide	H ₂ N-Asp-Lys-Tyr-Tyr-Ile-Val-Lys-Tyr-CONH ₂	459 ± 42 371 ± 58 355 ± 38	176 ± 13 165 ± 22 133 ± 7
Phe(3)-peptide	H ₂ N-Asp-Lys- Phe -Tyr-Ile-Val-Lys-Tyr-CONH ₂	12 ± 0.7 155 ± 12	11 ± 0.7 58 ± 2
Trp(3)-peptide	H ₂ N-Asp-Lys- Trp -Tyr-Ile-Val-Lys-Tyr-CONH ₂	51 ± 3	70 ± 11
Bip(3)-peptide	H ₂ N-Asp-Lys- Bip -Tyr-Ile-Val-Lys-Tyr-CONH ₂	16 ± 1	11 ± 1
His(3)-peptide	H ₂ N-Asp-Lys- His -Tyr-Ile-Val-Lys-Tyr-CONH ₂	>1000	>1000
link-Phe(3)-peptide	H ₂ N- Gly-Gly-Gly -Asp-Lys- Phe -Tyr-Ile-Val-Lys-Tyr-CONH ₂	26 ± 4	7 ± 1

Table 15: TR-FRET inhibition assay IC_{50} values for peptides

NB: Multiple IC_{50} values indicate the assay has been repeated on a different occasion.

It can be seen from Table 14 that overall the same trends are seen as when the peptides were tested with the ELISA (Tables 11 and 13). Lower IC_{50} values are generally obtained from the TR-FRET assay, as the concentrations of proteins are lower than in the ELISA and closer to the K_d of the IgE:FcεRI interaction, suggesting the TR-FRET assay is more sensitive and that less inhibitor is required to inhibit the IgE:FcεRI interaction. The **C-strand peptide** does not inhibit the IgE:FcεRI interaction, which confirms the previous ELISA results and indicates that this peptide may not be a good mimic the key binding region of FcεRI and therefore cannot compete with FcεRI for binding

to IgE. The **parent-peptide** showed moderate inhibition of the IgE:FcεRI interaction ($IC_{50} = 133 - 176 \mu\text{M}$ when pre-incubated with $\alpha\gamma$), however an improved inhibition is seen for **Phe(3)-peptide** and **Trp(3)-peptide** ($IC_{50} = 11 - 58 \mu\text{M}$ and $70 \mu\text{M}$ respectively when pre-incubated with $\alpha\gamma$), indicating that phenylalanine and tryptophan residues at position 3 make more favourable interactions with one of the proteins than tyrosine. **Bip(3)-peptide** also displayed good inhibition of the IgE:FcεRI interaction ($IC_{50} = 11 \mu\text{M}$ when pre-incubated with $\alpha\gamma$) which indicates that the larger biaryl group is also tolerated at position 3. **His (3)-peptide** did not inhibit the interaction, confirming the previous ELISA result and implying that histidine makes unfavourable interactions with one of the proteins, perhaps because of the charged nature of its side chain. The **link-Phe(3)-peptide** was also tested and showed good inhibition ($IC_{50} = 7 \mu\text{M}$ when preincubated with $\alpha\gamma$), implying that the extra glycine residues of the linker do not adversely affect the ability of the peptide to inhibit the IgE:FcεRI interaction, but actually give a slightly improved inhibition compared to the **Phe(3)-peptide**. Some variation between IC_{50} values for peptides tested on different occasions was seen. This could have been due to differences in the solubility of the peptides or between different synthesised batches of the same peptide or due to random error in the measurement.

It can also be seen that, on the whole, lower IC_{50} values are obtained when the peptide is pre-incubated for 1 hour with $\alpha\gamma$, rather than with IgE-Fc. As it is not known which protein the peptides bind to, these results could imply that the peptides bind to $\alpha\gamma$ rather than IgE-Fc. It was planned to further investigate this with subsequent biophysical and structural experiments. It would be important to deduce to which protein the peptides bind and try to obtain structural information about how they bind to that protein, to allow the rational design of peptides with improved affinity. There may be a slight disadvantage to an inhibitor binding to FcεRI, rather than to IgE-Fc, as binding to the receptor might cause a possible agonist effect and mast cell degranulation, so this is something that should be tested for in the future if it was confirmed that peptides do indeed bind to FcεRI.

4.4 Testing biotin-peptide inhibitors with the TR-FRET assay

It was planned to immobilise **b-Phe(3)-peptide** and **b-link-Phe(3)-peptide**, the biotin-labelled versions of the most active peptide **Phe(3)-peptide**, to an SPR chip and inject solutions of IgE-Fc and $\alpha\gamma$ over the chip, in the hope that the peptide would bind to one protein preferentially over the other. However, it was important to first check that these biotin-labelled peptides could still

inhibit the IgE:FcεRI interaction. These peptides were therefore tested in the TR-FRET assay using the same methodology as before and the results can be seen in Table 16.

Peptide name	Peptide sequence	IC ₅₀ (μM) Pre-inc. IgE-Fc	IC ₅₀ (μM) Pre-inc. αγ
b-Phe(3)-peptide	biotin-Asp-Lys- Phe -Tyr-Ile-Val-Lys-Tyr-CONH ₂	7 ± 1 60 ± 7	1 ± 1 15 ± 5
b-link-Phe(3)-peptide	biotin-Gly-Gly-Gly-Asp-Lys- Phe -Tyr-Ile-Val-Lys-Tyr-CONH ₂	13 ± 2	4 ± 0.4

Table 16: TR-FRET inhibition assay IC₅₀ values for biotin-peptides

NB: Multiple IC₅₀ values indicate the assay has been repeated on a different occasion.

It was found that the activity of both **b-Phe(3)-peptide** and **b-link-Phe(3)-peptide** was actually improved by having biotin on the N-terminus (IC₅₀ = 1 – 15 μM and 4 μM respectively when pre-incubated with αγ), rather than with a free N-terminus. This could imply that biotin makes a more favourable interaction with one of the proteins, or that simply not having a charged free N-terminus improves activity.

4.5 Testing biotin-peptide inhibitors with streptavidin in the TR-FRET assay

It was then planned to test these biotin-peptides with streptavidin in the TR-FRET assay, to check that the peptides could still inhibit the IgE:FcεRI interaction even when bound to streptavidin, as they would need to do this in the subsequent SPR experiments. In order to ensure that any inhibition was actually due to the streptavidin-bound peptide and not due to the free peptide, an excess of streptavidin was used to ensure that all biotin-peptide was bound to streptavidin. To ensure streptavidin was in excess, the concentration of biotin-peptide was decreased, from an upper concentration of 1 mM to an upper concentration of 125 μM, as it was predicated from their inhibition curves that they could still inhibit the IgE:FcεRI interaction even at the lower concentrations. The biotin-peptides were tested in the TR-FRET assay at these lower concentrations and the results can be seen in Table 17.

Peptide name	Peptide sequence	IC ₅₀ (μM) Pre-inc. αγ
b-Phe(3)-peptide (lower concentration) ^a	biotin-Asp-Lys- Phe -Tyr-Ile-Val-Lys-Tyr-CONH ₂	2 ± 4
b-link-Phe(3)-peptide (lower concentration)	biotin-Gly-Gly-Gly-Asp-Lys- Phe -Tyr-Ile-Val-Lys-Tyr-CONH ₂	98 ± 104

Table 17: TR-FRET inhibition assay IC₅₀ values for biotin-peptides at lower concentrations

^aMaximum concentration of peptide was reduced from 1 mM to 125 μM.

It can be seen that the peptides still showed inhibition at these lower concentrations and that **b-Phe(3)-peptide** showed particularly good inhibition ($IC_{50} = 2 \mu M$ when preincubated with $\alpha\gamma$). Both biotin-peptides were then tested at these lower concentrations with streptavidin (2 eq) in the TR-FRET assay and the results can be seen in Table 18.

Peptide name	Peptide sequence	IC_{50} (μM) Pre-inc. $\alpha\gamma$
b-Phe(3)-peptide (lower concentration) ^a + streptavidin (2 eq)	biotin-Asp-Lys- Phe -Tyr-Ile-Val-Lys-Tyr-CONH ₂	5 ± 1
b-link-Phe(3)-peptide (lower concentration) + streptavidin (2 eq)	biotin-Gly-Gly-Gly-Asp-Lys- Phe -Tyr-Ile-Val-Lys-Tyr-CONH ₂	>1000

Table 18: TR-FRET inhibition assay IC_{50} values for biotin-peptides with streptavidin

^aMaximum concentration of peptide was reduced from 1 mM to 125 μM .

It can be seen that **b-Phe(3)-peptide** still showed good inhibition of the IgE:Fc ϵ RI interaction even when it was bound to streptavidin ($IC_{50} = 5 \mu M$ when preincubated with $\alpha\gamma$), however **b-link-Phe(3)-peptide** did not show any inhibition. It was therefore decided to use **b-Phe(3)-peptide** for immobilisation to the SPR chip for subsequent SPR binding assays (discussed in section 4.7).

4.6 X-ray crystallography experiments

At the same time as testing all the peptides in the TR-FRET assay, x-ray crystallography experiments were also being carried out for both **Phe(3)-peptide** and **Trp(3)-peptide** with IgE-Fc, as these were the two most active peptides when the crystallography experiments were carried out. The aim was to obtain a co-crystal of IgE-Fc with a peptide bound in a particular position, to confirm that peptides do bind to IgE-Fc and to give structural information about their mode of action and facilitate improvements in inhibition. It was planned to carry out both co-crystallisation and soak crystallisation experiments and these are discussed in this section.

4.6.1 Co-crystallisations of peptides with IgE-Fc

First co-crystallisation experiments with Phe(3)-peptide and Trp(3)-peptide

Solutions of both **Phe(3)-peptide** and **Trp(3)-peptide** at concentrations of both 50 μM and 100 μM were incubated with IgE-Fc (27 μM) and IgE-Fc seeds (ground up apo crystals of IgE-Fc, provided by Dr Nyssa Drinkwater, KCL). More detailed experimental details can be found in section 6.6. After

approximately 5 days, oblong crystals measuring approximately 100 x 200 μm had formed for all four experiments. Single crystals from the co-crystallisations of both **Phe(3)-peptide** and **Trp(3)-peptide** at 100 μM were frozen in liquid nitrogen and x-ray diffraction data was collected at the Diamond Light Source synchrotron. Figure 43 shows photos of the crystals grown in the experiments and the x-ray diffraction patterns obtained and Table 19 shows the data collection statistics for the experiments.

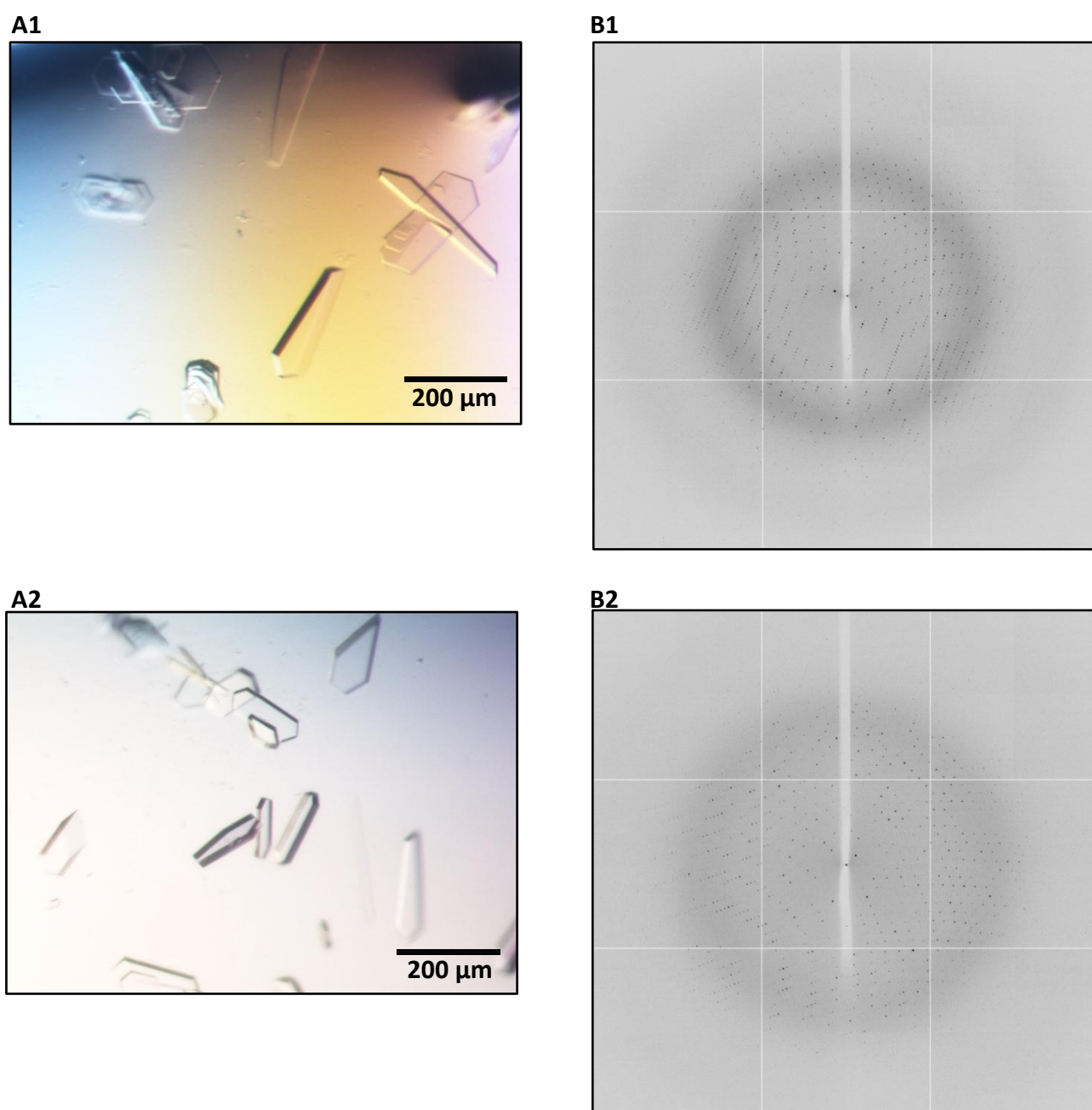


Figure 43: Crystal photos and x-ray diffractions - first co-crystallisations of peptides and IgE-Fc
A1 = Crystal photos and B1 = x-ray diffraction data for co-crystallisation experiment of **Phe(3)-peptide** (100 μM) with IgE-Fc (27 μM). A2 = Crystal photos and B2 = x-ray diffraction data for co-crystallisation experiment of **Trp(3)-peptide** (100 μM) with IgE-Fc (27 μM). Crystals measured approximately 100 μm x 200 μm . X-ray data collected at the Diamond Light Source synchrotron.

	Phe(3)-peptide	Trp(3)-peptide
Resolution (Å)	2.07	2.28
R_{merge}	0.099	0.069
I/sigma	11.2	11.5
Completeness (%)	99.7	98.7
Multiplicity	4.7	3.9
R_{factor}	0.2490	0.2380
R_{free}	0.2846	0.2838
Average unit cell	a = 128.33, b = 74.78, c = 79.33	a = 128.06, b = 74.86, c = 79.23
Space group	P 21 21 2	P 21 21 2

Table 19: Data collection statistics - first co-crystallisations of peptides and IgE-Fc

Co-crystallisation experiments of **Phe(3)-peptide** (100 μ M) with IgE-Fc (27 μ M) and **Trp(3)-peptide** (100 μ M) with IgE-Fc (27 μ M). Data collected at Diamond Light Source synchrotron.

As Table 18 shows, crystals from both experiments diffracted to a high resolution (2.07 Å for **Phe(3)-peptide** and 2.28 Å for **Trp(3)-peptide**) and refinement statistics were good. The crystal structures were solved by molecular displacement using a high resolution structure of IgE-Fc (PDB code 2WQR)²² and the CCP4 software Phenix Refine and Coot. Unfortunately, for both cases the structures were found to be of IgE-Fc only with no unaccounted electron density which would be indicative of a bound peptide. This could indicate that the peptides do not bind to IgE-Fc but instead bind to Fc ϵ RI, which would be consistent with the fact that in general lower IC₅₀ values were obtained in the TR-FRET assay when peptides were pre-incubated with $\alpha\gamma$ rather than with IgE-Fc. Or it could indicate that peptides do bind to IgE-Fc but were not able to form a co-crystal structure due to their affinity being too low, or that too low a concentration of peptide was used.

Second co-crystallisation experiments with Phe(3)-peptide and Trp(3)-peptide

It was therefore decided to repeat the co-crystallisation experiments for both **Phe(3)-peptide** and **Trp(3)-peptide** with IgE-Fc using higher peptide concentrations of 200 μ M and 300 μ M in the hope that this would be more amenable to co-crystallisation. Crystals were grown successfully in all four experiments after approximately 5 days as before. Crystals from the co-crystallisations of both peptides were frozen in liquid nitrogen and x-ray diffraction data was collected at KCL using a single crystal diffractometer. Figure 44 shows photos of the crystals obtained and Table 20 shows the data collection statistics for the experiments.

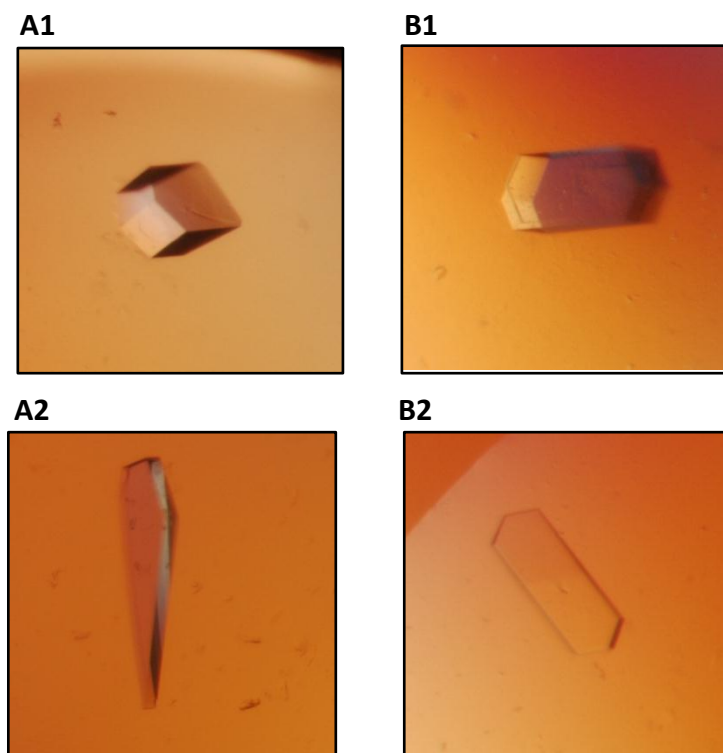


Figure 44: Crystal photos - second co-crystallisations of peptides and IgE-Fc

A1 = Co-crystallisation experiment of **Phe(3)-peptide** (200 μM) with IgE-Fc (27 μM). B1 = Co-crystallisation experiment of **Phe(3)-peptide** (300 μM) with IgE-Fc (27 μM). A2 = Co-crystallisation experiment of **Trp(3)-peptide** (200 μM) with IgE-Fc (27 μM). B2 = Co-crystallisation experiment of **Trp(3)-peptide** (300 μM) with IgE-Fc (27 μM). Crystals measured approximately 100 μm x 200 μm . Data collected at KCL using a single crystal diffractometer.

	Phe(3)-peptide	Trp(3)-peptide
Resolution (\AA)	2.6	2.4
R_{factor}	0.2646	0.2625
R_{free}	0.3253	0.3223

Table 20: Data collection statistics - second co-crystallisations of peptides and IgE-Fc

Co-crystallisation experiments of **Phe(3)-peptide** (300 μM) with IgE-Fc (27 μM) and **Trp(3)-peptide** (300 μM) with IgE-Fc (27 μM). Data collected at KCL using a single crystal diffractometer.

Crystals diffracted well, good refinement statistics were obtained and the structures were solved using molecular displacement as before. However, unfortunately the solved structures were of IgE-Fc only and no bound peptides were observed. It was therefore decided to try soak crystallisation experiments in case this was a more effective method of obtaining a co-crystal.

4.6.2 Soak crystallisations of peptides with IgE-Fc

Soak crystallisation experiments were carried out for both **Phe(3)-peptide** and **Trp(3)-peptide** with IgE-Fc. Solutions of both peptides at a concentration of 500 μ M were incubated with 4 – 6 apo crystals of IgE-Fc (provided by Dr Nyssa Drinkwater, KCL). The solutions were left for 5 – 10 days, after which crystals were frozen in liquid nitrogen and X-ray diffraction data was collected at Diamond light source. X-ray data collection for **Phe(3)-peptide** had low completeness and unfortunately data could not be obtained, however data was collected for **Trp(3)-peptide** and this can be seen in Table 21.

Resolution (Å)	2.08
R_{merge}	0.123
I/sigma	6.9
Completeness (%)	99.9
Multiplicity	4.4
R_{factor}	0.2461
R_{free}	0.2786
Average unit cell	a = 128.59, b = 75.05, c = 79.45
Space group	P 21 21 2

Table 21: Data collection statistics - soak crystallisation of IgE-Fc and Trp(3)-peptide

Soak crystallisation experiment of **Trp(3)-peptide** (500 μ M) with IgE-Fc crystals. Data collected at Diamond light source.

Trp(3)-peptide diffracted to a high resolution of 2.08 Å and good refinement statistics were obtained. The structure was solved using molecular displacement as described earlier, however unfortunately no peptide was found to be bound to IgE-Fc in the crystal structure. The fact that no co-crystal structure of IgE-Fc with a peptide bound in a particular position was obtained from either the co-crystallisation or soak crystallisation experiments with **Phe(3)-peptide** or **Trp(3)-peptide** is disappointing. However, it is beneficial that the conditions to grow crystals of IgE-Fc are optimised and if it was determined by other methods that peptides do actually bind to IgE-Fc and their binding affinity could be improved, this would improve the chances of obtaining a co-crystal. Alternative crystallisation experiments with IgE-Fc could be used, as mentioned earlier, for instance using IgE-Fc₃₋₄, or purifying IgE-Fc with the peptide bound and screening different crystallisation conditions, or even to form a covalent attachment between the peptide and IgE-Fc.

However, it was felt that efforts should first be focussed on obtaining conclusive information about which protein the peptides were binding to.

4.7 SPR experiments

SPR has proven a useful and varied technique for investigating peptide inhibitors of the IgE:FcεRI interaction as reported in the literature. It was decided to carry out SPR experiments with **Phe(3)-peptide** as overviewed in Scheme 9.

4.7.1 SPR with immobilised proteins

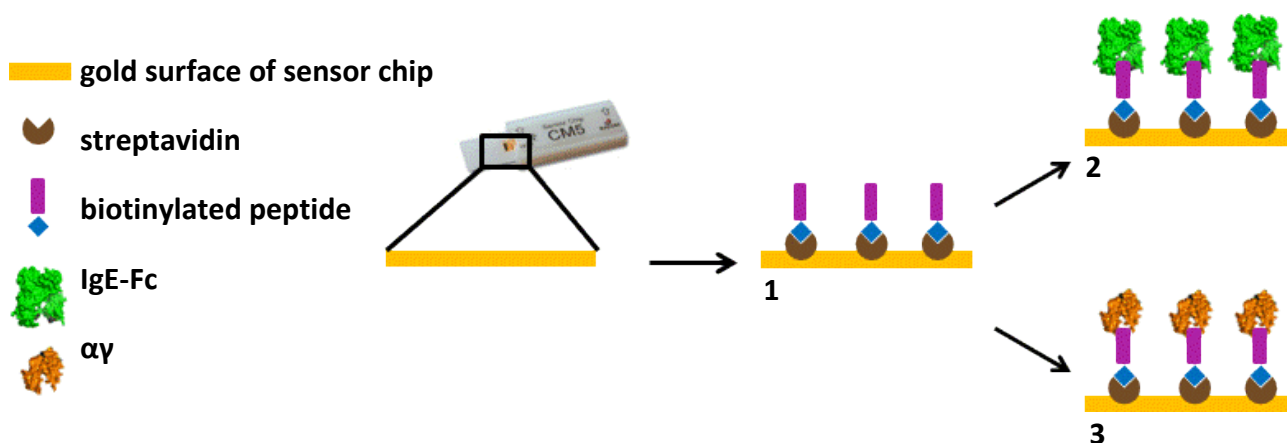
Inhibition of IgE-Fc binding to immobilised αγ by Phe(3)-peptide

Phe(3)-peptide was tested as an inhibitor of IgE-Fc binding to immobilised αγ in an inhibition assay. A solution of IgE-Fc (10 nM) and **Phe(3)-peptide** (150 μM) was injected over the immobilised αγ. However, a large increase in resonance units was observed along with sharp injection peaks for the peptide. This indicated poor solubility of the peptide in the SPR running buffer, as the sharp peaks could show the peptide was being injected in 'clumps' if precipitating out of solution. The large increase in resonance units was likely to indicate that the peptide was binding non-specifically to the chip due to its hydrophobic nature, despite the detergent present in the buffer. In fact, when studying the raw data it was found that the largest increase in signal was for the control flow cell with no protein bound to the surface, meaning the peptides could have been binding non-specifically to the CM matrix on the chip. Glycine pH 2.5, NaCl (5 M) and MgCl₂ (4 M) were all injected to try to remove the bound peptide but without success.

4.7.2 SPR with immobilised biotin-peptide

SPR experiments were then carried out with **Phe(3)-peptide** immobilised to the SPR chip instead of the proteins, as it was hoped this would overcome the problem of the peptide precipitating out of solution and binding non-specifically to the sensor chip. It would also mean that if a protein bound to the immobilised peptide, this would give a much larger increase in signal than if the peptide bound to an immobilised protein, due to the much larger molecular weight of the protein compared to the peptide. It was planned to use the biotin-labelled peptide **b-Phe(3)-peptide**, as described earlier, and immobilise this to a streptavidin coated SPR chip. A sensor chip pre-immobilised with streptavidin was chosen for the experiments, to avoid the extra streptavidin immobilisation step and give a more uniform density of streptavidin across the active and control flow cells of the sensor chip. It was planned to immobilise the **b-Phe(3)-peptide**, via the high-

affinity biotin-streptavidin interaction, then carry out direct binding assays where IgE-Fc and $\alpha\gamma$ are injected in turn over the peptide-chip (Scheme 16).



Scheme 16: Overview of SPR experiments with immobilised b-Phe(3)-peptide

1 = immobilisation of peptide to streptavidin coated SPR chip, 2 = direct binding assay with injection of IgE-Fc, 3 = direct binding assay with injection of $\alpha\gamma$.

Immobilisation of b-Phe(3)-peptide

The **b-Phe(3)-peptide** (100 nM) was injected over the streptavidin coated chip and the binding was allowed to reach saturation so the maximum density of immobilised peptide was achieved. An increase of ~ 350 resonance units was observed.

Initial binding of IgE-Fc and $\alpha\gamma$ to b-Phe(3)-peptide

IgE-Fc (13.3 μM) was then injected over the peptide-chip which gave an increase in signal of ~ 40 resonance units. This experiment was repeated with an injection of $\alpha\gamma$ (2.66 μM) over the peptide-chip which gave an increase in signal of ~ 70 resonance units. These initial results indicated that both proteins could have been binding to the peptide, but further assays with a dilution series of each protein and also a control protein were carried out to further confirm the results.

Binding assay with IgE-Fc, $\alpha\gamma$ and IgG₄ binding to immobilised b-Phe(3)-peptide

IgE-Fc was prepared in 12 different concentrations starting at 13.3 μM with 2-fold dilutions to a final concentration of 0.03 μM . $\alpha\gamma$ was prepared in 9 different concentrations starting at 3.0 μM with 2-fold dilutions to a final concentration of 0.06 μM . IgG₄ was used as a control protein as the peptide was not expected to bind to this. IgG₄ was prepared in 12 different concentrations starting at 4.0 μM with 2-fold dilutions to a final concentration of 0.03 μM . Due to the relatively weak binding of the peptide to the proteins, after the end of the injection the baseline had returned to its previous value, therefore no proteins stayed bound to the peptide and a glycine injection to remove any protein was not required. Further experimental details can be found in section 6.5.

The sensorgrams and corresponding Langmuir curves for each binding assay can be seen in Figures 45, 46 and 47. In each case the SPR binding assay was carried out twice to check the reproducibility and it was found that results were very consistent across the duplicate experiments. It can be seen that there was negligible binding of IgE-Fc to the immobilised **b-Phe(3)-peptide**, even at the highest concentration of 13.3 μM (Figure 45). Also, the control protein IgG₄ did not show any binding to immobilised **b-Phe(3)-peptide**, which was to be expected (Figure 46).

However, $\alpha\gamma$ appeared to bind to immobilised **b-Phe(3)-peptide** in a dose dependent manner and a series of sensorgrams were obtained (Figure 47, A1 and A2). These show that at the highest concentration of $\alpha\gamma$ (3.0 μM) there was an increase of nearly 60 resonance units. The Langmuir isotherm for $\alpha\gamma$ (Figure 47, B) also shows a dose dependent binding of $\alpha\gamma$ to immobilised **b-Phe(3)-peptide**. Even though this curve does not go to saturation, this was to be expected as the maximum concentration of $\alpha\gamma$ used in the assay was 3 μM , which is in the same range as the IC₅₀ value for **b-Phe(3)-peptide** (IC₅₀ = 1 – 15 μM when pre-incubated with $\alpha\gamma$ in the TR-FRET assay, Table 16). The upper concentrations of IgE-Fc, IgG₄ and $\alpha\gamma$ were chosen as they were the maximum concentrations available. If a higher concentration of $\alpha\gamma$ was able to be used, above the range of the IC₅₀ value for the peptide, then the Langmuir isotherm could indeed reach saturation.

These are interesting results and indicate that **Phe(3)-peptide** (and analogues) inhibit the IgE:Fc ϵ RI interaction by binding to Fc ϵ RI rather than by binding to IgE. This is consistent with the fact that a co-crystal structure of IgE-Fc and a peptide was not be obtained and also with the fact that peptides showed more potent inhibition in the TR-FRET assay when they were pre-incubated with $\alpha\gamma$. It is pleasing that it can be said with reasonable confidence that the peptides bind to Fc ϵ RI as it means that future biophysical and structural experiments with Fc ϵ RI could be planned to find out the mode of action of the peptides and to facilitate improvements in affinity.

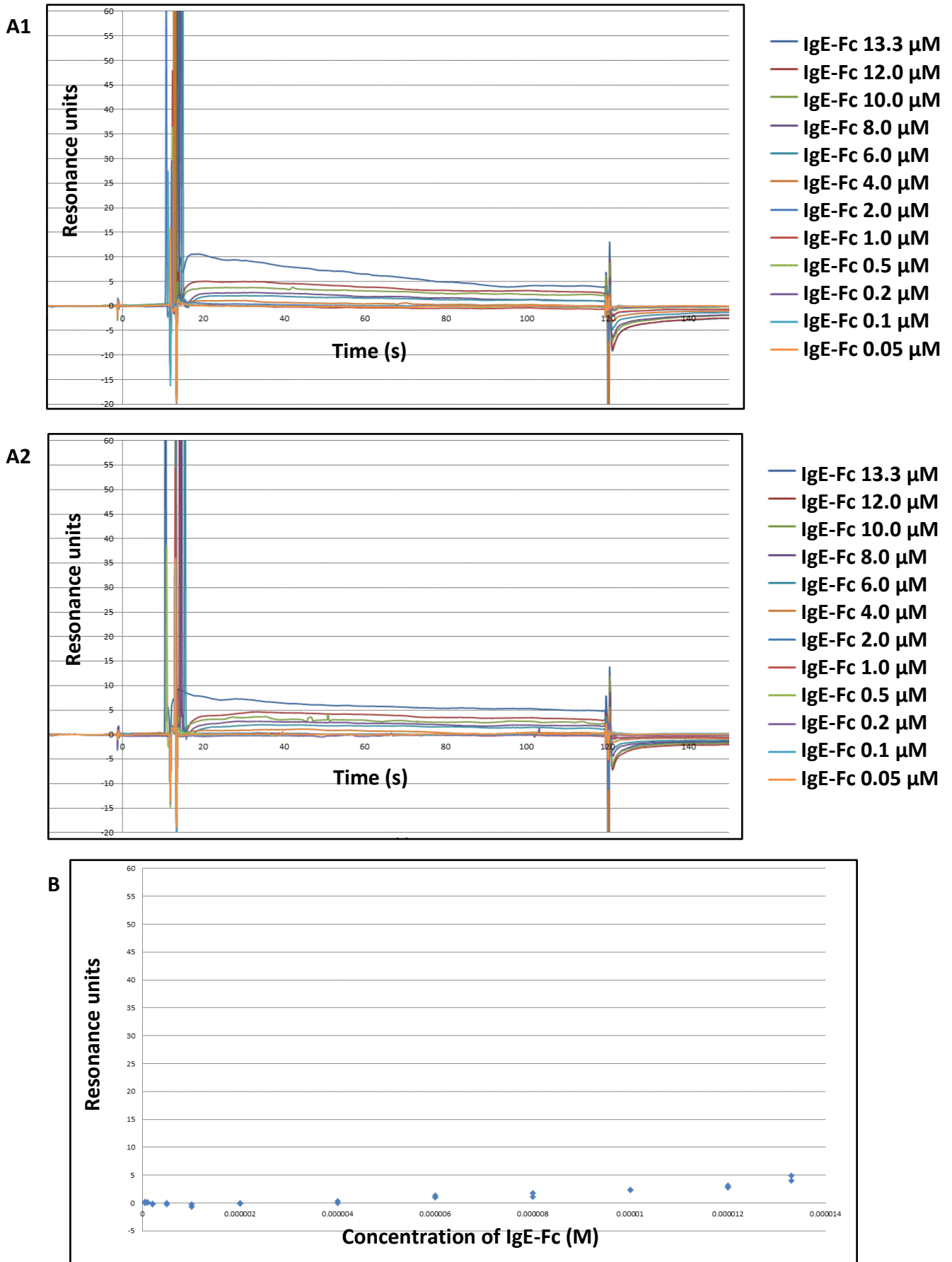


Figure 45: SPR sensorgrams and Langmuir isotherm - IgE-Fc binding to immobilised b-Phe(3)-peptide
 A1 and A2 = SPR sensorgrams (two repeats of the binding assay). B = Langmuir isotherm.

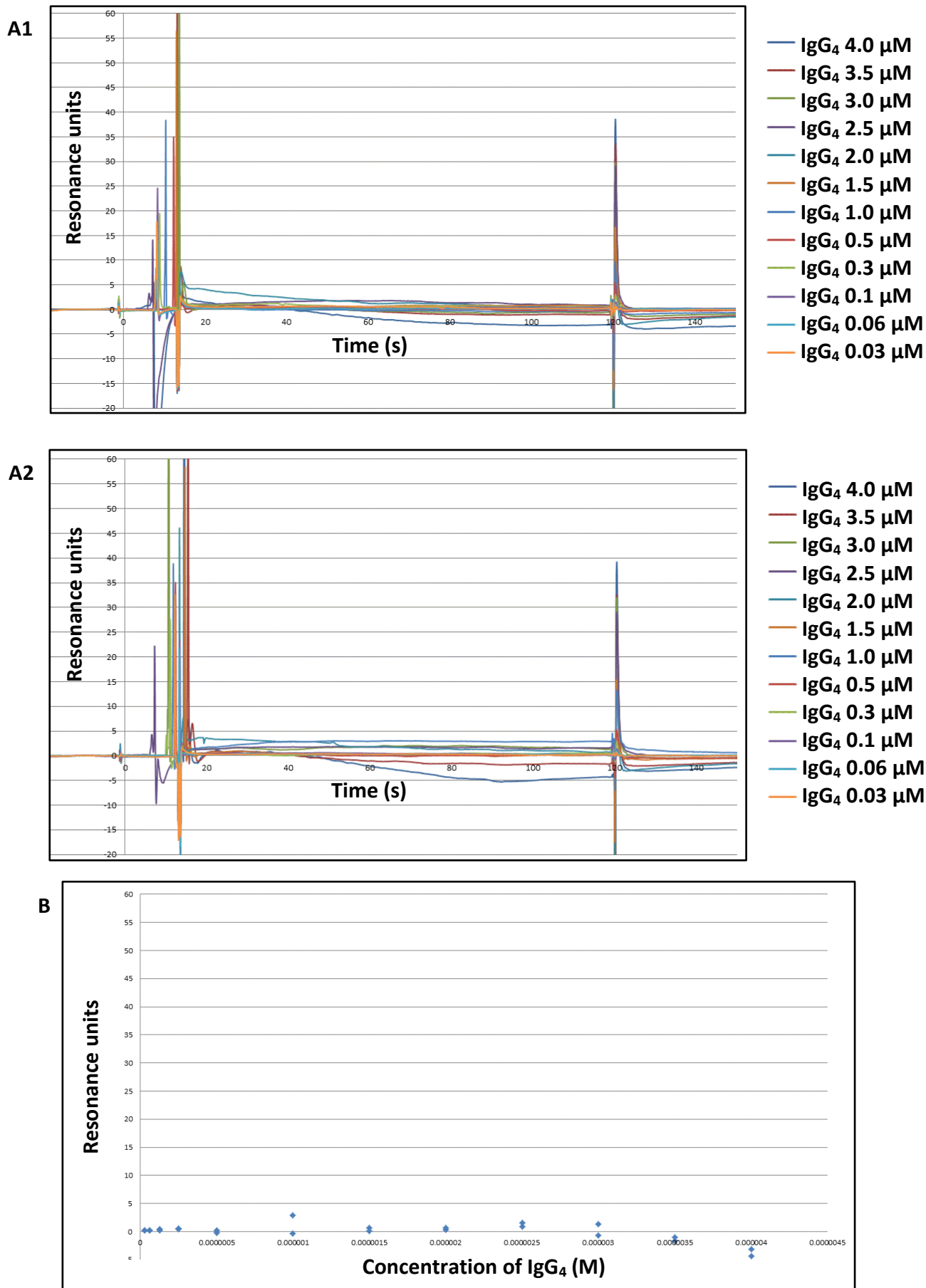


Figure 46: SPR sensorgrams and Langmuir isotherm - IgG₄ binding to immobilised b-Phe(3)-peptide
 A1 and A2 = SPR sensorgrams (two repeats of the binding assay). B = Langmuir isotherm.

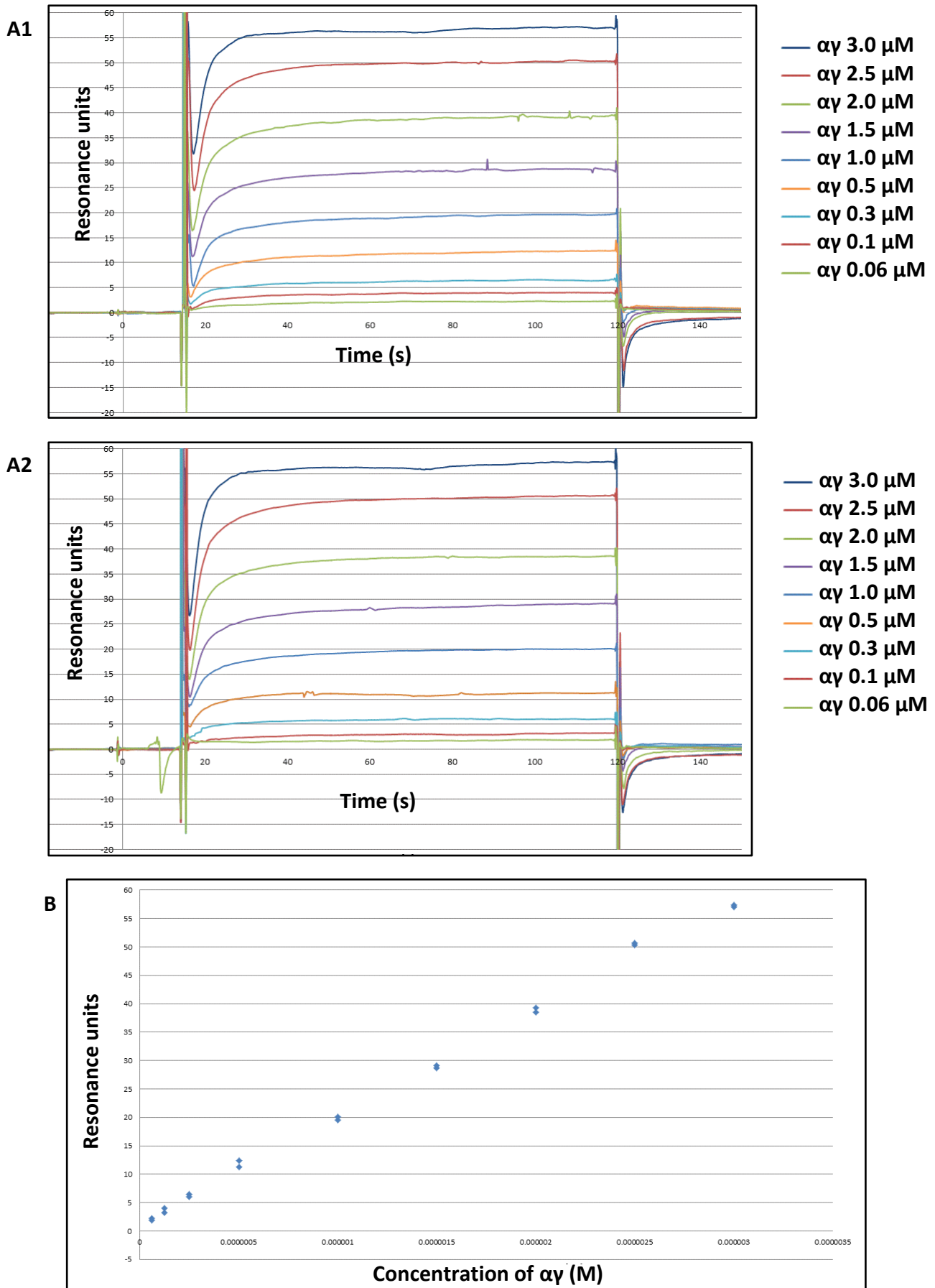


Figure 47: SPR sensorgrams and Langmuir isotherm - $\alpha\gamma$ binding to immobilised b-Phe(3)-peptide
 A1 and A2 = SPR sensorgrams (two repeats of the binding assay). B = Langmuir isotherm.

Chapter 5: Summary and future work

5.1 Summary

The main objectives of this PhD were to design and synthesise inhibitors of the PPI between IgE and FcεRI, which is a key component of the allergic reaction, and to develop and carry out assays and structural experiments to test these compounds. Two main series of compounds were studied as inhibitors of the IgE:FcεRI interaction; small molecules based on the natural product aspercyclide A and short, linear peptides derived from a sequence that was originally designed to mimic a key hotspot of the interaction.

A TR-FRET assay was developed and optimised to test the small molecule and peptide inhibitors. This involved labelling of the two proteins IgE and αγ with appropriate acceptor and long lifetime donor fluorophores and carrying out initial binding and inhibition assays to determine optimal protein concentrations, incubation times and assay format. The TR-FRET assay was found to be a more attractive assay than the previously developed ELISA, as it was carried out in solution, with no secondary reagents or washing steps required and it used less material. The TR-FRET assay was found to have a good S/B of 12.6 and an excellent Z-factor of 0.79. SPR experiments involving immobilisation of each of the two proteins were also investigated and individual domains of IgE were expressed and purified which could be used in subsequent experiments. The main results from the small molecule and peptide compound libraries are summarised in the following sections.

5.1.1 Small molecules

The natural product aspercyclide A was originally isolated from natural product extracts, tested in an ELISA and found to inhibit the IgE:FcεRI interaction with $IC_{50} = 200 \mu M$.⁸⁶ As this compound offered an interesting starting point for the design of potentially more potent inhibitors, co-workers in the Spivey research group at IC carried out the asymmetric synthesis of the natural product (+)-aspercyclide A and various analogues. (+)-Aspercyclide A and a benzoxathiazine-2,2-dioxide derivative were found to inhibit the IgE:FcεRI interaction when tested with an ELISA ($IC_{50} = 424 - 538 \mu M$ and $162 - 463 \mu M$ respectively) and the synthesis and assay results for these compounds were published recently.⁹² The structures of these compounds can be seen in Figure 48. The activity of the benzoxathiazine derivative was also confirmed by collaborators at Novartis, who also found that this compound showed inhibition of the IgE:FcεRI interaction when tested in an ELISA ($EC_{50} = 124 - 156 \mu M$).

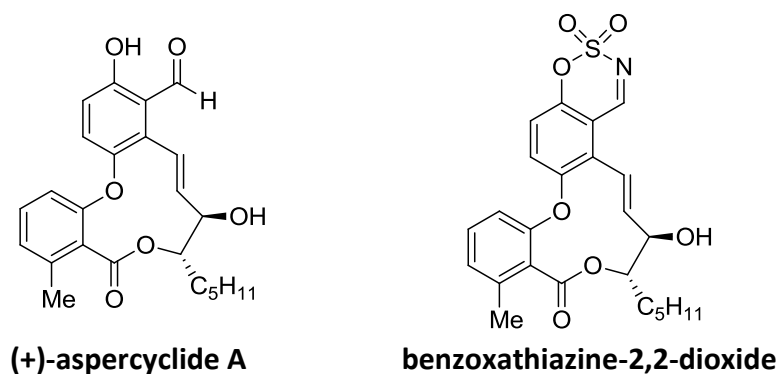


Figure 48: Structures of (+)aspercyclide A and its benzoxathiazine-2,2-dioxide derivative

These compounds were the most active small molecules at inhibiting the IgE:FcεRI interaction when tested with an ELISA ($IC_{50} = 424 - 538 \mu\text{M}$ for (+)-aspercyclide A and $162 - 463 \mu\text{M}$ for the benzoxathiazine derivative).

A dibenzofuran analogue, originally isolated as a byproduct during the final macrocyclisation reaction to form the aspercyclide A compounds, appeared to inhibit the IgE:FcεRI interaction when tested with the ELISA ($IC_{50} = 3 - 5 \mu\text{M}$). However, subsequent SPR inhibition assays found that this compound did not inhibit the IgE:FcεRI interaction and x-ray crystallography experiments with IgE-Fc found that this compound did not show any binding to IgE-Fc. On re-synthesis and re-testing of this compound with the ELISA, no inhibition was seen, therefore it was thought the initial result was a false positive and that the dibenzofuran was inhibiting another component of the ELISA and not the interaction between IgE and FcεRI.

5.1.2 Peptides

A short, linear peptide known as **parent-peptide** ($\text{H}_2\text{N-Asp-Lys-Tyr-Tyr-Ile-Val-Lys-Tyr-CONH}_2$), was previously found to inhibit the IgE:FcεRI interaction when tested with an ELISA¹³¹ and it was also found that Tyr(3) was key for the activity¹³⁹. A series of analogues with aromatic substitutions at position 3 were previously synthesised and tested in the ELISA and the analogous peptide **Phe(3)-peptide** ($\text{H}_2\text{N-Asp-Lys-Phe-Tyr-Ile-Val-Lys-Tyr-CONH}_2$) displayed an improved inhibition.¹³¹ A further peptide **Bip(3)-peptide** ($\text{H}_2\text{N-Asp-Lys-Bip-Tyr-Ile-Val-Lys-Tyr-CONH}_2$) was synthesised, to determine the effect of the unnatural amino acid biphenylalanine at position 3. The whole peptide library was tested with the new TR-FRET assay, to confirm the ELISA results and the **Phe(3)-peptide** and **Bip(3)-peptide** were found to show good inhibition of the interaction between IgE and FcεRI ($IC_{50} = 11 - 58 \mu\text{M}$ and $11 \mu\text{M}$ respectively). The structures of these peptides can be seen in Figure 49.

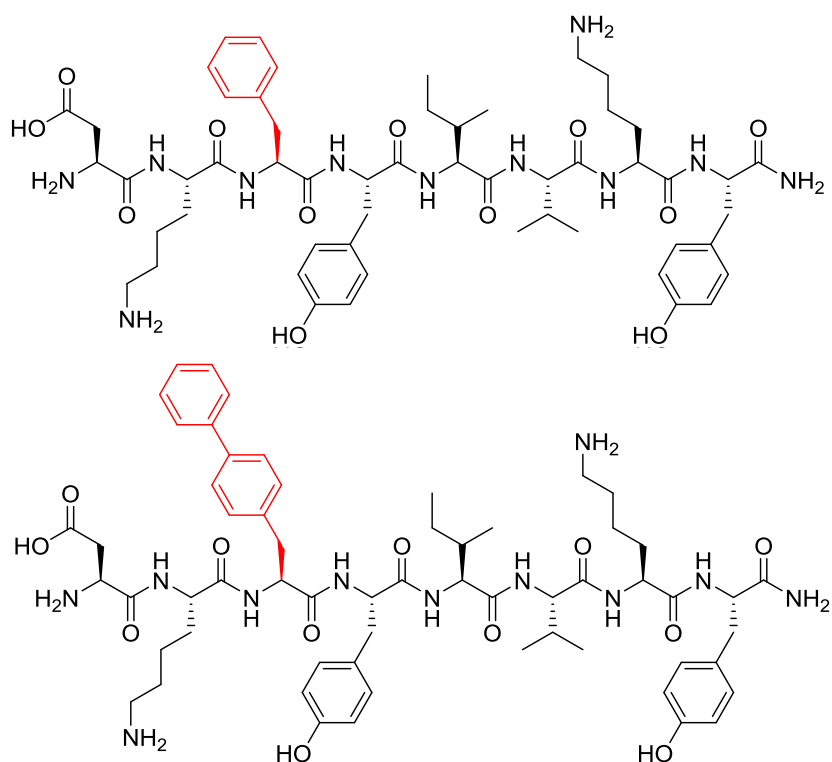


Figure 49: Structures of the most active peptides Phe(3)-peptide and Bip(3)-peptide

These were the two most active peptides at inhibiting the IgE:FcεRI interaction when tested with the TR-FRET assay ($IC_{50} = 11 - 58 \mu M$ for **Phe(3)-peptide** and $11 \mu M$ for **Bip(3)-peptide** when preincubated with α -Tb).

X-ray crystallography experiments for **Phe(3)-peptide**, and an analogue **Trp(3)-peptide**, with IgE-Fc were carried out, but a co-crystal structure of a peptide bound to IgE-Fc was not obtained. **Phe(3)-peptide** was then labelled with biotin on the N-terminus for subsequent SPR experiments; the peptide was immobilised to a streptavidin coated chip and solutions of both IgE and α were injected over the chip to try to determine to which protein the peptide was binding. It was found that the α bound to the immobilised **Phe(3)-peptide**, but neither the IgE-Fc or the control protein IgG₄ did, which indicated that this peptide inhibits the IgE:FcεRI by binding to FcεRI.

The fact that an 8-residue, linear peptide can inhibit this high affinity PPI with a low micromolar IC_{50} value, and that its protein partner has been identified, is an ideal starting point for future inhibitor investigations. Further structural and biophysical experiments focussing on the interaction between the peptide and FcεRI could now be carried out, with the aim of obtaining structural information about exactly how this peptide interacts with FcεRI which would facilitate the development of more potent peptide inhibitors.

5.2 Future work

5.2.1 Small molecules

Future work in the area of small molecule inhibitors of the IgE:FcεRI interaction should focus on the benzothiazine derivative of aspercyclide A; determining its protein binding partner, carrying out structural experiments and using this information to improve potency, whilst also improving other properties including solubility. As it is not known whether this compound binds to IgE or to FcεRI, or even to the protein complex, it would be important to determine this. It could be envisaged that this compound could be immobilised to an SPR chip and binding assays with both IgE-Fc and αγ could be carried with the aim of determining to which protein this compound binds. As this compound is small, it would be important to immobilise it via a number of different attachment points, to ensure an active orientation on the SPR chip. Attachment via the C19 methyl ether of the macrocycle could be a good first option for an immobilisation point, as the methyl ether group at this position does not seem to have any significant effect on the activity.

If the benzothiazine derivative of (+)-aspercyclide A was found to bind to IgE, then x-ray crystallography experiments with IgE-Fc could be carried out, along with STD and ¹⁵N-HSQC NMR experiments with the Cε2 and Cε3 domains of IgE-Fc as described earlier. If the compound was found to bind to αγ, then x-ray crystallography experiments with sFcεRIα could be carried out. This would hopefully give important structural information about the key areas of the protein that make contact with the compound and allow the development of more potent inhibitors. If the potency could be improved to the nanomolar range, it would then be important to determine the cell-based activity of this compound, by carrying out subsequent cell-based assays, for example monitoring the ability of the compound to inhibit IgE-triggered release of β-hexosaminidase or 5-hydroxytryptamine from RBL cells. Selectivity for the IgE:FcεRI interaction over any other immunoglobulin-receptor interactions would also need to be determined.

5.2.2 Peptides

As **Phe(3)-peptide** has been found to bind to αγ, the next important step should be x-ray crystallography with sFcεRIα to further confirm that this is the protein the peptide is binding to, and to identify contact residues on the protein. This information could then be used for the rational design of further peptide analogues with potentially improved activity. If a co-crystal structure was obtained of **Phe(3)-peptide** bound to sFcεRIα, it would be interesting to see how the residue in position 3 interacts with the protein. It has been found that peptides with either a

tyrosine, phenylalanine, tryptophan or biphenylalanine at position 3 all inhibit the interaction, but that a histidine is not tolerated at this position. If a biphenylalanine residue made a favourable interaction with the protein, for example a π -stacking or hydrophobic interaction, it would be interesting to carry out subsequent chemistry towards the synthesis of a library of peptides with various biaryl groups at position 3, to further probe the SAR at this position. Such modifications may give improved activity and stability, as discussed earlier, which would be advantageous. For example, Suzuki coupling could potentially be carried out if an iodo-phenylalanine was incorporated into the peptide during SPPS and then the peptide was reacted with a range of aryl boronic acids following the synthesis, which would build up a library of biaryl-containing peptides that could be tested. If more potent peptide inhibitors were developed, it would also be important to determine their cell-based activity and selectivity, as mentioned in section 5.2.1.

It could also be that a different series of peptides altogether would be a better starting point for the design of more potent peptide inhibitors of this interaction. As the TR-FRET assay has been found to be reasonably high throughput, if a larger library of peptide inhibitors was prepared, the library could be tested with the TR-FRET assay, perhaps even employing automation and robotic pipetting. Various methods could be used to synthesise a much larger library of peptides for screening, for instance SPOT technology to create a large library of peptides on a membrane^{146,147} or a technique known as split-intein circular ligation of peptides and proteins (SICLOPPS)¹⁴⁸ to make large libraries of small, cyclic peptides. Other assays to test inhibition, such as ITC, thermal melt experiments or a fluorescence polarisation assay could also be employed to measure the inhibition of peptide inhibitors, as an alternative to the TR-FRET assay.

5.2.3 Other future directions for investigating inhibitors of the IgE:Fc ϵ RI interaction

Various alternative methods could also be employed for the discovery and development of new inhibitors of the interaction between IgE and Fc ϵ RI and these are discussed in this section.

Fragment based approaches

Fragment-based screening is an alternative to HTS that uses low MW fragment molecules that generally conform to the 'Rule of 3' (MW < 300, < 3 H-bond donors, < 3 H-bond acceptors, cLogP < 3), have good aqueous solubility and typically bind with a weak affinity to a protein target.¹⁴⁹⁻¹⁵¹ These fragment libraries are screened for binding to a protein by various biophysical assays, such as thermal shift or SPR. Active fragments are good starting points for chemical expansion and can

then be linked together or optimised in some way to generate a set of drug-sized molecules which can then be screened for improved activity. This has the advantage over HTS in that a larger proportion of chemical space can be tested and also that the smaller fragments tend to be very atom efficient binders.¹⁵⁰

Tethering approaches

Another method of fragment discovery is to capture fragments that bind with a moderate affinity to a particular site on a protein using a 'tethering' approach.^{34,35} A library of fragments containing a disulfide bond could be added to a protein which had a cysteine mutation at a particular position. At equilibrium, the fragments that bound to the protein and formed a disulfide bond would be strongly bound to the protein.³⁴ Mass spectrometry of the protein/fragment library mixture could then be carried out to identify which fragments are conjugated to the protein. This approach could allow the screening of large libraries of fragments and also allow different regions of the protein to be studied by changing the position of the modified cysteine.³⁵

Virtual screening

Computational approaches have also been useful in identifying small molecules that target PPI interfaces.¹⁵²⁻¹⁵⁴ Virtual screening of small molecule libraries against the IgE:FcεRI interaction would be a useful approach to identify potential inhibitors and the results of such docking experiments, combined with advances in structural technique could be useful.

This PhD work has been a good step forward to the long-term goal of achieving potent, small molecule inhibitors of the IgE:FcεRI PPI and it will be interesting to see how further inhibitors of this important interaction develop in the coming years.

Chapter 6: Experimental

6.1 Expression and purification of IgE-Fc and $\alpha\gamma$

The following two proteins (used in the ELISA and labelled with fluorophores and used in the TR-FRET assay) were synthesised by the MRC/Asthma UK Centre in Allergic Mechanisms of Asthma Protein Production Facility at the Randall Division of Cell and Molecular Biophysics, KCL. For the experimental procedures see Dr Marie Pang, PhD thesis.¹⁵⁵

IgE-Fc: This protein consists of the C ϵ 2, C ϵ 3 and C ϵ 4 domains of IgE with a MW of 75,000. It was stored in aliquots of 1 mg/mL in PBS with 0.1% sodium azide at -80 °C (or at 4 °C if in use).

$\alpha\gamma$ (also referred to as Fc ϵ RI α :IgG₄-Fc): This fusion protein consists of the extracellular domains of the α -chain of Fc ϵ RI fused to the C γ 2 and C γ 3 domains of IgG₄ with a MW of 93,860. It was stored in aliquots of 0.25 mg/mL in PBS with 0.1% sodium azide at -80 °C (or at 4 °C if in use).

6.2 TR-FRET assay

6.2.1 TR-FRET assay general directions

Chemicals: NaHCO₃ and NaCl from Sigma-Aldrich. LanthaScreen amine reactive Tb chelate isothiocyanate and TR-FRET dilution buffer from Invitrogen. PBS Dulbecco A tablets from Oxoid.

Dialysis membrane: BioDesign Dialysis Tubing MW 8000 cut off, 6.4 mm diameter, 0.32 mL/cm volume from Fisher Scientific. **Protein concentration:** determined using UV absorption at 280 nm and 343 nm on a Nanodrop ND1000 spectrophotometer from Thermo Scientific. **SEC:** analysis of $\alpha\gamma$ -Tb carried out in PBS with 0.05% sodium azide using a dual wavelength of 280 nm and 343 nm, a flow rate of 0.3 mL/min and a run time of 15 min using a Superdex 200 5/150 mm GL column from GE Healthcare Life Sciences. Analysis of IgE-Fc-A647 carried out in PBS with 0.1% sodium azide using a wavelength of 280 nm, a flow rate of 0.75 mL/min and a run time of 40 min using a Superdex 200 10/300 GL column from GE Healthcare Life Sciences. Purification of IgE-Fc-A647 carried out in PBS with 0.1% sodium azide using a wavelength of 280 nm, a flow rate of 0.75 mL/min and a run time of 25 min using a Superdex 75 10/300 GL column from GE Healthcare Life Sciences. **Microplates:** assays carried out in white, polystyrene, flat bottom, small volume, medium-binding 384-well microplates from Greiner Bio-One. All assays were carried out at rt. **Plate reader:** plates excited at 340 nm and read at 620 nm and 665 nm using an HTRF-compatible microplate reader from Artemis. Delay time, integral time and number of flashes were all 100 μ s.

6.2.2 TR-FRET assay buffers

Sodium bicarbonate buffer: 125 mM NaCl, 100 mM NaHCO₃, pH adjusted to 8.3 with NaOH

TR-FRET dilution buffer: used as supplied by the manufacturers without dilution (exact buffer composition undisclosed by Invitrogen)

6.2.3 Labelling of IgE-Fc with Alexa Fluor 647 NHS ester

The labelling of IgE-Fc with Alexa Fluor 647 NHS ester was carried out by Dr Marie Pang, KCL. For the experimental procedure see Dr Marie Pang, PhD thesis.¹⁵⁵ A 2.5x molar excess of Alexa Fluor 647 NHS ester was used for the labelling of IgE-Fc and the resulting labelled protein (referred to as IgE-Fc-A647) had a dye:protein ratio of 1.9:1. IgE-Fc-A647 was stored in PBS with 0.1% azide at 4 °C.

6.2.4 Labelling of $\alpha\gamma$ with Tb chelate isothiocyanate

$\alpha\gamma$ conjugated to the donor fluorophore Tb chelate (the resulting labelled protein referred to as $\alpha\gamma$ -Tb) was prepared according to the following procedure. Lyophilised Lanthascreen™ amine reactive Tb chelate isothiocyanate (10 μ g) was reconstituted in DMSO (2 μ L) to obtain a 4.76 mM solution. To a solution of $\alpha\gamma$ in sodium bicarbonate buffer (37.8 μ M, 25 μ L) was added Tb chelate isothiocyanate (4.76 mM, 2 μ L) to achieve a 10x molar excess of fluorophore and the solution was shaken at rt in the dark for 3 h. The solution was then centrifuged at 12,000 rpm at rt for 2 min followed by the addition of PBS (175 μ L). The solution was dialysed into PBS (2 L) at 4 °C in the dark for 48 h, changing the buffer after 2 h and after 24 h. The final concentration of $\alpha\gamma$ -Tb was determined using a spectrophotometer and found to be 5.1 μ M. Labelling efficiency and removal of unreacted Tb chelate was determined using SEC and a dye:protein ratio of 6.3:1 was obtained. $\alpha\gamma$ -Tb was stored in PBS with 0.1% azide at 4 °C. The dye:protein ratio was calculated as follows:

$$\text{protein peak} = \frac{\text{Abs}_{280} - (\text{CF} \times \text{Abs}_{343})}{\epsilon_{\alpha\gamma}} \quad \text{dye peak} = \frac{\text{Abs}_{343}}{\epsilon_{\text{Tb}}}$$
$$\text{dye:protein ratio} = \frac{\text{dye peak}}{\text{protein peak}}$$

Abs₂₈₀ = absorbance at 280 nm for $\alpha\gamma$ (mV), CF = correction factor to account for Tb chelate absorption at 280 nm (CF = 1.1 for Tb chelate), Abs₃₄₃ = absorbance at 343 nm for Tb chelate (mV), $\epsilon_{\alpha\gamma}$ = extinction coefficient for $\alpha\gamma$ at 280 nm (M⁻¹ cm⁻¹) ($\epsilon_{\alpha\gamma}$ = 237,000 M⁻¹cm⁻¹) and ϵ_{Tb} = extinction coefficient for Tb chelate at 343 nm (M⁻¹ cm⁻¹) (ϵ_{Tb} = 12,570 M⁻¹cm⁻¹).

6.2.5 Optimisation of TR-FRET assay

Initial binding assays: Binding assays between IgE-Fc-A647 and $\alpha\gamma$ -Tb were carried out in triplicate with 20 μ L volume per well. The concentration of $\alpha\gamma$ -Tb was fixed at 0.5 nM, 1 nM, 2 nM and 5 nM and for each concentration, IgE-Fc-A647 was titrated up to a 10x molar excess, with 12 different IgE-Fc-A647 concentrations and a 2-fold dilution to obtain each concentration. The titration of IgE-Fc-A647 was carried out first, followed by the addition of a fixed concentration of $\alpha\gamma$ -Tb and the plate was then read immediately. It was found that 0.5 nM $\alpha\gamma$ -Tb and 1.25 nM IgE-Fc-A647 were ideal concentrations for use in subsequent inhibition assays. All solutions were prepared in TR-FRET dilution buffer.

Initial inhibition assays: Inhibition assays were carried out with either unlabelled IgE-Fc or unlabelled $\alpha\gamma$ as an inhibitor of the interaction between IgE-Fc-A647 and $\alpha\gamma$ -Tb. The assays were carried out in triplicate with 18 μ L volume per well. The concentration of $\alpha\gamma$ -Tb was fixed at 0.5 nM, the concentration of IgE-Fc-A647 was fixed at 1.25 nM and either unlabelled IgE-Fc or unlabelled $\alpha\gamma$ was titrated to a 10x molar excess. The titration of unlabelled protein was carried out first, then either 1) $\alpha\gamma$ -Tb was added, the plate was incubated at rt for 1 h, then IgE-Fc-A647 was added or 2) IgE-Fc-A647 was added, the plate was incubated at rt for 1 h, then $\alpha\gamma$ -Tb was added (this allowed the order of addition of the two fluorescently-labelled proteins to be investigated). The plate was then read immediately. All solutions were prepared in TR-FRET dilution buffer.

6.2.6 TR-FRET inhibition assay format

Inhibition assays were carried out in triplicate with 18 μ L volume per well. The concentration of $\alpha\gamma$ -Tb was fixed at 0.5 nM and the concentration of IgE-Fc-A647 was fixed at 1.25 nM. Inhibitors were prepared at 12 different concentrations with a maximum concentration of 1 mM and 2-fold dilutions to a final concentration of 0.49 μ M. The positive control was IgE-Fc-A647 (1.25 nM) and $\alpha\gamma$ -Tb (0.5 nM) as they would form a complex and give the maximum TR-FRET signal. The negative control was IgE-Fc-A647 (1.25 nM), $\alpha\gamma$ -Tb (0.5 nM) and either unlabelled IgE-Fc (5 nM) or unlabelled $\alpha\gamma$ (12.5 nM) as an excess of the unlabelled protein would inhibit the interaction between IgE-Fc-A647 and $\alpha\gamma$ -Tb and give the minimum TR-FRET signal. The background control was TR-FRET buffer with 2% DMSO. The titration of the inhibitor was carried out first, then either 1) $\alpha\gamma$ -Tb was added, the plate was incubated at rt for 1 h, then IgE-Fc-A647 was added or 2) IgE-Fc-A647 was added, the plate was incubated at rt for 1 h, then $\alpha\gamma$ -Tb was added (this allowed the

order of addition of the two fluorescently-labelled proteins to be investigated). The plate was then read immediately. All solutions were prepared in TR-FRET dilution buffer with 2% DMSO.

6.2.7 TR-FRET inhibition assay data analysis

The TR-FRET ratio was calculated as follows:

$$\text{TR-FRET ratio} = \frac{\text{emission at 665 nm}}{\text{emission at 620 nm}} \times 10,000$$

The TR-FRET ratio was then normalised with the background and positive controls to give a % response using the following equation:

$$\% \text{ response} = 100 \times \frac{\text{TR-FRET ratio} - \text{av BG}}{\text{av POS} - \text{av BG}}$$

av BG = average background control signal (TR-FRET dilution buffer with 2% DMSO)

av POS = average positive control signal (IgE-Fc-A647 and $\alpha\gamma$ -Tb)

This response was plotted against the concentration of inhibitor using GraFit version 7 (Leatherbarrow, R. J., Erithacus Software Ltd, Horley, UK, 2010) using a template that fitted data to a 4-parameter logistic IC₅₀ equation. IC₅₀ value = concentration of inhibitor that gives 50% response.

6.3 ELISA

6.3.1 ELISA general directions

Chemicals: PBS Dulbecco A tablets from Oxoid. Tween 20 for electrophoresis from Sigma-Aldrich. BSA lyophilised powder 96% (agarose gel electrophoresis) from Sigma-Aldrich. Biotinylated anti-human IgE epsilon chain specific affinity purified made in goat from Vector laboratories. ELISA grade streptavidin conjugated to HRP with preservative 0.01% thimerosal from Biosource. Stable peroxide substrate buffer 10x from Thermo Scientific. OPD dihydrochloride 5 mg tablets from Sigma-Aldrich. Na₂CO₃, NaHCO₃, DMSO and HCl from Sigma-Aldrich. All solvents and reagents used without further purification. **Microplates:** incubation carried out in Nunc microwell round bottom standard 96-well plates from Thermofisher Scientific and testing carried out in flat bottom F96 MaxiSorp 96-well ImmunoPlates from Scientific Laboratory Supplies Ltd. **Plate reader:** plates scanned at 492 nm in a Multiskan EX Microplate Photometer from ThermoScientific.

6.3.2 ELISA buffers

PBS: 140 mM NaCl, 8.10 mM Na₂HPO₄, 2.68 mM KCl, 1.47 mM KH₂PO₄, pH 7.3

PBS-T: as above with 0.1% (v/v) Tween 20

Carbonate buffer: 45.2 mM NaHCO₃, 18.1 mM Na₂CO₃, pH adjusted to 9.6 with acetic acid, buffer filtered using a cellulose acetate filter, pore size 0.45 µm and a glass fibre prefilter from Sartorius Stedim Biotech

6.3.3 ELISA inhibition assay format

The test plate was coated with αγ in carbonate buffer (0.02 µM, 100 µL per well) and incubated at 4 °C for 16 h then the solution was discarded and the test plate washed with PBS-T (300 µL per well) for 5 min x 3. The test plate was blocked with 2% BSA in PBS (300 µL per well) and incubated at 37 °C for 1 h then the solution was discarded and the test plate washed with PBS-T (300 µL per well) for 5 min x 3. Peptides and controls were prepared in the incubation plate with 110 µL volume in each well. The positive control was IgE-Fc (0.033 nM in PBS with 2% DMSO), which would bind to the immobilised αγ and give a maximum signal. The negative control was αγ (0.2 µM in PBS with 2% DMSO) and IgE-Fc (0.033 nM in PBS with 2% DMSO), which would form a complex and prevent IgE-Fc binding to immobilised αγ therefore giving a minimum signal. The background control was PBS (with 2% DMSO). Inhibitors were prepared in 12 different concentrations starting at 1 mM with 2-fold dilutions to a final concentration of 0.49 µM in PBS with 2% DMSO and each inhibitor solution contained 0.033 nM IgE-Fc. Inhibitors and controls were prepared in triplicate. The IgE-Fc was added last to all solutions and the plate was incubated at rt for 1 h.

Solutions in the incubation plate were then added to the test plate (100 µL per well) and incubated at 37 °C for 1 h then the solutions discarded and the test plate washed with PBS-T (300 µL per well) for 30 min and PBS-T (300 µL) for 5 min x 2. Biotinylated anti-human IgE was added to the test plate (0.1 µg/mL in PBS with 1% BSA, 100 µL per well) and incubated at 37 °C for 1 h then the solution discarded and the test plate washed with PBS-T (300 µL per well) for 5 min x 3. Streptavidin conjugated to HRP was added to the test plate (0.2 µg/mL in PBS with 1% BSA, 100 µL per well) and incubated at 37 °C for 1 h then the solution discarded and the test plate washed with PBS only (300 µL per well) for 5 min x 3. A solution of OPD dihydrochloride was added to the test plate (0.5 mg/mL in stable peroxide substrate buffer, 50 µL per well) and incubated in the dark at rt for 4 min following which 3 M HCl was added to the test plate (50 µL per well). The absorbance of the test plate was then measured at 492 nm.

6.3.4 ELISA inhibition assay data analysis

ELISA signal was normalised with the background and positive controls to give a % response using the following equation:

$$\% \text{ response} = 100 \times \frac{\text{TR-FRET ratio} - \text{av BG}}{\text{av POS} - \text{av BG}}$$

av BG = average background control signal (PBS with 2% DMSO)

av POS = average positive control signal (IgE-Fc and $\alpha\gamma$)

This response was plotted against the concentration of inhibitor using GraFit version 7 (Leatherbarrow, R. J., Erithacus Software Ltd, Horley, UK, 2010) using a template that fitted data to a 4-parameter logistic IC₅₀ equation. IC₅₀ value = concentration of inhibitor that gives 50% response.

6.4 Expression and purification of Cε2 and Cε3

6.4.1 Expression and purification of Cε2 and Cε3 general directions

Chemicals and reagents: Ampicillin and kanamycin from Melford Laboratories Ltd. LB Agar (Lennox L Agar) powder and LB Broth Base (Lennox L Broth Base) powder from Invitrogen. Super optimal broth with catabolite repression (SOC) medium from New England BioLabs. SDS for electrophoresis/molecular biology, 20% solution from Fisher BioReagents. Low MW calibration kit for SDS electrophoresis (14.4 kDa – 97.0 kDa) from GE Healthcare. Acrylamide ProtoFLOWGel (30% (w/v) acrylamide:0.8% (w/v) bis-acrylamide) protein and sequencing electrophoresis grade from Flowgen Bioscience. Sample buffer 2x from Sigma. Instant Blue coomassie based staining solution for protein gels from Expedeon Protein Solutions. All other chemicals from Sigma-Aldrich, Fisher Scientific Fisher BioReagents, Merck Millipore Calbiochem or VWR. ***E. coli*:** One Shot TOP10 chemically competent *E. coli* cells and BL21 Star (DE3) One Shot chemically competent *E. coli* cells from Invitrogen. **Plasmids:** the Cε2 plasmid (pET5a vector, ampicillin resistant) and Cε3 plasmid (pET28a vector, kanomycin resistant) supplied by Dr Anthony Keeble, KCL. **DNA purification:** using a Wizard Plus Maxipreps DNA purification system from Promega. **Agarose gel electrophoresis:** gels were run in 1x running buffer at 100 V for ~ 15 min then at 150 V for ~ 15 min and visualised using ethidium bromide fluorescence under UV light with a molecular imager Gel Doc XR+ imaging system from Bio-Rad. **Cε3 purification:** carried out on an AKTA fast protein liquid chromatography (FPLC) instrument from Amersham Pharmacia Biotech. **Protein concentration:** determined on a Nanodrop ND1000 spectrophotometer from Thermo Scientific measuring UV absorption at 280

nm. **SDS-PAGE:** 5 μg – 20 μg of protein in 1x sample buffer was heated to 100 °C for 10 min prior to loading into the gel. Gels were run in 1x running buffer at 160 V for ~ 25 min then at 180 V for ~ 25 min and visualised using Instant Blue staining solution. **C ϵ 3 mass spectra:** recorded on a Bruker Maxis time of flight (TOF) instrument with a Kd Scientific injector using ESI. A solution of C ϵ 3 (10 $\mu\text{g}/\text{mL}$, 200 μL) in 1:1 acetonitrile:H₂O with 0.1% formic acid was used to obtain the mass spectrum. **C ϵ 3 ¹H NMR spectra:** recorded at 500 MHz on a Bruker500 Ultrashield DRX500 instrument. Chemical shifts (δ_{H}) are quoted in ppm. A solution of C ϵ 3 (0.75 mg/mL, 580 μL) in PBS pH 7.3, 5% D₂O was used to obtain the ¹H NMR spectrum.

6.4.2 Buffers and solutions for expression of C ϵ 2 and C ϵ 3

LB agar (per L of H₂O): 12 g agar, 10 g peptone, 5 g yeast extract, 5 g NaCl

LB broth (per L of H₂O): 10 g peptone, 5 g yeast extract, 5 g NaCl

Minimal media (per L of H₂O): 6 g Na₂HPO₄, 3 g KH₂PO₄, 0.7 g NH₄Cl, 0.5 g NaCl, 2 mL 1M MgSO₄, 10 μL 1M CaCl₂, 10 mL 20% glucose

Tris/boric acid/EDTA (TBE) agarose gel electrophoresis running buffer (1x) (per L of H₂O): 10.8 g Tris, 5.5 g boric acid, 4 mL of 0.5 M ethylenediaminetetraacetic acid (EDTA)

Agarose gel (for 1 gel): 7 mL TBE buffer (10x), 63 mL agarose, 3.5 μL ethidium bromide

6.4.3 Buffers for purification of C ϵ 2 and C ϵ 3

Lysis buffer: 100 mM EDTA, 50 mM MgCl₂, 1 mM phenylmethylsulfonyl fluoride (PMSF), 1 mM dithiothreitol (DTT), 1% Triton-X, pH 7.4

Solubilisation buffer: 6 M guanidinium chloride, 0.5 M NaCl, 20 mM Na₂HPO₄, 1 mM DTT, pH 7.4

Binding buffer: 6 M guanidinium chloride, 0.5 M NaCl, 20 mM Na₂HPO₄, pH 7.4

Refolding buffer: 0.5 M NaCl, 20 mM Na₂HPO₄, pH 7.4

Elution buffer: 0.5 M NaCl, 20 mM Na₂HPO₄, pH 1.5

Gel filtration buffer: 0.5 M NaCl, 0.2 M arginine, 20 mM Na₂HPO₄, 0.02% sodium azide, pH 5.0

6.4.4 Buffers and solutions for SDS-PAGE

SDS-PAGE sample buffer (2x): 0.1 M tris-HCl, 24% glycerol, 4% 2-mercaptoethanol, 1% SDS, 0.02% brilliant blue G, pH 6.8

Resolving gel (for 2 gels): 5.0 mL acrylamide (30%), 2.6 mL 1.5 mM tris (0.1% SDS, pH 8.5), 2.3 mL H₂O, 50 μL 10% ammonium persulfate (APS), 10 μL tetramethylethylenediamine (TMEDA)

Stacking gel (for 2 gels): 3.4 mL 0.5 M tris (0.1% SDS, pH 6.8), 0.54 mL 30% acrylamide, 24 μ L 10% APS, 10 μ L TMEDA, 1 drop bromophenol blue

SDS-PAGE running buffer (1x) (per L of H₂O): 3 g tris, 14.4 g glycine, 1 g SDS

6.4.5 Expression of C ϵ 2 and C ϵ 3

Each plasmid (1 μ L) was transformed into chemically competent TOP10 *E. coli* cells, (20 μ L) incubated on ice for 30 min then incubated at 42 °C for 30 s to heat shock cells. Pre-warmed LB agar (250 μ L) containing 100 μ g/mL of ampicillin for C ϵ 2 or 30 μ g/mL kanamycin for C ϵ 3 was added. *E. coli* cells (100 μ L) were spread onto an LB agar plate containing 100 μ g/mL of ampicillin (C ϵ 2) or 30 μ g/mL kanamycin (C ϵ 3) and incubated at 37 °C overnight. 5 colonies were then removed and cultured in LB media (10 mL) containing 100 μ g/mL ampicillin (C ϵ 2) or 30 μ g/mL kanamycin (C ϵ 3) at 37 °C overnight. Plasmids were purified using a DNA purification kit according to the manufacturer's instructions and a brief outline is described here; cell resuspension solution (200 μ L), followed by cell lysis solution (200 μ L) was added and cells were incubated at rt for 10 min. Cell neutralisation solution (400 μ L) was added to precipitate cell organelles and leave the DNA dissolved in the supernatant. Centrifugation (4000 rpm, 4 °C, 15 min) was used to pellet the cell organelles and the supernatant was removed and added to a mini-column containing DNA resin (1 mL). The resin was washed with was solution (2 mL) then H₂O (50 μ L) pre-warmed to 70 °C was added to dissolve the DNA. The DNA concentration was measured using absorbance at 260 nm, the purity was measured using agarose gel electrophoresis and the DNA was sent for sequencing to confirm the correct sequence was obtained.

Each plasmid (1 μ L) was then transformed into chemically competent BL21 *E. coli* cells (100 μ L), incubated on ice for 20 min then incubated at 42 °C for 45 s to heat shock cells. SOC medium (200 μ L) was then added and the cells were incubated at 37 °C with shaking for 45 min. *E. coli* cells (200 μ L) were then spread onto LB agar plates containing 100 μ g/mL of ampicillin (C ϵ 2) or 30 μ g/mL kanamycin (C ϵ 3) and incubated at 37 °C overnight. A starter culture was set up by adding 1 colony to LB media (20 mL) containing 100 μ g/mL of ampicillin (C ϵ 2) or 30 μ g/mL kanamycin (C ϵ 3) and incubating overnight at 37 °C in a shaker. The starter culture was then centrifuged (4000 revolutions per minute (rpm), 20 °C, 5 min) to pellet cells, the supernatant was removed and cells were solubilised in minimal media (8 mL). This solution was then added to minimal media (2 L) containing 100 μ g/mL of ampicillin (C ϵ 2) or 30 μ g/mL kanamycin (C ϵ 3) and the solution shaken at 37 °C. OD was measured every hour and after ~ 8 hours when OD had reached at least 0.6, cells

were induced by the addition of 1 mM IPTG. Expression was allowed to continue for 20 h, then the solution was split into 2 x 1 L samples and centrifuged (4000 rpm, 4 °C, 20 min) to pellet cells. The supernatant media was removed and each cell sample was resuspended in PBS pH 7.3 (40 mL). The solutions were shaken, centrifuged (4000 rpm, 4 °C, 20 min) and supernatant PBS was removed. Cell pellets were stored at -20 °C until purification. SDS-PAGE analysis of induced vs uninduced cells was used to confirm that expression had taken place following induction with IPTG.

6.4.6 Purification of Cε3

Pelleted cells were resuspended in lysis buffer (20 mL) using a homogeniser to break up cell pellets, sonicated for 8 x 30 sec and centrifuged (10,000 g, 4 °C, 12 min). Supernatant lysis buffer was discarded, fresh lysis buffer was added (20 mL) using a homogeniser to break up cell pellets, cells were spun slowly at 4 °C for 40 min then centrifuged (10,000 g, 4 °C, 12 min). This was repeated twice more, supernatant lysis buffer was discarded, solubilisation buffer (20 mL) was added to solubilise the protein inclusion bodies and proteins were spun slowly at 4 °C overnight. The solution was then centrifuged (10,000 g, 4 °C, 15 min) to remove cell organelles and filtered through a 0.22 µm membrane.

Purification and refolding was carried out on an AKTA FPLC using a Ni²⁺ column. The Ni²⁺ column was equilibrated with binding buffer then Cε3 was loaded on to the column and washed with binding buffer. Cε3 was refolded by adding refolding buffer from a gradient of 0 – 100%, then eluted by adding elution buffer. One fraction (5 mL) containing pure protein was then run through a gel filtration column to remove any unfolded protein using gel filtration buffer and 8 pure fractions (each 10 mL) were obtained. These fractions were combined and concentrated by centrifugation (4000 rpm, 4 °C, 45 min) using a concentration tube with a 5,000 MW cut off until 1 mL of pure protein was obtained. The protein was buffer exchanged by adding PBS pH 5.0 (20 mL) and centrifuging (4000 rpm, 4 °C, 1.5 hour) and this was repeated 4 times. The concentration of refolded, pure Cε3 was measured using absorption at 280 nm and found to be 7.53 mg/mL. SDS-PAGE, MS and ¹H NMR analysis were carried out to determine the purity of Cε3. Cε3 was stored in PBS pH 5.0 with 0.01% sodium azide at 4 °C.

6.5 SPR experiments

6.5.1 SPR general directions

Chemicals: EDC, NHS and ethanolamine hydrochloride pH 8.5 from GE Healthcare. Sodium acetate pH 4.5 from Sigma-Aldrich. Glycine pH 2.0 and pH 2.5 solutions from GE Healthcare. Streptavidin from Sigma-Aldrich. Biotin-IgE-Fc was synthesised by Dr Marie Pang, KCL.¹⁵⁵ **SPR chips:** Series S sensor chip CM5 (carboxymethylated dextran matrix covalently attached to gold surface) and series S sensor chip SA (carboxymethylated dextran matrix pre-immobilised with streptavidin) both from GE Healthcare. New sensor chips stored under N₂ at 4 °C, sensor chips with immobilised proteins stored in running buffer with 0.1% azide at 4 °C. **SPR instrument:** experiments carried out at 25 °C on a Biacore T200 biosensor from GE Healthcare.

6.5.2 SPR buffers

HBS running buffer: 150 mM NaCl, 10 mM HEPES, 3 mM EDTA, 0.005% Tween 20, pH 7.4.

PBS running buffer: 140 mM NaCl, 8.10 mM Na₂HPO₄, 2.68 mM KCl, 1.47 mM KH₂PO₄, 2% DMSO, 0.005% Tween 20, pH 7.3.

6.5.3 Immobilisation of $\alpha\gamma$ onto CM5 sensor chip

The carboxymethylated matrix was activated by adding EDC (0.2 M) and NHS (0.05 M) for 420s at a flow rate of 10 μ L/min. Following activation, $\alpha\gamma$ (100 nM) in sodium acetate buffer (10 mM, pH 4.5) was added for between 500 and 2000s at a flow rate of 10 μ L/min. To cap the surface, ethanolamine hydrochloride pH 8.5 (1.0 M) was added for 420s at a flow rate of 10 μ L/min. The $\alpha\gamma$ immobilisation was carried out on one flow cell only. Another flow cell was used as a control surface that had been activated and capped only, without addition of $\alpha\gamma$. All immobilisation steps were carried out in HBS running buffer.

6.5.4 Initial binding of IgE-Fc to immobilised $\alpha\gamma$

To determine if the immobilised $\alpha\gamma$ was an active surface, IgE-Fc (10 nM) was added for 180s at a flow rate of 20 μ L/min. Glycine (10 mM, pH 2.5) was then added for 60s at a flow rate of 20 μ L/min to remove IgE-Fc bound to the immobilised $\alpha\gamma$. This was repeated and if reproducible results were obtained then the chip was deemed ready to use for subsequent inhibition assays. Binding experiments were carried out in PBS running buffer with 2% DMSO.

6.5.5 Immobilisation of IgE-Fc onto CM5 sensor chip

The carboxymethylated matrix was activated by adding EDC (0.2 M) and NHS (0.05 M) for 420s at a flow rate of 10 $\mu\text{L}/\text{min}$. Following activation streptavidin (160 nM) in sodium acetate buffer (10 mM, pH 4.5) was added for 300s at a flow rate of 10 $\mu\text{L}/\text{min}$. To cap the surface ethanolamine hydrochloride pH 8.5 (1.0 M) was added for 420s at a flow rate of 10 $\mu\text{L}/\text{min}$. Biotin-IgE-Fc (125 nM) was then added for between 700 and 1000s at a flow rate of 10 $\mu\text{L}/\text{min}$. The streptavidin immobilisation was carried out on two flow cells, the biotinylated IgE-Fc binding was carried out on one streptavidin flow cell only, with the other being used as a control surface. All immobilisation steps were carried out in HBS running buffer.

6.5.6 Initial binding of $\alpha\gamma$ to immobilised IgE-Fc

To determine if the immobilised IgE-Fc was an active surface, $\alpha\gamma$ (10 nM) was added for 180s at a flow rate of 20 $\mu\text{L}/\text{min}$. Glycine (10 mM, pH 2.5) was then added for 60s at a flow rate of 20 $\mu\text{L}/\text{min}$ to remove $\alpha\gamma$ bound to the immobilised IgE-Fc. This was repeated and if reproducible results were obtained then the chip was deemed ready to use for subsequent inhibition assays. Binding experiments were carried out in PBS running buffer with 2% DMSO.

6.5.7 Inhibition assay with dibenzofuran (\pm)-11, IgE-Fc and immobilised $\alpha\gamma$

Initial inhibition assays were carried out using the flow cell with immobilised $\alpha\gamma$. Dibenzofuran (\pm)-11 (HJD-107) was prepared in 10 different concentrations starting at 160 μM with 2-fold dilutions to a final concentration of 0.313 μM . Each inhibitor solution contained a fixed concentration of IgE-Fc (10 nM) and all inhibitor/IgE-Fc solutions were made in PBS 2% DMSO SPR running buffer. The inhibitor/IgE-Fc solutions were allowed to incubate for at least 1 h, then injected over the immobilised $\alpha\gamma$ for 180s at a flow rate of 20 $\mu\text{L}/\text{min}$. After the injection of each different inhibitor/IgE-Fc solution, an injection of glycine (10 mM, pH 2.5) for 60s at a flow rate of 20 $\mu\text{L}/\text{min}$ removed any bound IgE-Fc. The inhibition assay was carried out in PBS 2% DMSO SPR running buffer.

6.5.8 Immobilisation of b-Phe(3)-peptide onto SA sensor chip

B-Phe(3)-peptide (LDS-002-1A) (100 nM, in HBS) was added to one flow cell for 120s at a flow rate of 20 $\mu\text{L}/\text{min}$ which gave an increase in signal of ~ 100 resonance units. **B-Phe(3)-peptide** (100 nM, in HBS) was then added to the same flow cell for a further 1200s at a flow rate of 5 $\mu\text{L}/\text{min}$ which

gave an increase in signal of ~ 350 resonance units and saturation of the chip surface. All immobilisation steps were carried out in HBS running buffer.

6.5.9 Initial binding of IgE-Fc to immobilised b-Phe(3)-peptide

IgE-Fc (13.3 μM , in PBS) was added for 120s at a flow rate of 5 $\mu\text{L}/\text{min}$ in HBS running buffer which gave an increase in signal of ~ 40 resonance units. The IgE-Fc was injected over both the flow cell with immobilised **b-Phe(3)-peptide** (LDS-002-1A) and the flow cell with immobilised streptavidin only as a control. The data for the streptavidin flow cell was subtracted from the data for the peptide flow cell.

6.5.10 Initial binding of $\alpha\gamma$ to immobilised b-Phe(3)-peptide

$\alpha\gamma$ (2.66 μM , in PBS) was added for 120s at a flow rate of 5 $\mu\text{L}/\text{min}$ in HBS running buffer which gave an increase in signal of ~ 70 resonance units. The $\alpha\gamma$ was injected over both the flow cell with immobilised **b-Phe(3)-peptide** (LDS-002-1A) and the flow cell with immobilised streptavidin only as a control. The data for the streptavidin flow cell was subtracted from the data for the peptide flow cell.

6.5.11 Binding assays of IgE-Fc, $\alpha\gamma$ and IgG₄ to immobilised b-Phe(3)-peptide

IgE-Fc was prepared in 12 different concentrations (13.3 μM , 12 μM , 10 μM , 8 μM , 6 μM , 4 μM , 2 μM , 1 μM , 0.5 μM , 0.2 μM , 0.1 μM , 0.05 μM) with dilutions made in HBS. $\alpha\gamma$ was prepared in 9 different concentrations (3 μM , 2.5 μM , 2 μM , 1.5 μM , 1 μM , 0.5 μM , 0.25 μM , 0.125 μM , 0.06 μM) with dilutions made in HBS. IgG₄ (provided by Dr Anna Davies, KCL) was used as a control protein as the peptide was not expected to bind to this. IgG₄ was prepared in 12 different concentrations (4 μM , 3.5 μM , 3 μM , 2.5 μM , 2 μM , 1.5 μM , 1 μM , 0.5 μM , 0.25 μM , 0.125 μM , 0.06 μM , 0.03 μM) with dilutions made in HBS. Each different concentration of each protein was added in turn for 120s at a flow rate of 20 $\mu\text{L}/\text{min}$ in HBS running buffer. Each injection was carried out twice to obtain duplicate results. The proteins were injected over both the flow cell with immobilised **b-Phe(3)-peptide** (LDS-002-1A) and the flow cell with immobilised streptavidin only as a control. The data for the streptavidin flow cell was subtracted from the data for the peptide flow cell to give the signal for this experiment.

6.6 Protein crystallography

6.6.1 Protein crystallography general directions

Chemicals: Li_2SO_4 , tris, PEG, NaCl, sodium azide, ethylene glycol and hexylene glycol from Sigma-Aldrich. **Microplates:** co-crystallisations carried out in a MRC 96-well 2-drop UV sitting drop crystallisation plate from Molecular Dimensions. Soak crystallisations carried out in a MRC MAXI 48-well polystyrene crystallisation plate from Molecular Dimensions. **Protein crystal seeds:** generated using a PTFE Seed Bead from Hampton Research. **Automated pipetting:** carried out using a mosquito liquid handler from TTP Labtech. **Sealing sheets:** UV transparent ClearVue sheets from Molecular Dimensions. **Apo IgE-Fc crystals:** grown under the co-crystallisation conditions outlined below but with no inhibitor or ligand present, provided by Dr Nyssa Drinkwater, KCL. **Data collection:** carried out either at the Diamond Light Source synchrotron in Oxfordshire, UK using beamline I04 or at KCL using an Xcalibur PX Nova CCD single crystal diffractometer from Oxford Diffraction. **Data analysis:** crystal structures were solved by molecular displacement using a high resolution IgE-Fc structure with the PDB code 2WQR²² and with the CCP4 software Phenix Refine and Coot. IgE-Fc space group = $P2_12_12$, $a = 128.5$, $b = 75.0$, $c = 79.5$, $\alpha = \beta = \gamma = 90^\circ$.

6.6.2 Protein crystallography buffers and solutions

Co-crystallisation reservoir solution: 0.2 M Li_2SO_4 , 0.1M tris (pH 7.5 – 9.0), PEG 8K (14 – 24%)

IgE-Fc/inhibitor buffer: 25 mM tris pH 7.5, 20 mM NaCl, 0.05% azide

Stabilising solution: 0.2 M Li_2SO_4 , 0.1 M tris pH 7.5, 24% PEG 8K

Cryoprotectant solution: 0.2 M Li_2SO_4 , 0.1M tris pH 7.0, 24% PEG 8K, 16% ethylene glycol, 16% hexylene glycol

6.6.3 Co-crystallisations

Four experiments, each of 24 wells, were set up in one 96-well plate. Each well contained 70 μL reservoir solution and across the 24 wells the pH of the tris buffer was varied between 7.5 and 9.0 (0.5 increments), the concentration of PEG 8K was varied between 14% and 24% (2% increments) and the concentration of Li_2SO_4 was kept constant. IgE-Fc/inhibitor solutions were prepared with IgE-Fc (26.7 μM) and inhibitor (50 μM , 100 μM , 200 μM or 300 μM) in IgE-Fc/inhibitor buffer and incubated for 1 h. Next to each well were two 'sitting drops' containing 1 μL IgE-Fc/inhibitor solution, 400 nL reservoir solution and 100 nL seed solution (ground up apo crystals of IgE-Fc in stabilising solution). One drop contained seed solution diluted by a factor of 5 and one drop contained seed solution diluted by a factor of 10. The plate was covered and incubated at 18 $^\circ\text{C}$ for

~ 10 - 20 days, with plate-shaped, oblong crystals forming after ~ 5 days. Individual crystals were then added to the corresponding inhibitor (500 μ M) in cryoprotectant solution and frozen in liquid nitrogen.

6.6.4 Soak crystallisations

Two experiments, each of 1 well, were set up in one 24-well plate. Each well contained 100 μ L cryoprotectant solution. Inhibitor solutions were prepared with inhibitor (500 μ M or 2.5 mM) in cryoprotectant solution. Next to each well was one sitting drop containing 5 μ L inhibitor solution and 4 – 6 apo crystals of IgE-Fc. The plate was covered and incubated at 18 °C for ~ 5 - 10 days, after which individual crystals were frozen in liquid nitrogen.

6.7 Synthesis of aspercyclide A and analogues

All compounds in Table 22 were synthesised by Dr Jimmy Sejberg (IC).^{91,92}

(±)-1 (JS-039)		(+)-3 (JS-287)	
(+)-1 (JS-039-E1)		(+)-4 (JS-289)	
(+)-2a (JS-291)		(+)-5 (JS-312)	
(+)-2b (JS-256-P)			

Table 22: Aspercyclide A and analogues used in experiments

NB: The references in parenthesis indicated the Spivey research group compound reference number.

6.8 Synthesis of dibenzofuran and analogues

All compounds in Table 23 were synthesised by Dr Helena Dennison¹³⁸, Dr Jimmy Sejberg or Dr Daniel Offerman (IC).

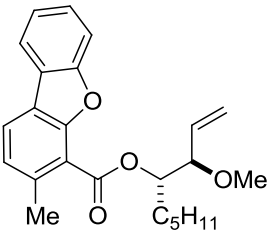
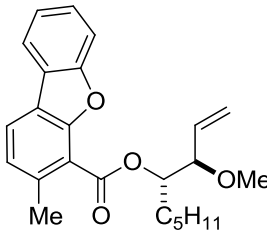
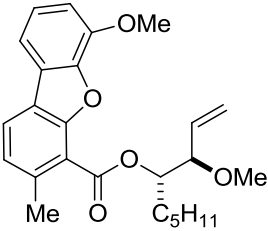
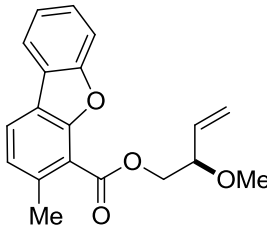
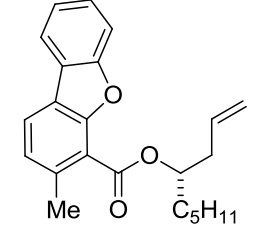
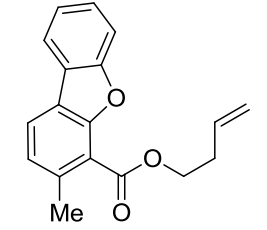
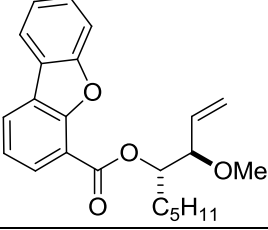
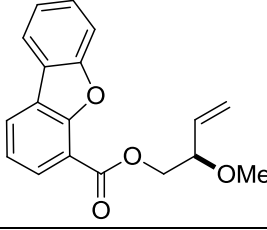
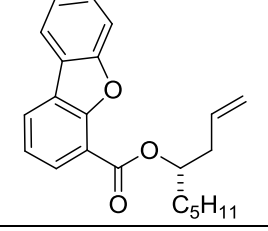
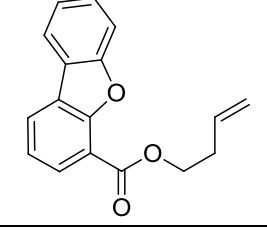
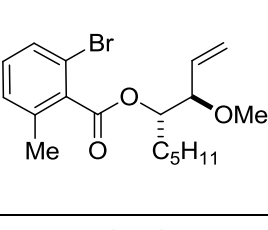
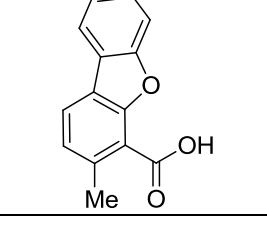
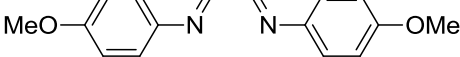
(±)-11 (HJD-107)		(±)-23 (JS-331)	
(±)-12 (HJD-115)		14 (HJD-210)	
13 (HJD-205)		15 (HJD-211)	
(±)-16 (HJD-186)		18 (HJD-214)	
17 (HJD-213)		19 (HJD-212)	
(±)-20 (JS-004/26)		21 (JS-322)	
8 (DAO-268)			

Table 23: Dibenzofurans and analogues used in experiments

NB: The references in parenthesis indicated the Spivey research group compound reference number. HJD, JS and DAO refer to compounds synthesised by Dr Helena Dennison, Dr Jimmy Sejberg and Dr Daniel Offerman respectively.

6.9 Peptide synthesis

6.9.1 Peptide synthesis general directions

Reagents and solvents: Fmoc-protected L-amino acids (side-chain protecting groups in parenthesis) Ala, Asp(O^tBu), His, Ile, Lys(Boc), Phe, Trp(Boc), Tyr(^tBu) and Val from AGTC Bioproducts. Fmoc-protected unnatural amino acid L-biphenylalanine (Bip) from VWR International. (+)-Biotin-NHS ester from VWR International. HATU and HBTU from AGTC Bioproducts. TentaGel S Rink Amide Resin (0.23 mmol/g loading) from RAPP Polymere. NMM, NMP, DMF, DIPEA, piperidine, acetic anhydride, dichloromethane, methanol, diethyl ether, TFA, TIS and TBME from Sigma-Aldrich or VWR International. All solvents and reagents were used without further purification. **Deionised water:** obtained from Elix and MilliQ Millipore water purification systems. **Peptide synthesis:** carried out using an Intavis AG ResPep SL instrument. **Centrifugation:** carried out using a Jouan BR4 centrifuge. **LC-MS:** carried out using a Waters HPLC system equipped with a 2767 Sample Manager, a 515 HPLC Pump, a 3100 Mass Detector with ESI and a 2998 Photodiode Array Detector (detection at 200 - 600 nm). The system was fitted with Waters XBridge C18 columns (4.6 mm × 100 mm for analytical LC-MS and 19.0 mm × 100 mm for preparative LC-MS). **LC-MS solvent evaporation:** carried out using a Genevac EZ-2 plus, HCl compatible personal evaporator. **Lyophilisation:** carried out using a Christ Alpha 1-4 instrument.

6.9.2 Automated SPPS

All peptides were synthesised on a 20 µmol scale from the C-terminus to the N-terminus using standard, automated Fmoc SPPS. The rink amide resin (20 µmol per well of the peptide synthesiser) was placed into the peptide synthesiser and swelled in DMF for 1 h, then the DMF removed by filtration. Fmoc deprotection (initially of the resin, then afterwards of each Fmoc-protected amino acid) was achieved with 20% piperidine in DMF (400 µL) for 10 min x 3, followed by washing the resin with DMF (400 µL) x 8. Coupling of the subsequent Fmoc-protected amino acid was carried out with HBTU in NMP (0.5 M, 170 µL), NMM in NMP (4 M, 52 µL), NMP (5 µL) and the Fmoc-protected amino acid in NMP (0.5 M, 175 µL) for 35 min. This coupling reaction was then repeated for 45 min. A cap mixture consisting of 5% acetic anhydride in DMF (400 µL) was then added for 5 min (this capped any unreacted N-terminal free amines on the growing peptide) followed by washing the resin with DMF (600 µL) x 2 and DMF (500 µL) x 5. This cycle of Fmoc-deprotection, washing, coupling, capping and washing was repeated until each peptide was the desired length. Deprotection of the N-terminal Fmoc protecting group on all peptides was then carried out with 20% piperidine in DMF (400 µL) for 10 min x 3, followed by washing the resin with DMF (400 µL) x

8 and dichloromethane (600 μ L) x 3. After the peptide synthesis was complete, the resin was removed from the synthesiser, placed in a syringe fitted with a polystyrene frit, washed with DMF (3 mL) x 3, dichloromethane (3 mL) x 3, methanol (3 mL) x 3 and diethyl ether (3 mL) x 3 and dried in a desiccator under vacuum for at least 16 h.

Unnatural amino acid coupling: Synthesis was carried out as above, except the coupling of the unnatural amino acid Bip was carried out with the alternative coupling agent HATU in DMF (0.4 M, 170 μ L), NMM in NMP (4 M, 52 μ L), NMP (5 μ L) and the Fmoc-protected Bip in DMF (0.6 M, 175 μ L). The reaction time was increased to 50 min and the reaction was then repeated for 50 min.

6.9.3 Cleavage from resin and side-chain deprotection of peptides

Cleavage of the peptide from the resin and simultaneous side chain deprotection was achieved using a deprotection mixture of 95% TFA, 2.5% H₂O and 2.5% TIS (1.5 mL) and shaking at rt for 3 h. The mixture was removed by filtration and the resin washed with deprotection mixture (1 mL) and TFA (1 mL). The filtrate and washings were combined and the TFA removed under nitrogen to leave a volume of approximately 1 mL. Ice-cold TBME (10 mL) was added with vigorous shaking to precipitate the deprotected, cleaved peptide. The mixture was centrifuged (4000 rpm) at 5 °C for 15 min and the supernatant TBME was removed. Fresh ice-cold TBME (10 mL) was added, the peptide pellet broken up, the mixture centrifuged (4000 rpm) at 5 °C for 15 min and the supernatant TBME removed. This process was repeated once more, then the peptide was dried in a desiccator under vacuum for at least 16 h.

6.9.4 On-resin biotin labelling of peptides

The biotin labelling reaction was carried out on the N-terminus of the resin-bound, side-chain protected peptide after SPPS.

First biotin labelling reaction: The resin was shaken in DMF (2 mL) at rt for 1 h to swell the resin, then the DMF removed by filtration. Biotin-labelling solution (biotin-NHS ester 5 eq, 50 mM and DIPEA 1 eq, 10 mM, 2 mL) was added with shaking at rt for 1 h, then the solution removed by filtration and the resin washed with DMF (2 mL). This was repeated by adding fresh biotin-labelling solution (biotin-NHS ester 5 eq, 50 mM and DIPEA 1 eq, 10 mM, 2 mL) and shaking at rt for 1 h, then the solution removed by filtration. The resin was washed with DMF (3 mL) x 3,

dichloromethane (3 mL) x 3, methanol (3 mL) x 3 and diethyl ether (3 mL) x 3 and dried in a desiccator under vacuum for at least 16 h.

Optimised biotin labelling reaction: The reaction was carried out as above, except after the initial labelling reaction for 1 h, fresh biotin-labelling solution was added and the resin shaken at rt for an increased reaction time of 16 h.

Following the biotin labelling, the peptides were then cleaved from the resin with simultaneous side-chain deprotection as described in section 6.9.3.

6.9.5 LC-MS analysis and purification of peptides

LC-MS was used to analyse and purify all peptides. LC-MS grade methanol and deionised water, both degassed and containing 0.1% formic acid, were used as the mobile phases.

Analytical LC-MS: a small amount of peptide (~ 0.1 mg) was dissolved in a solution of 5% methanol in H₂O. A linear gradient of 5 – 98% methanol, a run time of 18 min and a flow rate of 1.2 mL/min was used.

Preparative LC-MS: all of the crude peptide (~ 17 – 20 mg per well of the peptide synthesiser) was dissolved in a solution of 5% methanol in H₂O, then filtered through a 0.45 µm membrane low protein binding syringe filter to give a clear solution. A linear gradient of 5 – 98% methanol, a run time of 18 min and a flow rate of 20 mL/min was used.

Following preparative LC-MS, methanol was evaporated from pure fractions and the remaining aqueous solution was frozen in liquid nitrogen and lyophilised for at least 24 h to yield the pure peptide as a white amorphous powder. Pure peptides were further analysed using analytical LC-MS (as described above) to check purity, then stored as solids at – 20 °C.

6.9.6 LC-MS characterisation data for all pure peptides

LC-MS characterisation data for all pure peptides synthesised during the PhD can be seen in Table 24.

Name/Reference	Sequence	MW	Mass (mg)	Yield ^a (%)	Rt (min)	m/z (ES-)
Parent-peptide (LDS-001-1A)	H ₂ N-Asp-Lys-Tyr-Tyr-Ile-Val-Lys-Tyr-CONH ₂	1090.27	6.8	31	8.36	1088.73
Phe(3)-peptide (LDS-001-2A)	H ₂ N-Asp-Lys-Phe-Tyr-Ile-Val-Lys-Tyr-CONH ₂	1074.27	6.2	29	8.87	1072.60
Bip(3)-peptide (LDS-001-3A)	H ₂ N-Asp-Lys-Bip-Tyr-Ile-Val-Lys-Tyr-CONH ₂	1150.37	7.7	33	9.90	1148.68
C-strand peptide (LDS-001-4A)	H ₂ N-Tyr-Lys-Val-Ile-Tyr-Tyr-Lys-Asp-CONH ₂	1090.27	8.4	39	6.94	1088.79
link-Phe(3)-peptide (LDS-002-2B-free)	H ₂ N-Gly-Gly-Gly-Asp-Lys-Phe-Tyr-Ile-Val-Lys-Tyr-CONH ₂	1245.45	2.9	23	8.35	1243.68
b-Phe(3)-peptide (LDS-002-1A)	biotin-Asp-Lys-Phe-Tyr-Ile-Val-Lys-Tyr-CONH ₂	1300.59	1.8	8	10.16	1298.84
b-Phe(3)-peptide (LDS-002-1B)	biotin-Asp-Lys-Phe-Tyr-Ile-Val-Lys-Tyr-CONH ₂	1300.59	3.3	15	9.96	1298.85
b-link-Phe(3)-peptide (LDS-002-2A)	biotin-Gly-Gly-Gly-Asp-Lys-Phe-Tyr-Ile-Val-Lys-Tyr-CONH ₂	1471.74	0.9	4	9.97	1469.91
b-link-Phe(3)-peptide (LDS-002-2B)	biotin-Gly-Gly-Gly-Asp-Lys-Phe-Tyr-Ile-Val-Lys-Tyr-CONH ₂	1471.74	0.8	3	9.90	1470.12

Table 24: LC-MS characterisation data for all pure peptides synthesised during PhD

^ayield based on maximum theoretical yield of 20 μmol peptide per well of the peptide synthesiser.

NB: H₂N- denotes a free N-terminus and –CONH₂ denotes an amidated C-terminus. The references in parenthesis indicated the Spivey research group compound reference number.

6.9.7 Other peptides used in experiments

Some of the peptides used during the PhD were synthesised during the MRes research project¹³¹ as outlined in Table 25 below.

Name/Reference	Sequence	Synthesised by
Phe(3)-peptide (LDS-001-3A-MRes)	H ₂ N-Asp-Lys-Phe-Tyr-Ile-Val-Lys-Tyr-CONH ₂	Lucy Smith – MRes (IC)
Trp(3)-peptide (LDS-001-4A-MRes)	H ₂ N-Asp-Lys-Trp-Tyr-Ile-Val-Lys-Tyr-CONH ₂	Lucy Smith – MRes (IC)
His(3)-peptide (LDS-005-5A-MRes)	H ₂ N-Asp-Lys-His-Tyr-Ile-Val-Lys-Tyr-CONH ₂	Lucy Smith – MRes (IC)

Table 25: Other peptides used in experiments

6.10 Novartis testing of small molecules and peptides

The following compounds were tested in ELISA, FRET and SPR experiments by Dr Jeffrey Stonehouse (Investigator III, Global Discovery Chemistry, Novartis Institutes for Biomedical Research, Horsham Research Centre, Wimblehurst Road, Horsham, West Sussex, RH12 5AB, UK) and his team: **(±)-1** (JS-039), **(+)-2b** (JS-256), **(+)-5** (JS-312), **13** (HJD-205), **(±)-16** (HJD-186), **21** (JS-322), **(±)-23** (JS-331), **parent peptide** (LDS-001-1) and **Phe(3)-peptide** (LDS-001-2). 100 µL solutions of the above inhibitors at 50 mM in DMSO were shipped to Novartis on solid CO₂. Compounds were screened by Novartis as full dose-response IC₅₀ curves to a maximum concentration of 650 µM in the ELISA and FRET assays and were screened at 200 µM and 20 µM in the SPR experiments. ELISA buffer was: PBS, 3 mM EDTA, 0.1% Tween 30. FRET buffer was: 50 mM HEPES, 3 mM EDTA, 0.02% Tween 20. Further assay procedures were not disclosed by Novartis.

7: References

- (1) Gupta, R.; Sheikh, A.; Strachan, D. P.; Anderson, H. R. *Clin. Exp. Allergy* **2004**, *34*, 520.
- (2) Eder, W.; Ege, M. J.; von Mutius, E. *N. Engl. J. Med.* **2006**, *355*, 2226.
- (3) Chang, T. W. *Nat. Biotechnol.* **2000**, *18*, 157.
- (4) Gould, H. J.; Sutton, B. J.; Bevil, A. J.; Bevil, R. L.; McCloskey, N.; Coker, H. A.; Fear, D.; Smurthwaite, L. *Annu. Rev. Immunol.* **2003**, *21*, 579.
- (5) Gould, H. J.; Sutton, B. J. *Nat. Rev. Immunol.* **2008**, *8*, 205.
- (6) Cookson, W.; Moffatt, M. F. *Science* **1997**, *275*, 41.
- (7) Mincarini, M.; Pasquali, M.; Cosentino, C.; Fumagalli, F.; Scordamaglia, A.; Quaglia, R.; Canonica, G. W.; Passalacqua, G. *Pulm. Pharmacol. Ther.* **2001**, *14*, 267.
- (8) Raphael, G. D.; Angello, J. T.; Wu, M. M.; Druce, H. A. *Ann. Allerg. Asthma Im.* **2006**, *96*, 606.
- (9) Kay, G. G.; Harris, A. G. *Clin. Exp. Allergy* **1999**, *29*, 147.
- (10) Cazzola, M.; Segreti, A.; Matera, M. G. *Curr. Opin. Pulm. Med.* **2010**, *16*, 6.
- (11) Stoloff, S. W.; Kelly, H. W. *Curr. Opin. Allergy Clin. Immunol.* **2011**, *11*, 337.
- (12) Holgate, S. T.; Chuchalin, A. G.; Hebert, J.; Lotvall, J.; Persson, G. B.; Chung, K. F.; Bousquet, J.; Kerstjens, H. A.; Fox, H.; Thirlwell, J.; Della Cioppa, G.; Omalizumab 011 Int Study, G. *Clin. Exp. Allergy* **2004**, *34*, 632.
- (13) Holgate, S.; Casale, T.; Wenzel, S.; Bousquet, J.; Deniz, Y.; Reisner, C. *J. Allergy Clin. Immunol.* **2005**, *115*, 459.
- (14) Holgate, S.; Buhl, R.; Bousquet, J.; Smith, N.; Panahloo, Z.; Jimenez, P. *Resp. Med.* **2009**, *103*, 1098.
- (15) Garman, S. C.; Wurzburg, B. A.; Tarchevskaya, S. S.; Kinet, J. P.; Jardetzky, T. S. *Nature* **2000**, *406*, 259.
- (16) Wan, T.; Bevil, R. L.; Fabiane, S. M.; Bevil, A. J.; Sohi, M. K.; Keown, M.; Young, R. J.; Henry, A. J.; Owens, R. J.; Gould, H. J.; Sutton, B. J. *Nat. Immunol.* **2002**, *3*, 681.
- (17) Garman, S. C.; Sechi, S.; Kinet, J. P.; Jardetzky, T. S. *J. Mol. Biol.* **2001**, *311*, 1049.
- (18) Henry, A. J.; Cook, J. P. D.; McDonnell, J. M.; Mackay, G. A.; Shi, J. G.; Sutton, B. J.; Gould, H. *J. Biochemistry* **1997**, *36*, 15568.
- (19) Cook, J. P. D.; Henry, A. J.; McDonnell, J. M.; Owens, R. J.; Sutton, B. J.; Gould, H. *J. Biochemistry* **1997**, *36*, 15579.
- (20) Sayers, I.; Cain, S. A.; Swan, J. R. M.; Pickett, M. A.; Watt, P. J.; Holgate, S. T.; Padlan, E. A.; Schuck, P.; Helm, B. A. *Biochemistry* **1998**, *37*, 16152.
- (21) Sayers, I.; Helm, B. A. *Clin. Exp. Allergy* **1999**, *29*, 585.

- (22) Holdom, M. D.; Davies, A. M.; Nettleship, J. E.; Bagby, S. C.; Dhaliwal, B.; Girardi, E.; Hunt, J.; Gould, H. J.; Beavil, A. J.; McDonnell, J. M.; Owens, R. J.; Sutton, B. J. *Nat. Struct. Mol. Biol.* **2011**, *18*, 571.
- (23) Hunt, J.; Keeble, A. H.; Dale, R. E.; Corbett, M. K.; Beavil, R. L.; Levitt, J.; Swann, M. J.; Suhling, K.; Ameer-Beg, S.; Sutton, B. J.; Beavil, A. J. *J. Biol. Chem.* **2012**, *287*, 17459.
- (24) Hunt, J.; Beavil, R. L.; Calvert, R. A.; Gould, H. J.; Sutton, B. J.; Beavil, A. J. *J. Biol. Chem.* **2005**, *280*, 16808.
- (25) Hunt, J.; Bracher, M. G.; Shi, J.; Fleury, S.; Dombrowicz, D.; Gould, H. J.; Sutton, B. J.; Beavil, A. J. *J. Biol. Chem.* **2008**, *283*, 29882.
- (26) Dhaliwal, B.; Yuan, D. P.; Pang, M. O. Y.; Henry, A. J.; Cain, K.; Oxbrow, A.; Fabiane, S. M.; Beavil, A. J.; McDonnell, J. M.; Gould, H. J.; Sutton, B. J. *Proc. Natl. Acad. Sci. U.S.A.* **2012**, *109*, 12686.
- (27) Borthakur, S.; Hibbert, R. G.; Pang, M. O. Y.; Yahya, N.; Bax, H. J.; Kao, M. W.; Cooper, A. M.; Beavil, A. J.; Sutton, B. J.; Gould, H. J.; McDonnell, J. M. *J. Biol. Chem.* **2012**, *287*, 31457.
- (28) Wurzburg, B. A.; Jardetzky, T. S. *J. Mol. Biol.* **2009**, *393*, 176.
- (29) Wurzburg, B. A.; Kim, B.; Tarchevskaya, S. S.; Egel, A.; Vogel, M.; Jardetzky, T. S. *J. Biol. Chem.* **2012**, *287*, 36251.
- (30) Yuan, D. P.; Keeble, A. H.; Hibbert, R. G.; Fabiane, S.; Gould, H. J.; McDonnell, J. M.; Beavil, A. J.; Sutton, B. J.; Dhaliwal, B. *J. Biol. Chem.* **2013**, *288*, 21667.
- (31) Dhaliwal, B.; Pang, M. O. Y.; Yuan, D. P.; Yahya, N.; Fabiane, S. M.; McDonnell, J. M.; Gould, H. J.; Beavil, A. J.; Sutton, B. J. *Mol. Immunol.* **2013**, *56*, 693.
- (32) Dhaliwal, B.; Pang, M. O. Y.; Yuan, D. P.; Beavil, A. J.; Sutton, B. J. *Acta Crystallogr. F.* **2014**, *70*, 305.
- (33) Drinkwater, N.; Cossins, B. P.; Keeble, A. H.; Wright, M.; Cain, K.; Hailu, H.; Oxbrow, A.; Delgado, J.; Shuttleworth, L. K.; Kao, M. W. P.; McDonnell, J. M.; Beavil, A. J.; Henry, A. J.; Sutton, B. J. *Nat. Struct. Mol. Biol.* **2014**, *21*, 397.
- (34) Arkin, M. R.; Wells, J. A. *Nat. Rev. Drug Discov.* **2004**, *3*, 301.
- (35) Yin, H.; Hamilton, A. D. *Angew. Chem. Int. Ed.* **2005**, *44*, 4130.
- (36) Wells, J. A.; McClendon, C. L. *Nature* **2007**, *450*, 1001.
- (37) Zinzalla, G.; Thurston, D. E. *Future Med. Chem.* **2009**, *1*, 65.
- (38) Wilson, A. J. *Chem. Soc. Rev.* **2009**, *38*, 3289.
- (39) Buchwald, P. *IUBMB Life* **2010**, *62*, 724.
- (40) Moreira, I. S.; Fernandes, P. A.; Ramos, M. J. *Proteins* **2007**, *68*, 803.

- (41) Hajduk, P. J.; Bures, M.; Praestgaard, J.; Fesik, S. W. *J. Med. Chem.* **2000**, *43*, 3443.
- (42) Lipinski, C. A.; Lombardo, F.; Dominy, B. W.; Feeney, P. J. *Adv. Drug Deliver. Rev.* **1997**, *23*, 3.
- (43) Stigers, K. D.; Soth, M. J.; Nowick, J. S. *Curr. Opin. Chem. Biol.* **1999**, *3*, 714.
- (44) McDonnell, J. M.; Beavil, A. J.; Mackay, G. A.; Jameson, B. A.; Korngold, R.; Gould, H. J.; Sutton, B. J. *Nat. Struct. Biol.* **1996**, *3*, 419.
- (45) Hill, T. A.; Shepherd, N. E.; Diness, F.; Fairlie, D. P. *Angew. Chem. Int. Ed.* **2014**, *53*, 13020.
- (46) Kotha, S.; Lahiri, K. *Bioorg. Med. Chem. Lett.* **2001**, *11*, 2887.
- (47) Kotha, S.; Lahin, K. *Biopolymers* **2003**, *69*, 517.
- (48) Smith, L. D.; Leatherbarrow, R. J.; Spivey, A. C. *Future Med. Chem.* **2013**, *5*, 1423.
- (49) Hamburger, R. N. *Science* **1975**, *189*, 389.
- (50) Hamburger, R. N. *Immunology* **1979**, *38*, 781.
- (51) Stanworth, D. R.; Humphrey, J. H.; Bennich, H.; Johansson, S. G. O. *Lancet* **1968**, *292*, 17.
- (52) Burt, D. S.; Stanworth, D. R. *Eur. J. Immunol.* **1987**, *17*, 437.
- (53) Stanworth, D. R.; Jones, V. M.; Lewin, I. V.; Nayyar, S. *Lancet* **1990**, *336*, 1279.
- (54) Helm, B. A.; Spivey, A. C.; Padlan, E. A. *Allergy* **1997**, *52*, 1155.
- (55) Spivey, A. C.; McKendrick, J. E.; Srikanan, R.; Helm, B. A. *J. Org. Chem.* **2003**, *68*, 1843.
- (56) Offermann, D. A.; McKendrick, J. E.; Sejberg, J. J. P.; Mo, B. L.; Holdom, M. D.; Helm, B. A.; Leatherbarrow, R. J.; Beavil, A. J.; Sutton, B. J.; Spivey, A. C. *J. Org. Chem.* **2012**, *77*, 3197.
- (57) McDonnell, J. M.; Beavil, A. J.; Mackay, G. A.; Henry, A. J.; Cook, J. P. D.; Gould, H. J.; Sutton, B. J. *Biochem. Soc. T.* **1997**, *25*, 387.
- (58) McDonnell, J. M.; Fushman, D.; Cahill, S. M.; Sutton, B. J.; Cowburn, D. *J. Am. Chem. Soc.* **1997**, *119*, 5321.
- (59) Danho, W.; Makofske, R.; Swistok, J.; Mallamaci, M.; Nettleton, M.; Madison, V.; Greeley, D.; Fry, D.; Kochan, J. *Peptides Am. Symp.* **1997**, *15*, 539.
- (60) Sandomenico, A.; Monti, S. M.; Marasco, D.; Dathan, N.; Palumbo, R.; Saviano, M.; Ruvo, M. *Mol. Immunol.* **2009**, *46*, 3300.
- (61) Sandomenico, A.; Monti, S. M.; Palumbo, R.; Ruvo, M. *J. Pept. Res.* **2011**, *17*, 604.
- (62) Zhou, J. S.; Sandomenico, A.; Severino, V.; Burton, O. T.; Darling, A.; Oettgen, H. C.; Ruvo, M. *Mol. Biosyst.* **2013**, *9*, 2853.
- (63) Nakamura, G. R.; Starovasnik, M. A.; Reynolds, M. E.; Lowman, H. B. *Biochemistry* **2001**, *40*, 9828.
- (64) Nakamura, G. R.; Reynolds, M. E.; Chen, Y. M.; Starovasnik, M. A.; Lowman, H. B. *Proc. Natl. Acad. Sci. U.S.A.* **2002**, *99*, 1303.

- (65) Stamos, J.; Eigenbrot, C.; Nakamura, G. R.; Reynolds, M. E.; Yin, J. P.; Lowman, H. B.; Fairbrother, W. J.; Starovasnik, M. A. *Structure* **2004**, *12*, 1289.
- (66) Fassina, G.; Verdoliva, A.; Odierna, M. R.; Ruvo, M.; Cassini, G. *J. Mol. Recognit.* **1996**, *9*, 564.
- (67) Fassina, G.; Verdoliva, A.; Palombo, G.; Ruvo, M.; Cassani, G. *J. Mol. Recognit.* **1998**, *11*, 128.
- (68) Fassina, G.; Ruvo, M.; Palombo, G.; Verdoliva, A.; Marino, M. *J. Biochem. Biophys. Meth.* **2001**, *49*, 481.
- (69) Palombo, G.; De Falco, S.; Tortora, M.; Cassani, G.; Fassina, G. *J. Mol. Recognit.* **1998**, *11*, 243.
- (70) Palombo, G.; Rossi, M.; Cassani, G.; Fassina, G. *J. Mol. Recognit.* **1998**, *11*, 247.
- (71) Palombo, G.; Verdoliva, A.; Fassina, G. *J. Chromatogr. B* **1998**, *715*, 137.
- (72) Verdoliva, A.; Basile, G.; Fassina, G. *J. Chromatogr. B* **2000**, *749*, 233.
- (73) Verdoliva, A.; Pannone, F.; Rossi, M.; Catello, S.; Manfredi, V. *J. Immunol. Methods* **2002**, *271*, 77.
- (74) Marino, M.; Ruvo, M.; De Falco, S.; Fassina, G. *Nature Biotechnol.* **2000**, *18*, 735.
- (75) Marino, M.; Rossi, M.; Ruvo, M.; Fassina, G. *Curr. Drug Targets* **2002**, *3*, 223.
- (76) Rossi, M.; Ruvo, M.; Marasco, D.; Colombo, M.; Cassani, G.; Verdoliva, A. *Mol. Immunol.* **2008**, *45*, 226.
- (77) Ratcliffe, N. A.; Mello, C. B.; Garcia, E. S.; Butt, T. M.; Azambuja, P. *Insect Biochem. Mol. Biol.* **2011**, *41*, 747.
- (78) Buku, A.; Maulik, G.; Hook, W. A. *Peptides* **1998**, *19*, 1.
- (79) Buku, A. *Peptides* **1999**, *20*, 415.
- (80) Buku, A.; Price, J. A. *Peptides* **2001**, *22*, 1987.
- (81) Buku, A.; Price, J. A.; Mendlowitz, M.; Masur, S. *Peptides* **2001**, *22*, 1993.
- (82) Buku, A.; Mendlowitz, M.; Condie, B. A.; Price, J. A. *J. Med. Chem.* **2003**, *46*, 3008.
- (83) Buku, A.; Mendlowitz, M.; Condie, B. A.; Price, J. A. *J. Pept. Res.* **2004**, *10*, 313.
- (84) Buku, A.; Condie, B. A.; Price, J. A.; Mezei, M. *J. Pept. Res.* **2005**, *66*, 132.
- (85) Buku, A.; Keselman, I.; Lupyan, D.; Mezei, M.; Price, J. A. *Chem. Biol. Drug Des.* **2008**, *72*, 133.
- (86) Singh, S. B.; Jayasuriya, H.; Zink, D. L.; Polishook, J. D.; Dombrowski, A. W.; Zweerink, H. *Tetrahedron Lett.* **2004**, *45*, 7605.
- (87) Pospisil, J.; Muller, C.; Furstner, A. *Chem. Eur. J.* **2009**, *15*, 5956.
- (88) Yoshino, T.; Sato, I.; Hirama, M. *Org. Lett.* **2012**, *14*, 4290.

- (89) Yoshino, T.; Yamashita, S.; Sato, I.; Hayashi, Y.; Hiram, M. *Chem. Lett.* **2014**, *43*, 349.
- (90) Carr, J. L.; Offermann, D. A.; Holdom, M. D.; Dusart, P.; White, A. J. P.; Bevil, A. J.; Leatherbarrow, R. J.; Lindell, S. D.; Sutton, B. J.; Spivey, A. C. *Chem. Commun.* **2010**, *46*, 1824.
- (91) Carr, J. L.; Sejberg, J. J. P.; Saab, F.; Holdom, M. D.; Davies, A. M.; White, A. J. P.; Leatherbarrow, R. J.; Bevil, A. J.; Sutton, B. J.; Lindell, S. D.; Spivey, A. C. *Org. Biomol. Chem.* **2011**, *9*, 6814.
- (92) Sejberg, J. J. P.; Smith, L. D.; Leatherbarrow, R. J.; Bevil, A. J.; Spivey, A. C. *Tetrahedron Lett.* **2013**, *54*, 4970.
- (93) Charneira, C.; Godinho, A. L. A.; Oliveira, M. C.; Pereira, S. A.; Monteiro, E. C.; Marques, M. M.; Antunes, A. M. M. *Chem. Res. Toxicol.* **2011**, *24*, 2129.
- (94) Cheng, Y. S.-E. L., Y.; Chu, J.; Kinet, J.-P.; Jouvain, M.-H.; Sudo, Y.; Quian, X. *WO 9740033* **1997**.
- (95) Cheng, Y. S.-E. L., Y.; Chu, J.; Kinet, J.-P.; Jouvain, M.-H.; Sudo, Y.; Quian, X. *US 5965605* **1999**.
- (96) Wiegand, T.; Williams, P.; Dreskin, S.; Jouvin, M.; Kinet, J.; Tasset, D. *J. Immunol.* **1996**, *157*, 221.
- (97) Eggel, A.; Baumann, M. J.; Amstutz, P.; Stadler, B. M.; Vogel, M. *J. Mol. Biol.* **2009**, *393*, 598.
- (98) Baumann, M. J.; Eggel, A.; Amstutz, P.; Stadler, B. M.; Vogel, M. *Immunol. Lett.* **2010**, *133*, 78.
- (99) Eggel, A.; Buschor, P.; Baumann, M. J.; Amstutz, P.; Stadler, B. M.; Vogel, M. *Allergy* **2011**, *66*, 961.
- (100) Kim, B.; Eggel, A.; Tarchevskaya, S. S.; Vogel, M.; Prinz, H.; Jardetzky, T. S. *Nature* **2012**, *491*, 613.
- (101) Eggel, A.; Baravalle, G.; Hobi, G.; Kim, B.; Buschor, P.; Forrer, P.; Shin, J. S.; Vogel, M.; Stadler, B. M.; Dahinden, C. A.; Jardetzky, T. S. *J. Allergy Clin. Immunol.* **2014**, *133*, 1709.
- (102) Zhang, J. H.; Chung, T. D. Y.; Oldenburg, K. R. *J. Biomol. Screen.* **1999**, *4*, 67.
- (103) Sittampalam, G. S.; Kahl, S. D.; Janzen, W. P. *Curr. Opin. Chem. Biol.* **1997**, *1*, 384.
- (104) Engvall, E.; Perlmann, P. *Immunochemistry* **1971**, *8*, 871.
- (105) Vanweeme.Bk; Schuurs, A. H. W. *FEBS Lett.* **1971**, *15*, 232.
- (106) Lequin, R. M. *Clin. Chem.* **2005**, *51*, 2415.
- (107) Arkin, M. R.; Glicksman, M. A.; Fu, H.; Havel, J. J.; Du, Y. *Assay Guidance Manual (Chapter 14: Inhibition of Protein-Protein Interactions: Non-Cellular Assay Formats)* **2012**, *1*.

- (108) Selvin, P. R. *Method Enzymol.* **1995**, *246*, 300.
- (109) Selvin, P. R. *Nat. Struct. Biol.* **2000**, *7*, 730.
- (110) Förster, T. *Annalen der Physik* **1948**, *437*, 55.
- (111) Ormo, M.; Cubitt, A. B.; Kallio, K.; Gross, L. A.; Tsien, R. Y.; Remington, S. J. *Science* **1996**, *273*, 1392.
- (112) Selvin, P. R.; Hearst, J. E. *Proc. Natl. Acad. Sci. U.S.A.* **1994**, *91*, 10024.
- (113) Li, M.; Selvin, P. R. *J. Am. Chem. Soc.* **1995**, *117*, 8132.
- (114) Selvin, P. R. *IEEE J. Sel. Top. Quantum Electron.* **1996**, *2*, 1077.
- (115) Li, M.; Selvin, P. R. *Bioconjugate Chem.* **1997**, *8*, 127.
- (116) Chen, J. Y.; Selvin, P. R. *Bioconjugate Chem.* **1999**, *10*, 311.
- (117) Xiao, M.; Selvin, P. R. *J. Am. Chem. Soc.* **2001**, *123*, 7067.
- (118) Selvin, P. R. *Annu. Rev. Bioph. Biom.* **2002**, *31*, 275.
- (119) Ge, P. H.; Selvin, P. R. *Bioconjugate Chem.* **2003**, *14*, 870.
- (120) Riddle, S. M.; Vedvik, K. L.; Hanson, G. T.; Vogel, K. W. *Anal. Biochem.* **2006**, *356*, 108.
- (121) Ge, P. H.; Selvin, P. R. *Bioconjugate Chem.* **2008**, *19*, 1105.
- (122) Ge, O. H.; Selvin, P. R. *Bioconjugate Chem.* **2004**, *15*, 1088.
- (123) Kim, B.; Tarchevskaya, S. S.; Eggel, A.; Vogel, M.; Jardetzky, T. S. *Anal. Biochem.* **2012**, *431*, 84.
- (124) Pope, A. J.; Haupts, U. M.; Moore, K. J. *Drug Discov. Today* **1999**, *4*, 350.
- (125) Jameson, D. M.; Croney, J. C. *Comb. Chem. High T. Scr.* **2003**, *6*, 167.
- (126) Bingham, B. R.; Monk, P. N.; Helm, B. A. *J. Biol. Chem.* **1994**, *269*, 19300.
- (127) Giannetti, A. M.; Koch, B. D.; Browner, M. F. *J. Med. Chem.* **2008**, *51*, 574.
- (128) Rich, R. L.; Myszka, D. G. *J. Mol. Recognit.* **2011**, *24*, 892.
- (129) Meyer, B.; Peters, T. *Angew. Chem. Int. Edit.* **2003**, *42*, 864.
- (130) Mayer, M.; Meyer, B. *J. Am. Chem. Soc.* **2001**, *123*, 6108.
- (131) Smith, L. D. *MRes Thesis* **2011**, Imperial College London.
- (132) Panchuk-Voloshina, N.; Haugland, R. P.; Bishop-Stewart, J.; Bhalgat, M. K.; Millard, P. J.; Mao, F.; Leung, W. Y. *J. Histochem. Cytochem.* **1999**, *47*, 1179.
- (133) Berlier, J. E.; Rothe, A.; Buller, G.; Bradford, J.; Gray, D. R.; Filanoski, B. J.; Telford, W. G.; Yue, S.; Liu, J. X.; Cheung, C. Y.; Chang, W.; Hirsch, J. D.; Beechem, J. M.; Haugland, R. P. *J. Histochem. Cytochem.* **2003**, *51*, 1699.
- (134) Johnson, I.; Spence, M. T. Z. *The Molecular Probes Handbook - A Guide to Fluorescent Probes and Labelling Technologies*; 11th ed.; Life Technologies, 2010.

- (135) McDonnell, J. M.; Calvert, R.; Beavil, R. L.; Beavil, A. J.; Henry, A. J.; Sutton, B. J.; Gould, H. J.; Cowburn, D. *Nat. Struct. Biol.* **2001**, *8*, 437.
- (136) Price, N. E.; Price, N. C.; Kelly, S. M.; McDonnell, J. M. *J. Biol. Chem.* **2005**, *280*, 2324.
- (137) Harwood, N. E.; Price, N. C.; McDonnell, J. M. *FEBS Lett.* **2006**, *580*, 2129.
- (138) Dennison, H. J. *PhD Thesis* **2011**, Imperial College London.
- (139) Mo, B. *PhD Thesis* **2011**, Imperial College London.
- (140) Merrifield, R. *J. Am. Chem. Soc.* **1963**, *85*, 2149.
- (141) Carpino, L. A.; Han, G. Y. *J. Am. Chem. Soc.* **1970**, *92*, 5748.
- (142) Carpino, L. A.; Han, G. Y. *J. Org. Chem.* **1972**, *37*, 3404.
- (143) Jones, J. *The Chemical Synthesis of Peptides*; Oxford University Press, 1994.
- (144) Chan, W. C.; White, P. D. *Fmoc Solid Phase Peptide Synthesis: A Practical Approach*; Oxford University Press, 1999.
- (145) Afonso, A.; Roses, C.; Planas, M.; Feliu, L. *Eur. J. Org. Chem.* **2010**, 1461.
- (146) Frank, R. *J. Immunol. Methods* **2002**, *267*, 13.
- (147) Hilpert, K.; Winkler, D. F. H.; Hancock, R. E. W. *Nat. Protoc.* **2007**, *2*, 1333.
- (148) Lennard, K. R.; Tavassoli, A. *Chem. Eur. J.* **2014**, *20*, 10608.
- (149) Coyne, A. G.; Scott, D. E.; Abell, C. *Curr. Opin. Chem. Biol.* **2010**, *14*, 299.
- (150) Scott, D. E.; Coyne, A. G.; Hudson, S. A.; Abell, C. *Biochemistry* **2012**, *51*, 4990.
- (151) Scott, D. E.; Ehebauer, M. T.; Pukala, T.; Marsh, M.; Blundell, T. L.; Venkitaraman, A. R.; Abell, C.; Hyvonen, M. *ChemBioChem* **2013**, *14*, 332.
- (152) Zhong, S. J.; Macias, A. T.; MacKerell, A. D. *Curr. Top. Med. Chem.* **2007**, *7*, 63.
- (153) Fletcher, S.; Hamilton, A. D. *Curr. Top. Med. Chem.* **2007**, *7*, 922.
- (154) Caputo, G. A.; Litvinov, R. I.; Li, W.; Bennett, J. S.; DeGrado, W. F.; Yin, H. *Biochemistry* **2008**, *47*, 8600.
- (155) Pang, M. *PhD Thesis* **2013**, King's College London.

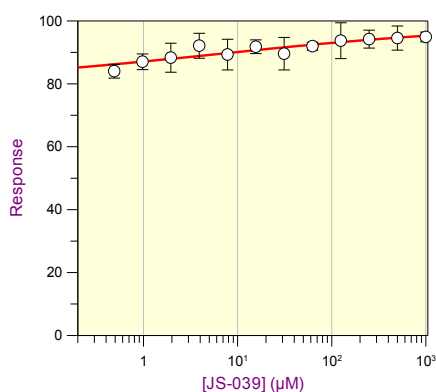
8: Appendices

8.1 Aspercyclide A and analogues – ELISA inhibition assay IC₅₀ curves

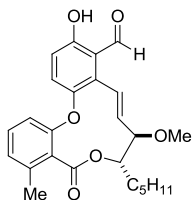
(±)-1 (JS-039)

IC₅₀ > 1000 μM (solubility issues)

IC₅₀ Data



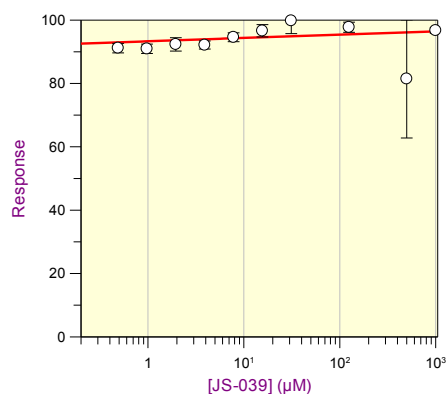
Parameter	Value	Std. Error
Y Range	19.5307	2.0955
IC 50	5.5361	6.4355
Slope factor	-0.2731	0.0591
Background	79.5631	1.2078



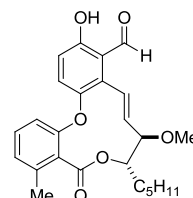
(±)-1 (JS-039) (repeat)

IC₅₀ > 1000 μM (solubility issues)

IC₅₀ Data



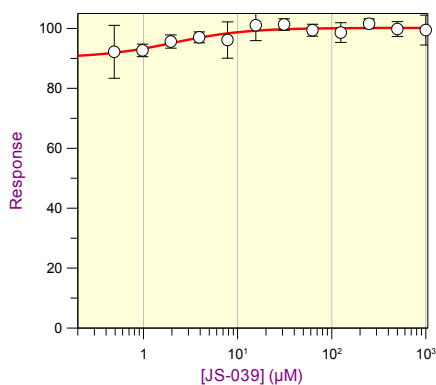
Parameter	Value	Std. Error
Y Range	29.8026	8.7337
IC 50	0.0624	0.7269
Slope factor	-0.0630	0.0840
Background	77.1070	4.9824



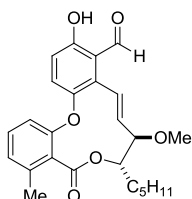
(±)-1 (JS-039) (repeat)

IC₅₀ > 1000 μM

IC₅₀ Data



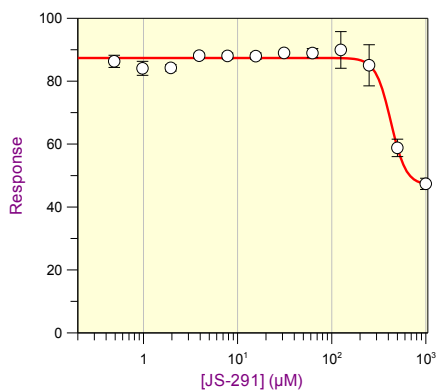
Parameter	Value	Std. Error
Y Range	9.9643	2.9013
IC 50	2.0637	1.2106
Slope factor	-1.1184	0.4730
Background	90.2083	2.7190



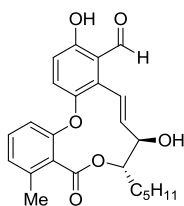
(+)-2a (JS-291)

IC₅₀ = 424 ± 27 μM

IC₅₀ Data



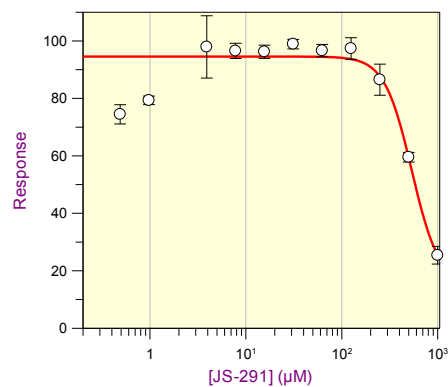
Parameter	Value	Std. Error
Y Range	40.3960	2.4397
IC 50	424.4460	27.1284
Slope factor	5.4040	1.5864
Background	46.9803	2.2968



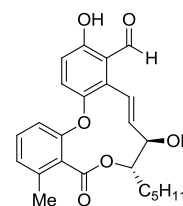
(+)-2a (JS-291) (repeat)

IC₅₀ = 538 ± 222 μM

IC₅₀ Data



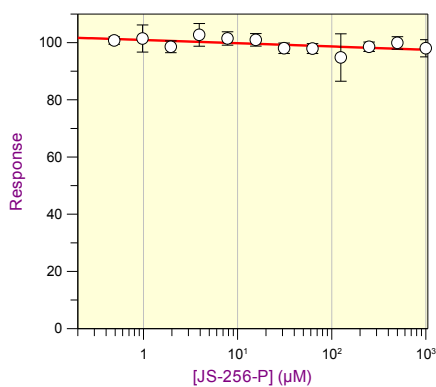
Parameter	Value	Std. Error
Y Range	79.3420	35.7175
IC 50	537.5600	222.2826
Slope factor	3.0682	3.3086
Background	15.2210	34.5955



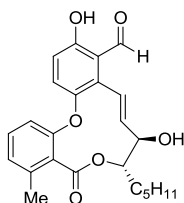
(+)-2b (JS-256-P)

IC₅₀ > 1000 μM

IC₅₀ Data



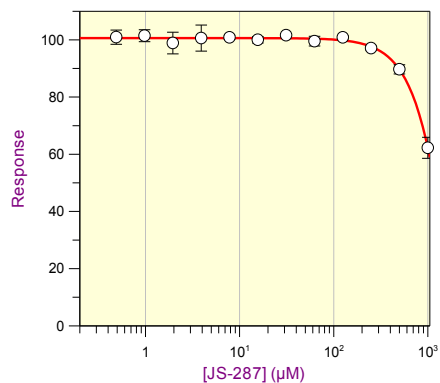
Parameter	Value	Std. Error
Y Range	17.9189	9.6541
IC 50	30.0574	408.0740
Slope factor	0.1108	0.0867
Background	90.2885	4.9575



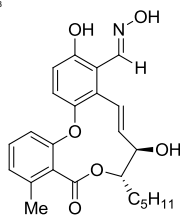
(+)-3 (JS-287)

IC₅₀ > 1000 μM

IC₅₀ Data



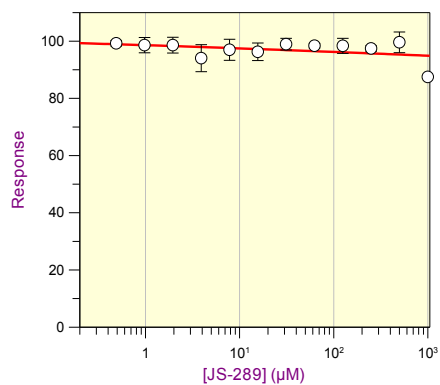
Parameter	Value	Std. Error
Y Range	380.0372	2115.6735
IC 50	3138.1557	11313.0996
Slope factor	1.9122	0.6232
Background	-279.4234	2115.5445



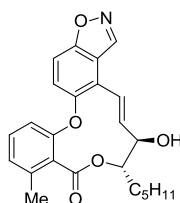
(+)-4 (JS-289)

IC₅₀ > 1000 μM

IC₅₀ Data



Parameter	Value	Std. Error
Y Range	21.2087	4.3749
IC 50	10100.4242	43943.7944
Slope factor	0.1121	0.0788
Background	82.9515	2.8177

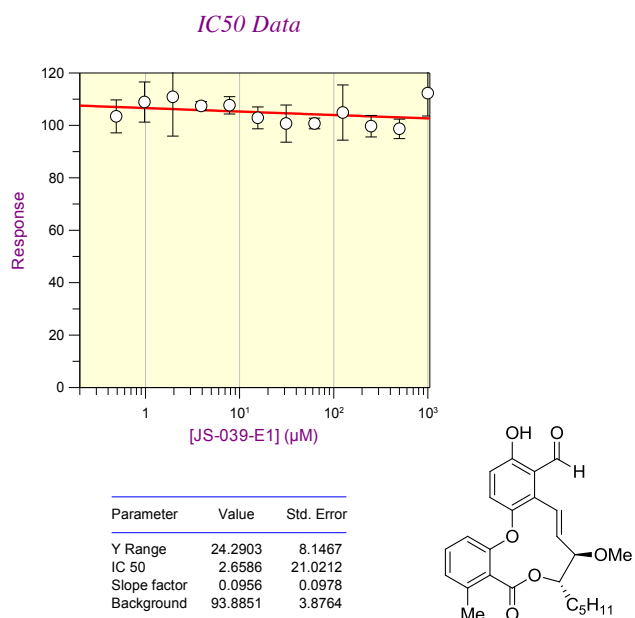


8.2 Aspercyclide A and analogues – TR-FRET inhibition assay IC₅₀ curves

(+)-1 (JS-039-E1)

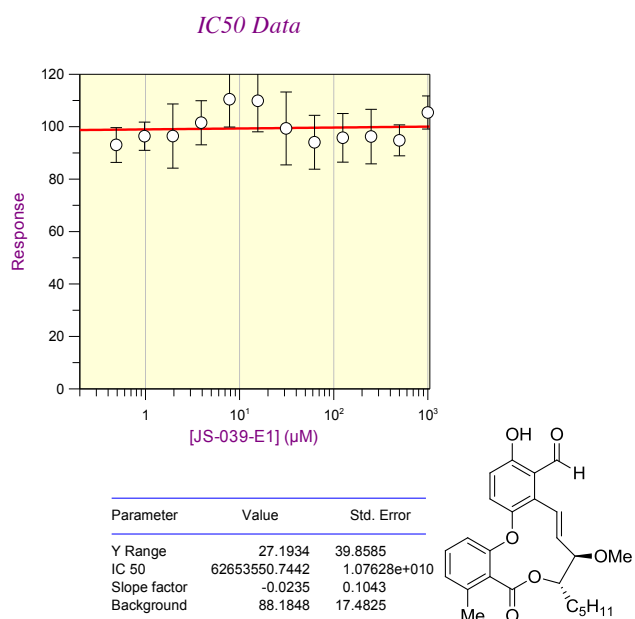
Pre-incubated with IgE-Fc-A647:

IC₅₀ > 1000 μ M



Pre-incubated with α -Tb:

IC₅₀ > 1000 μ M

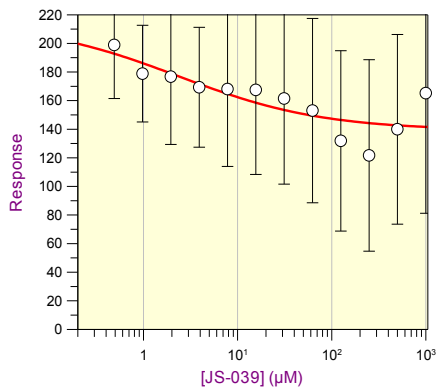


(±)-1 (JS-039)

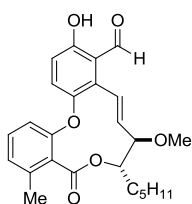
Pre-incubated with IgE-Fc-A647:

IC₅₀ > 1000 μM

IC50 Data



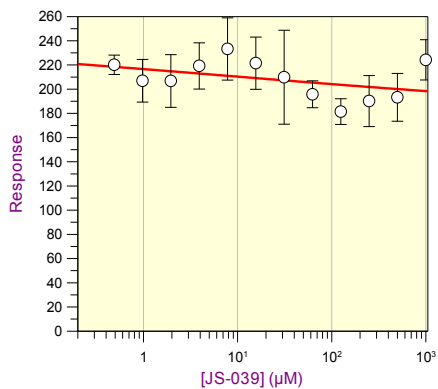
Parameter	Value	Std. Error
Y Range	75.6852	72.9397
IC 50	2.3545	5.9691
Slope factor	0.5640	0.5326
Background	139.1852	14.0184



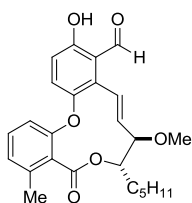
Pre-incubated with αγ-Tb:

IC₅₀ > 1000 μM

IC50 Data



Parameter	Value	Std. Error
Y Range	68.5902	80.3172
IC 50	7.4169	169.2438
Slope factor	0.1592	0.2120
Background	176.8879	39.6322

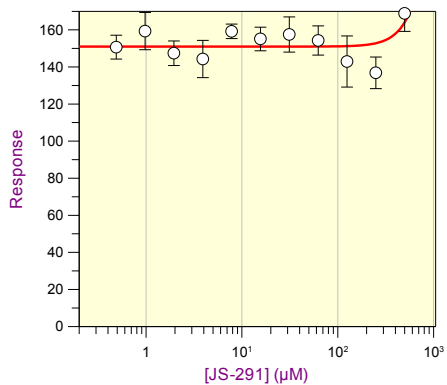


(+)-2a (JS-291)

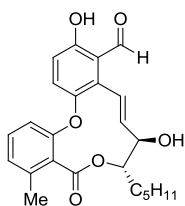
Pre-incubated with IgE-Fc-A647:

IC₅₀ > 1000 μM

IC₅₀ Data



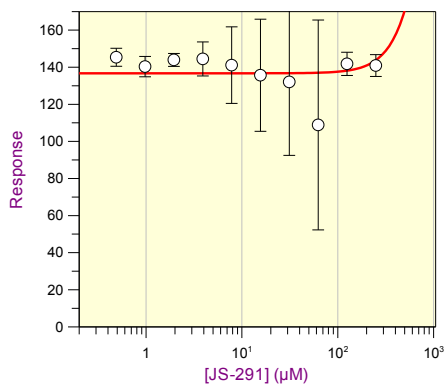
Parameter	Value	Std. Error
Y Range	1423.1823	3293.8143
IC 50	2556.6931	2193.9780
Slope factor	-2.8677	0.9290
Background	150.9864	2.8344



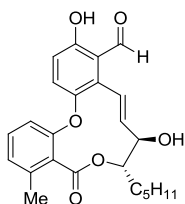
Pre-incubated with αγ-Tb:

IC₅₀ > 1000 μM

IC₅₀ Data



Parameter	Value	Std. Error
Y Range	573.6960	1103.9519
IC 50	1642.3440	1865.3926
Slope factor	-2.3297	0.6696
Background	136.7255	3.8465

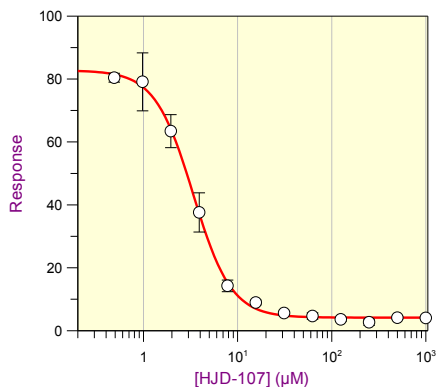


8.3 Dibenzofurans – ELISA inhibition assay IC₅₀ curves

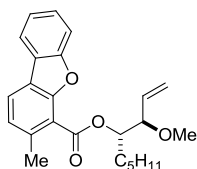
(±)-11 (HJD-107)

IC₅₀ = 4 ± 0.1 μM

IC₅₀ Data



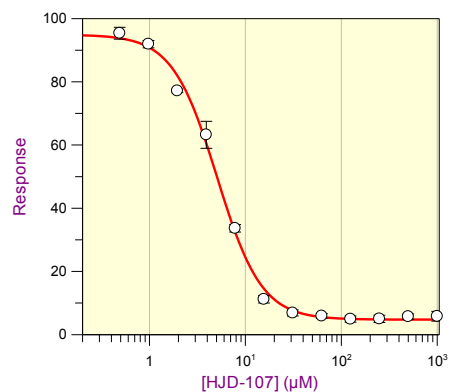
Parameter	Value	Std. Error
Y Range	78.5781	1.4538
IC 50	3.3668	0.1074
Slope factor	2.1389	0.1236
Background	4.1590	0.5049



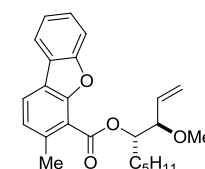
(±)-11 (HJD-107) (repeat)

IC₅₀ = 5 ± 0.3 μM

IC₅₀ Data



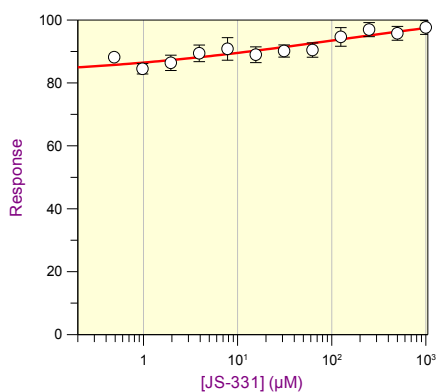
Parameter	Value	Std. Error
Y Range	90.1722	2.6975
IC 50	5.0631	0.2943
Slope factor	1.8719	0.1741
Background	4.7443	1.0884



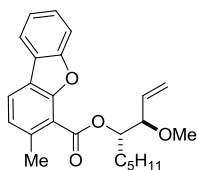
(±)-23 (JS-331)

IC₅₀ > 1000 μM

IC₅₀ Data



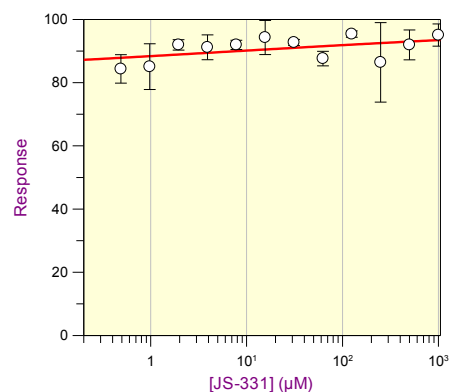
Parameter	Value	Std. Error
Y Range	23.4509	3.0096
IC 50	116.7188	89.0590
Slope factor	-0.3041	0.0580
Background	82.0045	1.3686



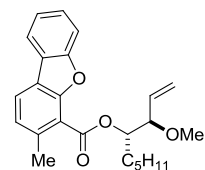
(±)-23 (JS-331) (repeat)

IC₅₀ > 1000 μM

IC₅₀ Data



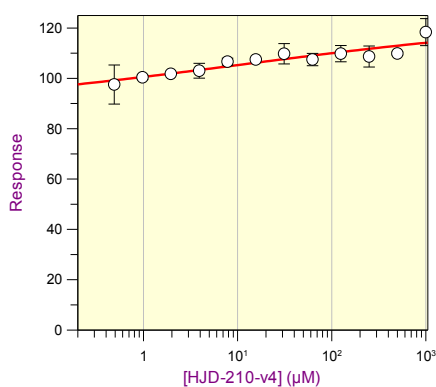
Parameter	Value	Std. Error
Y Range	19.5632	5.4841
IC 50	5.2603	29.3293
Slope factor	-0.1562	0.1084
Background	79.8735	2.9287



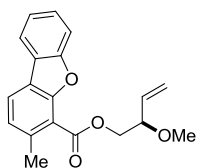
14 (HJD-210)

IC₅₀ > 1000 μM (solubility issues)

IC₅₀ Data



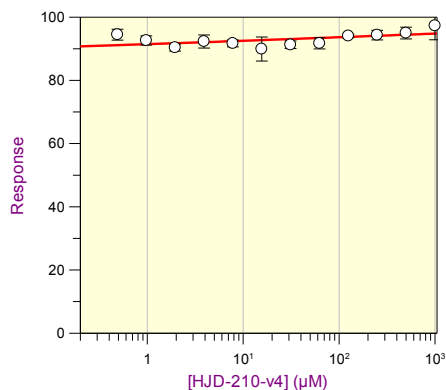
Parameter	Value	Std. Error
Y Range	35.9082	10.7683
IC 50	10.8775	38.4092
Slope factor	-0.2334	0.0907
Background	87.4992	5.7732



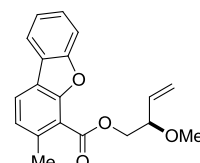
14 (HJD-210) (repeat)

IC₅₀ > 1000 μM

IC₅₀ Data



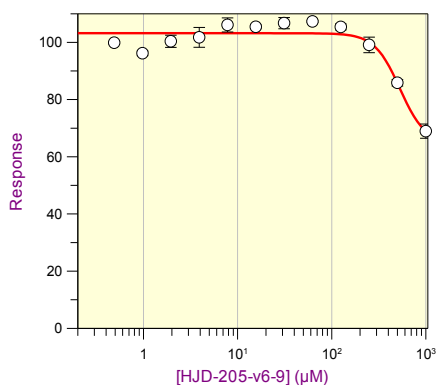
Parameter	Value	Std. Error
Y Range	16.9769	3.4620
IC 50	265.1282	670.8035
Slope factor	-0.1171	0.0599
Background	85.6419	1.6181



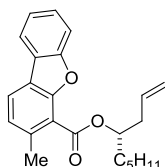
13 (HJD-205)

IC₅₀ = 529 ± 148 μM (solubility issues)

IC₅₀ Data



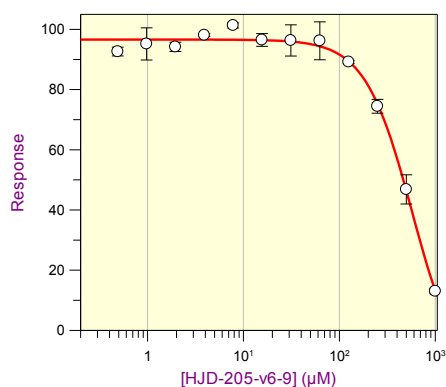
Parameter	Value	Std. Error
Y Range	38.5671	11.7728
IC 50	529.2105	147.5827
Slope factor	3.2321	2.1939
Background	64.6221	11.3966



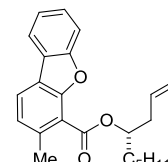
13 (HJD-205) (repeat)

IC₅₀ = 576 ± 122 μM

IC₅₀ Data



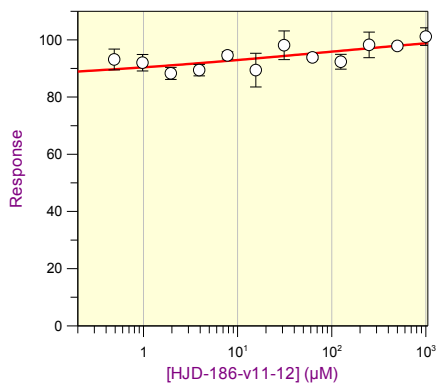
Parameter	Value	Std. Error
Y Range	114.8860	18.2971
IC 50	576.0253	121.7170
Slope factor	1.7698	0.2976
Background	-18.2787	17.9798



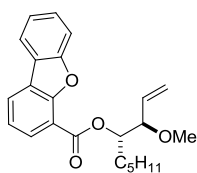
(±)-16 (HJD-186)

IC₅₀ > 1000 μM (solubility issues)

IC₅₀ Data



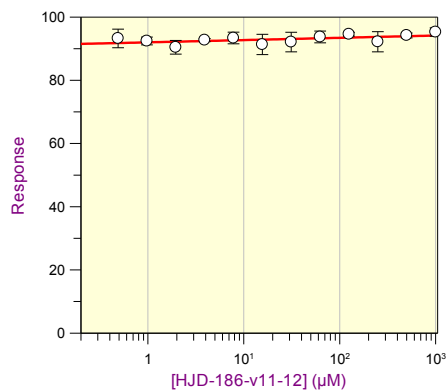
Parameter	Value	Std. Error
Y Range	22.8379	5.1843
IC 50	101.0696	152.2007
Slope factor	-0.2270	0.0878
Background	84.4657	2.4699



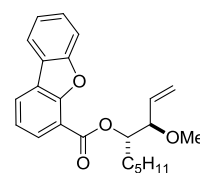
(±)-16 (HJD-186) (repeat)

IC₅₀ > 1000 μM

IC₅₀ Data



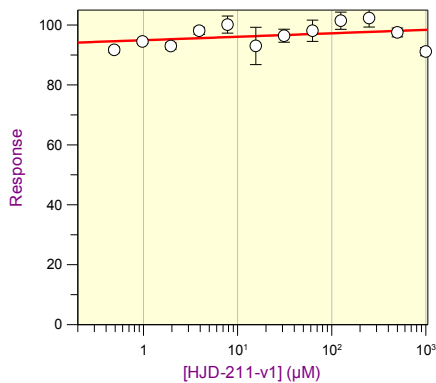
Parameter	Value	Std. Error
Y Range	14.1715	2.0054
IC 50	27.9316	81.9264
Slope factor	-0.0884	0.0458
Background	85.9554	1.0048



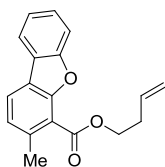
15 (HJD-211)

IC₅₀ > 1000 μM

IC₅₀ Data



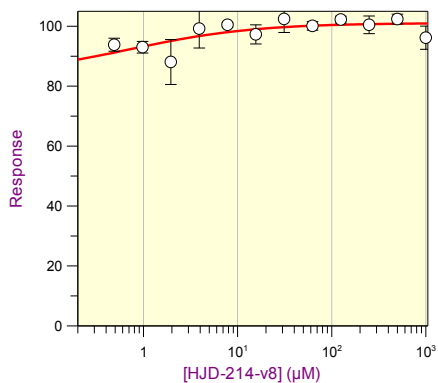
Parameter	Value	Std. Error
Y Range	20.5808	6.4135
IC 50	35.1731	310.7567
Slope factor	-0.0983	0.0975
Background	86.4149	3.1577



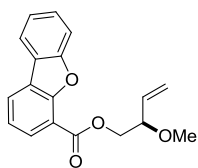
18 (HJD-214)

IC₅₀ > 1000 μM

IC₅₀ Data



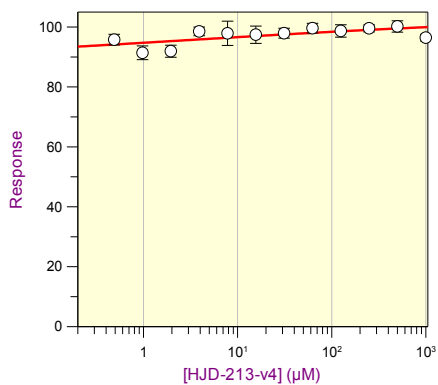
Parameter	Value	Std. Error
Y Range	17.4248	8.0068
IC 50	0.7300	0.8402
Slope factor	-0.6552	0.5233
Background	83.6437	7.7484



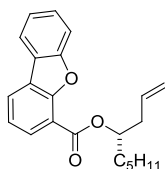
17 (HJD-213)

IC₅₀ > 1000 μM

IC₅₀ Data



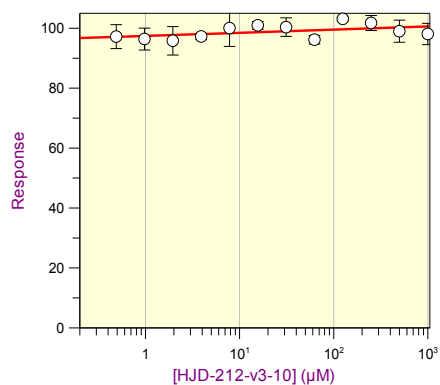
Parameter	Value	Std. Error
Y Range	17.7228	3.2980
IC 50	2.4578	8.4589
Slope factor	-0.1850	0.0813
Background	86.6092	1.8627



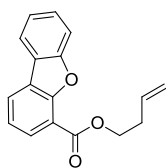
19 (HJD-212)

IC₅₀ > 1000 μM

IC₅₀ Data



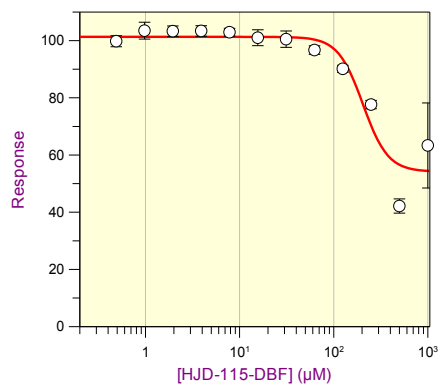
Parameter	Value	Std. Error
Y Range	17.0673	3.8897
IC 50	81.8792	405.3635
Slope factor	-0.1093	0.0691
Background	90.9172	1.8695



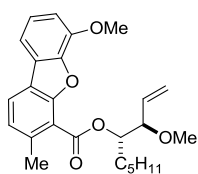
(±)-12 (HJD-115)

IC₅₀ = 205 ± 51 μM

IC₅₀ Data



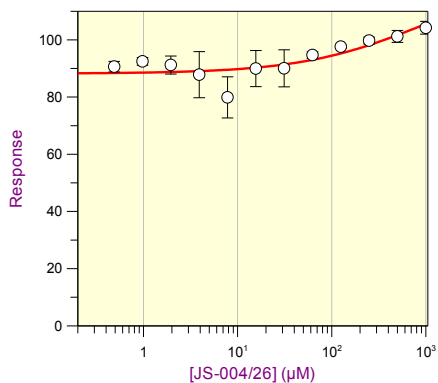
Parameter	Value	Std. Error
Y Range	47.1163	8.1350
IC 50	204.5460	51.3388
Slope factor	3.2796	1.4730
Background	54.1939	7.3900



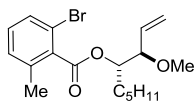
(±)-20 (JS-004/26)

IC₅₀ > 1000 μM

IC₅₀ Data



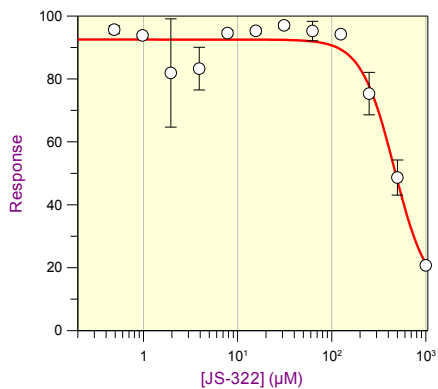
Parameter	Value	Std. Error
Y Range	33.8366	12.1187
IC 50	927.6961	989.0379
Slope factor	-0.6667	0.2529
Background	88.2013	1.9983



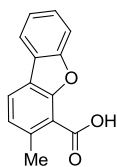
21 (JS-322)

IC₅₀ = 462 ± 89 μM

IC₅₀ Data



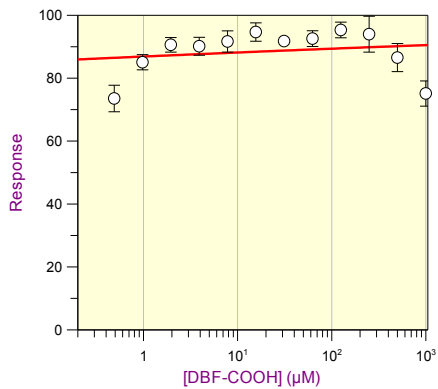
Parameter	Value	Std. Error
Y Range	81.7617	14.3337
IC 50	461.5029	89.2540
Slope factor	2.4648	1.0681
Background	10.7535	13.8172



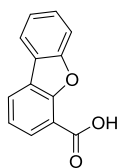
Dibenzofuran-4-carboxylic acid

IC₅₀ > 1000 μM

IC₅₀ Data



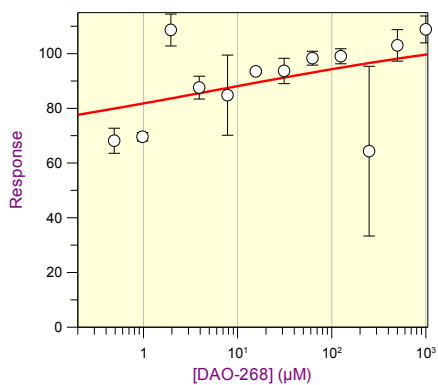
Parameter	Value	Std. Error
Y Range	29.1432	10.3910
IC 50	0.0074	0.1764
Slope factor	-0.0810	0.1076
Background	69.4504	6.4988



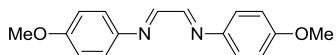
8 (DAO-268)

IC₅₀ > 1000 μM

IC₅₀ Data



Parameter	Value	Std. Error
Y Range	52.6518	21.9857
IC 50	5.7809	34.5005
Slope factor	-0.2108	0.1878
Background	60.2782	12.0854



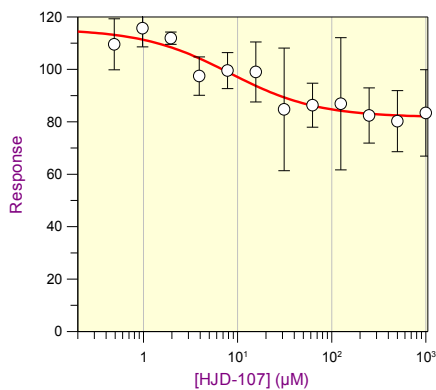
8.4 Dibenzofurans – TR-FRET inhibition assay IC₅₀ curves

(±)-11 (HJD-107)

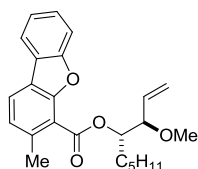
Pre-incubated with IgE-Fc-A647:

IC₅₀ > 1000 μM

IC₅₀ Data



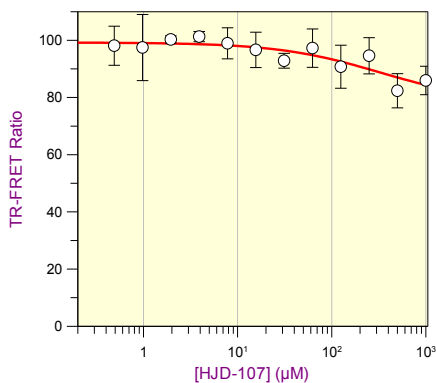
Parameter	Value	Std. Error
Y Range	33.7453	9.1271
IC 50	8.2552	5.0845
Slope factor	0.9267	0.5156
Background	81.6949	3.3924



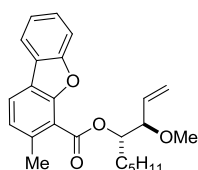
Pre-incubated with αγ-Tb:

IC₅₀ > 1000 μM

IC₅₀ Data



Parameter	Value	Std. Error
Y Range	20.7127	25.4681
IC 50	316.9788	1019.5650
Slope factor	0.8030	0.9001
Background	78.5119	24.0296

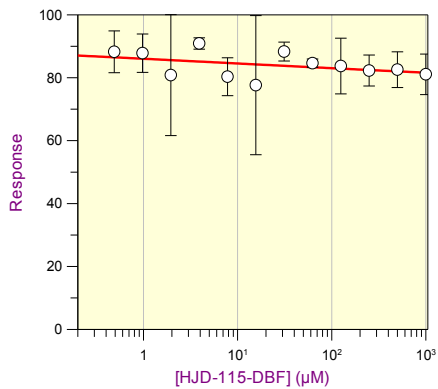


(±)-12 (HJD-115)

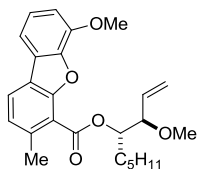
Pre-incubated with IgE-Fc-A647:

IC₅₀ > 1000 μM

IC₅₀ Data



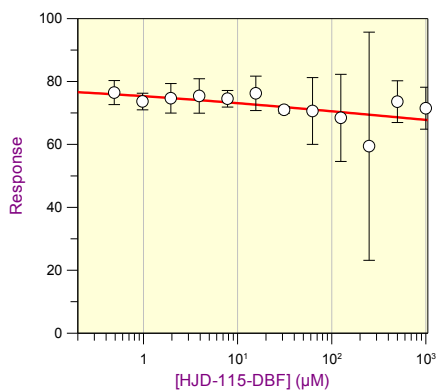
Parameter	Value	Std. Error
Y Range	21.8146	6.6620
IC 50	7.4471	41.4835
Slope factor	0.1200	0.0981
Background	73.8132	3.2512



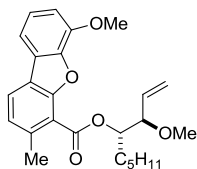
Pre-incubated with αγ-Tb:

IC₅₀ > 1000 μM

IC₅₀ Data

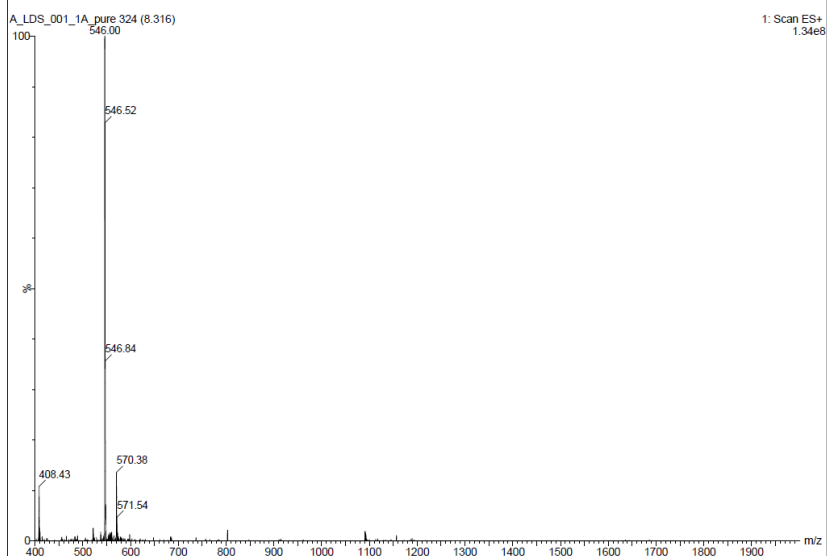
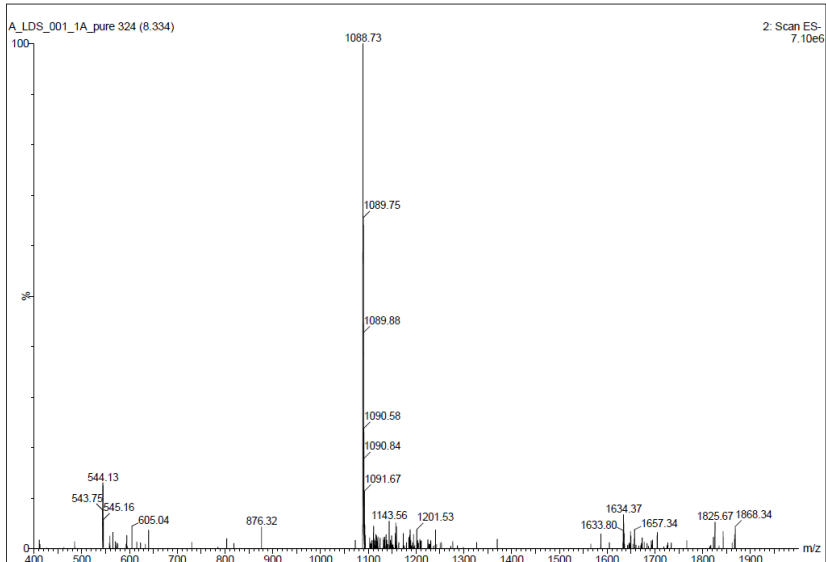
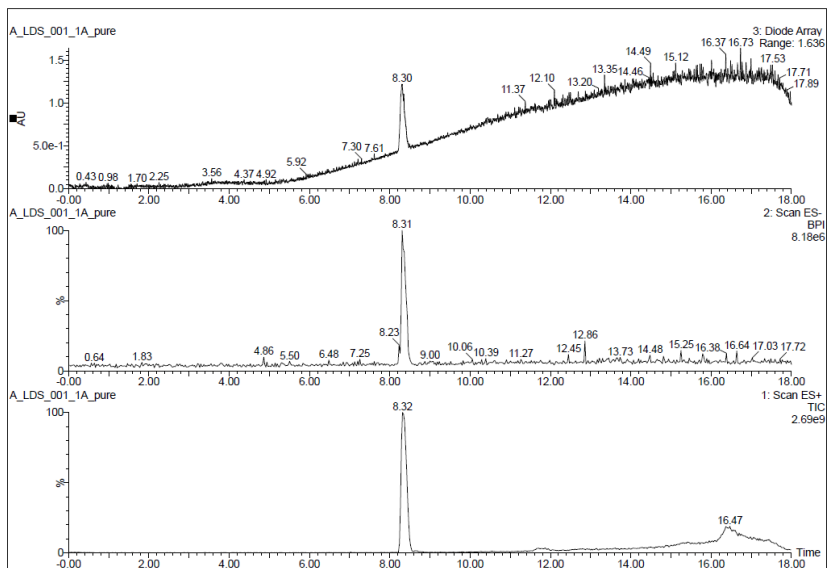


Parameter	Value	Std. Error
Y Range	24.2672	5.4036
IC 50	367.7044	1229.5099
Slope factor	0.1964	0.1242
Background	56.8540	3.3906

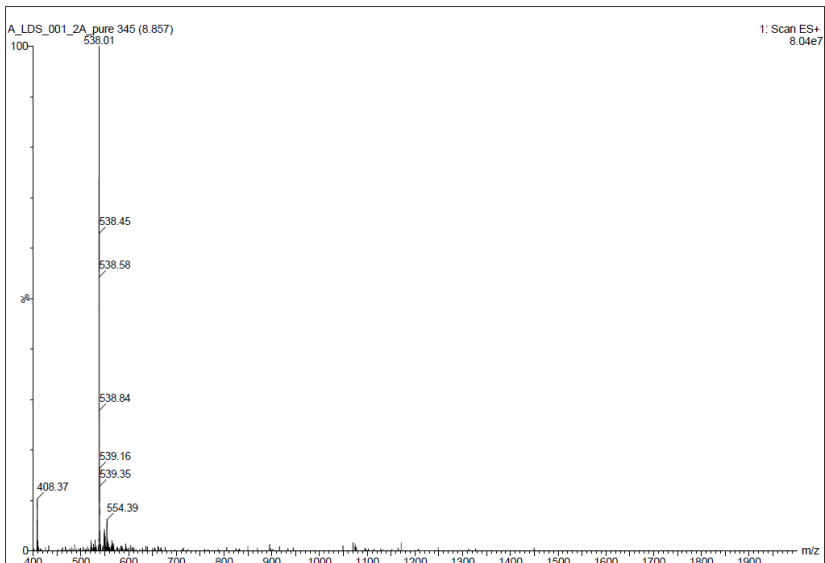
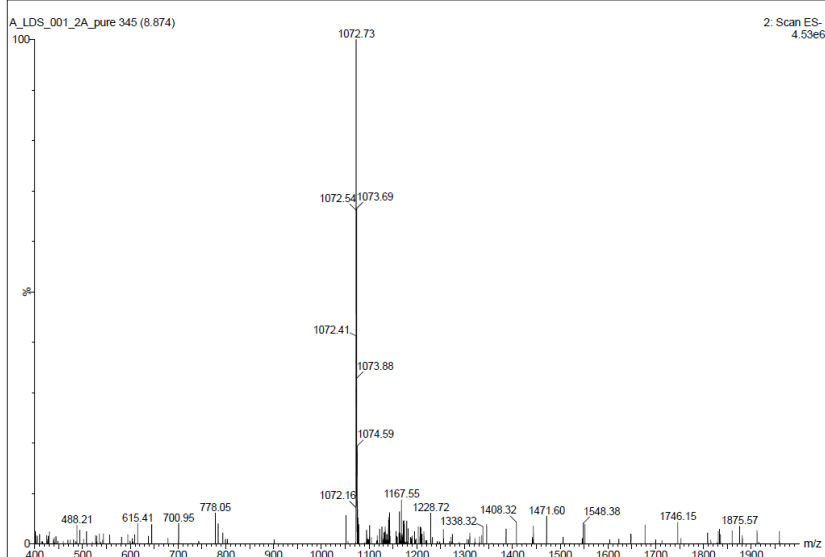
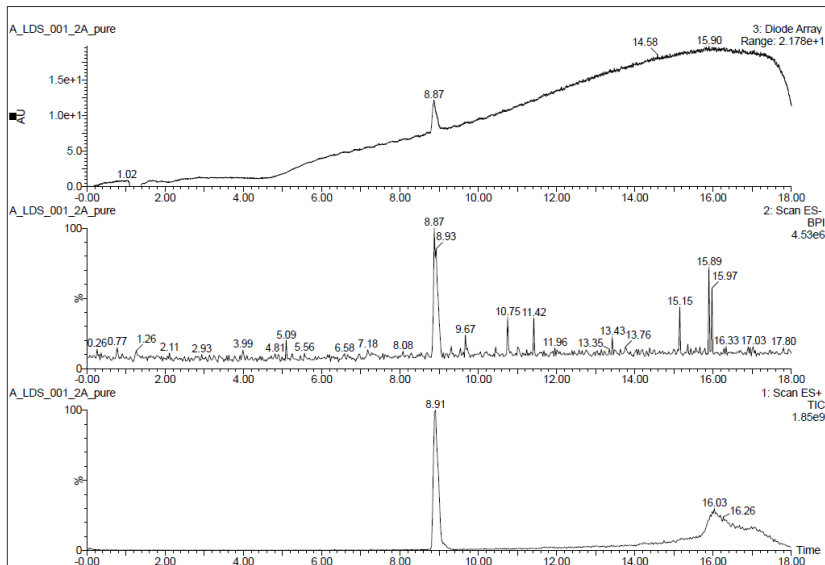


8.5 LC-MS chromatograms and mass spectra of pure peptides

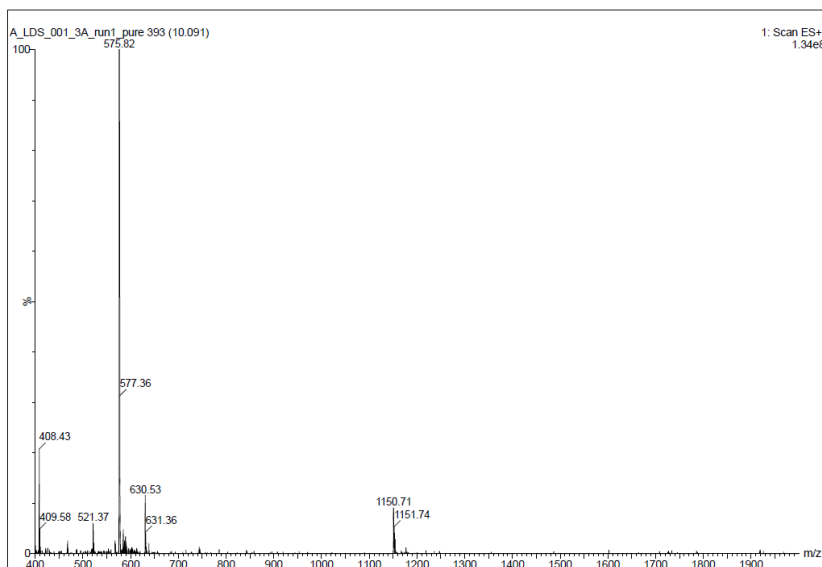
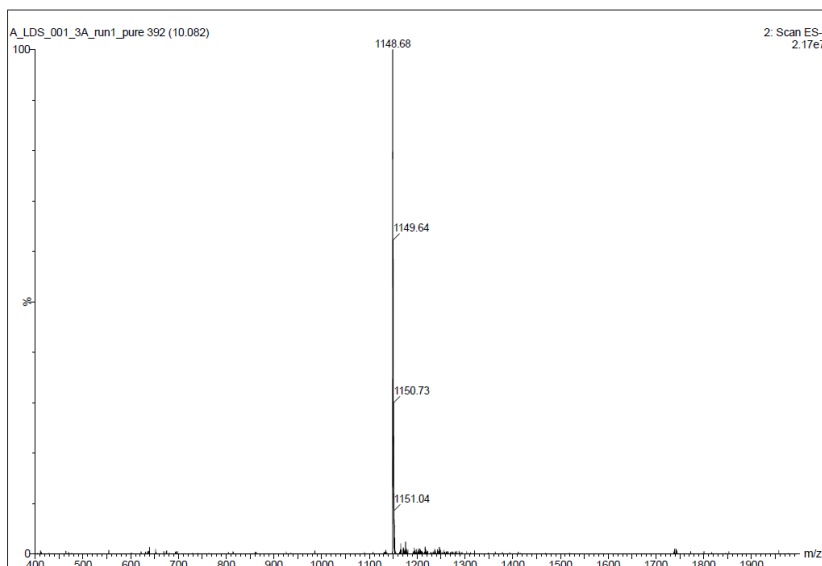
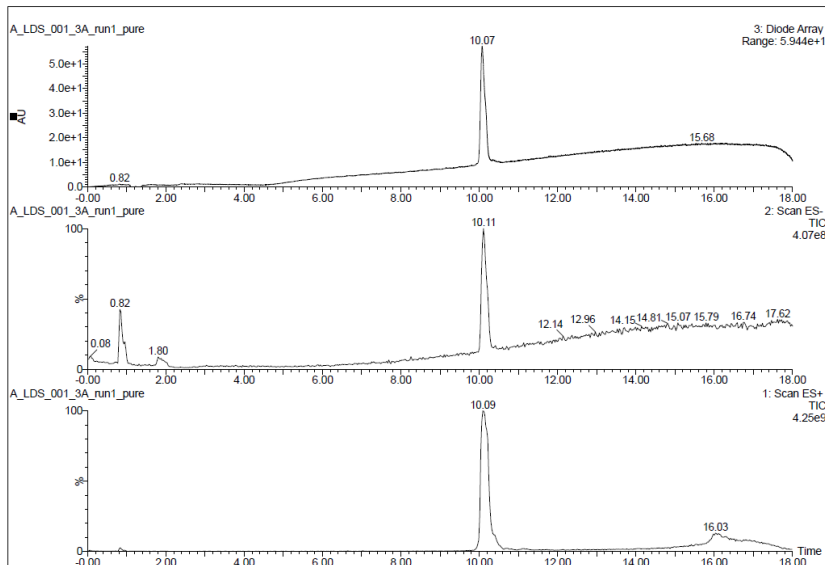
C-strand peptide ($\text{H}_2\text{N-Asp-Lys-Tyr-Tyr-Ile-Val-Lys-Tyr-CONH}_2$) (LDS-001-1A)



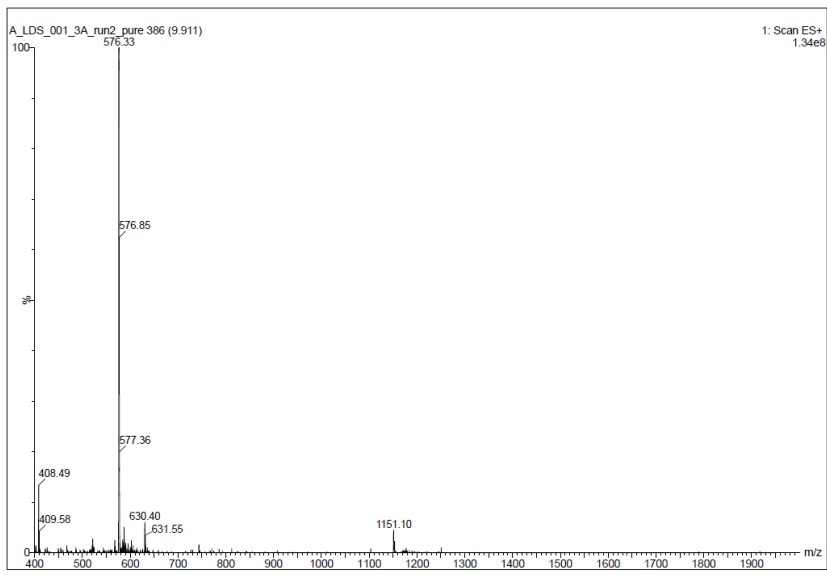
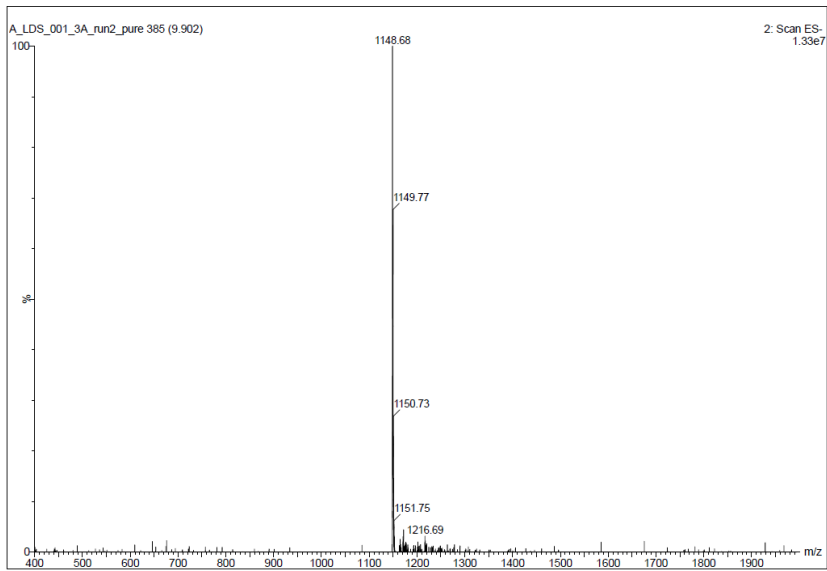
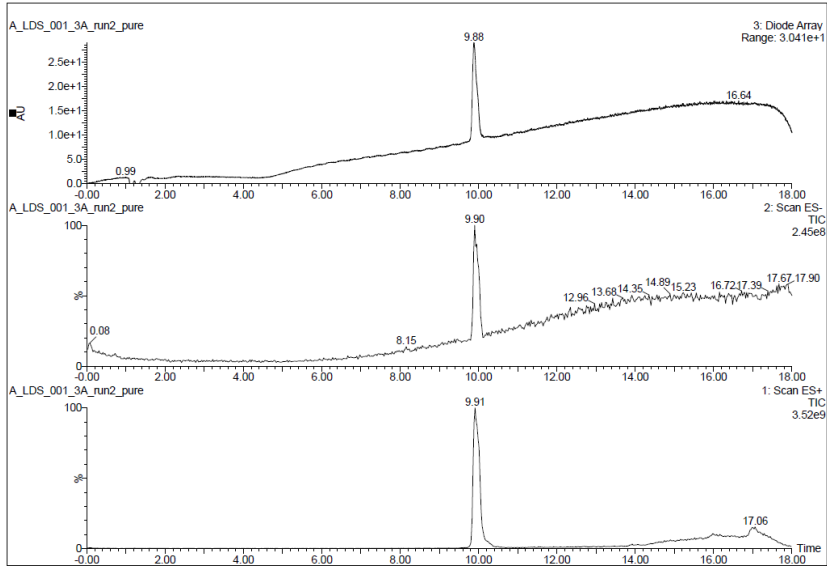
Phe(3)-peptide (H₂N-Asp-Lys-Phe-Tyr-Ile-Val-Lys-Tyr-CONH₂) (LDS-001-2A)



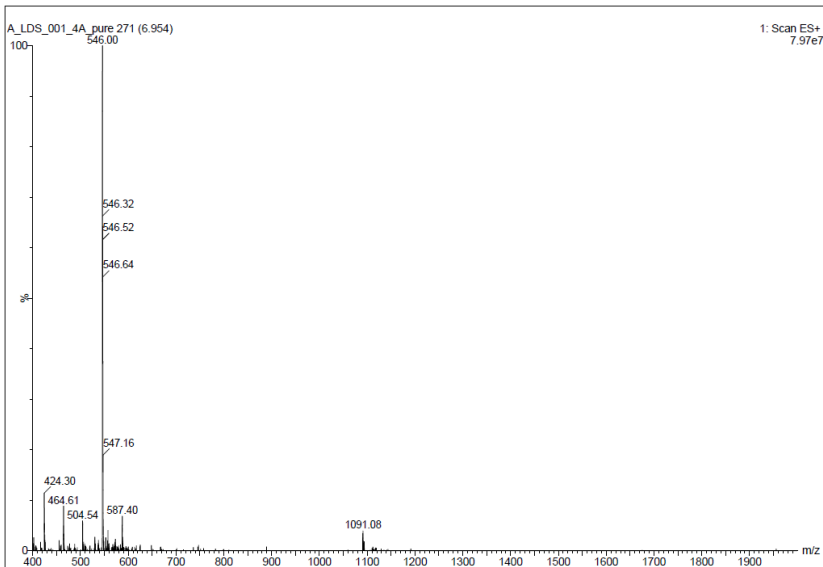
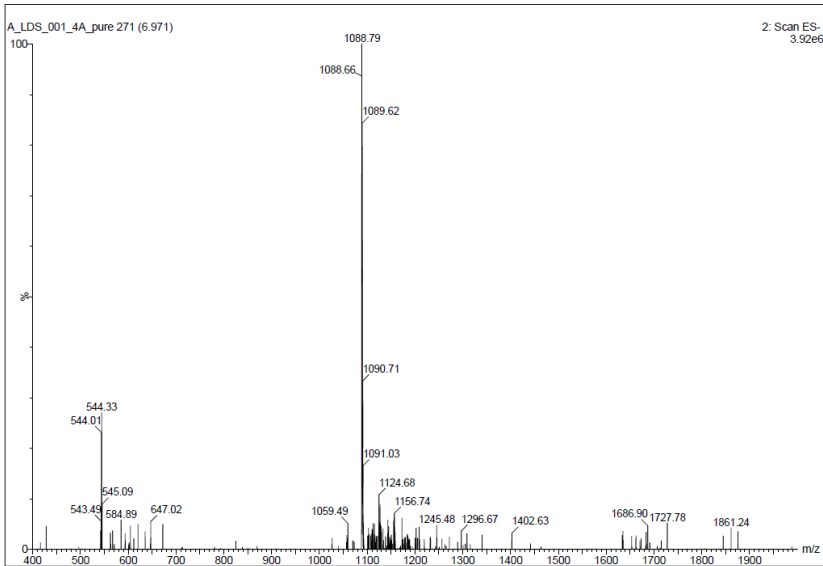
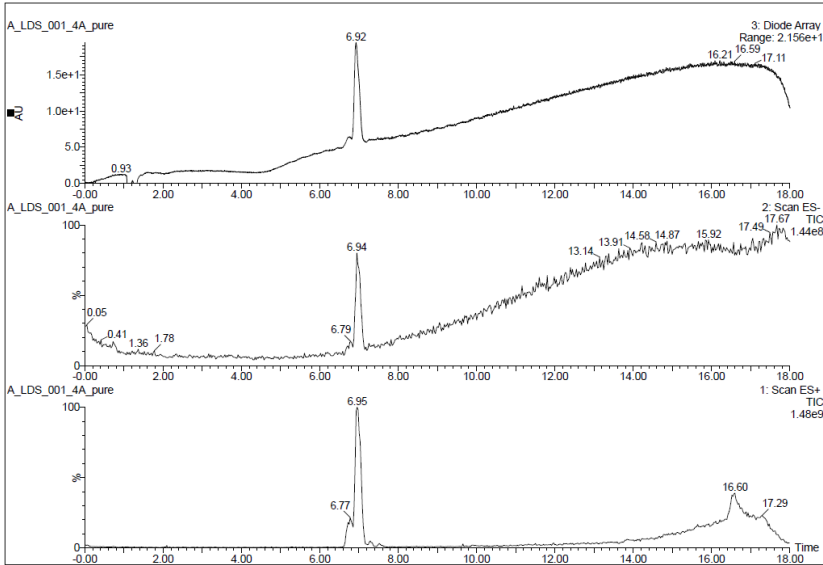
Bip(3)-peptide (H₂N-Asp-Lys-Bip-Tyr-Ile-Val-Lys-Tyr-CONH₂) (LDS-001-3A_run 1)



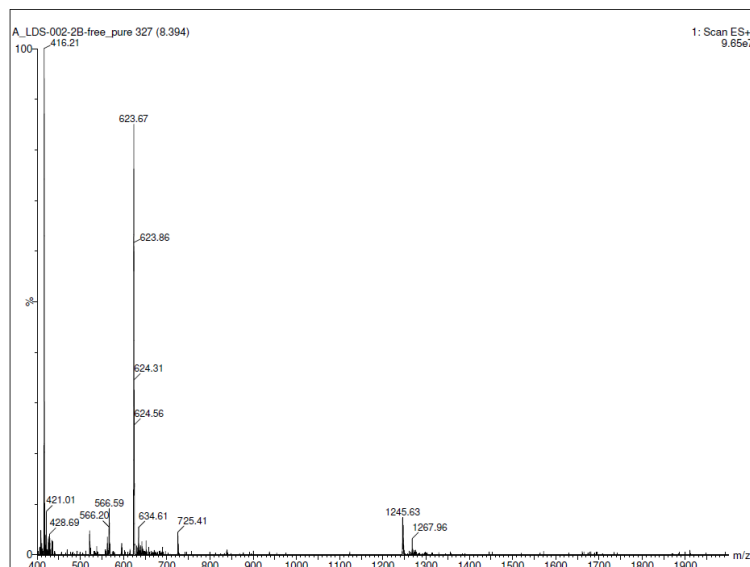
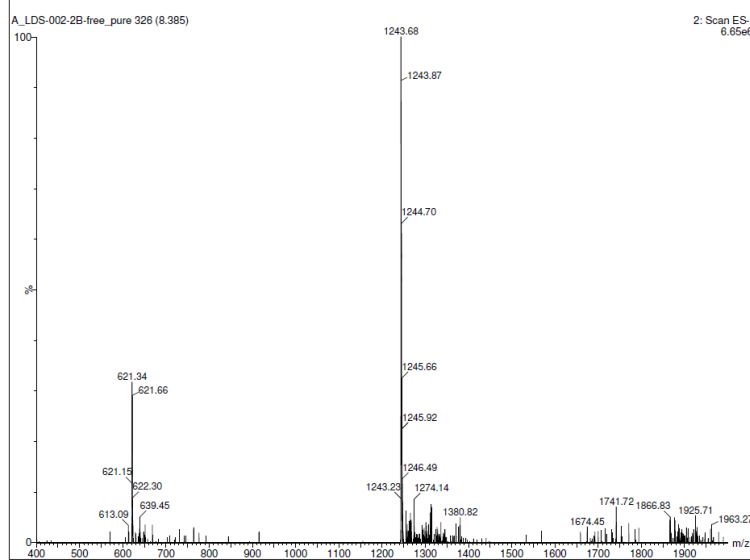
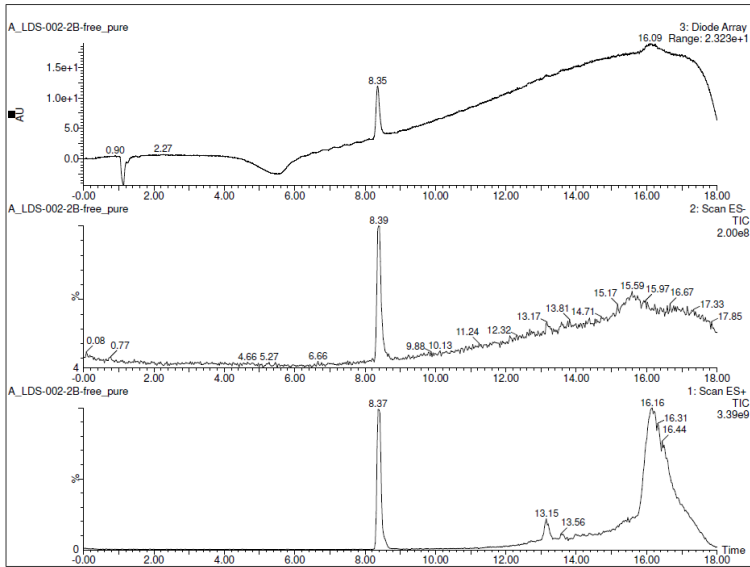
Bip(3)-peptide (H₂N-Asp-Lys-Bip-Tyr-Ile-Val-Lys-Tyr-CONH₂) (LDS-001-3A_run 2)



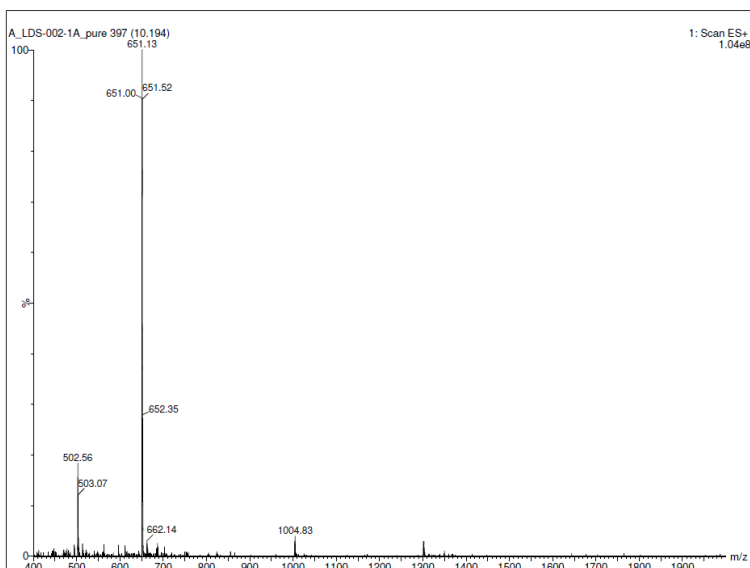
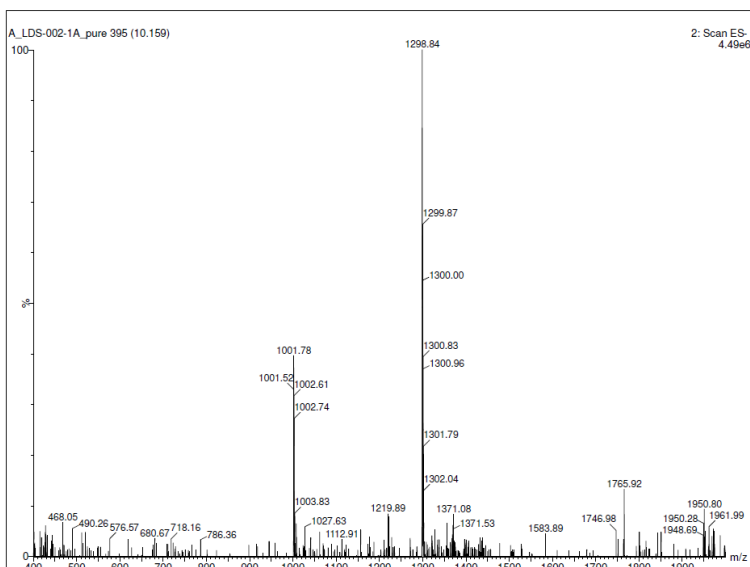
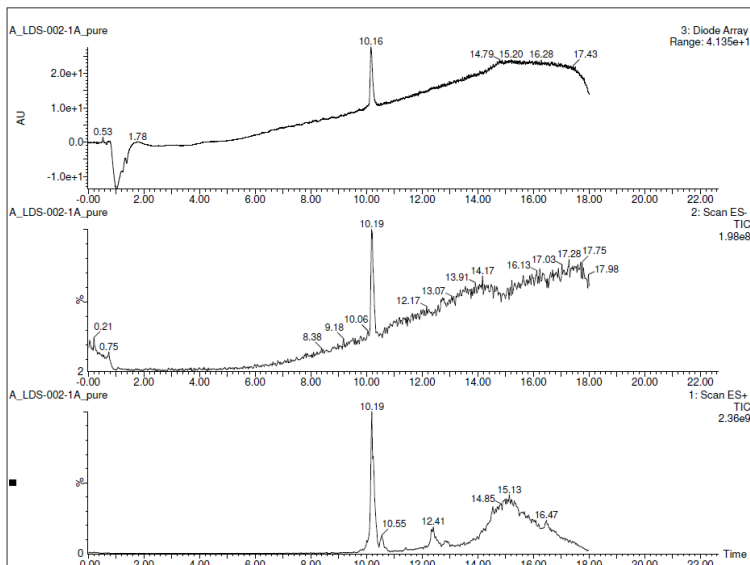
C-strand peptide (H₂N-Tyr-Lys-Val-Ile-Tyr-Tyr-Lys-Asp-CONH₂) (LDS-001-4A)



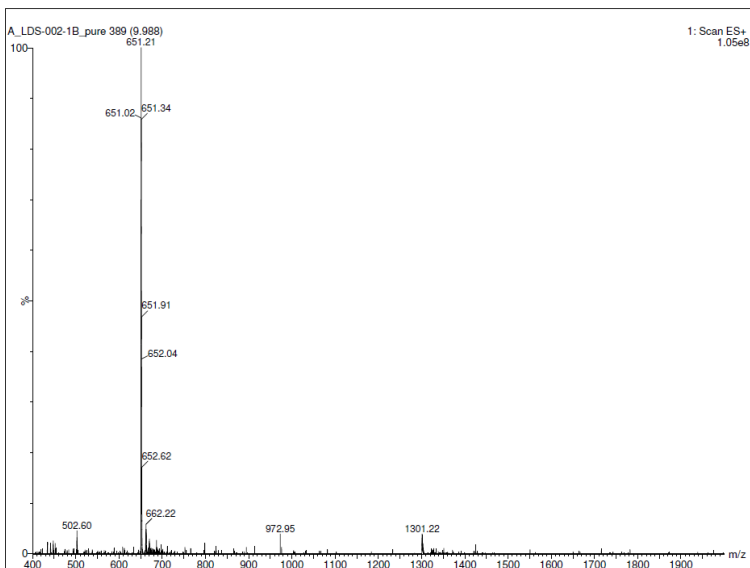
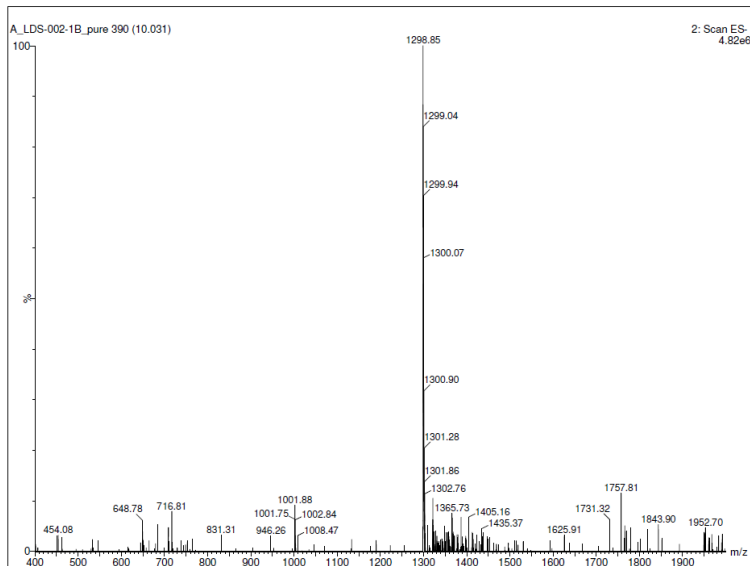
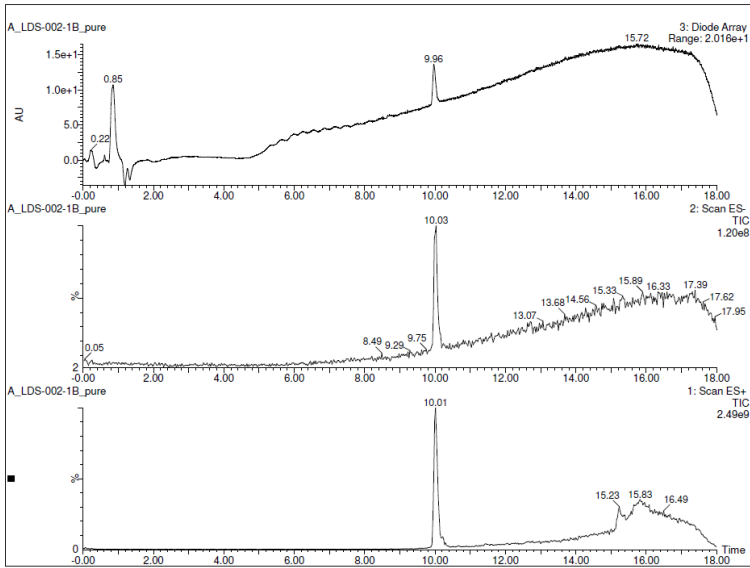
link-Phe(3)-peptide (H₂N-Gly-Gly-Gly-Asp-Lys-Phe-Tyr-Ile-Val-Lys-Tyr-CONH₂) (LDS-002-2B-free)



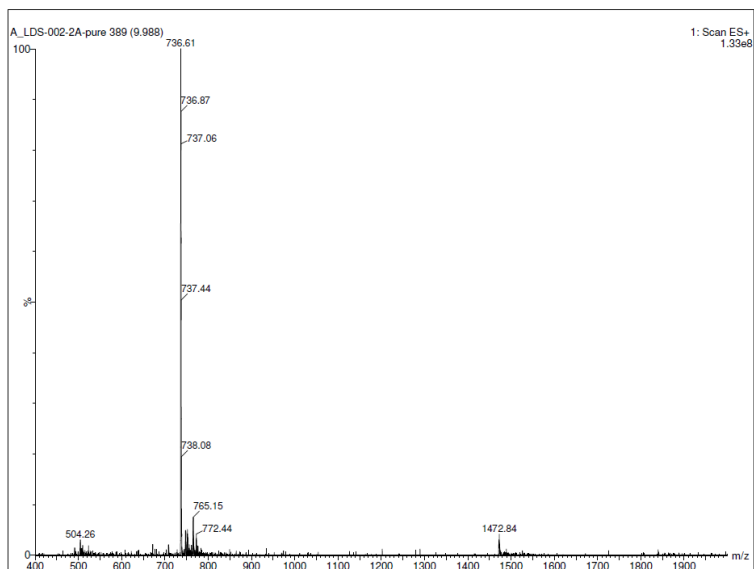
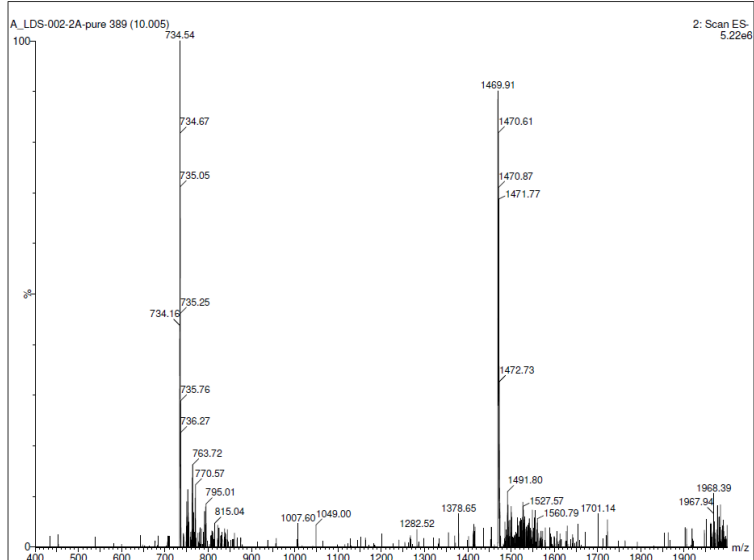
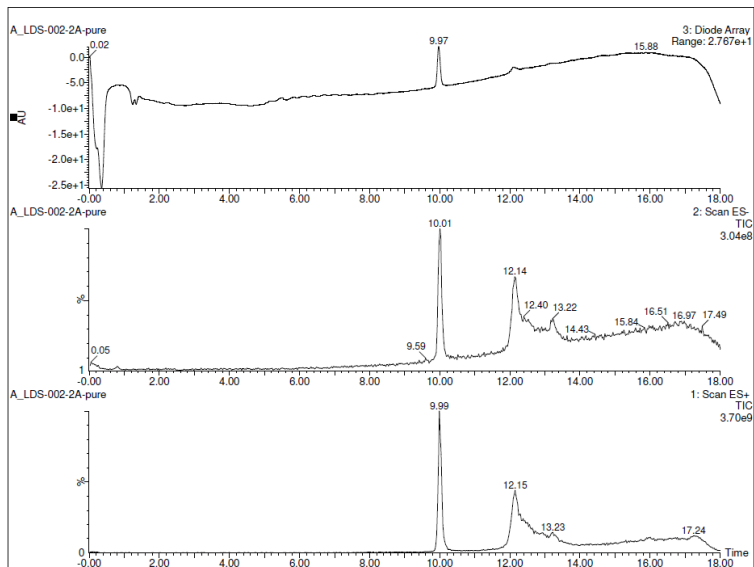
b-Phe(3)-peptide (biotin-Asp-Lys-Phe-Tyr-Ile-Val-Lys-Tyr-CONH₂) (LDS-002-1A)



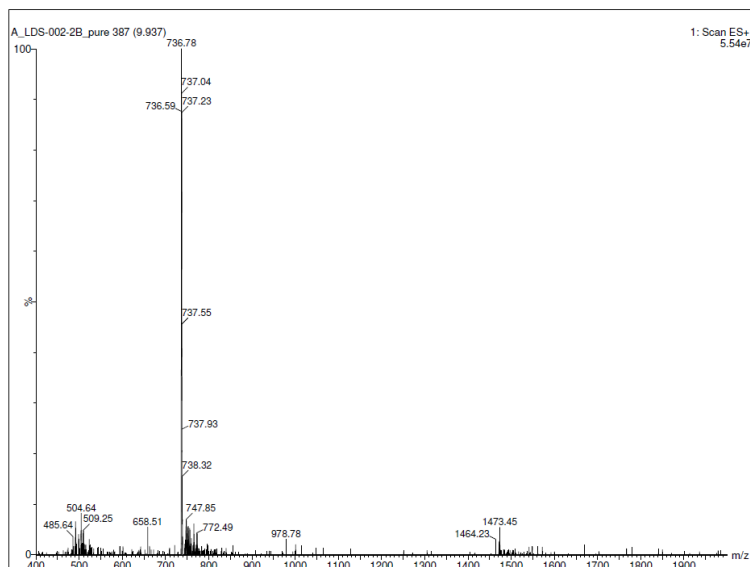
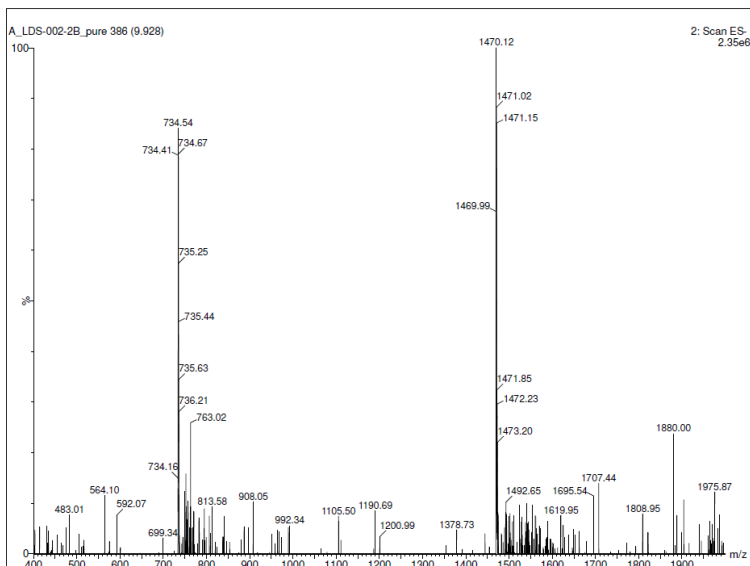
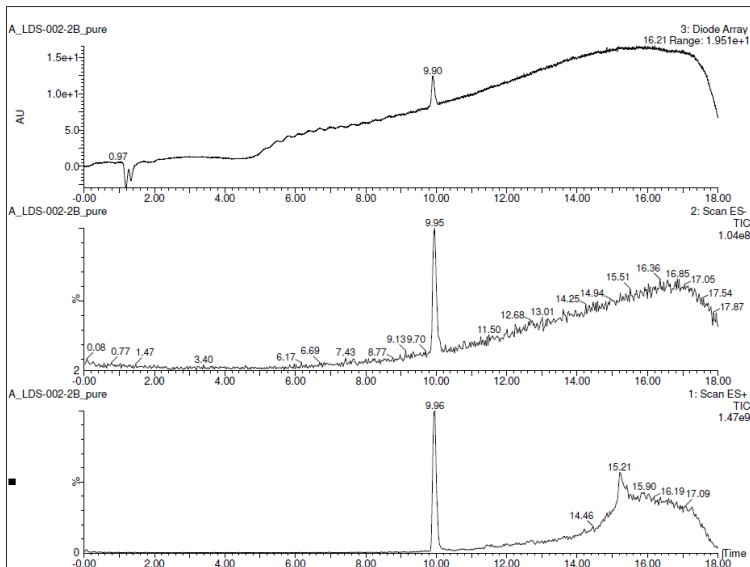
b-Phe(3)-peptide (biotin-Asp-Lys-Phe-Tyr-Ile-Val-Lys-Tyr-CONH₂) (LDS-002-1B)



b-link-Phe(3)-peptide (biotin-Gly-Gly-Gly-Asp-Lys-Phe-Tyr-Ile-Val-Lys-Tyr-CONH₂) (LDS-002-2A)



b-link-Phe(3)-peptide (biotin-Gly-Gly-Gly-Asp-Lys-Phe-Tyr-Ile-Val-Lys-Tyr-CONH₂) (LDS-002-2B)

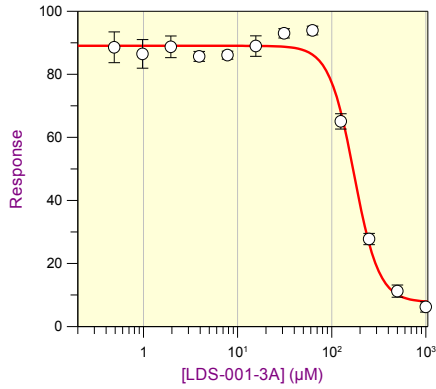


8.6 Peptides - ELISA inhibition assay IC₅₀ curves

Bip(3)-peptide (H₂N-Asp-Lys-Bip-Tyr-Ile-Val-Lys-Tyr-CONH₂) (LDS-001-3A)

IC₅₀ = **173 ± 12 μM**

IC₅₀ Data

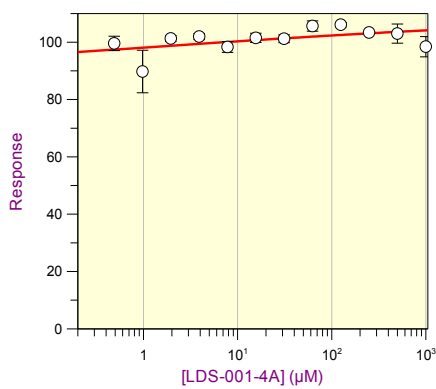


Parameter	Value	Std. Error
Y Range	81.3212	3.6697
IC 50	172.5720	11.9625
Slope factor	3.2840	0.5444
Background	7.7108	3.2766

C-strand peptide (H₂N-Tyr-Lys-Val-Ile-Tyr-Tyr-Lys-Asp-CONH₂) (LDS-001-4A)

IC₅₀ > **1000 μM**

IC₅₀ Data



Parameter	Value	Std. Error
Y Range	25.2476	5.4783
IC 50	0.6042	3.1197
Slope factor	-0.1537	0.0936
Background	84.9971	3.2611

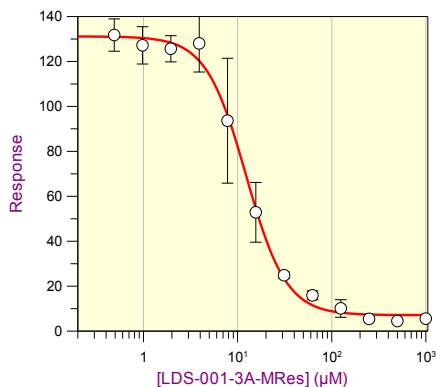
8.7 Peptides - TR-FRET inhibition assay IC₅₀ curves

Phe(3)-peptide (H₂N-Asp-Lys-Phe-Tyr-Ile-Val-Lys-Tyr-CONH₂) (LDS-001-3A-MRes)

Pre-incubated with IgE-Fc-A647:

IC₅₀ = **12 ± 0.7 μM**

IC₅₀ Data

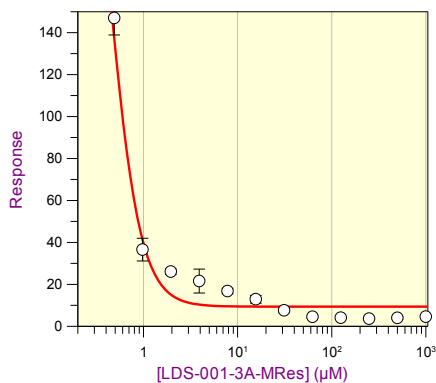


Parameter	Value	Std. Error
Y Range	124.0105	3.3636
IC 50	12.3321	0.7114
Slope factor	2.0385	0.2105
Background	7.1114	1.9435

Pre-incubated with αγ-Tb:

IC₅₀ = **0.4 ± 0.2 μM**

IC₅₀ Data

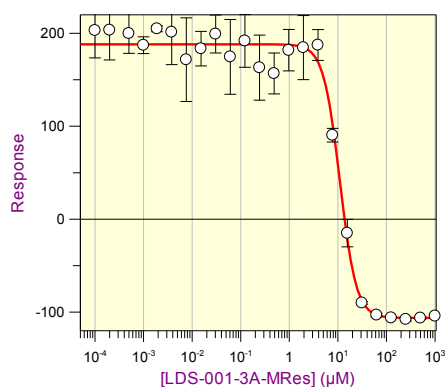


Parameter	Value	Std. Error
Y Range	319.3328	105.5412
IC 50	0.4183	0.1549
Slope factor	2.5988	0.5854
Background	9.3717	2.7835

Pre-incubated with αγ-Tb (repeat):

IC₅₀ = **11 ± 0.7 μM**

IC₅₀ Data



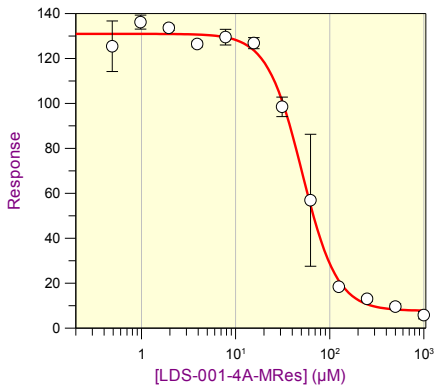
Parameter	Value	Std. Error
Y Range	294.4099	7.3191
IC 50	10.9801	0.7374
Slope factor	2.5797	0.3648
Background	-106.2377	6.2337

Trp(3)-peptide (H₂N-Asp-Lys-Trp-Tyr-Ile-Val-Lys-Tyr-CONH₂) (LDS-001-4A-MRes)

Pre-incubated with IgE-Fc-A647:

IC₅₀ = **51 ± 3 μM**

IC50 Data

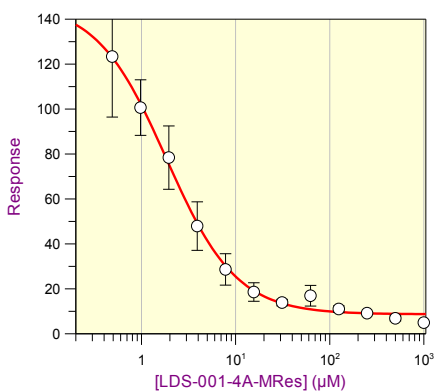


Parameter	Value	Std. Error
Y Range	123.2418	3.1987
IC 50	50.8515	2.6388
Slope factor	2.3376	0.2498
Background	7.6930	2.4660

Pre-incubated with αγ-Tb:

IC₅₀ = **2 ± 0.3 μM**

IC50 Data

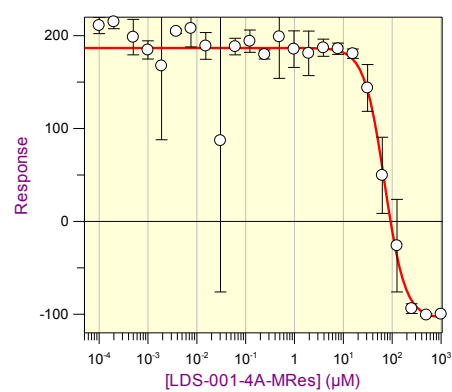


Parameter	Value	Std. Error
Y Range	138.5473	12.0254
IC 50	1.8367	0.3159
Slope factor	1.1689	0.1342
Background	8.6529	1.4961

Pre-incubated with αγ-Tb (repeat):

IC₅₀ = **70 ± 11 μM**

IC50 Data



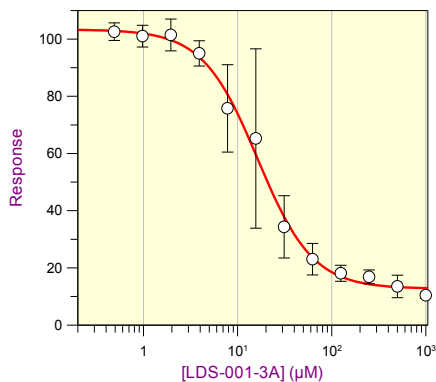
Parameter	Value	Std. Error
Y Range	291.1433	20.3019
IC 50	69.9084	10.7972
Slope factor	2.0885	0.5853
Background	-104.3774	18.8240

Bip(3)-peptide (H₂N-Asp-Lys-Bip-Tyr-Ile-Val-Lys-Tyr-CONH₂) (LDS-001-3A)

Pre-incubated with IgE-Fc-A647:

IC₅₀ = **16 ± 1 μM**

IC50 Data

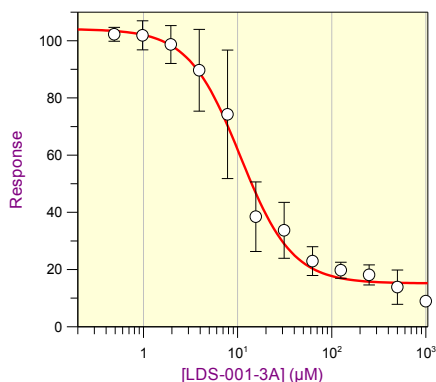


Parameter	Value	Std. Error
Y Range	90.6039	3.4248
IC 50	16.3649	1.4005
Slope factor	1.4845	0.1739
Background	12.7424	1.9983

Pre-incubated with αγ-Tb:

IC₅₀ = **11 ± 1 μM**

IC50 Data



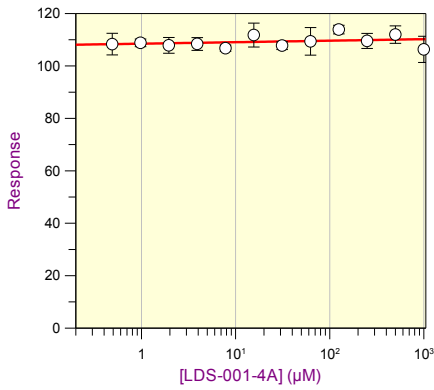
Parameter	Value	Std. Error
Y Range	88.9443	4.8121
IC 50	10.6751	1.2691
Slope factor	1.5752	0.2580
Background	15.1533	2.4636

C-strand peptide (H₂N-Tyr-Lys-Val-Ile-Tyr-Tyr-Lys-Asp-CONH₂) (LDS-001-4A)

Pre-incubated with IgE-Fc-A647:

IC₅₀ > 1000 μM

IC50 Data

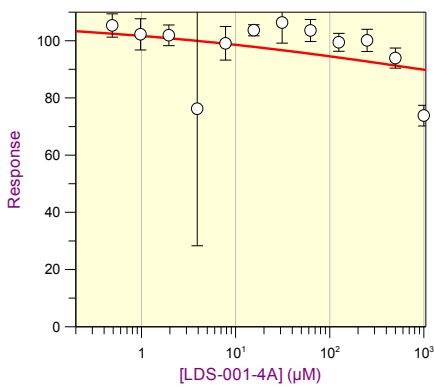


Parameter	Value	Std. Error
Y Range	18.3368	12.8257
IC 50	482.1486	20461.9832
Slope factor	-0.0548	0.0731
Background	100.8534	6.1099

Pre-incubated with αγ-Tb:

IC₅₀ > 1000 μM

IC50 Data



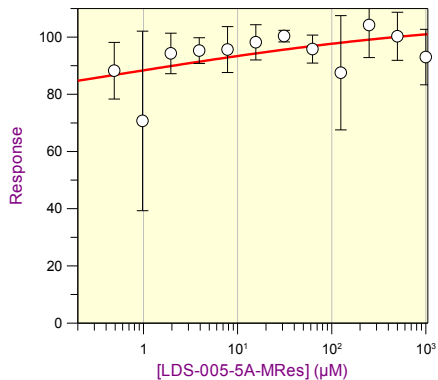
Parameter	Value	Std. Error
Y Range	38.9160	13.4702
IC 50	1913.3454	4945.5284
Slope factor	0.2184	0.1996
Background	69.0267	9.0238

His(3)-peptide (H₂N-Asp-Lys-His-Tyr-Ile-Val-Lys-Tyr-CONH₂) (LDS-005-5A-MRes)

Pre-incubated with IgE-Fc-A647:

IC₅₀ > 1000 μM

IC50 Data

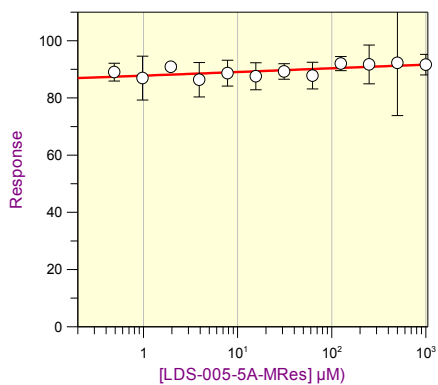


Parameter	Value	Std. Error
Y Range	40.6322	10.4612
IC 50	0.5645	5.2410
Slope factor	-0.2234	0.1392
Background	66.7657	6.4364

Pre-incubated with αγ-Tb:

IC₅₀ > 1000 μM

IC50 Data



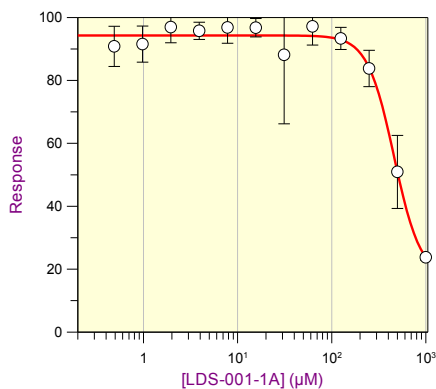
Parameter	Value	Std. Error
Y Range	15.0273	2.7646
IC 50	30.9598	63.2773
Slope factor	-0.1517	0.0663
Background	82.1861	1.3967

Parent peptide (H₂N-Asp-Lys-Tyr-Tyr-Ile-Val-Lys-Tyr-CONH₂) (LDS-001-1A)

Pre-incubated with IgE-Fc-A647:

IC₅₀ = 459 ± 42 μM

IC50 Data

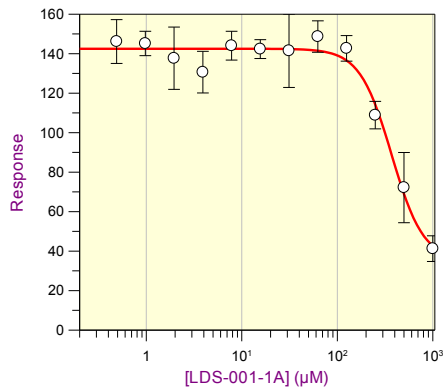


Parameter	Value	Std. Error
Y Range	76.9040	7.1167
IC 50	459.3115	42.3843
Slope factor	3.0799	0.6977
Background	17.3841	6.8334

Pre-incubated with IgE-Fc-A647 (repeat):

IC₅₀ = 371 ± 58 μM

IC50 Data

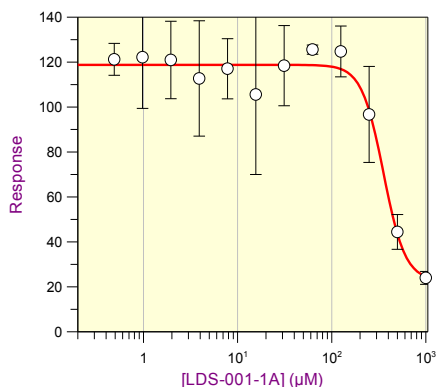


Parameter	Value	Std. Error
Y Range	107.2458	13.4761
IC 50	370.5129	57.6934
Slope factor	2.6137	0.6679
Background	35.2346	12.9041

Pre-incubated with IgE-Fc-A647 (repeat):

IC₅₀ = 355 ± 38 μM

IC50 Data

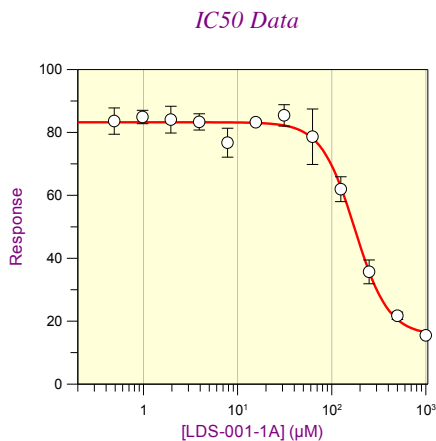


Parameter	Value	Std. Error
Y Range	96.0282	8.4021
IC 50	354.6023	37.8480
Slope factor	3.7665	1.0718
Background	22.7332	7.9763

Parent peptide (H₂N-Asp-Lys-Tyr-Tyr-Ile-Val-Lys-Tyr-CONH₂) (LDS-001-1A)

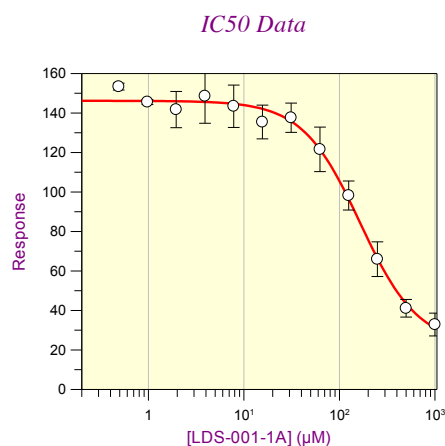
Pre-incubated with α-Tb:

IC₅₀ = **176 ± 13 μM**



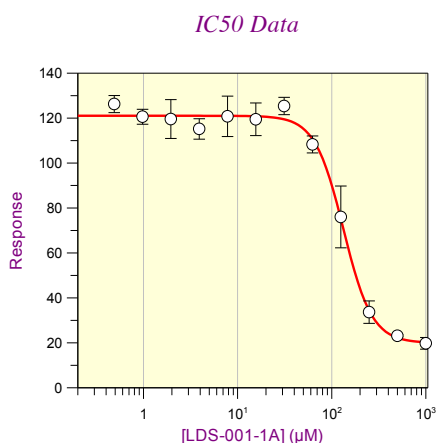
Pre-incubated with α-Tb (repeat):

IC₅₀ = **176 ± 13 μM**



Pre-incubated with α-Tb (repeat):

IC₅₀ = **133 ± 7 μM**

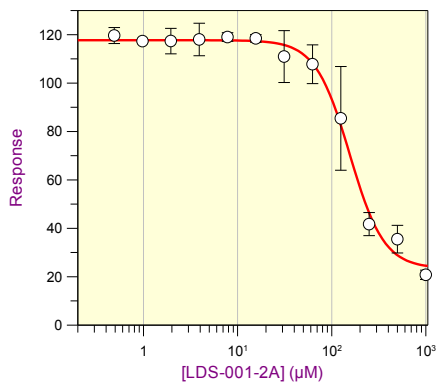


Phe(3)-peptide (H₂N-Asp-Lys-Phe-Tyr-Ile-Val-Lys-Tyr-CONH₂) (LDS-001-2A)

Pre-incubated with IgE-Fc-A647:

IC₅₀ = **155 ± 12 μM**

IC50 Data

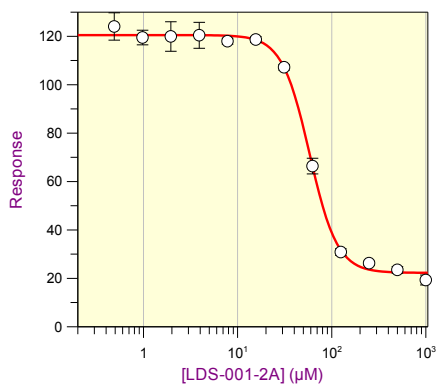


Parameter	Value	Std. Error
Y Range	94.2846	4.3234
IC 50	155.4465	11.8742
Slope factor	2.3926	0.3469
Background	23.4399	3.8417

Pre-incubated with αγ-Tb:

IC₅₀ = **58 ± 2 μM**

IC50 Data



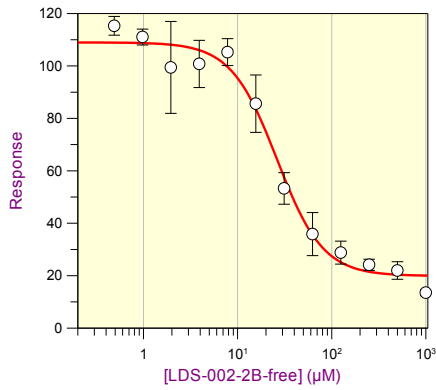
Parameter	Value	Std. Error
Y Range	98.2161	1.6460
IC 50	58.2653	1.7468
Slope factor	2.9510	0.2372
Background	22.2817	1.2859

link-Phe(3)-peptide (H₂N-Gly-Gly-Gly-Asp-Lys-Phe-Tyr-Ile-Val-Lys-Tyr-CONH₂) (LDS-002-2B-free)

Pre-incubated with IgE-Fc-A647:

IC₅₀ = **26 ± 4 μM**

IC50 Data

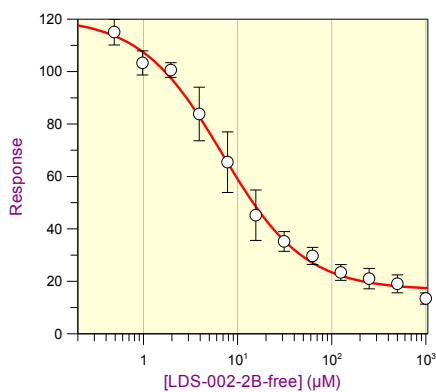


Parameter	Value	Std. Error
Y Range	89.0711	5.3054
IC 50	26.1771	3.5038
Slope factor	1.7765	0.3481
Background	19.8993	3.5913

Pre-incubated with α-Tb:

IC₅₀ = **7 ± 0.9 μM**

IC50 Data



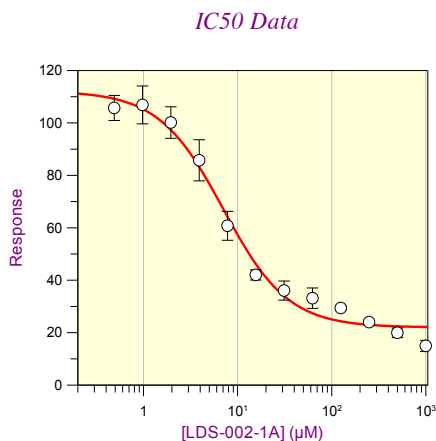
Parameter	Value	Std. Error
Y Range	103.8823	6.0949
IC 50	6.8557	0.9012
Slope factor	0.9962	0.1151
Background	16.7139	2.0576

8.8 Biotin-peptides – TR-FRET inhibition assay IC₅₀ curves

b-Phe(3)-peptide (biotin-Asp-Lys-Phe-Tyr-Ile-Val-Lys-Tyr-CONH₂) (LDS-002-1A)

Pre-incubated with IgE-Fc-A647:

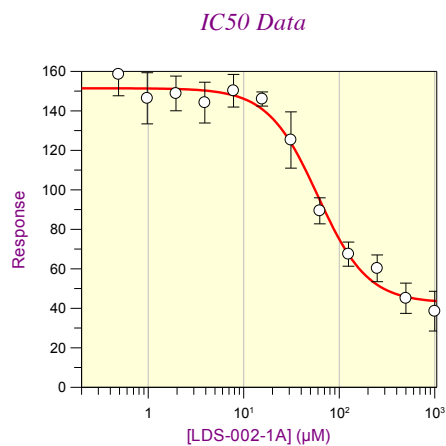
IC₅₀ = **7 ± 1 μM**



Parameter	Value	Std. Error
Y Range	90.1878	7.3429
IC 50	7.0599	1.2209
Slope factor	1.2635	0.2291
Background	21.9947	2.7647

Pre-incubated with IgE-Fc-A647 (repeat):

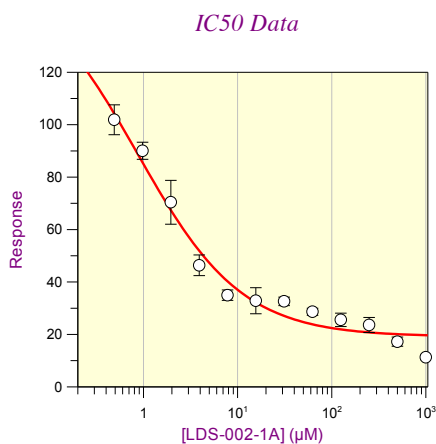
IC₅₀ = **60 ± 7 μM**



Parameter	Value	Std. Error
Y Range	108.7017	6.2333
IC 50	59.5128	7.3681
Slope factor	1.6622	0.2939
Background	42.7315	4.9287

Pre-incubated with αγ-Tb:

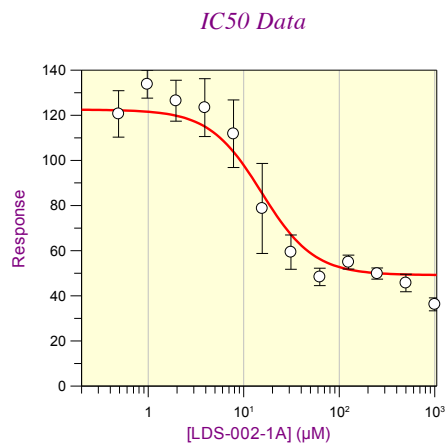
IC₅₀ = **0.9 ± 1 μM**



Parameter	Value	Std. Error
Y Range	139.4480	65.2422
IC 50	0.8657	1.1355
Slope factor	0.7836	0.2933
Background	19.1381	3.7068

Pre-incubated with αγ-Tb (repeat):

IC₅₀ = **15 ± 5 μM**



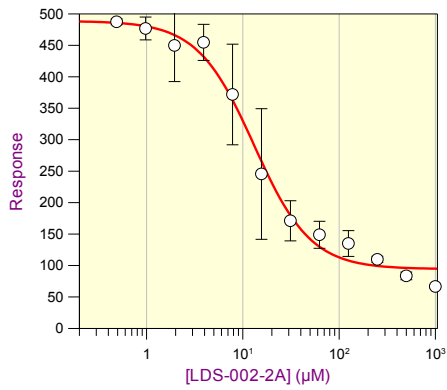
Parameter	Value	Std. Error
Y Range	73.3568	16.2747
IC 50	15.3492	5.4283
Slope factor	1.5860	0.3511
Background	49.1450	8.1412

b-link-Phe(3)-peptide (biotin-Gly-Gly-Gly-Asp-Lys-Phe-Tyr-Ile-Val-Lys-Tyr-CONH₂) (LDS-002-2A)

Pre-incubated with IgE-Fc-A647:

IC₅₀ = **13 ± 2 μM**

IC50 Data

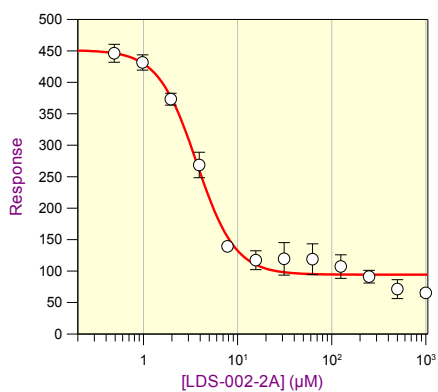


Parameter	Value	Std. Error
Y Range	394.3169	22.6089
IC 50	13.0591	1.6864
Slope factor	1.4784	0.2487
Background	94.3801	12.2034

Pre-incubated with αγ-Tb:

IC₅₀ = **4 ± 0.4 μM**

IC50 Data



Parameter	Value	Std. Error
Y Range	356.8550	21.9218
IC 50	3.6622	0.3980
Slope factor	2.1148	0.3987
Background	94.3160	7.8688

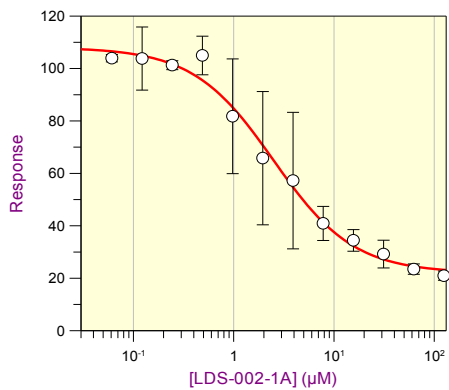
b-Phe(3)-peptide (biotin-Asp-Lys-Phe-Tyr-Ile-Val-Lys-Tyr-CONH₂) (LDS-002-1A)

(maximum concentration reduced from 1 mM to 125 μM)

Pre-incubated with αγ-Tb:

IC₅₀ = **2 ± 0.4 μM**

IC50 Data



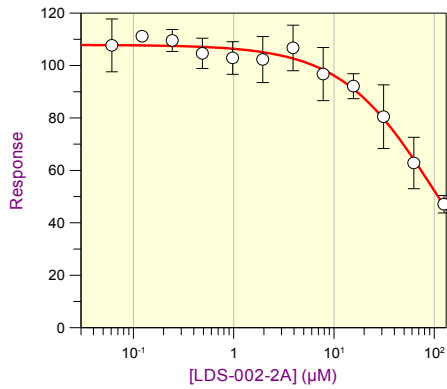
Parameter	Value	Std. Error
Y Range	86.0704	6.4386
IC 50	2.4945	0.4160
Slope factor	1.0847	0.1956
Background	21.9748	3.7161

b-link-Phe(3)-peptide (biotin-Gly-Gly-Gly-Asp-Lys-Phe-Tyr-Ile-Val-Lys-Tyr-CONH₂) (LDS-002-2A)
(maximum concentration reduced from 1 mM to 125 μM)

Pre-incubated with αγ-Tb:

IC₅₀ = **98 ± 104 μM**

IC50 Data



Parameter	Value	Std. Error
Y Range	109.9581	53.5881
IC 50	97.6188	103.5828
Slope factor	0.9336	0.2473
Background	-2.0997	52.7474

8.9 Biotin-peptides and streptavidin – TR-FRET inhibition assay IC₅₀ curves

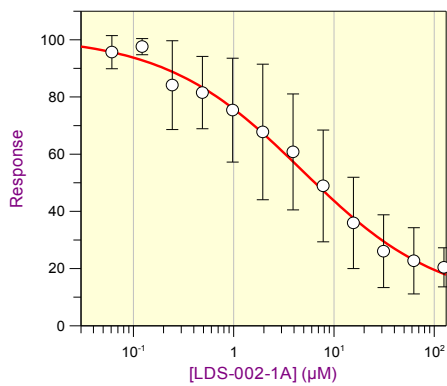
b-Phe(3)-peptide (biotin-Asp-Lys-Phe-Tyr-Ile-Val-Lys-Tyr-CONH₂) (LDS-002-1A)

(maximum concentration reduced from 1 mM to 125 μM) and 2 eq streptavidin

Pre-incubated with αγ-Tb:

IC₅₀ = **5 ± 1 μM**

IC50 Data



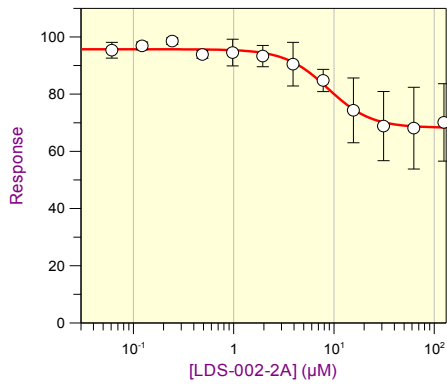
Parameter	Value	Std. Error
Y Range	93.8841	13.3578
IC 50	4.7919	1.3596
Slope factor	0.6291	0.1419
Background	7.4441	8.6986

b-link-Phe(3)-peptide (biotin-Gly-Gly-Gly-Asp-Lys-Phe-Tyr-Ile-Val-Lys-Tyr-CONH₂) (LDS-002-2A)
(maximum concentration reduced from 1 mM to 125 μ M) **and 2 eq streptavidin**

Pre-incubated with $\alpha\gamma$ -Tb:

IC₅₀ > 1000 μ M

IC50 Data



Parameter	Value	Std. Error
Y Range	27.4592	1.5819
IC 50	8.7044	1.0056
Slope factor	2.0208	0.3977
Background	68.2386	1.2771